Measurement of human skin mechanical properties : variations according to the effect of different stresses.

Bastien Blanchard

THÈSE

UNIVERSITE DE PAU ET DES PAYS DE L'ADOUR

École doctorale des Sciences Exactes et de leurs Applications (ED 211)

Présentée et soutenue le 19 Décembre 2023

par **Bastien BLANCHARD**

pour obtenir le grade de docteur
de l'Université de Pau et des Pays de l'Adour
Spécialité : Physique des polymères

Mesure des propriétés mécaniques de la peau humaine : variations sous l'effet de différents *stress*

Measurement of human skin mechanical properties: variations according to the effect of different stresses

MEMBRES DU JURY

RAPPORTEURS

• Muriel BRACCINI	Chargée de recherche HDR CNRS / SIMAP, Grenoble
• Nicolas L'HEUREUX	Directeur de recherche INSERM / BIOTIS, Bordeaux

EXAMINATEURS

• Éric PAPON	Professeur / LCPO, Bordeaux
• Giuseppe PERCOCO	Ingénieur de recherche - PhD / Eurofins BIO-EC, Longjumeau (invité)
• Francis EHRENFELD	Ingénieur d'études CNRS / IPREM, Pau (invité)

DIRECTEURS

• Christophe DERAIL	Professeur / IPREM, Pau
• Corinne NARDIN	Professeur / IPREM, Pau

UNIVERSITÉ DE PAU ET DES PAYS DE L'ADOUR

Remerciements

Ces remerciements sont dédiés à toutes les personnes qui m'ont accompagnées durant ces 3 années de doctorat et qui m'ont permis de vivre une très belle aventure scientifique et humaine.

Je souhaite tout d'abord remercier mes directeurs de thèse, Christophe Derail et Corinne Nardin, de m'avoir embarqué dans une superbe aventure sur un sujet de thèse très innovant mais aussi très risqué. Je les remercie pour ces 3 années de recherche et d'enseignement passées avec eux. Merci pour leurs aides, leurs disponibilités, leur écoute, leur bienveillance, leurs accompagnements et leurs conseils prodigués tout au long de la thèse.

Un grand merci à Francis Erhenfeld et Anthony Laffore, qui complètent l'équipe MECAPEAU avec mes directeurs de thèse, pour leur travail tout au long de la thèse sur l'instrumentation. On sera passé par toutes les émotions ensemble, mais je trouve que la fin de l'histoire est plutôt belle.

Je souhaite également remercier l'ensemble des membres du jury de thèse d'avoir lu et évalué ce manuscrit, de m'avoir permis de soutenir et de m'avoir donné de nombreuses remarques pertinentes sur ce travail de recherche.

Je tiens également à remercier le Laboratoire Eurofins BIO-EC, et plus particulièrement Giuseppe Percoco, d'avoir collaboré avec nous sur ce projet, en me permettant de réaliser plusieurs campagnes de tests chez eux, à Longjumeau.

Pour la partie « enseignement » de ma thèse, que j'ai d'ailleurs tout particulièrement appréciée, j'aimerais remercier Delphine Bessières et Sylvie Dagreou pour leur accompagnement et pour l'organisation de ces heures d'enseignement réalisées à l'UPPA. Merci également à l'ensemble des enseignants-chercheurs avec lesquels j'ai pu collaborer pour donner des cours.

En parlant des enseignants-chercheurs, je tiens également à remercier tous ceux que j'ai pu côtoyer tout au long de mon parcours universitaire à l'UPPA : de la Licence Physique-Chimie, en passant par le Master IMECA, jusqu'à ce doctorat. Merci sincèrement à vous de m'avoir transmis la passion de la recherche et de l'enseignement !

Un très grand merci également à notre équipe de doctorants de l'IPREM, qui ne sont plus des collègues mais des amis maintenant : Alexandre, Alexis, Arnaud, Axelle, Beatrice, François, Grégoire, Léonard, Marine, Marion, Maud, Nabil, Quentin, Théo et Valentina. Une sacrée belle équipe avec laquelle j'ai passé de super moments ! C'était vraiment top de vous côtoyer au quotidien dans les bons comme dans les moins bons moments.

Enfin, je remercie de tout mon cœur ma famille de m'avoir accompagné et soutenu sans cesse durant ce travail de thèse.

Un dernier grand merci à vous tous !!!

Table of contents

Introduction Générale 1

General Introduction 7

Chapter 1: State of the art 13

1.1 Human skin anatomy 16

1.1.1 Skin tissue structure 16

1.1.2 Vascularisation, cutaneous innervation, and cutaneous appendages 28

1.2 Skin functions and their alterations 32

1.2.1 The different functions of the skin 33

1.2.2 Skin ageing and effects of different stresses 36

1.3 Mechanical properties of human skin 43

1.3.1 Intrinsic mechanical properties of skin components 44

1.3.2 Non-linearity of the skin properties 47

1.3.3 Viscoelasticity of the skin 49

1.3.4 Anisotropy and pre-tension state of the skin 51

1.3.5 Contribution of the different skin layers to the mechanical properties 53

1.3.6 Parameters affecting mechanical properties 55

1.4 Techniques for characterising human skin 60

1.4.1 Direct techniques 60

1.4.2 Indirect techniques 69

1.5 Modelling the mechanical behaviour of human skin 76

1.5.1 Phenomenological and microstructural models 77

1.5.2 Elastic and hyperelastic models 79

1.5.3 Viscoelastic models 79

1.6 General conclusion of the literature review 80

Chapter 2: Materials and Methods 81

2.1 Development of an original equipment for measuring the mechanical properties of skin 83

2.1.1 Initial state: Principle and description of the device 83

2.1.2 Main improvements to the device 90

2.1.3 Final state of the device 95

2.1.4 Experimental validation of the device using different materials 98

2.1.5 Conclusion on the development of the equipment 102
2.2 Methods 103
2.2.1 Test protocol 103
2.2.2 The different types of mechanical tests possible 105
2.2.3 Methods for analysing results 109
2.2.4 Conclusion on methods 115
2.3 Human skin 115
2.3.1 Ethics: human skin models as an alternative to animal experimentation 115
2.3.2 *Ex vivo* explants 116
2.4 General conclusion on materials and methods 118

Chapter 3: Preliminary studies on human skin and method validation 119

3.1 Notion of skin preconditioning 121
3.2 Test repeatability 124
3.3 Test reproducibility 125
3.4 Study of the effect of strain rate 127
3.5 Study on the effect of compression force on the skin 129
3.6 Study on the pre-tension state of the skin 131
3.7 Notion of skin anisotropy 136
3.8 General conclusion of “Preliminary studies” 140

Chapter 4: Characterisation of human skin mechanical properties 141

4.1 Characterisation of *ex vivo* skin mechanical properties 144
4.1.1 Tensile test 145
4.1.2 Comparison of our results with those of the scientific literature 149
4.1.3 Dynamic tests 150
4.1.4 Loading-unloading cycles 158
4.1.5 Stress relaxation test 160
4.1.6 Conclusion on the characterisation of *ex vivo* skin mechanical properties 162
4.2 Study on the viability of *ex vivo* skin explants 164
4.3 Study of the variability of mechanical properties within the same plasty 167
4.4 Comparison of the mechanical properties of skin of different ages 168
4.5 General conclusion on the mechanical properties of *ex vivo* skin explants 173

Chapter 5: Evaluation of the effect of stress on human skin mechanical properties 175

5.1 Study of the mechanical properties of a skin lesion: stretch marks 177

5.1.1 Introduction and literature review on stretch marks 178

5.1.2 Methodology and presentation of the results 180

5.1.3 Conclusion 186

5.2 Effect of freezing on the mechanical properties of human skin 188

5.2.1 Introduction and literature review on the effect of freezing 188

5.2.2 Methodology and presentation of the results 190

5.2.3 Conclusion 193

5.3 Effect of enzymatic stress on the mechanical properties of human skin 194

5.3.1 Introduction and literature review on proteolytic enzymes 194

5.3.2 Methodology and presentation of the results 196

5.3.3 Conclusion 205

5.4 Effect of collagenases, elastases, and inhibitors of these proteolytic enzymes on the mechanical properties of human skin 207

5.5 General conclusion of the effect of stress 213

Conclusions and Prospects 215

Conclusions et Perspectives 223

References 233

APPENDIX 255

Appendix 1: Minor modifications to the device 257

Appendix 2: Latest version of the LabVIEW® interface that enables the operator to carry out mechanical tests with the device 259

Appendix 3: Power supply principle and communication principle of the device 264

Appendix 4: The Cutometer® 266

Appendix 5: Injuries and wound healing 269

Abstracts & Résumés de la thèse 273

Introduction Générale

Suite à l'interdiction des essais sur animaux pour la cosmétique en 2009 [Règlementation CE n°1223/2009], une forte demande pour de nouvelles solutions d'étude sur des modèles de peau *in vitro* et *ex vivo* a vu le jour. Cette interdiction a marqué une nouvelle ère et un besoin d'aller au-delà des connaissances acquises sur les tissus humains, y compris pour les applications médicales. Le projet proposé s'inscrit dans ce contexte avec un besoin marqué des industriels du domaine d'obtenir des données fiables sur les effets des produits cosmétiques et des traitements thérapeutiques. Au-delà de ce besoin, une meilleure compréhension des relations entre les propriétés mécaniques de la peau humaine et sa structure composite est un enjeu afin de disposer de leviers pour prévoir leur variation et ainsi être capable de les prévenir. Cet enjeu scientifique et technique implique la capacité à mesurer ces propriétés dans des conditions qui se rapprochent le plus possible du vivant, à évaluer quantitativement les effets de différents *stress*, et à trouver des moyens de les atténuer.

L'enjeu socio-économique repose sur la mise sur le marché de produits ayant le moins d'impact possible sur la détérioration des tissus cutanés, et dans le développement de solutions pour contrer les effets néfastes des divers *stress* sur la peau.

La peau est l'enveloppe du corps humain, c'est la première barrière protectrice de notre organisme. Le terme *exposome* décrit un concept lié à l'ensemble des expositions environnementales externes et internes auxquelles un individu est soumis de sa conception à sa mort (concept qui exclut les facteurs génétiques) [Krutmann *et al.*, 2017]. L'*exposome* de la peau n'a cependant jusqu'à présent pas reçu une attention adéquate.

En effet, la peau humaine est sujet à une exposition, tout au long de la vie, à une grande variété de facteurs. Ces derniers agissent non seulement sur le vieillissement de la peau mais aussi sur le développement de pathologies. Si le rôle de la peau vis-à-vis de « l'intrusion » de substances néfastes pour la santé est plutôt bien connu et étudié, afin de maitriser, notamment, la diffusion de substances à l'intérieur du corps, il n'en est pas de même du rôle des propriétés mécaniques globales de la peau.

Les propriétés mécaniques d'un tel matériau hautement déformable renvoient à ce que les physiciens appellent ses propriétés viscoélastiques. Selon la littérature, celles-ci semblent varier en fonction du type de contrainte et de ses paramètres. Les propriétés viscoélastiques de la peau humaine jouent un rôle clé dans son intégrité, car elles confèrent au tissu cutané sa capacité à rester intact. Les dommages cutanés, tels que les vergetures, les rides et les blessures comme les escarres, sont soit le résultat de déformations très importantes entraînant des dommages irréversibles, soit dus au vieillissement naturel aboutissant à une capacité moindre de la peau à se déformer de façon réversible. L'ensemble de ces comportements est lié aux propriétés mécaniques qui sont pilotées par ailleurs par la structure composite de la peau. Ce sont différentes couches superposées qui vont assurer un ensemble de propriétés à ce tissu, chacune ayant des propriétés et fonctions dédiées. Des efforts importants sont faits pour pallier à l'ensemble des effets néfastes du vieillissement ou de fortes contraintes sur la peau. Paradoxalement, peu de techniques instrumentales semblent exister pour suivre le comportement mécanique de la peau, même si certains dispositifs sont référencés dans ce domaine.

La mesure des propriétés mécaniques de la peau présente en général un triple intérêt [Ossant *et al.*, 2001] :

i. Obtenir une description de l'histoire naturelle de la peau au fil des ans, en particulier lors des phases de croissance et de vieillissement ;
ii. Disposer d'une méthode d'évaluation objective de l'effet de certains produits médicaux ou cosmétiques ;
iii. Observer et quantifier les pathologies cutanées pouvant entraîner une altération des propriétés mécaniques : collagénoses et hyperkératoses par exemple.

Mesurer les propriétés de la peau humaine s'est longtemps résumé à des mesures en surface. L'apparition de techniques comme l'imagerie médicale a permis des avancées importantes [Tran, 2007], car couplées à une mesure mécanique il est possible de constater les modifications structurales de la peau.
Les techniques de sollicitation de la peau sont de diverses natures comme l'indentation, la traction, la succion, la ballistométrie. L'indentation semble être très prisée et une équipe en France (Laboratoire de Tribologie et Dynamique des Systèmes, Lyon) travaille sur cette technique de manière intensive [Pailler-Mattéi *et al.*, 2012].
Cependant, le plus souvent les expériences sont réalisées *in vivo* avec les erreurs inhérentes à une mesure directe sur un lieu du corps mal défini pour une expérience de mécanique et à la variabilité biologique due à la statistique sur un nombre limité d'individus. Ces tests *in vivo* sont donc réalistes car pratiqués directement sur le corps humain vivant, mais sont complexes à mettre en place sur le plan expérimental et ne permettent pas de réaliser des mesures invasives et destructrices. Au contraire, les mesures *ex vivo* permettent d'explorer de nombreux paramètres mécaniques tout en isolant la peau afin de ne caractériser que cet organe. De plus, les conditions *ex vivo* permettent d'obtenir des échantillons qui peuvent être modifiés ou attaqués avec de fortes contraintes : chimiques, biologiques, mécaniques. Il est évident que chacune de ces approches présentera des points positifs et négatifs pour une interprétation appropriée.

Dans ce contexte, un instrument spécifique pour évaluer les propriétés viscoélastiques de la peau humaine *ex vivo* a été développé. Ce travail de thèse est basé sur une technologie originale [Derail *et al.*, 2022]. Ce travail a bénéficié de différents soutiens financiers avec la pré-maturation et les *phd talents* du projet I-SITE E2S (label national d'excellence pour le projet « Solutions pour l'Energie et l'Environnement »), et le projet de maturation d'Aquitaine Science Transfert.
Cette nouvelle instrumentation permet de caractériser le comportement classique en traction ainsi que les deux composantes mécaniques de la peau, l'élasticité et la dissipation, à différentes fréquences afin de discriminer chaque phénomène. Une vision nouvelle sera apportée en mesurant les propriétés viscoélastiques globales et notamment en tenant compte des paramètres de dissipation, peu explorés par ailleurs. Ceci nous permettra une analyse énergétique qui n'existe pas dans la littérature. L'approche proposée est de réaliser des analyses spectromécaniques pour finalement établir un lien phénoménologique avec la structure de la peau, dans le même esprit que pour les matériaux polymères.

L'enjeu est donc de suivre ces paramètres mécaniques sur une peau humaine *ex vivo*, maintenue vivante comme une peau *in vivo* durant plus de sept jours par une « alimentation » au contact d'un milieu nutritif dédié (collaboration avec le laboratoire Eurofins BIO-EC).

Le projet repose sur le développement de cette instrumentation innovante pouvant mesurer différents paramètres mécaniques, et sur le suivi de leurs évolutions en fonction de divers traitements et *stress* subis par la peau dans ces conditions physiologiques pendant plusieurs jours.

Cette nouvelle instrumentation pourrait avoir un impact dans les domaines scientifique et médical. Elle permet d'avoir une meilleure connaissance du comportement mécanique de la peau humaine et de suivre de manière objective l'évolution des propriétés mécaniques de celle-ci au cours d'un traitement médical par exemple.

Le projet de thèse repose en premier lieu sur la consolidation de cet outil original existant, et sur la proposition d'une approche basée sur des échantillons de peaux *ex vivo* maintenus en conditions physiologiques durant plus de sept jours. La finalité de ce développement instrumental est de démontrer la robustesse et la fiabilité de cette instrumentation innovante.

Le second objectif est de caractériser les propriétés mécaniques de la peau en identifiant plus précisément ses propriétés d'élasticité et de dissipation.

Le troisième objectif est d'évaluer l'évolution de ces propriétés mécaniques en fonction de différentes contraintes (agressions extérieures ou produits cosmétiques). L'objet de ce travail consiste à mettre en évidence les mécanismes de dégénérescence de la peau humaine sur son élasticité en fonction de ces divers *stress*. Ces évolutions de propriétés mécaniques seront analysées en lien avec la structure de la peau. L'outil original développé lors de cette thèse sera utilisé pour caractériser et étudier les effets combinés de facteurs de *stress* sur les propriétés mécaniques de la peau et de suivre l'adaptation du tissu à ces *stress*.

L'objectif final est de réaliser des études sur l'effet de *stress* sur la peau dans le but de montrer que cette instrumentation peut contribuer à aider au développement de produits destinés aux traitements. Afin de répondre à l'enjeu de la mesure de l'efficacité d'un traitement *ex vivo*, l'objectif, qui est en lien avec l'univers médical et cosmétique, est de pouvoir analyser et évaluer de manière objective sur les propriétés viscoélastiques de la peau humaine, (i) les effets de différentes agressions extérieures (vergetures, exposition aux rayons UV, pollution par un produit chimique ou par l'atmosphère, incision, etc.), et (ii) les effets de produits médicaux ou dermo-cosmétiques (crèmes hydratantes, crèmes anti-vergetures, pansements cicatrisants, etc.).

Ce manuscrit de thèse se compose de cinq chapitres :

Le premier chapitre est consacré à un travail de recherches bibliographiques qui a été réalisé afin de connaitre la littérature scientifique du domaine. Afin de connaitre au mieux notre « matériau » peau, une large étude générale sur la physiologie de la peau humaine est réalisée. Les fonctions de cet organe essentiel à l'Homme ainsi que ses possibles altérations sont ensuite analysées. Une attention particulière est prise concernant le thème principal de cette thèse : les propriétés mécaniques de la peau. Une revue des différentes techniques de caractérisation de la peau humaine ainsi que des modélisations de son comportement mécanique sont enfin réalisée.

Dans le deuxième chapitre, le développement continu de cette nouvelle instrumentation innovante pour caractériser les propriétés mécaniques de la peau humaine est décrit. Ce travail de développement fut important car la pertinence de la thèse, en termes de débouchés et d'applications, repose sur la performance et la fiabilité de l'instrumentation. Cette partie permet de montrer l'amélioration et l'évolution continue de l'instrument et des méthodes de mesures tout au long de la thèse. Les éléments forts du travail instrumental et de l'évolution du dispositif sont présentés. L'instrumentation finale proposée permet donc de mesurer, de façon fiable et précise, les propriétés mécaniques de tissus mous comme la peau humaine.

Le troisième chapitre porte sur les premiers tests effectués sur des explants de peau humaine *ex vivo* du laboratoire Eurofins BIO-EC. Ces premiers tests sur la peau humaine *ex vivo* permettent dans un premier temps de confronter et d'adapter notre instrumentation à l'étude d'échantillons biologiques. Ensuite, ces études préliminaires permettent de valider la fiabilité de l'instrumentation développée ainsi que les protocoles de tests, les essais mécaniques et les méthodes de mesures. Les notions de pré-conditionnement, d'état de pré-tension cutané et d'anisotropie mécaniques sont, entre autres, analysées dans cette partie.

Le quatrième chapitre se consacre à la caractérisation expérimentale des propriétés mécaniques d'explants de peau humaine *ex vivo* sans *stress*. Il s'agit donc d'explorer les propriétés rhéologiques globales de la peau. L'ensemble des résultats issus de cette nouvelle instrumentation sont présentés, analysés et interprétés en vue de mettre en évidence les paramètres les plus pertinents à mesurer qui permettront de relever les effets d'un *stress* sur la viscoélasticité de la peau. Les tests réalisés dans cette partie permettent également d'étudier la viabilité des explants dans le temps et la notion de vieillissement cutané.

Enfin, le cinquième chapitre est dédié aux caractérisations expérimentales des propriétés mécaniques d'explants de peau humaine *ex vivo* sous *stress*. En effet, cette nouvelle instrumentation, associée à l'utilisation d'explants de peau *ex vivo* dans des conditions physiologiques pendant plusieurs jours, permet finalement d'évaluer l'effet de différentes contraintes sur les propriétés mécaniques de la peau. La variation des propriétés mécaniques de la peau et l'adaptation du tissu sont corrélées à une exposition à différents *stress*.
Une caractérisation complète de zones de peaux endommagées telles que les vergetures est réalisée. Dans un second temps, l'effet de contraintes sur la viscoélasticité de la peau est étudié. La congélation des explants, processus utilisé pour conserver les tissus dans le temps, ainsi que la mise en contact de la peau avec des enzymes protéolytiques (collagénase et élastase), imitant un processus naturel de vieillissement accéléré du tissu, sont les deux *stress* étudiés.

Une conclusion générale ainsi que les perspectives de ce travail de thèse complètent et finalisent ce manuscrit. Plusieurs conclusions sont émises : sur la partie instrumentale de la thèse qui est liée au développement de l'instrumentation, sur l'avancée scientifique du travail de thèse ainsi que sur l'avancement du projet Mécapeau. Les perspectives d'évolution de l'instrumentation et les perspectives du projet global sont finalement détaillées.

Les différents travaux menés lors de cette thèse permettent de montrer que cette nouvelle instrumentation peut contribuer à répondre à des questions scientifiques et techniques et peut aider au développement de produits destinés aux traitements.

General Introduction

Following the ban on animal testing for cosmetics in 2009 [Regulations CE n°1223/2009], there has been a strong demand for new study solutions using *in vitro* and *ex vivo* skin models. This ban marked a new era and a need to go beyond the knowledge acquired on human tissues, including for medical applications. The proposed project falls within this context, with a marked need for actors in the field to obtain reliable data on the effects of cosmetic products and therapeutic treatments. Beyond this need, a better understanding of the relationship between the mechanical properties of human skin and its composite structure is essential in order to have the levers to predict their variation and thus be able to prevent them. This scientific and technical challenge involves the ability to measure these properties under conditions that are as close as possible to physiological conditions, to quantitatively assess the effects of different stresses, and to find ways of mitigation.

The socio-economic challenge is to market products that have as little impact as possible on the deterioration of the skin tissue, and to develop solutions to counter the harmful effects of various stresses on the skin.

The skin is the envelope of the human body and is our body's first protective barrier. The term "exposome" describes a concept linked to the totality of external and internal environmental exposures to which an individual is subjected from cradle to grave (concept that excludes genetic factors) [Krutmann *et al.*, 2017]. However, the skin exposome has not received adequate attention to date.

The human skin is subject to exposure to a wide variety of factors throughout life. These factors have an impact not only on the ageing of the skin, but also on the development of pathologies. While the skin's role in preventing the 'intrusion' of substances that are harmful to health is well known and studied, in particular to control the spread of substances within the body, the same cannot be written about the global mechanical properties of the skin.

The mechanical properties of such a highly deformable material refer to what physicists call its viscoelastic properties. According to the literature, these seem to vary depending on the type of stress and its intrinsic parameters. The viscoelastic properties of human skin play a key role in its integrity, as they give skin tissue its ability to remain intact. Skin damage, such as stretch marks, wrinkles, and wounds like bedsores, are either the result of very large deformations leading to irreversible damages, or due to natural ageing leading to a reduced capacity of the skin to deform reversibly. All of these behaviours are linked to the mechanical properties, which are also controlled by the composite structure of the skin. The various superimposed layers provide a range of properties for this tissue, each with its own dedicated properties and functions. Major efforts are being made to mitigate all the harmful effects of ageing or of severe stress on the skin. Paradoxically, few instrumental techniques exist to monitor the mechanical behaviour of the skin even if some devices are references in this domain.

Measuring the mechanical properties of the skin is generally of threefold interest [Ossant *et al.*, 2001]:

iv. To obtain a description of the natural history of the skin over the years, in particular during the growth and ageing phases;
v. To provide a method for objectively assessing the effect of some medical or cosmetic products;
vi. To observe and quantify skin pathologies that can lead to an alteration of the tissue mechanical properties, such as collagenosis and hyperkeratosis.

For a long time, measuring the properties of human skin was limited to surface measurements. The emergence of techniques such as medical imaging has led to major advances [Tran, 2007], because coupled with mechanical measurement it is possible to observe structural changes in the skin.
Various techniques are used to test the skin, including indentation, traction, suction and ballistometry. Indentation seems to be very popular and a team in France (Laboratoire de Tribologie et Dynamique des Systèmes, Lyon) is working intensively on this technique [Pailler-Mattéi *et al.*, 2012].

However, experiments are usually carried out *in vivo*, with the inherent errors of direct measurement on a poorly defined part of the body for a mechanical experiment and biological variability due to statistics on a limited number of individuals. These *in vivo* tests are therefore realistic because they are carried out directly on the living human body, but they are complex to set up experimentally and do not allow invasive and destructive measurements to be made. *Ex vivo* measurements, on the other hand, allow many mechanical parameters to be explored while isolating the skin in order to characterise only this tissue. In addition, *ex vivo* conditions enable to obtain samples that can be modified or attacked under severe chemical, biological and mechanical stress. It is obvious that each of these approaches will present positive and negative outcomes for appropriate interpretation.

In this context, a specific instrument for evaluating the viscoelastic properties of human skin *ex vivo* has been developed. This thesis work is based on an original equipment [Derail *et al.*, 2022]. This work has benefited from different financial supports with pre-maturation and *phd talents* of E2S I-SITE project (national label of excellence for the "Energy Environment Solutions" project), and maturation project of *Aquitaine Science Transfert.*
This new device makes it possible to characterise classical traction behaviour as well as the two mechanical components of the skin, elasticity and dissipation, at different frequencies in order to discriminate each phenomenon. A new vision will be provided by measuring the overall viscoelastic properties and in particular by taking into account the dissipation parameters, which have been little explored otherwise. This will enable us to carry out an energy analysis that was not reported so far in the literature. The proposed approach is to carry out spectromechanical analyses in order to establish a phenomenological link between the mechanical properties and the structure of the skin, with the same approach as for polymer materials.

The challenge is therefore to monitor these mechanical parameters on *ex vivo* human skin, kept alive in physiological-like *in vivo* skin for more than seven days by "feeding" in contact with a dedicated nutrient medium (collaboration with the Eurofins BIO-EC laboratory). The project is based on the development of this innovative instrumentation capable of measuring various mechanical

parameters, and on monitoring their changes as a function of different treatments and stresses undergone by the skin in these physiological conditions over several days.

This new instrumentation shall have an impact in the scientific and medical fields. It will provide a deeper understanding of the mechanical behaviour of human skin and enable to objectively monitor the evolution of the skin's mechanical properties during medical treatment, for example.

The thesis project is primarily based on the consolidation of this original existing tool, and on the proposal of an approach based on *ex vivo* skin samples maintained in physiological conditions for more than seven days. The aim of this instrumental development is to demonstrate the robustness and reliability of this innovative device.

The second objective is to characterise the mechanical properties of the skin by identifying more precisely its elasticity and dissipation properties.

The third objective is to evaluate the evolution of these mechanical properties as a function of different stresses (external aggressions or cosmetic products). The aim of this work is to highlight the degenerative mechanisms affecting the elasticity of human skin as a function of these various stresses. These changes in mechanical properties will be analysed in relation to the structure of the skin. The original tool developed during this thesis will be used to characterise and study the combined effects of stress factors on the mechanical properties of the skin and to monitor the adaptation of the tissue to these stresses.

The final objective is to carry out studies on the effect of stress on the skin with the aim of showing that this instrumentation can help in the development of products intended for cures. In order to meet the challenge of measuring the effectiveness of an *ex vivo* treatment, the objective, which is linked to the medical and cosmetic fields, is to be able to analyse and evaluate objectively the viscoelastic properties of human skin, (i) the effects of various external aggressions (stretch marks, exposure to UV rays, chemical or atmospheric pollution, injuries, etc.), and (ii) the effects of medical or dermo-cosmetic products (moisturising creams, anti-stretch mark creams, healing dressings, etc.).

This thesis manuscript is composed of five chapters:

The first chapter is devoted to a bibliographical research work which was carried out in order to identify the existing scientific literature in the field of the thesis. In order to better understand our skin "material", a broad general study of the physiology of human skin is carried out. The functions of this organ, which is essential to humans, and its possible alterations are then analysed. Particular attention is paid to the main theme of this thesis: the mechanical properties of the skin. Finally, a review of the various techniques for characterising human skin and modelling its mechanical behaviour is carried out.

The second chapter describes the ongoing development of this innovative new equipment for characterising the mechanical properties of human skin. This development work was essential because the relevance of the thesis, in terms of opportunities and applications, is based on the performance and reliability of the instrumentation. This section shows the continuous improvement and development of the instrument and measurement methods throughout the thesis. The key elements of the instrumental work and the evolution of the device are presented. The proposed instrumentation will therefore enable the mechanical properties of soft tissues such as human skin to be measured reliably and accurately.

The third chapter focuses on the first tests carried out on *ex vivo* human skin explants from the Eurofins BIO-EC laboratory. These initial tests on *ex vivo* human skin firstly enable us to compare and adapt our instrumentation to the study of biological samples. These preliminary studies are then used to validate the reliability of the instrumentation developed, as well as the test protocols, mechanical tests and measurement methods used. The concepts of pre-conditioning, skin pre-tension state and mechanical anisotropy are analysed in this section, among others.

The fourth chapter is devoted to the experimental characterisation of the mechanical properties of human skin explants *ex vivo* without stress. The aim is to explore the overall rheological properties of the skin. All the results from this new instrumentation are presented, analysed, and interpreted in order to highlight the most relevant parameters to be measured, which will enable to identify the effects of stress on the viscoelasticity of the skin. The tests carried out in this section also enable to study the viability of the explants over time and the notion of skin ageing.

Finally, the fifth chapter is devoted to experimental characterisation of the mechanical properties of *ex vivo* human skin explants under stress. This new device, combined with the use of *ex vivo* skin explants under physiological conditions for several days, enables to assess the effect of different stresses on the mechanical properties of the skin. The variation in the mechanical properties of the skin and the adaptation of the tissue are correlated with exposure to different stresses.
A complete characterisation of damaged areas of skin such as stretch marks is carried out. Secondly, the effect of stress on skin viscoelasticity is studied. The freezing of explants, a process used to preserve tissue over time, and the exposure of skin to proteolytic enzymes (collagenase and elastase), mimicking a natural process of accelerated tissue ageing, are the two stresses studied.

A general conclusion and the prospects for this thesis work complete and finalise this manuscript. Several conclusions are drawn: on the instrumental part of the thesis, which is linked to the development of the equipment, on the scientific progress of the thesis work and on the progress of the Mécapeau project. Finally, the prospects for the development of the device and the overall project are detailed.

The work carried out during this thesis show that this new instrumentation can contribute to answering scientific and technical questions and can help in the development of products for treatments.

Chapter 1.

State of the art

The skin, also known as the integument (from the Latin *tegumentum*, covering), is the envelope of the human body. This organ forms an interface between the outside and the inside of the body. It is the first protective barrier of our organism against mechanical, biological, and chemical aggressions for example.

The skin is the heaviest and most extensive organ in our body. In adults, the skin tissue covers an area of about 1.75 -2 m^2 [Marino, 2001]. The combination between epidermis and dermis weights 3.5 - 4 kg, representing about 5.5% of the total body mass [Edwards *et al.*, 1995]. The thickness of the skin, again limited to the epidermis and dermis, is 2 mm on average, but varies from 0.5 mm at the eyelids (thin skin) to 4 mm at the palms and soles (thick skin) [Della Volpe *et al.*, 2012]. Finally, the skin is made of approximately 70% of water.

According to Wilson [Wilson, 1992], the first anatomical study of this organ dates back to 1698 with the work of the surgeon Cowper [Cowper, 1698]. The skin, observed with the aid of an optical microscope, was then described not as a homogeneous structure but as a stack of several layers that could vary in thickness depending on the area of the body. Subsequently, the work of the French Dupuytren [Dupuytren, 1834] and the Austrian Langer [Langer, 1861a,b,c,d] showed that in addition to being heterogeneous, the skin is subject to a non-uniform natural tension. Indeed, a circular incision made on the integument changes its shape to become elliptical. The work of Cowper, Dupuytren and Langer alone shows the complexity of the skin: heterogeneous, multilayered, and prestressed. Subsequent studies have continued to confirm this complexity.

The skin is anatomically made up of three tissue layers (Figure 1.1) which are, starting from the surface: the epidermis, the dermis, and the hypodermis.

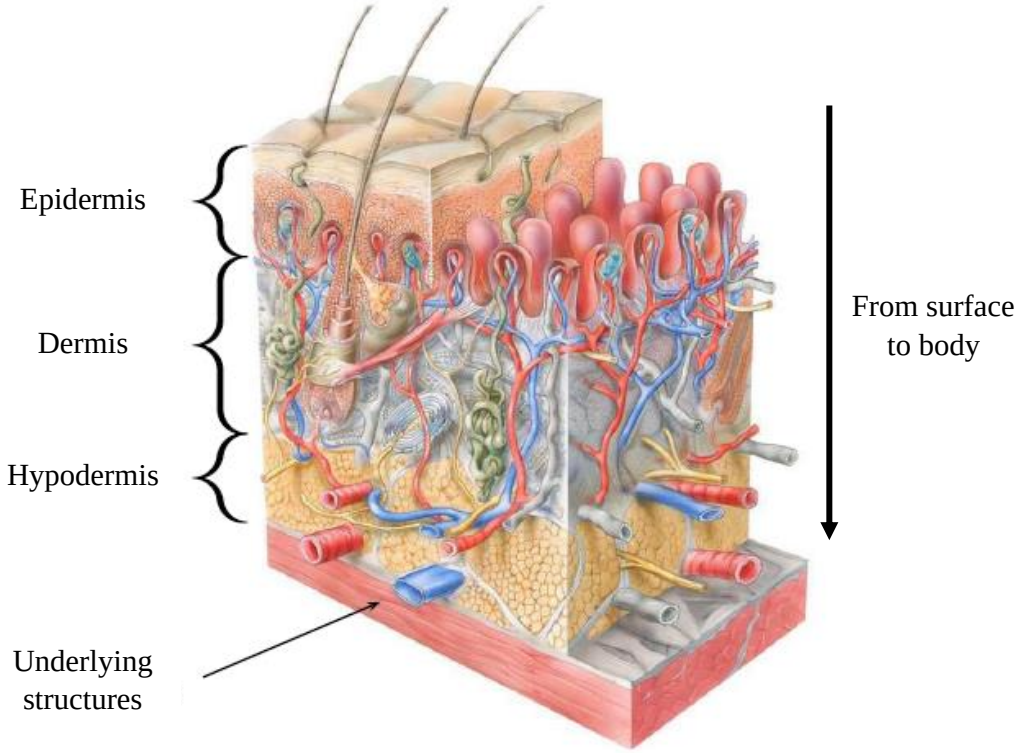

Figure 1.1: Cross-section of human skin – [Boyer, 2010]

1.1 Human skin anatomy

The structure of the human skin is known for its complexity due to the fact that each layer represents a system that is itself made up of several parts [McGrath *et al.*, 2010]. In addition, the skin contains a multitude of other cells and elements such as the vascularisation system, the innervation system, the immune system, and the cutaneous appendages.

1.1.1 Skin tissue structure

The skin is a complex organ composed of several superimposed layers. It owes its suppleness and resistance to the different tissue layers that make it up: the outermost tissue is the epidermis (from the Greek "*epi*", above, and "*derma*", skin), the intermediate tissue is the dermis and the deepest tissue is the hypodermis (from the Greek "*hypo*", below).

These tissue layers have different thicknesses and each has a structure and composition that gives it specific functions. The epidermis has an average thickness of 0.1 mm, the dermis is 1 mm thick and the hypodermis varies greatly in thickness, depending on the area of the body, from 1 mm to 20 mm.

Each of these layers and the skin appendages are described below.

1.1.1.A The epidermis

The epidermis is the superficial layer of the skin. Its thickness can range from 0.05 mm on the eyelids to more than 1.5 mm on the soles of the feet and palms. It is a stratified, keratinised, and squamous, covering the epithelium[1]. The epidermis is made up of layers of cells, called keratinocytes, stacked one on top of the other, which are bathed in a nutritive liquid, the cellular lymph, necessary for the metabolism of the cells. Its construction mechanism is very particular as it is constantly renewed. The outermost cells are worn out by contact with the environment and are quickly abandoned. This loss, called desquamation (9 to 17 mg/day), is usually invisible; it becomes so, for example, during sunburn. The epidermis is neither vascularised nor innervated, and nutrients reach it from the dermis and penetrate by diffusion.

The stratified nature of the epidermis is due to the superposition of several layers which are, from the inside to the outside: the basal layer, the spinous layer, the granular layer, the clear layer and the horny layer or *stratum corneum* (Figure 1.2).

[1] **Stratified, keratinised and squamous epithelium:** tissue, formed of juxtaposed keratin-loaded cells, which covers the surface of the body. It is a multi-layered tissue with flattened surface cells.

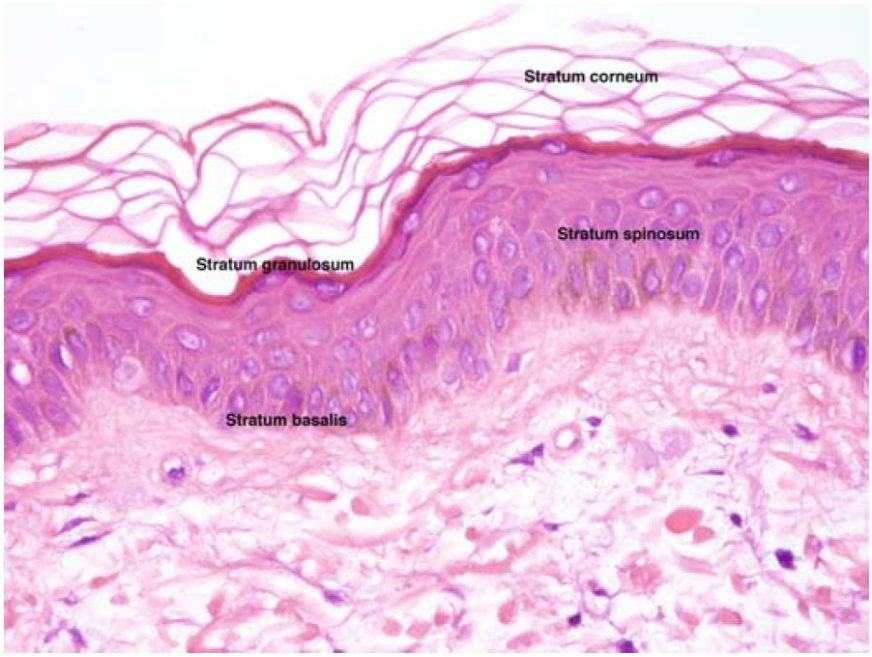

Figure 1.2: Overview of the epidermis (without the clear layer) – [Hiatt et al., 2009]

i) *The different cells of the epidermis*

All cells originate from the deepest layer of the epidermis, called the basal or germinal layer. The epidermis contains four different types of cells:

+ Keratinocytes:

These are the main cells of the epidermis, representing more than 80% of the cells contained in this part of the skin. These are the cells that give birth to the most superficial part of the epidermis, i.e. the horny layer. In fact, keratinocytes mutate and evolve into corneocytes, leading to the formation of horny cells in successive stages. This is the cellular differentiation of keratinocytes, known as keratinisation.

Keratinisation is a continuous process from the stem cells, throughout cell maturation, from the depth to the surface. The formed corneocytes (or corneal cells) are flat, keratinised and anucleate squamous cells. Every day we shed the layers formed by these cells, which is known as desquamation. Their production accelerates in the areas most subject to friction (hands, feet).

Keratinocytes migrate from the basal layer to the skin surface producing keratin, a very resistant fibrous protein with an α-helical structure[2]. Keratins play an important cyto-architectural role; indeed, these cytoskeletal proteins form a filamentous network that ensures the cohesion of cellular junctions in the epidermis [Bousquet *et al.*, 2002].

[2] **α-helical structure:** secondary structure of a protein (α-helix). It is formed by the regular winding on itself of the helical-shaped polypeptide chain which allows the formation of hydrogen bonds between its amino acids.

+ Melanocytes:

Melanocytes are the cells responsible for the pigmentation of the skin and hair, their function is to produce melanin. They represent about 13% of the cell population of the epidermis. The melanocytes are not homogeneously distributed and are located in the basal layer of the epidermis, between the keratinocytes. These cells are larger than the keratinocytes because they contain numerous extensions, dendrites, which can reach the granular layer (Figure 1.3). Their density is on average 2000 $.mm^{-2}$ and decreases with age.

The melanocytes therefore produce melanin, a brown-black pigment which gives the skin its colouring. The production and distribution of melanin grains in the epidermis is called melanogenesis and is carried out via melanosomes. These grains, containing melanin, are transferred to neighbouring keratinocytes by dendrites. The main role of melanin is to provide photoprotection against the sun (note that the epidermis thickens under the influence of solar radiation). It acts as a filter that diffracts and reflects the incident rays, protecting the genetic material of the cell. In addition to pigmenting the skin, melanocytes have a photoprotective function that allows them to absorb non-reflected rays such as ultraviolet (UV) light.

Skin colour, which varies between ethnic groups, is expressed mainly at the level of melanosomes [Flagothier *et al.*, 2005]. Racial differences in pigmentation are not based on the number of melanocytes, but on whether or not melanosomes disintegrate during the migration of keratinocytes to the surface.

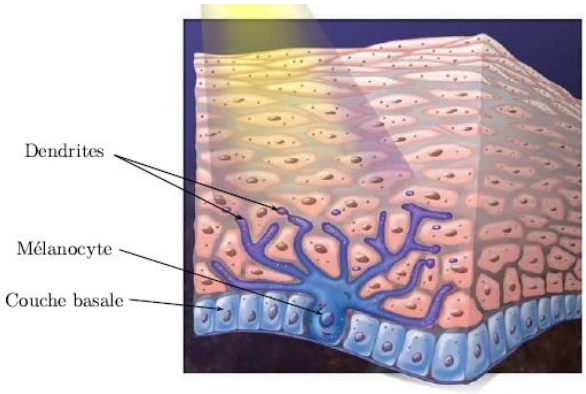

Figure 1.3: Melanocyte – [Boyer, 2010]

+ Langerhans cells:

These are immune system cells, formed by dozens of dendrites, distributed in the epidermis with a population varying between 2 and 5%. These cells originate and renew themselves from the bone marrow and are transported through the blood to the epidermis. They are able to detect and to ingest foreign particles that may have passed through the skin barrier, such as antigens, and then 'inform' the immune system. They are able to phagocytose foreign particles, but less efficiently than macrophages. The main function of these cells is therefore the immunisation of the skin against antigens applied to it. Their density is on average 700 $.mm^{-2}$ and decreases with age and UV radiation.

+ Merkel cells:

Merkel cells are the fourth cell population of the epidermis. These cells, which have a flattened shape, ensure the function of tactile sensitivity. They are mechanoreceptor cells which play a sensory role. They register the vibrations perceived by the skin and transmit them to the nerve endings. They are irregularly distributed on the surface of the human body and are located in the basal layer of the epidermis. They are particularly abundant on the lips, palms of the hands, fingertips and soles of the feet.

ii) The five layers of the epidermis

As we have already mentioned, the epidermis is divided into five layers (Figure 1.2) which are, from the inside out:

+ The basal layer (or germinal layer). This is the deepest layer and is in contact with the dermis. This is where all the cells of the epidermis are formed, from skin stem cells. It is a layer composed of a single row of cylindrical cells, called germinal cells, implanted perpendicularly on the papillae of the dermis[3]. It ensures the continuous regeneration of the skin by cell division: the cells produced gradually migrate to the upper layers by undergoing various mutations. One of the two daughter cells remains in place to divide again, while the other detaches from the mother cell and begins its vertical migration, pushing the previous one towards the upper layer. The body of the cells, the cytoplasm, extends outside the cells and is equipped with desmosomes, strong attachments that hold the cells together. Between these basal cells are inserted the melanocytes, responsible for melanogenesis.
Implanted along the dermal papillae, the germinative layer is undulated, allowing an increase in the exchange surface between the epidermis and the dermis.

+ The spinous layer (or mucous layer or *stratum spinosum*). The keratinocytes which make up this layer are voluminous and polygonal in shape. They gradually flatten out as they migrate towards the surface. These cells are superimposed in 3 to 10 layers. The spinous layer contains melanin-rich cells dispersed in the keratinocytes. As with the basal layer, numerous cytoplasmic extensions can be seen at the periphery of the cell, which are attached to the extensions of neighbouring cells by means of desmosomes, thus ensuring a high degree of cohesion of the whole.

+ The granular layer (*stratum granulosum*). This layer consists of 3 to 5 layers of flattened keratinocytes. This is where the keratinisation of the keratinocytes (which evolve into corneocytes) begins. The cell structure is profoundly modified: the cytoplasmic organs become rarefied, the plasma membrane thickens and the bundles of tonofibrils, precursors of keratin, clump together.

+ The clear layer (*stratum lucidum*). This layer of the epidermis only appears in thick areas of the skin. It contains several layers of flat, light-coloured cells of uniform appearance. This layer corresponds to a transition phase between the granular layer and the *stratum corneum*.

+ The stratum corneum. This is the outermost layer of the epidermis. It is composed of 15 to 20 layers of cells depending on the area of the skin. The cells are anucleate and very flat: 26 to 45 µm

[3] **Dermal papillae:** small protuberances in the dermis that dip into the epidermis.

in diameter and 0.3 to 0.7 µm thick. The cells are completely keratinised: they are corneocytes, dead cells (the nucleus and cytoplasmic organs have completely disappeared and the cell is filled with keratin) that are glued together with lipid cement. This is the result of the final phase of mutation of the keratinocytes which gradually rise from the basal layer. The *stratum corneum* is often compared to a "brick and mortar" structure, with the corneocytes in the role of bricks and an intercellular cement formed of lipids in the role of mortar. The composition of the *stratum corneum* also varies depending on the location on the body [Brancaleon *et al.*, 2001]. The thickness of the *stratum corneum* varies from 15 to 20 µm. This layer protects the body against external aggressions and represents a barrier preventing the entry of external elements such as microbes and dust into our body. It is constantly being renewed through spontaneous desquamation. The cells of the *stratum corneum* are gradually shed by rubbing and cleaning, leaving room for new cells.

iii) The skin film and surface flora

The surface of the skin is not in direct contact with the outside, a continuous film covers this surface. This film is made up of several elements including:

+ The products of keratinisation: keratin from desquamating horny cells and lipids that form the inter-cellular cement.

+ A hydrolipidic film, formed by an emulsion of water and fat. The quantity and composition of this film vary according to the parts of the body, sex, and age, but also according to exogenous (air humidity, season) and endogenous (stress, illness) factors. It is mainly composed of a water-soluble fraction made up of water, water-soluble elements and organic substances, as well as a fat-soluble fraction made up of sebum and residues of substances from the keratinisation process. This film forms a protective "acid mantle" (pH between 4.6 and 6.1) which limits the multiplication of foreign germs, controls the proliferation of the resident flora and prevents the penetration of foreign substances. In addition to being a protective barrier, it also avoids excessive moistening or drying, thus allowing the epidermis to remain supple.

+ The cutaneous microbiota (or cutaneous flora), is a population of micro-organisms (bacteria, mites, micro-fungi), specialised or opportunistic, saprobionts[4], often symbionts and sometimes pathogenic. The skin's hydrolipidic film is colonised by this microbial flora which is essential for its protection and our immune system. In general, bacterial biodiversity limits the risk of colonisation of the skin by pathogenic bacteria and provides protection against skin inflammation; it is essential to the individual's good health. This flora resides stably on the skin: it is referred to as resident, permanent or commensal bacterial flora. It is composed of non-pathogenic organisms such as Gram-positive germs[5], coagulase-negative *staphylococci*, propionibacteria, etc. However, its composition varies according to climate, individuals, age and region of the body. The density of this flora is variable but remains constant and is rapidly renewed, even after disinfection or daily bathing [Hartmann, 1979]. The skin of an adult hosts on average 1012 bacteria of more than 200 different species. It should be noted that this environment can also be temporarily colonised by other

[4] **Saprobiont micro-organisms:** micro-organisms that live at the expense of decomposing organic matter or are involved in this decomposition.

[5] **Gram-positive germs:** germs that appear purple under the microscope when using the gram staining technique.

potentially pathogenic organisms (enterobacteria, staphylococcus aureus, streptococci), which form a transitory bacterial flora. This micro-ecosystem is organised as a biofilm and feeds on both molecules and compounds excreted by the skin itself, and on compounds secreted by these communities of micro-organisms.

Iv) Summary of the epidermis

The epidermis, which is the top layer of the skin, is the tissue that is in direct contact with the environment and is home to the skin microbiota. It is the most superficial and thinnest part of the skin. Its structure and construction process are particularly complex. It is an epithelial covering tissue, i.e. a tissue made up of closely juxtaposed cells, without the interposition of fibres or ground substance[6].

The outermost surface of the epidermis is covered with hard, dead cells called corneocytes. Over time, they fall off like scales and are replaced by new underlying cells. The average turnover time of the epidermis, necessary for complete cell turnover (time from division to shedding of a keratinocyte), is about 39 days. This time can be affected by various diseases, such as psoriasis.

The structure and cells of the epidermis (Figure 1.4) give it a triple protective role: it is a highly resistant protective barrier against external mechanical and chemical aggression, a barrier against harmful radiation from the sun and an immunological barrier. Its role in the overall mechanical behaviour of the skin is generally neglected compared to the role played by the dermis. However, we will see that its particular topography (see Part 1.2.2) is still largely responsible for the skin's suppleness, which is necessary for body movements.

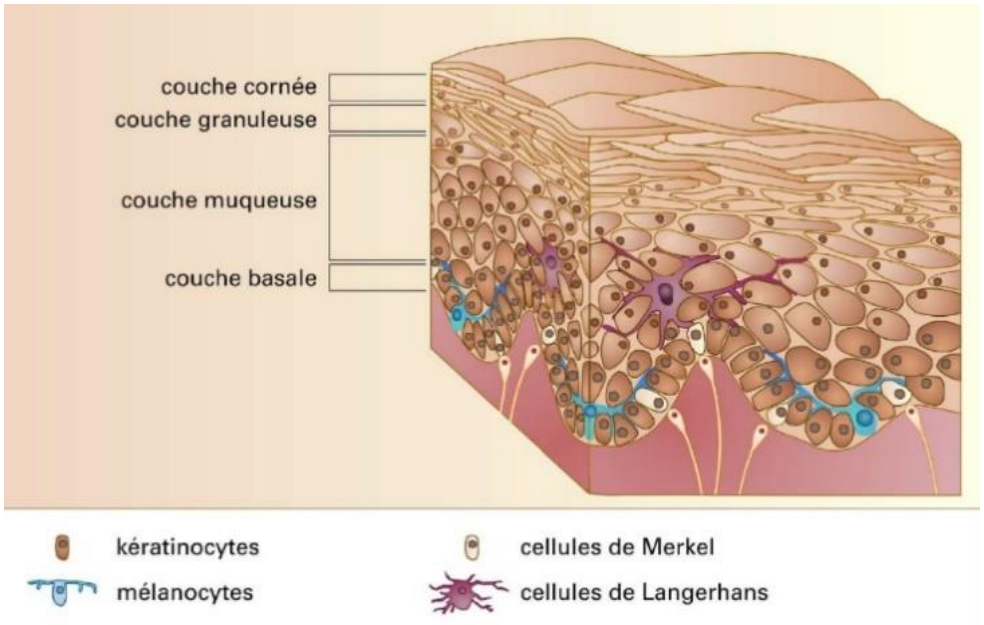

Figure 1.4: Microscopic structure of the epidermis (without the clear layer) – [Dubertret, encyclopédie]

[6] **Ground substance:** amorphous gel-like substance present in the composition of various connective tissues.

1.1.1.B The dermal-epidermal junction

The dermal-epidermal junction (DEJ) is an extra-cellular matrix that separates the epidermis from the dermis and ensures metabolic exchanges between the two layers. The main function of this zone is adhesion, anchoring the epidermis in the dermis, but it also enables the maintenance of a functional epidermis by ensuring its nutrition by the underlying tissues and by promoting its healing.

It is made up of four layers which are, from the epidermis to the dermis:

- The plasma membrane of the basal keratinocytes.
- The *lamina lucida*, containing numerous anchoring filaments composed of laminin, collagen XVII and integrin, among others. They connect the dense lamina to the hemidesmosomes of the keratinocytes of the basal layer of the epidermis.
- The dense lamina (*lamina densa*), composed massively of type IV collagen with a grid architecture which allows great mechanical and physiological stability.
- The fibrillar zone or submembranous space (*sublamina densa*) which contains anchoring fibrils composed of collagen VII and dermal microfibrils.

The dermal papillae induce an undulating shape, visible in Figure 1.5, which allows for a very large exchange surface.

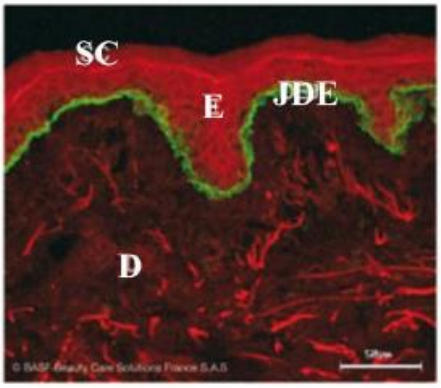

Figure 1.5: Dermal-Epidermal Junction ("Jonction Dermo-Épidermique" (JDE) in French) – [Azzez, 2019]

This part of the skin connecting the first two layers, despite their differences, ensures the mechanical continuity of the skin structure. Indeed, on the epidermis side, the junction allows the anchoring of the keratinocytes; on the dermis side, it is the collagen fibres that anchor there, thus ensuring mechanical continuity.

1.1.1.C The dermis

The dermis is a dense fibrous connective tissue. It is the middle layer of the skin and represents its dominant mass. It is an elastic connective tissue that is considerably thicker than the epidermis. It has properties that ensure the main mechanical structure of the skin. Indeed, this tissue gives the skin its strength, solidity, and elasticity; it is responsible for the skin's resistance and flexibility.

This layer houses the vascular system of the skin, which contains the blood vessels that supply nutrients to the epidermis and the lymphatic vessels. The dermis is also the ground for the skin appendages and contains nerve fibres and sensory receptors for pressure, touch, pain, temperature, and itching.

Its gelatinous structure enables to connect and support the various tissues and organs that make it up. The dermis is made up of a ground substance in which various cells, fibres and structural glycoproteins are embedded (Figure 1.6).

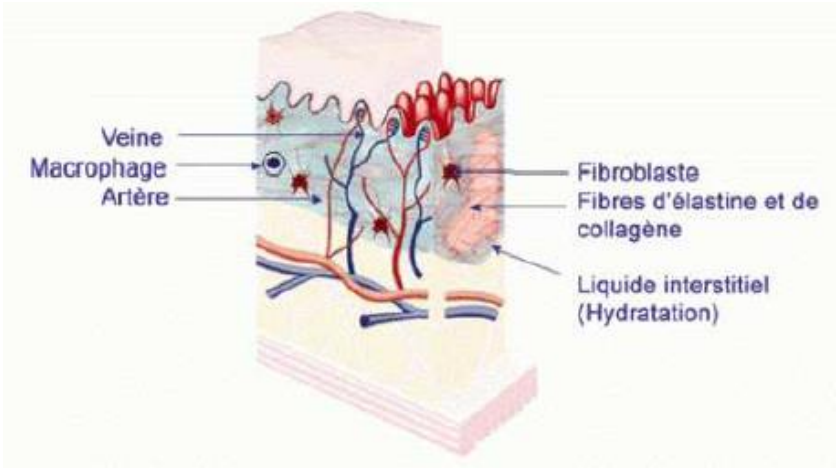

Figure 1.6: Diagram of the dermis – [Azzez, 2019]

i) *The different components of the dermis*

The dermis contains different types of molecules and cells.

+ The extracellular matrix (ECM):

It comprises a variety of elements, of which **proteoglycans** are the most important because of their water retention capacity. These complex proteins represent only about 0.2% of the dry weight of the skin, but their primary function is of the utmost importance: they retain water, up to 1000 times their own volume. These proteoglycans will thus act as a reservoir of moisture and will also absorb proenzymes and precursors of growth factors that will only be activated in the event of a wound and will contribute to the first stages of healing.

These proteoglycans are complex proteins that consist of a "core protein" with one or more glycosaminoglycan (GAG) chains covalently attached (Figure 1.7). GAGs are long-chain amino polysaccharides; the most common in the dermis are hyaluronic acid and dermatan sulphate. GAGs are also charged molecules, which contribute to the retention of water molecules resulting in the formation of a viscous and elastic gel, resistant to mechanical stress. This gel is called ground substance. This allows the metabolic transmission to take place. It is formed by the activity of the fibroblasts, on the one hand, and by the infiltration of blood elements, on the other hand.

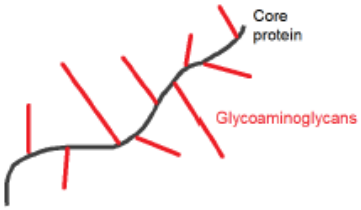

Figure 1.7: Schematic representation of a proteoglycan: a central protein with covalently linked glycosaminoglycan (GAG) chains – [Lynch, 2015]

This matrix also contains fibres, which are the most common proteins in our skin tissue. The dermis contains two types of fibres that give the skin flexibility and elasticity.

On the one hand, **collagen fibres**, which are fibrous macromolecules of glycoprotein nature. The main function of these fibres is to ensure the structural integrity and cohesion of the tissue, in particular owing to their great strength. These fibrous proteins are said to be structural; they are in fibrillar form and give the tissue significant mechanical resistance to stretching. The collagen fibres in the dermis can be of different types: I, III, V, VI, XII, XIV and XVI. It should be noted that collagen is the most abundant protein in the body, with twenty-eight types of collagen identified [Shoulders *et al.*, 2009]. The most abundant type is collagen I, which represents about 80% of the total amount of collagen in the dermis. Collagen I, unlike the other types of collagen (with the exception of collagen III), forms long and wide fibres, arranged in a tight network. These collagen fibres represent about 70% of the volume of the dermis or 75% of the dry weight of the skin [Silver *et al.*, 2001].

On the other hand, **elastin fibres** are non-glycolysed, very hydrophobic, and very long proteins. Elastin is a protein that forms small fibres, much finer than collagen fibres, as shown in Figure 1.8. As presented later in Part 1.3.1, elastin fibres have, to a lesser extent than collagen fibres, a high level of chemical and physical resistance. Elastin forms elastic fibres and is often presented as providing elasticity to the skin [Gahagnon, 2009]; [Ventre *et al.*, 2009]. These elastin fibres are wrapped around collagen fibres, forming a three-dimensional network of fibres in the dermis. These fibres represent only about 4% of the dry weight of the skin.

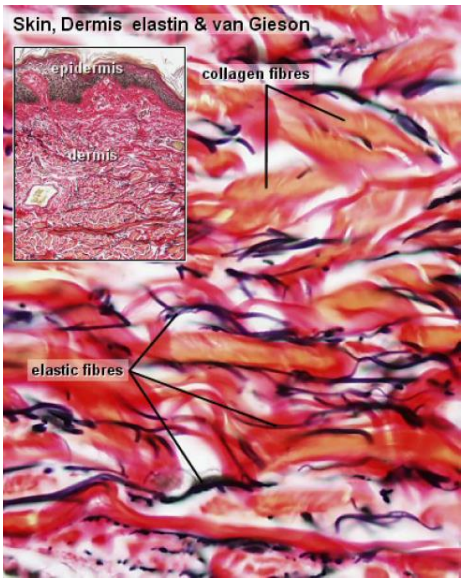

Figure 1.8: Histological section of skin (cross section) stained with van Gieson's stain. Van Gieson's stain colours the collagen pink and the elastic fibres purple – [Lynch, 2015]

Scott [Scott, 1991, 2003] and Hulmes [Hulmes, 2002] have demonstrated that there is a structure in the extracellular matrix. Indeed, the proteoglycans that form the ground substance attach to collagen fibres at regular intervals, and run perpendicularly from one fibre to the next. Proteoglycans are therefore important structural components of the dermis, contributing to the transmission of stress and maintenance of the overall network [Cribb *et al.* 1995].

The extracellular matrix also contains other proteoglycans such as tenascin and fibronectins which play a very important role in wound healing and skin regeneration after injury.

All these macromolecules are arranged in the extracellular space to form the extracellular matrix.

+ The cells:

There are two types of cells. On the one hand, the fibroblasts which synthesise and maintain the components of the extracellular matrix. These will secrete the various macromolecules that form the fibres of the connective tissue as well as the glycoproteins of the ground substance. Their activity is particularly intense during wound healing. On the other hand, there are leukocytes, mast cells and macrophages which play an important role in defence and immune surveillance, as well as mechanoreceptors which are part of the skin innervation.

ii) The parts of the dermis

The dermis is separated into two parts according to the morphology of the collagen network: the papillary dermis and the reticular dermis. Figure 1.9 shows scanning electron microscope (SEM) images of the location of the dermis and collagen parts, demonstrating the differences in structure between the papillary and reticular dermis.

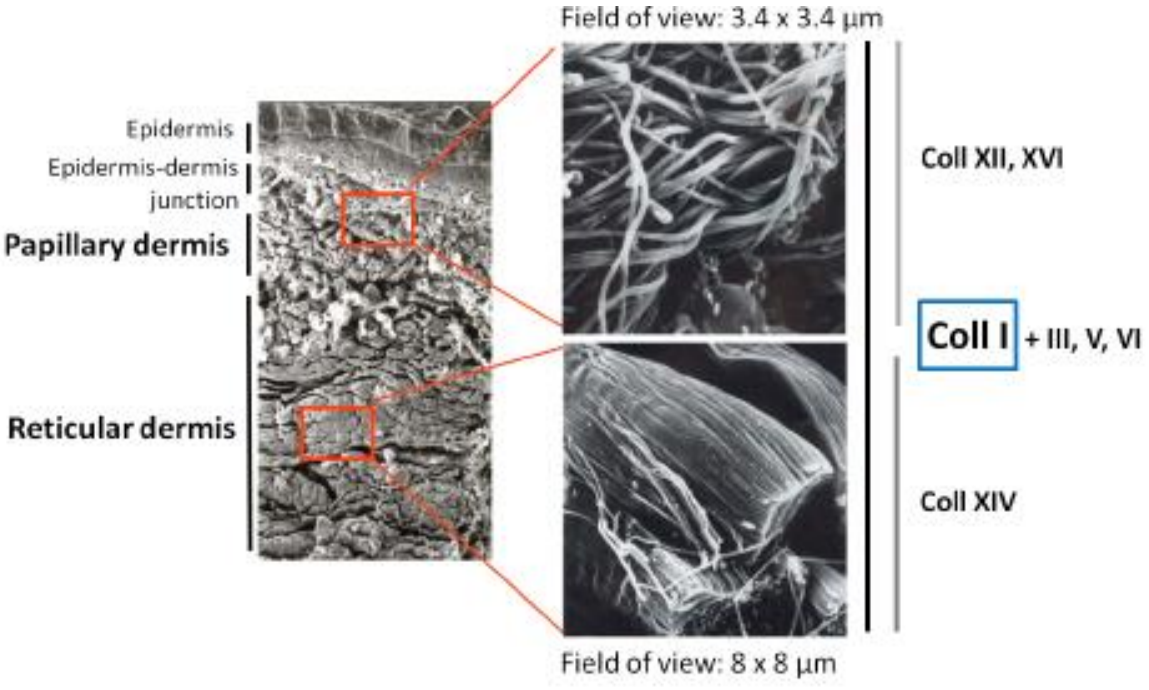

Figure 1.9: SEM images of the two parts of the dermis and the respective distribution of collagen types – [Garrone et al., 1997]

+ The papillary dermis (superficial dermis):

The layer of dermis closest to the epidermis is called the papillary dermis and owes its name to the finger-like structures at the dermal-epidermal junction, called papillae. This intermediate layer is in permanent symbiosis with the epidermis. The major component of the papillary dermis is the ground substance, hence its character as that of a loose connective tissue. It is also rich in fine collagen and elastin fibres which are interwoven and oriented perpendicular to the epidermis. The collagen fibres are quite small, curled and loosely arranged. On the immune and nervous system side, it contains the arterial, venous, and lymphatic subpapillary plexus, allowing nutrient exchange with the epidermis, as well as numerous free nerve endings.

+ The reticular dermis (deep and middle dermis):

The deepest layer of the dermis is called the reticular dermis. This part of the dermis represents 80% of the volume of the dermis. Thus, if we model the skin as a single layer, we can say that the mechanical properties we determine are mostly related to the reticular dermis. This is a dense connective tissue composed of a large network of elastin fibres and collagen fibres. The elastin fibres are thicker and form a branched network with the dense network of collagen fibres (Figure 1.10). In addition, the elastin fibres are also connected to those of the papillary dermis to form a very dense and disordered three-dimensional network. The collagen fibres, on the other hand, are grouped into dense bundles which are straighter and thicker than in the papillary dermis. Unlike those in the papillary dermis, the collagen fibres here run parallel to the skin surface and in random directions. The continuity of these fibres represents the lines of skin tension, known as Langer's lines. This part of the dermis also contains blood and lymph vessels, nerves, fibroblasts, but above all the skin appendages such as hairs, sweat glands and sebaceous glands.

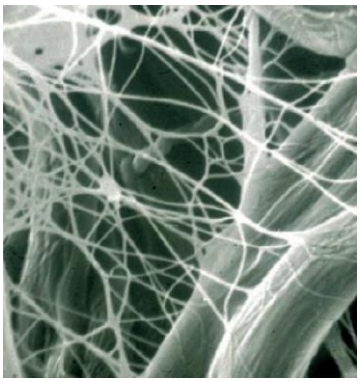

Figure 1.10: Elastin fibre network – [Quatresooz et al., 2006]

iii) Summary of the dermis

The dermis is the thickest and most important layer of the skin for structure and mechanical strength. It is a collagenous tissue in the general sense described as a heterogeneous structure composed of a few cells and an extracellular matrix. Certain cells found in the dermis, such as fibroblasts, have an important role to play in synthesising the components of the extracellular matrix that makes up the majority of the dermis. These components are collagen fibres of various types, elastin fibres and the ground substance. The main component of the ground substance and of the dermis in general is water, which accounts for 64% of the total skin.

The dermis is a composite structure in the mechanical sense: a combination of collagen fibres and elastin fibrils surrounded by a host structure (the ground substance), thus giving it the main role in the mechanical structure function of the skin. Its complexity allows for a very particular behaviour (see Chapter 4) necessary to ensure effective resistance to the many mechanical aggressions of daily life.

In addition to its structural and mechanical role, the dermis also plays a key role in thermoregulation and healing as well as in the elimination of toxic products [Dubertret, encyclopaedia].

1.1.1.D The hypodermis

The hypodermis is the deepest layer of human skin, coming just after the dermis and attached to it by expansions of collagen and elastin fibres. The hypodermis is also the thickest and heaviest layer of the skin, accounting for 15% to 20% of the human body mass. It is an adipose tissue which is composed of fat cells, the adipocytes, which are organised in lobules. These adipose lobules[7] are separated by connective partitions which allow the passage of nerves and vessels. In these partitions, trabeculae of collagen fibres from the dermis attach to the aponeuroses[8] of the muscles or the periosteum[9] of the bones, thus limiting the mobility of the skin.

The hypodermis therefore represents an interface between the dermis and the mobile structures just below the skin tissue such as muscles, tendons and bones (Figure 1.11). This layer is highly vascularised and innervated as blood is necessary for the metabolism and proper functioning of the adipocytes. These fat cells therefore represent a nutritional and energy reservoir for storing lipids. In addition, they supply fatty acids by lipolysis in the event of an energy demand: 85% of energy requirements are thus covered by withdrawals from these adipose reserves. It is in the cells of this layer, the adipocytes, that half of the body's fat is stored. The distribution of this tissue varies according to sex: predominantly in the upper parts of the body in men, it is located below the navel in women. It should be noted that certain areas are devoid of adipocytes, such as the eyelids or the ears for example. Finally, there are numerous capillary roots and sweat glands.

The hypodermis is a thermal insulator and its two main roles are to store energy and to protect the body against mechanical shocks. In fact, it forms a fatty mattress of very variable thickness which moulds itself to the underlying muscles and organs, thus protecting them from shocks.

[7] **Adipose lobules:** clusters of cells composed of unilocular adipocytes.
[8] **Muscle aponeuroses:** membranes made up of dense connective fibres which envelop a muscle.
[9] **Bone periosteum:** fibrous membrane that envelops the bones.

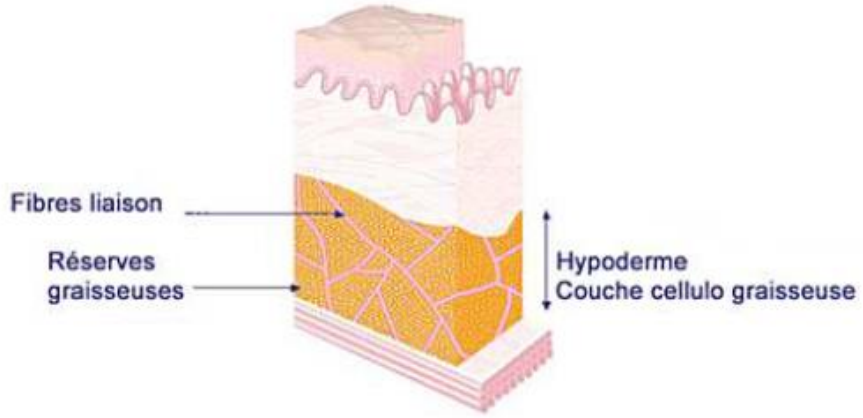

Figure 1.11: Diagram of the hypodermis – [Azzez, 2019]

1.1.2 Vascularisation, cutaneous innervation, and cutaneous appendages

1.1.2.A Skin vascularisation

Like all the organs of the human body, the human skin is highly vascularised. It is crossed by a multitude of blood vessels ensuring the survival and proper functioning of the various cells that make it up. The vascularisation is localised in the dermis and hypodermis; no blood vessels exist in the epidermis (Figure 1.12). Arterial blood enters the skin via subcutaneous arteries crossing the inter globular partitions of the fat. A first arterial network, fed by these arteries, is located in the deep dermis. Arterioles then leave this first network to create a second network in the superficial dermis and the sub-papillary plexus. Capillaries then reach the dermal papillae.

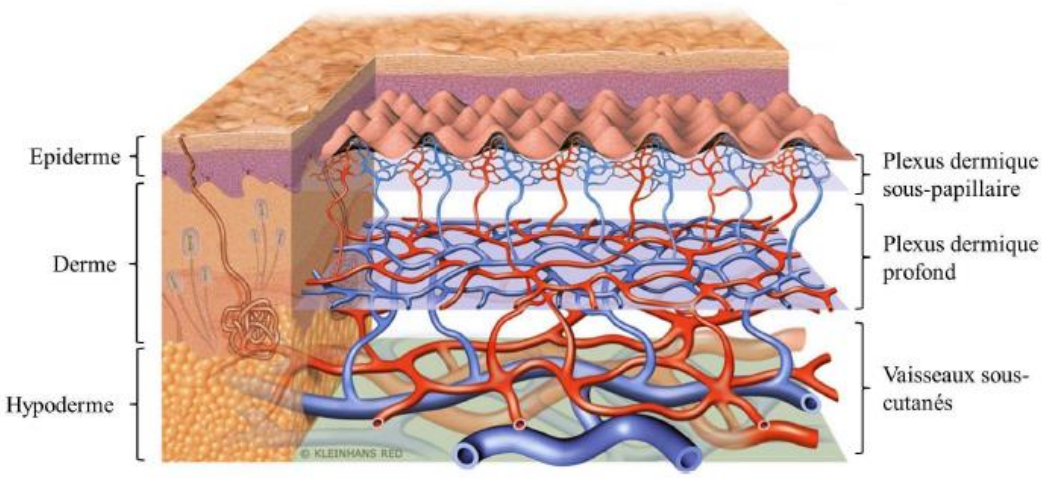

Figure 1.12: Skin vascularisation – [Azzez, 2019]

The skin blood volume represents 9-12% of the total blood volume, with a flow rate of 0.5-7 $L.min^{-1}$.There is one metre of blood capillaries per square centimetre of skin. The reason for the widespread presence of the vascular system is that it has many functions. It transports nutrients and oxygen to the layers and cells of which they are composed, and removes waste products in return. The cutaneous vascular network plays a key role in thermoregulation and the balance of

blood pressure, as well as maintaining the homeostasis of the internal environment and the organic balance of the body. It is as useful to the whole organism as it is to the preservation of skin functions alone.

1.1.2.B Skin innervation

Cutaneous innervation in the dermis and hypodermis is important. Being a sensory organ, the skin tissue is the site of several nerve transmissions. The density of innervation is highly variable, ranging from 5 to 10 sensors per square centimetre to 2,000 sensors per square centimetre in the fingers, an area of the body where touch is particularly sensitive. The transmissions are carried out by nerve endings that transport the information to the cerebral cortex (Figure 1.13).

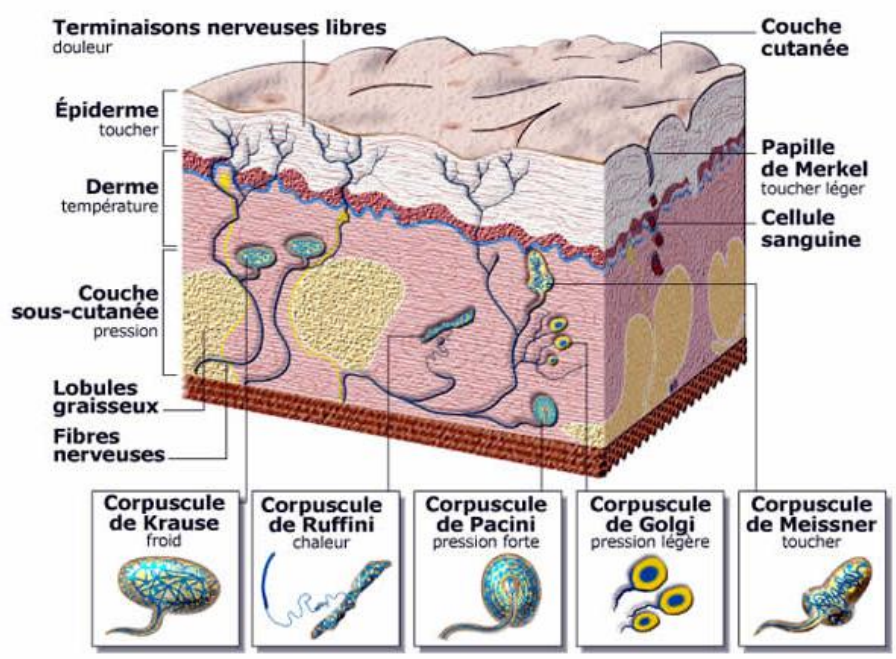

Figure 1.13: Cutaneous innervation – [CNRS Peau]

The innervation of the skin includes on the one hand the nerve endings of the autonomic nervous system (confined to the dermal vessels, sweat glands and the hair arrector muscles or horripilator muscles) and on the other hand the nerve endings of the sensory pathways, including:

- The free nerve endings. These endings are fine branches located in the superficial dermis or epidermis and include mechanoreceptors (slow adaptation), thermoreceptors (heat) and nocereceptors (pain).
- Corpuscular endings. These include Meissner's, Pacini's, Ruffini's and Golgi's corpuscles, which are mechanoreceptors involved in the sense of touch. They provide the function of tactile sensitivity and perceive pressure.
- The dilated endings. They come into contact with Merkel cells, neuroendocrine cells of the epidermis.

1.1.2.C Cutaneous appendages

In addition to all the components that make up the human skin, several types of skin appendages are anchored to it. These are complex epithelial formations which develop thanks to a collaboration between the dermis and the epidermis. There are two main categories of these appendages: the glands (sweat glands and sebaceous glands) and the phanera (from the Greek word *"phaneros"* which means apparent; these are the hairs and nails).

i) *Sweat and sebaceous glands*

The origin of the sweat glands is deep in the dermis. They then extend through a duct to the surface of the dermis with a pore that opens outwards (Figure 1.14a). They secrete sweat and provide an important part of thermoregulation. There are between 2 and 5 million sweat glands, particularly numerous in the armpits, inguinal folds, and especially on the soles and palms. In addition to thermoregulation, other functions of sweat should be noted. It keeps the stratum corneum minimally hydrated, thus preserving its mechanical properties. On the palms and soles, the non-thermo-dependent secretion improves the gripping of objects. Sweat also has antiseptic and antifungal properties due to its acidic pH.

The sebaceous glands are located in the mid-dermis and are vascularised and non-innervated (Figure 1.14b). They are distributed all over the body except for the palms and soles and are more numerous on the face. Most of these glands are attached to the hairs. The sebaceous glands are responsible for the secretion of sebum via a hairs canal. Sebum is formed from mature sebaceous cells and contains mainly lipids. The amount of sebum varies from person to person and its production is regulated by the sebaceous glands. They perform several functions such as lubricating the skin and hair, thus preventing water loss and hair breakage. Seborrhoea, the secretion of sebum, also helps to protect the skin against external aggression and to balance the bacterial flora of the skin. Indeed, sebum is part of the hydrolipidic film that protects the epidermis.

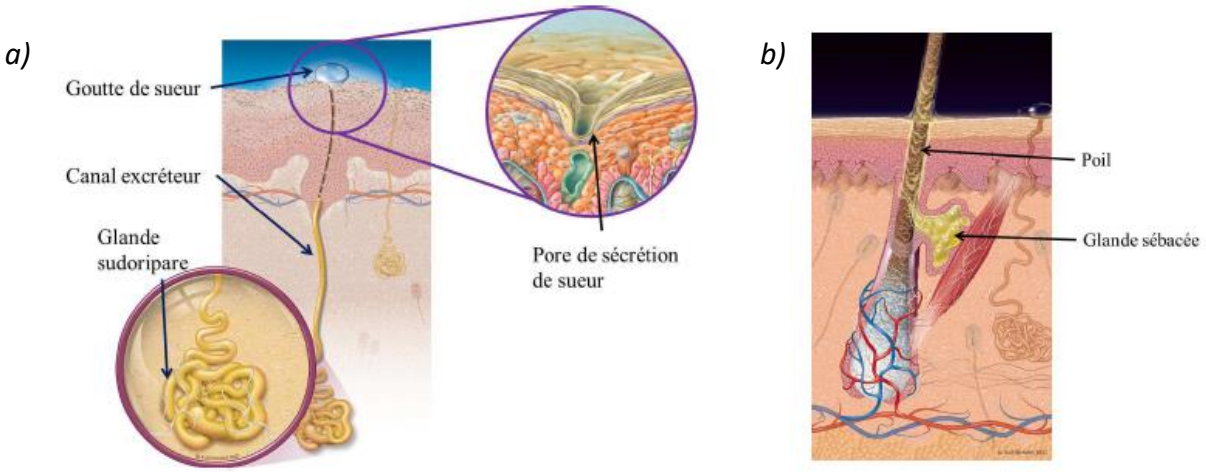

Figure 1.14: Glands. a) Diagram of a sweat gland. b) Diagram of a sebaceous gland – [Azzez, 2019]

ii) Hairs and nails

Hairs play a role in decorating the body, in protecting it from external aggression and in the sensitivity of the skin through sensitive sensors located around their roots in the dermis. Spread over the entire surface of the body except for the palms and soles of the feet, there are up to 5 million hairs, of which 1 million are located on the head. Hair follicles are associated with a sebaceous gland and their base, called the papilla, is highly innervated and vascularised (Figure 1.15a). Each hair also has its own pilomotor muscle which allows the hair to be bristled. Note that the hair shaft is formed by differentiation of keratinocytes (in the same way as the epidermis). In addition to their sensory function, hairs protect against the sun's rays thanks to the melanin present in the stem (especially on the scalp). They also play a role in thermal protection by trapping an insulating layer of air around the skin.

The nails are located in two areas of the skin, namely the dorsal surface of the fingertips and the toes. The nail is a hard and flexible rectangular plate and is a specialised keratinised skin appendage. The nail implants into the skin through a root, which runs almost parallel to the skin surface (Figure 1.15b). It is a cutaneous appendage vascularised and innervated by nerve endings beneath the nail bed. The nail has several functions such as protection and grip in the case where the nail protrudes from the digital pulp.

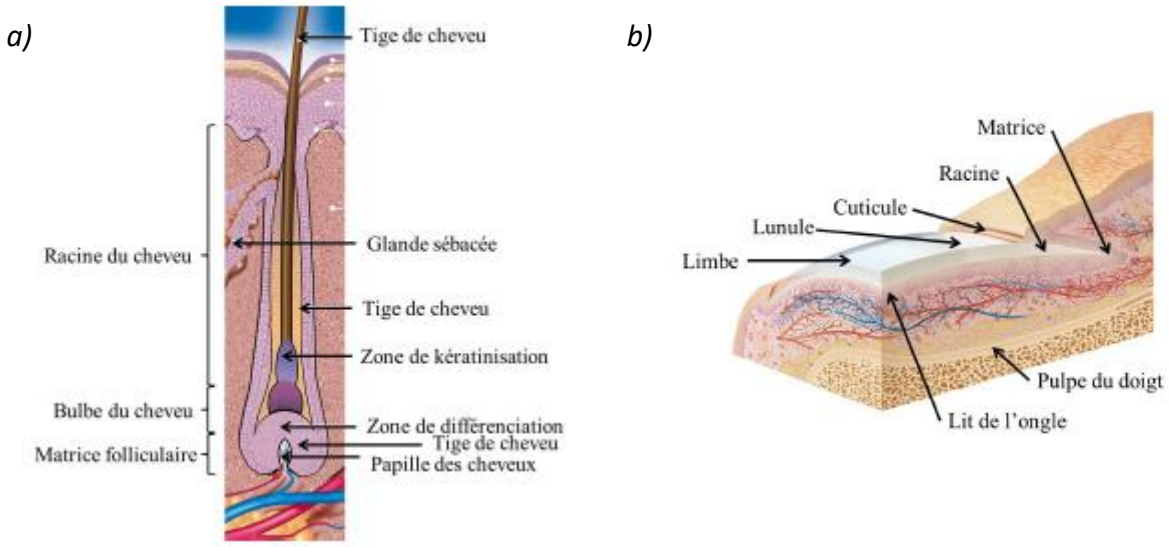

Figure 1.15: The phanera. a) Diagram of a hair follicle. b) Diagram of a nail – [Azzez, 2019]

1.1.3 Summary: skin, a complex organ.

This description of the functioning and organisation of the skin shows that this tissue has a very complex structure composed of multiple elements.
The skin is anatomically made up of three tissue layers which are, starting from the surface: the epidermis, the dermis and the hypodermis. Each of these tissue layers represents a rather complex system formed by several parts containing numerous cells. In addition, the skin also contains a

multitude of other cells and elements, namely the vascularisation system, the innervation system, the immune system and the cutaneous appendages.
Although generally presented in a structured way, there is a real continuity between all the elements [Guimberteau *et al.*, 2005], and each one will contribute to the properties of the tissue.

This organisation, as well as the multiple elements that make up the skin, enable many functions that are essential for the survival of the organism.

1.2 Skin functions and their alterations

The skin is a rigid and elastic structure composed of three layers: the epidermis, the dermis and the hypodermis. It is an organ in constant renewal. As we have seen previously, it is made up of numerous components and specialised cells that ensure its different functions.

The skin is first of all the envelope of our human body, it is the first protective barrier of our organism. Its role as the boundary between the body and the outside world requires very specific characteristics that allow both the exchange of information and the protection of the body.

The main function of the skin is therefore to protect the body from external physical, chemical and infectious aggressions. It is an essential border organ for the protection of the body.
However, the skin is much more than a simple protective envelope covering our body. It is in fact the home to numerous vital functions: thermoregulatory function, sensory function, exchange function (thermal and hydric exchanges which are essential for maintaining homeostasis), metabolic functions. It has the characteristic of being both impermeable as an inside-outside boundary (impermeable to a certain extent to chemical, mechanical, light and microbial aggressions), and permeable as a privileged exchange zone (permeable to substances that can enter or pass through the skin).
The skin also participates in social communication; it is a mirror organ where most internal diseases are manifested, but also reactions to environmental changes and, in particular, emotions.

Finally, the skin can also suffer significant damages due to its role as a border with the external environment. Indeed, it can undergo very large deformations which can lead to irreversible damage, but it can also be impacted by various constraints which can alter its main functions. Finally, like the rest of our body, the skin ages naturally, which also results in a reduced capacity to perform its functions.

All the main functions of the skin and the effect of various stresses that can alter them are described in this Section.

1.2.1 The different functions of the skin

The skin is the site of many vital functions that are essential for maintaining the body's homeostasis. These main functions are described below.

1.2.1.A Protective function

The skin primarily has a protective function against all external aggressions (heat, sun, water, infections, etc.). The protective function is mainly provided by the *stratum corneum* of the epidermis which is the body's first line of defence against external aggressions. The situation of the corneocytes is unique in the body since a dead cell is usually useless, but this is far from being the case for the *stratum corneum* [Elias, 2005].

The skin is a protective physical barrier that also allows control of water, electrolyte, and macromolecule losses. The absence of the stratum corneum would allow water and extracellular fluids to leak out: a loss of this layer of more than 50% of the body surface area is therefore lethal (dehydration in burn victims is a major factor in mortality).

i) *Against mechanical aggression*

The skin plays an important role in structural support and protection against mechanical impacts and external pressure. Indeed, the skin undergoes distortions due to movements, but it also adapts to weight variations or to punctual modifications of a part of the body such as pregnancy. The mechanical strength of the skin is crucial in this respect.
Each layer of the skin, due to its own composition, organisation and thickness, has a different mechanical function. It is a flexible and effective protection on 3 levels:

+ the keratin of the *stratum corneum*, a strong continuous barrier;

+ the dermis fibres: collagen and elastin fibres which give the skin its tensile strength and which allow the skin to return to its original position after stretching. These fibres are responsible for the cohesion of the tissues and their resistance. As already mentioned, the dermis is similar to a composite material, which ensures the main role in the mechanical structure of the skin;

+ the fat pad of the hypodermis, which protects the underlying organs, muscles and bones against physical shocks and pressures; it acts as a shock absorber.

This allows the skin to become a physical barrier that preserves the internal environment. The elasticity and strength of the skin provides effective resistance to the many mechanical stresses of daily life while allowing movement.

ii) Against chemical aggression

The *stratum corneum* and the hydrolipidic film, formed among other things by sweat and sebum, act as a protective barrier against chemical agents. The hydrolipidic film forms a protective "acid

mantle" (pH between 4.6 and 6.1) which limits the multiplication of foreign germs, controls the proliferation of resident flora and prevents the penetration of foreign substances.

However, this barrier is not impenetrable. Some products can slowly penetrate through the skin into the general circulation. This penetration can be used for the application of certain drugs. On the other hand, it represents a danger with regard to toxic products capable of penetrating this barrier (case of heavy metals for example).

iii) Against microbes

The skin's defence is provided by the *stratum corneum*, the immune cells of the dermis, and also by the microbial flora that exists on the skin's surface. Indeed, the *stratum corneum* is the habitat of the cutaneous microbiota, a population of micro-organisms that is essential to our protection and to our immune system in general. Its main function is to form a protective barrier against bacteria and fungi.

The cutaneous flora, known as saprophyte, opposes the development of the flora known as pathogenic, i.e., generating diseases (*streptococcus, staphylococcus aureus*, etc). This surface flora must therefore be respected and is essential for good health. In general, bacterial biodiversity limits the risk of colonisation of the skin by pathogenic bacteria and provides protection against skin inflammation. The skin is thus our first barrier against micro-organisms.

iv) Against solar radiation

The skin protects the internal organs from external radiation, in particular UV radiation from the sun, which is an important factor in the development of cancer. It provides photoprotection against the sun.

The skin benefits from the dual protection of the *stratum corneum*, which thickens under the influence of solar radiation and thus increases the effectiveness of the skin barrier, and of melanin, whose secretion increases. Indeed, the skin is the site of melanin production, which determines the colour of the skin and prevents damage from sun exposure [Scott, 1989]. It acts as a filter that diffracts and reflects incident rays, protecting the genetic material of the cell. Melanin production is a dynamic phenomenon: UV radiation induces a rapid reaction (browning) which starts 5 to 10 minutes after exposure and can last 36 hours. A delayed reaction appears 72 hours later, corresponding to tanning; a neo synthesis of melanin and melanosomes occurs. It should be noted that hair also constitutes an interface that can protect against UV rays. However, when burned, the skin's protective function against UV is impaired.

1.2.1.B Role in the general metabolism

The skin also plays an important role in the general metabolism, for example in thermal regulation through sweating (excretion from the sweat glands) or in the synthesis of vitamin D under the action of sunlight.

i) *Temperature control function*

The skin is an essential organ of thermal regulation. This thermoregulation of the skin contributes effectively to maintaining the body temperature around 37°C. It is the result of the production and loss of thermal energy.

With regard to heat, the evacuation of excess heat is ensured by sweating and by the active dilation of the small blood vessels (vasodilatation) of the dermis. Evaporation through sweat, or body perspiration, is the only way to remove heat quickly. This perspiration also regulates the balance of body fluids and allows the elimination of toxic products. On the other hand, the constriction of the small blood vessels (vasoconstriction) in the skin, the presence of the fatty cushion of the hypodermis and the contraction of the small hair muscles (muscle activation linked to the "goose bumps" phenomenon) counteract the cooling of the body.

Precise control of body temperature is of the utmost importance: below 32°C and above 41.6°C body temperature, a human being is considered to be in danger of death.

ii) Vitamin D synthesis

In addition to the production of melanin by melanocytes, vitamin D is synthesised by sunlight. A balance of sunlight exposure is therefore necessary for good health: too much sunlight destroys cells, but not enough sunlight will not maintain a sufficient level of vitamin D [Sinclair, 2006]. Vitamin D is a fat-soluble vitamin synthesised in the human body from a cholesterol or ergosterol derivative under the action of ultraviolet B (UVB) radiation from the sun. This synthesis of vitamin D increases the capacity of the intestine to absorb calcium and phosphorus and thus ensures the mineralisation of bones, cartilage and teeth.

iii) Role in immunity

The skin actively participates in the immune response due to the presence of immune cells. The antimicrobial and antifungal properties of the skin's surface and the resident skin flora of the epidermis also contribute to immune surveillance. In addition to a passive physical barrier, some elements of the immune system, both innate and adaptive, are fully integrated into the skin. For example, Langerhans cells in the epidermis play a crucial role in immunity: these peripheral sentinels detect the presence of antigens that may have passed through the skin barrier. They capture the antigens and present them to T cells to initiate the immune response chain.

1.2.1.C Sensation function

The skin has a very important sensory role in terms of the surface area it comes into contact with the environment. The skin is therefore an organ of perception thanks to the vast network of nerve cells it contains. Indeed, the skin, with its wealth of sensory fibres, informs the body about four major groups of sensations: touch, pain, temperature and pressure.

The skin contains several types of receptors. For example, it contains mechanoreceptors sensitive to touch and pressure, nociceptors sensitive to pain and thermoreceptors sensitive to cold or heat. It constantly informs the brain through these many specialised sensors responsible for perception. It should be noted that hairs also play a role in the sensitivity of the skin through sensors located around their roots in the dermis. The tactile sense was the first sensory organ to appear during evolution and the last to disappear during the ageing process.

1.2.2 Skin ageing and effects of different stresses

Over the course of a lifetime, the physical properties of the skin's layers and its appearance change. Skin ageing is an inescapable phenomenon, which is complex in terms of both its causes and its mechanisms and manifestations. It is the result of a variety of factors, which can be divided into 2 different groups: individual genetic factors known as intrinsic (age, genetics) and environmental factors known as extrinsic (UV radiation, tobacco, nutrition, etc.) [Lambert, 2018], [Boismal *et al.*, 2020], [Rorteau *et al.*, 2020].

Healthy skin is elastic, smooth, and resilient. However, many factors can stress our largest organ in different ways. Ageing and stresses will lead to a decrease in the properties of this organ and a reduced capacity to perform its functions. Even if the primordial function of protection is well organised and in place, the skin will suffer damage as a result of major aggressions that will alter its functions. Natural ageing and the effects of various stresses on the skin are described in this Section.

1.2.2.A Visual representation of skin ageing

The natural ageing of the skin consists of the progressive degradation of the functions of the skin tissue as well as the components that make it up. Indeed, with age the skin gradually loses its suppleness and firmness, and becomes less and less sensitive to everything it used to perceive with the touch. This ageing is manifested by the appearance of fine lines and wrinkles, especially on the face, and deep furrows all over the skin's surface. This network of lines, apparent on the surface, is called the skin's microrelief.

This micro-relief can be characterised by a topographic study of the skin surface. Four categories of furrows are distinguished:

- First-order furrows, or primary lines, are the most visible; they range in depth from 70 µm to 200 µm. They are oriented in at least two directions and delimit plateaus of varying shapes. The follicular orifices are at the intersection of these grooves, whereas the sweat pores are located on the plateaus or in the secondary lines.
- The secondary lines are less apparent than the primary lines with a depth between 30 µm and 70 µm.
- For the tertiary and quaternary lines, they can only be seen with a microscope, the former delineates groups of corneocytes and the latter gives the relief of each corneocyte with a depth of less than 1 µm.

This microrelief varies according to age and ethnicity [Guinot *et al.*, 2006]. Isotropic and tight in a young person, the network becomes increasingly wide and anisotropic in an elderly person, reflecting the disorganisation of the dermis (Figure 1.16). Indeed, from a topographical point of view, ageing results in the disappearance of secondary lines and the strengthening of primary furrows, which leads to a lower overall furrow density.

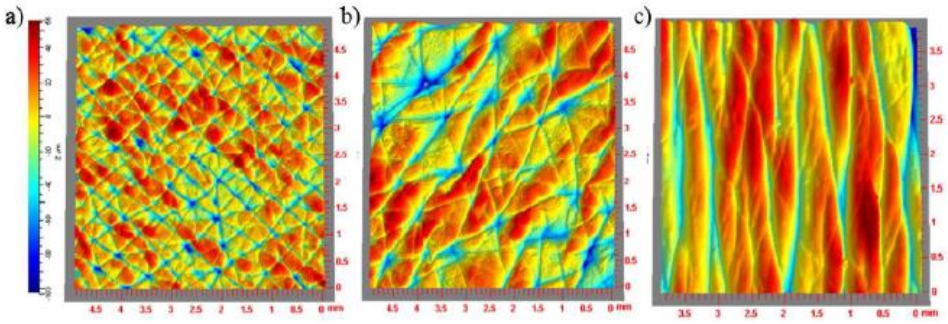

Figure 1.16: Topography of the skin tissue, size: 5x5 mm^2. a) 30-40 years. b) 50-60 years. c) 70-80 years – [Zahouani et al., 2011]

1.2.2.B Intrinsic skin ageing and alterations

i) *Intrinsic skin ageing*

It is a natural, slow, and progressive phenomenon, based on 2 fundamental principles. Firstly, the biological clock, known as "chronological ageing" or "senescence", which is due to wear and tear on our bodies as the years go by. On the other hand, genetic inheritance, specific to each individual, which "genetically programmes" skin ageing. Intrinsic ageing is therefore a chronological, genetically programmed skin ageing. It will manifest itself through cellular changes that will have both functional and clinical consequences.

The following intrinsic factors group together the causes of intrinsic skin ageing:

- Innate genetic factors. Innate genetic factors include phototype and hereditary genetic background, which have an influence on skin ageing specific to each individual.
- Acquired genetic factors: chronological factors. Chronological factors are directly correlated with the passage of time, wear and tear on the body. They are the result of a combination of genetics (programmed skin ageing) and the accumulation of errors over time.

ii) Intrinsic alterations: the case of stretch marks

Certain phases of life bring about significant morphological and physical changes, such as pregnancy or substantial weight changes. These internal physical phenomena can cause scarring of the skin, known as stretch mark. Stretch marks, *or striae distensae* (SD), are linear dermal scars accompanied by epidermal atrophy. They frequently occur during times of rapid tissue expansion, such as in adolescence or during pregnancy. They appear as parallel streaks (*striae*) aligned perpendicular to the direction of skin tension (Figure 1.17).

Figure 1.17: Laddering pattern of skin colours in striae distensae – [Devillers et al., 2010]

The mechanism by which stretch marks appear is still unknown, but their development in certain physiological or pathological conditions is described by three main histopathogenic theories: skin rupture by mechanical stretching, hormonal changes, and genetic factors that lead to a reduction in the genetic expression of collagen, elastin, and fibronectin [Elsedfy, 2020]. Histologic and biochemical analyses have revealed that SD are characterized by [Kim *et al.*, 2019; Stamatas *et al.*, 2014; Cho *et al.*, 2018]:

- a thin epidermis with a rougher surface and an anisotropic surface texture;
- a flattening of the dermal-epidermal junction;
- a decrease in extracellular matrix (ECM) components in the dermis: collagen, fibrillin and elastin;
- a strong alignment of collagen fibres;
- a decrease in elasticity.

SD appear correlated with loss of synthetic capacity of fibroblasts and strong alteration of connective tissue structure. At an early stage in striae formation, the inflammatory reaction causes destruction of collagen and elastin fibres network. As in any other damage, this would be followed by regeneration of new elastin and collagen, this time oriented in the direction of stress imposed by mechanical forces [Zheng *et al.*, 1985].

1.2.2.C Extrinsic skin ageing and alterations

i) Extrinsic skin ageing

As a barrier organ exposed to environmental factors, the skin undergoes what is known as "extrinsic" ageing, which is linked to multiple environmental factors, identified under the term "exposome" [Krutmann *et al.*, 2017]. Extrinsic skin ageing can be considered as "lifestyle" ageing. This is ageing caused by all the environmental factors to which the body is exposed throughout its life, the main and most damaging of which is UV radiation. This extrinsic ageing of the skin has mechanisms similar to intrinsic ageing, which both amplify the latter and maintain its deficiencies.

Extrinsic factors can be divided into 2 groups: non-modifiable environmental factors that the individual cannot influence, and modifiable environmental factors that are directly linked to the individual's behaviour.
The non-modifiable environmental factors are mainly ultra-violet radiation (photo-induced ageing) and atmospheric pollution (Figure 1.18). For some authors, photo-induced and environmental factors are as important as chronological ageing [Giacomoni *et al.*, 2004]. The modifiable environmental factors include tobacco, nutrition, and alcohol.

Regarding atmospheric pollution, the skin is affected every day by many air pollutants such as nitrogen dioxide or airborne particles related to exhaust gases. Skin cultures exposed to polluted air show an increase in the number of abnormal or dying cells, demonstrating damage to the cells' DNA [Svoboda, 2018]. These factors such as pollution or smoking will notably accelerate ageing [Boisnic *et al.*, 2005]; [Leung *et al.*, 2002]; [Bernhard *et al.*, 2007].

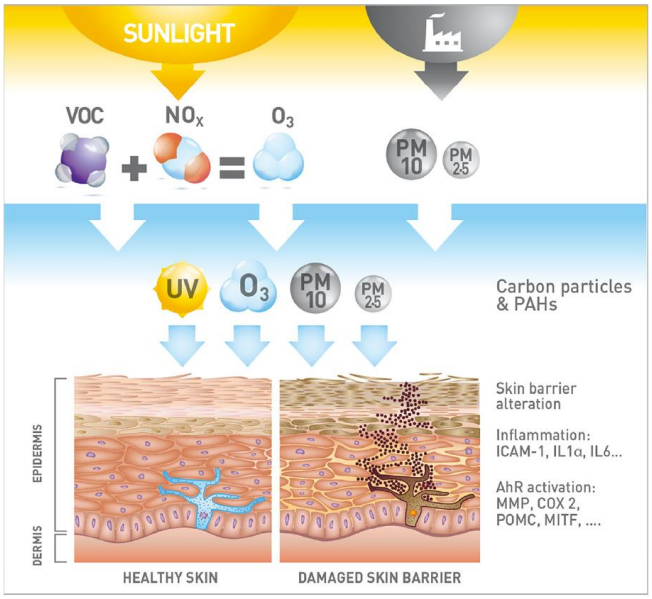

Figure 1.18: Damage to the skin caused by pollution – [Lambert, 2018]

ii) Extrinsic alterations: the case of Ultraviolet (UV) radiation

Although the sun is essential to the human body, prolonged and intense exposure to its rays, without precaution, can lead to sunburn (erythema) or deeper lesions. Indeed, ultraviolet radiation is both a nutrient and an aggression for the skin.

UV radiation is the main factor in extrinsic ageing. They are part of solar radiation, which can be broken down into several types of radiation: infrared, visible, and invisible (ultraviolet UVA, UVB and UVC). Each type of radiation has a specific wavelength, which determines its energy potential: the longer the wavelength, the lower the energy. The following types of radiation can be described in detail (Infrared (IR): 3000 to 800 nm; Visible rays: 800 to 400 nm; Ultraviolet: 400 to 100 nm). Ultraviolet radiation is considered the most dangerous to the skin and is divided into three bands (Figure 1.19):

+ UVA, which has a wavelength of 320 to 400 nm. Although their energy is lower than that of UVB, they penetrate the dermis and are responsible for immediate tanning, premature ageing of the skin and may play a role in the development of some skin cancers. UVA radiation has no known health benefits and causes photo-oxidative damage to all cellular structures. UVA is not easily absorbed by the ozone layer; about 95% of it passes through;

+ UVB, which has a wavelength of 280 to 320 nm. They mainly penetrate the protective layer of the epidermis. It is this UVB radiation that is responsible for the synthesis of vitamin D. UVB is also responsible for long-term tanning and sunburn, as well as most skin cancers, because it damages DNA, proteins, and cell lipids. Both UVB and UVA have an immunosuppressive action [Dubertret, encyclopedia]. A large proportion of UVB is absorbed by the ozone layer; only 5% reaches the earth's surface;

+ UVC has a wavelength of 100 to 280 nm and is the most energetic UV radiation. They are very dangerous to all forms of life (even at very low doses) but do not penetrate the ozone layer and never reach the earth.

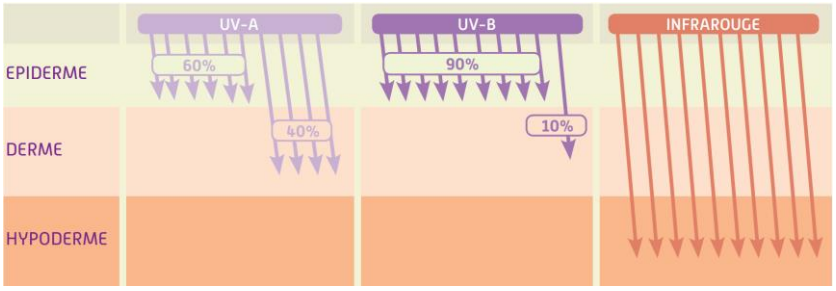

Figure 1.19: Penetration of UV radiation into the skin – [Lambert, 2018]

The skin has a system for protecting itself from UV rays, notably via natural pigmentation (melanin synthesis by melanocytes) and repair systems in the event of cellular, molecular or DNA damage. UV rays will be beneficial in small quantities (vitamin D synthesis which is essential for Calcium assimilation) but, when exposure is repeated and excessive, UV rays will have harmful effects, as the repair systems are overwhelmed. These repeated exposure to solar UV radiation causes skin damage similar to that resulting from the normal ageing process. The skin thins in places and loses its elasticity, while whitish patches, freckles and wrinkles appear.

More precisely, skin ageing is accelerated by UV rays via various mechanisms, similar to those of intrinsic ageing:

+ Direct damage to DNA. UV rays have a direct toxic effect on the skin by interacting with the DNA of keratinocytes, causing lesions and mutations that can lead to cell death or carcinogenesis;

+ Production of reactive oxygen species (ROS), which create unstable states. The result is a situation of oxidative stress induced by the free radicals that UVs helps to form on the skin, sources of squamous cell carcinoma[10] [Svoboda, 2018]. When they strike molecules on the skin's surface that contain oxygen, unstable compounds called free radicals are created. To stabilise, free radicals steal electrons from neighbouring molecules, the process of oxidation. This process can damage the DNA of skin cells, leading to tissue inflammation, accelerating skin ageing, and promoting mutations that contribute to cancer [Quatresooz *et al.*, 2005];

+ Increased activation of proteolytic enzymes such as collagenases and elastase. UV exposure results in a significant increase in elastase and matrix metalloproteinases (MMPs) activities within the dermal tissue resulting in the destruction of both the collagen and elastic fibre network [Jenkins, 2002]. The alteration of the ECM and its components by enzymes causes the skin to become more fragile, leading to the appearance of wrinkles.

1.2.2.D Physiological and clinical consequences of skin ageing

Skin ageing has several consequences which have a direct impact on the skin and its visual appearance [Lambert, 2018]. On a microscopic scale, the different layers and the constitutive cells are subject to innumerable modifications [Ebling, 1982]; [Waller *et al.*, 2006], starting with their thickness. The thickness of the epidermis decreases by 7% per decade compared to a decrease of 6% every ten years for the dermis. The skin becomes thinner and more fragile over the years. In fact, the skin cells do no longer regenerate at the same rate as they are destroyed, and their number and production decrease.

i) *Epidermis layer*

In the stratum corneum, there is an increase in the size of the corneocytes, which leads to a decrease in their desquamation and a reduction in their cohesion. Moreover, the rate of lipid contained in the stratum corneum decreases, which leads to a decrease in skin hydration. The skin becomes dull, dry, and rough. Overall, the epidermis atrophies and thins. In the case of keratinocytes, there is a reduction in their size and number, as well as in their ability to proliferate, leading to a drop in skin renewal. In addition, the decrease in melanogenesis induces a non-uniform colouring of the skin. This phenomenon affects the skin's barrier function, as it becomes increasingly difficult to prevent the penetration of UV rays. This barrier function of the skin is also disturbed because of the decrease in the number and synthesis of Langerhans cells; the healing process loses its effectiveness.

[10] **Squamous cell carcinoma:** skin cancer that develops in the cells of the spinous layer of the epidermis.

ii) Dermal-Epidermal Junction

The DEJ shows a characteristic structural change: it flattens. This is due to the reduction and even disappearance of the elastic fibres involved in the structure of the dermal papillae. As a result, the DEJ loses its exchange surface area.

iii) Dermis layer

Regarding the dermis, ageing manifests itself through disorganisation, reduced vascularisation, and a drop in cellular and protein content. The result is a thinner dermis. As far as dermal cells are concerned, fibroblasts decrease in activity, size, and number (by 50% on average between the ages of 20 and 80). This leads to a progressive decrease in fibroblast metabolism and in particular in their capacity to generate the elements of the extracellular matrix. As a direct consequence of this decrease in metabolism, the synthesis and therefore the density of the collagen and elastin fibre network decreases. At the same time, we observe a contradictory increase in the expression of elastases and collagenases, leading to a respective deterioration and degradation of elastic and collagen fibres [Boisnic *et al.*, 2005]. The particularity of elastic fibres is that the consequences of ageing vary according to their location: in the papillary dermis, their number will decrease, while it will increase in the reticular dermis, but they will be disordered and fragmented. We also observe that the ground substance becomes increasingly fluid [Agache *et al.*, 1980]; [Daly *et al.*, 1979].

The natural tension of the skin then decreases considerably and the fibres progressively follow their preferred direction, the anisotropy thus becoming more pronounced. This multitude of structural modifications manifests itself in the overall mechanical behaviour of the skin, which gradually deteriorates. Indeed, the elasticity of the skin decreases with age due to the degradation of the fibre network. The disorganised and weakened extracellular matrix results in less dense connective tissue, which loses its protective function and support for the cutaneous vessels.

iv) Hypodermis layer

In the hypodermis, intrinsic ageing causes a redistribution of fat: fat cells decline on the face, back, hands and arch of the foot, causing subcutaneous atrophy, while they increase on the stomach and thighs.

1.2.3 Summary: skin, a complex organ with multiple functions

The skin, described in Part 1.1, is an organ with a very complex structure composed of multiple elements that perform many functions essential to the survival of the organism [Agache, 2000]. The skin is at the same time impermeable, resistant and flexible, and is populated by organelles specialised in alertness, defence and repair.

The skin is an organ that constitutes an interface between the outside and inside of the body, forming an envelope. The properties and characteristics of this organ, which is in charge of the border function, are therefore essential to ensure the protection of the body. In addition to its main function of protecting the body from external aggressions (mechanical, chemical and infectious aggressions), the skin is home to many vital functions such as thermal regulation and sensory function. The skin is also an organ that allows thermal and hydric exchanges between the body and the external environment, which are essential for maintaining homeostasis.

Although the slightest hitch easily damages this structure, involving a process of repair and internal maintenance, its advantages are multiple. It is very flexible, allowing for unparalleled freedom of movement, a multitude of exchanges with the outside world, and can also be damaged without endangering the body.

Finally, the natural ageing of the skin leads to a reduced capacity of this organ to ensure these main functions. Skin ageing varies from one person to another depending on age and gender, but from the age of thirty onwards, we observe that the tissues lose their elasticity. The alteration of these functions can also be accelerated by the effect of certain constraints, aggressions of the external environment on its structure, such as excessive exposure to the sun. The same applies when the skin is affected by pathologies (solar elastosis[11], senile elastosis, cutis laxa, etc.). The skin can be a good indicator of the general state of health, the presence of certain cutaneous or internal diseases and the effects of the cutaneous application of certain substances.

The elements described in these first two Sections will allow us to better understand the behaviour of the skin under mechanical stress. The study of the mechanical properties of the skin is of paramount importance for many fields and in particular for the medical and cosmetic world.

1.3 Mechanical properties of human skin

The mechanical properties of the skin are of great importance in many clinical and cosmetic applications. They have therefore been extensively studied experimentally both *ex vivo* and *in vivo* [Xu *et al.*, 2008]; [Pissarenko *et al.*, 2020]; [Arnold *et al.*, 2023].

The skin is a complex multifunctional organ that has to meet many specifications. It has to be highly resistant, flexible in all directions and able to return to its original state under all circumstances. The description of the skin tissue shows a multitude of components which, because of the strong cohesion between them, all participate in their own way in the mechanical behaviour of the skin

[11] **Elastosis:** alteration of the elastic tissue of the dermis.

which will be different according to the body area. However, the dermis remains the main structure and will largely control its behaviour.

The combination of collagen and elastin fibres in the form of networks will give the human tissues they compose very different properties as shown in *Table 1.1*. While the fibres individually exhibit linear behaviour, the structure generated by their arrangement generally moves toward a non-linear behaviour [Hendriks, 2001]. In addition to the type of structure, the density of the collagen fibres will generally have a strong impact on the mechanical properties of the tissue [Roeder *et al.*, 2002].

Table 1.1: General mechanical properties of tissues – [Holzapfel, 2000]

Material	Ultimate tensile strength [Mpa]	Ultimate tensile strain [%]	Collagen (% dry weight)	Elastin (% dry weight)
Tendon	50-100	10-15	75-85	< 3
Ligament	50-100	10-15	70-80	10-15
Aorta	0.3-0.8	50-100	25-35	40-50
Skin	1-20	30-70	60-80	5-10
Articular Cartilage	9-40	60-120	40-70	-

The skin being a multi-functional and multi-component organ will therefore generate a complex range of mechanical properties. Indeed, the skin is characterised by a non-homogeneous, non-linear, viscoelastic and anisotropic behaviour with a natural pre-stress [Wilkes *et al.*, 1973]; [Agache, 2000].

First, the intrinsic mechanical properties of dermal fibres will be presented. We will then break down the different aspects of the global behaviour of the skin by detailing the link with its microstructure. Finally, a general synthesis of the mechanical properties of human skin will be made.

1.3.1 Intrinsic mechanical properties of skin components

1.3.1.A Collagen fibres

The skin belongs to the family of tissues called connective tissues, i.e. tissues "rich in collagen". Collagens are proteins which are macromolecules formed by one or more long chains of amino acids. These proteins are assembled in a triple helix, a structure formed by linking together three chains of amino acids, called α-chains, in what is called a tropocollagen. The stability of the triple helix is ensured by hydrogen bonds between specific amino acids of different α-chains. A tropocollagen triple helix is shown schematically in Figure 1.20.

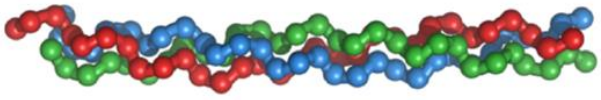

Figure 1.20: Triple helix of tropocollagen linking 3 α-chains together – [Lynch, 2015]

The structural organisation of collagen is summarised in Figure 1.21: the α-chains assemble into tropocollagens, which assemble into fibrils, which aggregate to form fibres, which in turn organise themselves into a tissue-specific microstructure [Gautieri *et al.*, 2011]. Collagen fibres can extend to a few millimetres in length and a few micrometres in diameter. The structure of collagen fibres has been studied for quite some time using X-ray and electron microscopy [Hulmes, 2002].

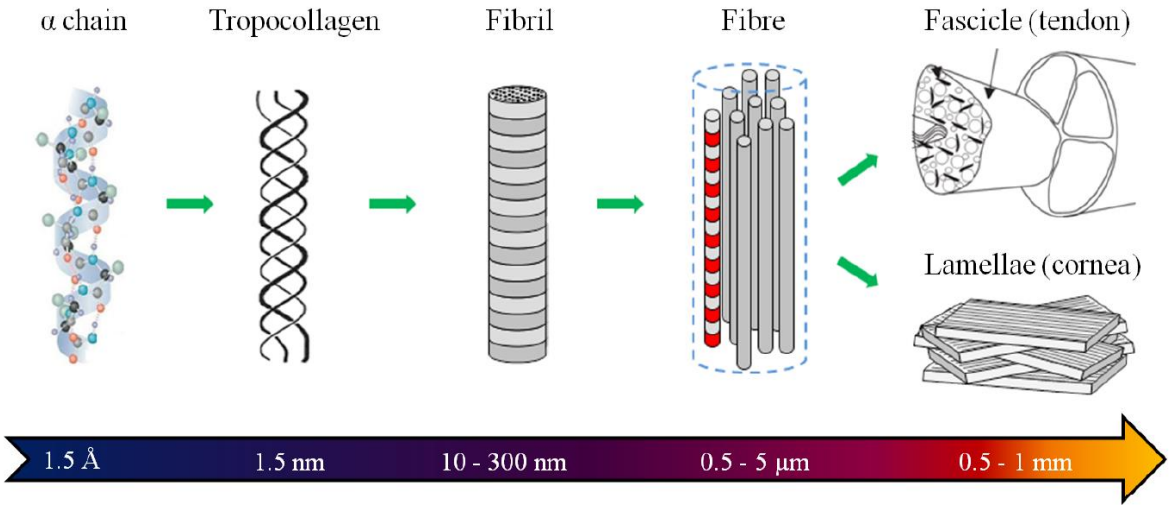

Figure 1.21: Structural organisation of fibrillar collagen – [Bancelin, 2013]

At least 28 different collagens are known in vertebrates [Shoulders *et al.*, 2009]. The most important and abundant type of collagen in collagen-rich tissues is collagen I: it is responsible for most of their structural properties. While most collagens can have breaks in their triple helix regions, collagen I has no imperfections [Kadler *et al.*, 2007].

The skin, as seen in Figure 1.22, has a very disorganised tangle of thick fibre bundles. The fibres are often coiled or wavy. This organisation is ideal for allowing the skin to be mechanically stimulated in all directions. The orientation of the fibres is always closely related to the directions in which the tissue is mechanically stressed.

Figure 1.22: Skin observed by Transmission Electron Microscopy (horizontal section) – [Ushiki, 2002]

Numerous studies have been conducted to determine their mechanical properties [Gautieri *et al.*, 2011]; [Ushiki, 2002]; [Shen *et al.*, 2008]; [Wenger *et al.*, 2007]; [Sun *et al.*, 1996]. Atomic force microscopy (AFM), microelectromechanical systems (MEMS) and optical tweezers are the most commonly used experimental devices.

Collagen fibres, like all slender structures, are anisotropic in the mechanical sense. While they have low bending or torsional strength, they have high tensile strength in their main direction, attributed to intermolecular covalent cross-links. The behaviour of these fibres is accepted as linear elastic [Hendriks, 2001]. It is described using a modulus of elasticity, also called Young's modulus, whose values, which are given in *Table 1.2*, vary from 20 MPa to more than 4 GPa.

Table 1.2: Mechanical properties of collagen and elastin fibres according to the literature.

Young's modulus of collagen fibres	Young's modulus of elastin fibres	References
	0,3 MPa	[Agache, 2000]
695 MPa - 2 GPa		[Daly, 1966]
1 GPa	0,6 MPa	[Delalleau, 2007]
1 GPa	0,2 MPa	[Lapierre *et al.*, 1984]
20 - 73 MPa		[Manschot *et al.*, 1986]
500 MPa	0,1 MPa	[Silver *et al.*, 1992]
4,4 GPa	4 MPa	[Silver *et al.*, 2001]

Thus, collagen is characterised by significant stiffness and a low elongation capacity: from 5 to 15% maximum [Roche, 1997]; [Silver *et al.*, 1992]; [Fung, 1993].
Note also the intrinsic viscoelastic nature of collagen fibres, illustrated in Figure 1.23 by the hysteresis that occurs during cyclic loading on a single fibril [Van der Rijt, 2004].

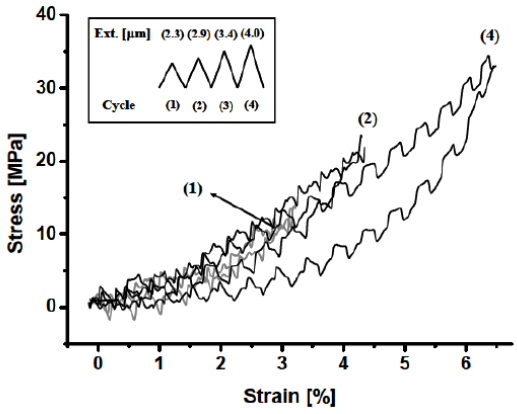

Figure 1.23: Stress-strain curve for cyclic loading on a single collagen fibril using AFM – [Van der Rijt, 2004]

1.3.1.B Elastin fibres

Elastin, like collagen, is made up of proteins which are formed by long chains of amino acids.
Elastin is first produced by the fibroblasts in the form of a precursor, tropoelastin, a very hydrophobic polypeptide. Inter-chain links will progressively form elastin fibrils and then elastin fibres. Elastin fibres therefore have the same microstructure as collagen fibres. The origin of the remarkable physical properties of elastin fibres is linked to the presence of a "cross-linking agent" within the fibres, desmosin, a lysine tetra-peptide whose role is similar to the disulphide bridges in

keratins, but more flexible. These fibres, which appear as a tight, three-dimensional interweaving of fibrils, give elasticity and strength to the tissue. Indeed, they are known to ensure the elastic return of the skin when stressed. They have a modulus of elasticity much lower than that of collagen fibres (*Table 1.2*), of the order of 0.1 MPa to 4.5 MPa [Silver *et al.*, 1992, 2001]; [Fung, 1993].

They are much more extensible than collagen, their rupture only occurs for deformations of a few hundred percent, 120 to 300%, and under low stresses of the order of 0.1 MPa [Silver *et al.*, 1992], hence their second name: elastic fibres. Their very high elongation capacity makes it necessary to use hyperelastic laws to describe their behaviour under large deformations. These fibres give the skin a high degree of extensibility and allow to maintain the tissue natural state of tension [Wilkes *et al.*, 1973].

1.3.1.C Other components

The ground substance represents about 20% of the dry weight of the dermis and has the characteristics of a semi-fluid gel [Wheater *et al.*, 2004] Its mechanical properties will therefore not be predominant in the mechanical response of the tissue [Silver *et al.*, 1992] However, it will play a role in the viscous component of the mechanical behaviour [Minns *et al.*, 1973]; [Hendriks, 2001].

There are also reticular fibres, which constitute only 0.4% of the dry weight of the dermis, whose properties are similar to those of collagen [Hendriks, 2001].

1.3.2 Non-linearity of the skin properties

The non-linear elasticity of the human skin was predicted in 1861 by Langer and demonstrated in 1966 by Daly. Skin extension will see a phase of tensioning of elastin fibres and orientation of collagen fibres to resist traction, followed by a phase of stretching of collagen fibres which explains the non-linearity.

The non-linear elasticity of skin, and more generally that of all soft collagenous tissues, can be illustrated in a uni-axial quasi-static tensile test by the typical stress-strain curve shown in Figure 1.24a.

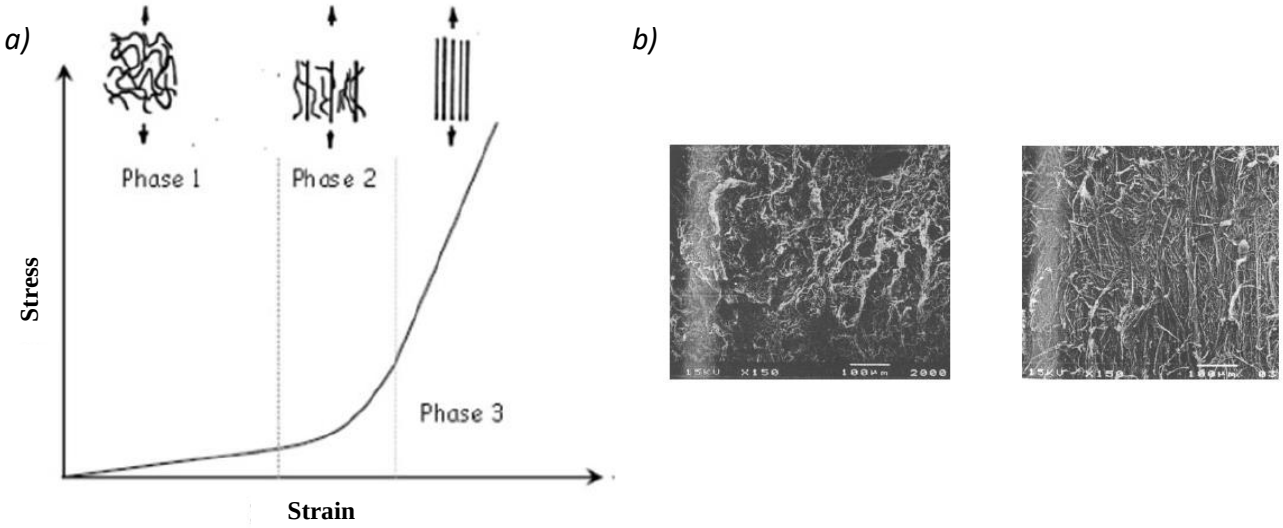

Figure 1.24: Non-linear behaviour of skin in tension. a) Typical stress-strain curve for skin and diagram of collagen fibres orientation – [Wilkes et al., 1973]. b) Scanning Electron Microscopy observation of rat skin collagen fibres: i) initail and ii) stretched state in tension – [Belkoff et al., 1991]

It is commonly described as a three-part curve [Holzapfel, 2000]; [Brown, 1973]:

+ In the first region, a high extension of the skin is observed under low loading. The stresses remain relatively low and the behaviour is linear. This observation can be interpreted on a microscopic scale by the elongation of the elastin fibres contained in the dermis, as these fibres have a lower elastic modulus than the collagen fibres. Indeed, in this phase, the collagen fibres are entangled and wavy, not contributing to the mechanical response of the material. [Schmid *et al.*, 2005] shows the increase in the period of waviness of collagen fibres in this first tensile phase. The elastin fibres are fully stretched, resulting in a linear isotropic behaviour in the absence of the effect of the collagen fibres [Silver *et al.*, 2003]. Elastin fibres are highly extensible and therefore contribute at the beginning of traction up to about 30% of deformation [Brèque, 2002]. At the molecular level, some authors suggest that elastin fibres can store energy during traction by transforming α-helices into other more extended conformations [Silver *et al.*, 2002].

+ The second region is a transition phase. For deformations between 30 and 60%, the stress as well as the stiffness increase. This is due to the reorientation and elongation of collagen fibres in the dermis, which have a higher modulus of elasticity than elastin fibres. The elastin fibres take over and solicit the collagen fibres which begin to respond mechanically to the solicitation. In fact, the collagen fibres, which are undulating in their natural state, progressively unfold to reorient themselves in the direction of traction. The process of unfolding and reorientation of the collagen fibres continues until about 60% deformation, the beginning of the last phase. This reorientation phenomenon, shown in Figure 1.24b, was studied by scanning electron microscopy on rat skin [Belkoff *et al.*, 1991].

+ The third region is a new linear region where we observe the stabilisation of the stiffness. This region reflects the elastic modulus of collagen fibres that are sufficiently aligned in the tensile direction and provide maximum strength [Bischoff *et al.*, 2000]. The linearity is due to

the behaviour of these collagen fibres. The stress increases linearly as a function of the deformation until rupture, which is manifested by the alteration of the collagen fibres, known as defibrillation [Wilkes *et al.*, 1973]; [Silver *et al.*, 1992]. This last phase marks the beginning of tissue failure, with a plateau of force followed by progressive rupture; the tissue is then damaged. The skin can usually withstand very high elongation, up to strains of over 50% [Silver *et al.*, 1992]; [Yamada, 1970].

The first phase (Phase 1 in Figure 1.24a) and the last phase (Phase 3 in Figure 1.24a) are almost linear and thus allow the definition of two elastic moduli, noted E_1 for the first phase and E_2 for the last. The values of E_1 vary between 5 and 700 kPa according to the authors [Brèque, 2002]; [Daly, 1982]; [Silver, 1987] whereas those of E_2 vary between 300 kPa and more than 100 MPa. Although these three phases are characteristic of the skin's response, a large number of authors limit themselves to global values of the modulus of elasticity, without specifying the part of the curve considered.

Unfolding of collagen fibres and their reorientation in the direction of loading seem to be accepted phenomena responsible for the non-linear tensile characteristic of a connective tissue [Roche, 1997]. Non-linear stiffening is generally interpreted as a way for soft collagenous tissues to meet two conflicting needs. Under relatively low stresses, the material must be easy to remodel, while at higher stresses, the tissue must be stiff enough to ensure cell and tissue integrity.

1.3.3 Viscoelasticity of the skin

Skin, like all soft collagenous tissues, is a viscoelastic material: it has both elastic and viscous characteristics. The first discovery of the viscoelasticity of skin was made by Wilkes [Wilkes *et al.*, 1973]. He found that skin has a dissipative behaviour probably due to the flow of fluid contained in the dermis' ground substance. However, the viscoelastic behaviour of the skin is only demonstrated for strains of less than 30% [Dunn *et al.*, 1983]. The viscous aspect therefore does not seem to be verified at large strains, at which the elastic component takes over from the viscous component.

The viscoelasticity of the skin can therefore be attributed to several factors, such as:

+ Fluid flows and the intrinsic viscoelasticity of the ground substance [Hendriks, 2001]. According to Wilkes [Wilkes *et al.*, 1973], the movements of this semi-fluid structure within the fibre network dissipate energy;

+ The intrinsic viscoelasticity of collagen fibres. Minns [Minns *et al.* 1973] showed the rate-dependent behaviour of collagen;

+ Dissipative friction between fibres and mesh rearrangement [Dellaleau *et al.*, 2008a]. Guimberteau [Guimberteau *et al.*, 2005] observed *in vivo* a phenomenon of sliding and reorganisation of the fibres, contributing to the dissipation of energy during stress;

It is likely that different structural levels contribute to viscoelasticity at one or more time scales [Xu *et al.*, 2008]; [Gautieri *et al.*, 2011].

The following are examples of experimental behaviours derived from different type of mechanical tests which can be attributed to the viscoelasticity of the skin:

+ Creep and relaxation tests. If the stress is held constant, the strain increases with time (creep) and if the strain is held constant, the stress decreases with time (relaxation) [Xu *et al.*, 2008]; [Barbenel *et al.*, 1977]. Relaxation experiments are shown in Figure 1.25a;

+ Incremental deformation tests. Incremental stress-strain curves are obtained by constraining the skin through a series of strain increments and allowing the stress to relax at each increment until it stabilises in the short term [Silver *et al.*, 2002]. The total instantaneous strain can be separated into an elastic and a viscous part. An incremental deformation experiment is shown in Figure 1.25b;

+ Cyclic loading, showing the presence of hysteresis [Liu *et al.*, 2010]; [Diridollou *et al.*, 1998]. An example is shown in Figure 1.25c;

+ The dependence of mechanical properties on strain rate [hergold *et al.*, 2006], **and on dynamic test frequency** [Lamers *et al.*, 2013]; [Nicolle *et al.*, 2023]. An example of strain rate dependence is shown in Figure 1.25d;

+ The dependence of mechanical properties on loading history [Shergold *et al.*, 2006]. In particular, it is possible to precondition, with repeated cycles at a given small strain: after a few cycles, the stress-strain curve converges to a single cycle, as shown in Figure 1.25c. This effect is close to the Mullins effect observed in elastomers [Diani *et al.*, 2009].

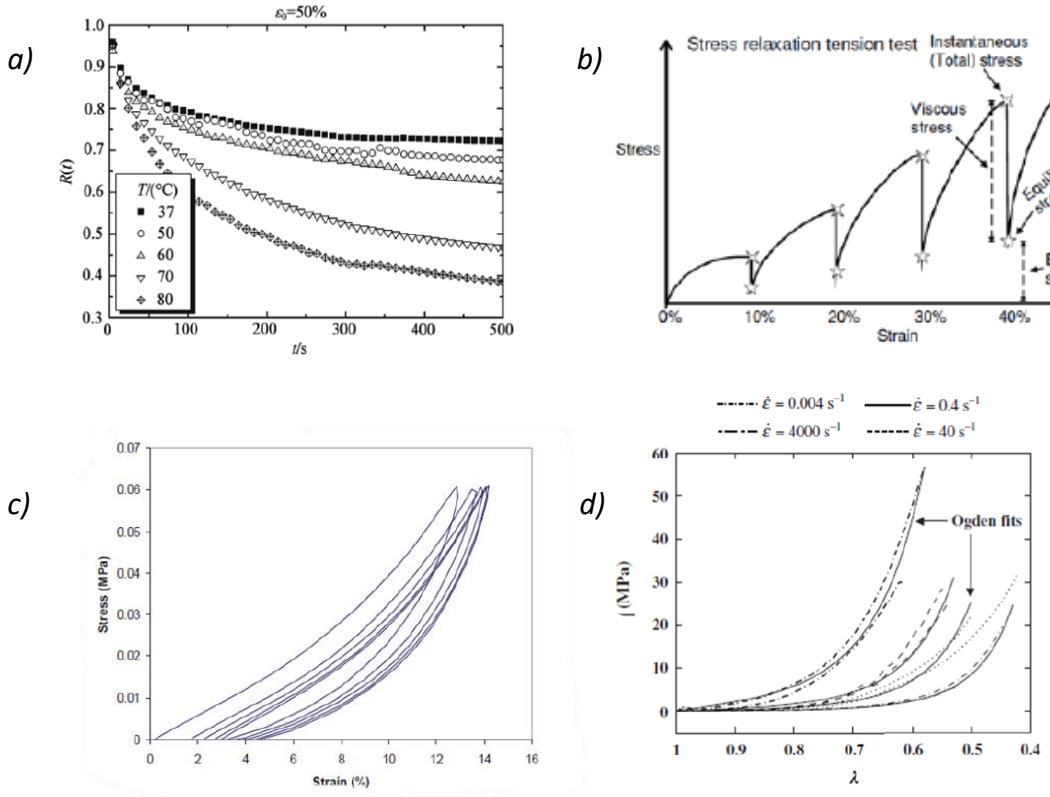

Figure 1.25: Mechanical tests revealing the viscoelastic properties of the skin: a) Relaxation experiments (strain held constant and stress released) – [Xu et al., 2008]. b) Typical curve of incremental strain experiments – [Silver et al., 2002]. c) Cyclic loading experiments. Loading and unloading curves are different (hysteresis), and cycles converge to a single curve after a few cycles (preconditioning) – [Liu et al., 2010]. d) Strain rate dependence. The faster the sample is stretched, the stiffer it appears – [Shergold et al., 2006]

These points imply that the response of the tissue will depend on the loading history. [Liu et al, 2008] showed that depending on the direction of loading, the number of cycles to stabilise the behaviour of the skin varies. Another effect that is also present and influences the time dependence of the behaviour is the Mullins effect or preconditioning effect, which corresponds to a reorganisation of the tissue during loading [Munnoz *et al.*, 2008]. Due to the viscoelasticity of the skin, preconditioning is important to study the mechanical behaviour of the skin.

1.3.4 Anisotropy and pre-tension state of the skin

Skin is an anisotropic material. Anisotropy is the property of being direction-dependent. Skin therefore has different mechanical characteristics depending on its orientation.

The first discovery of the anisotropy of human skin was made by Dupuytren [Dupuytren, 1834], who observed that circular wounds evolve into ellipses over time. This discovery was further investigated by the Austrian anatomist Karl Langer in 1861 [Langer, 1978]. He made circular incisions in cadavers to study the natural tension and anisotropy of the skin. He found that by drilling these circular holes in the skin of a corpse, the resulting wounds were ellipsoidal and always oriented in the same direction at a given point in the body, revealing the existence of a pre-stressed state (Figure 1.26a). By making several incisions close together, he was able to delineate and map lines of tension, called "Langer lines", shown in Figure 1.26b. Langer defines them as the major axis of the ellipse obtained after the circular incision. These skin tension lines represent the directions of maximum tension in the skin.

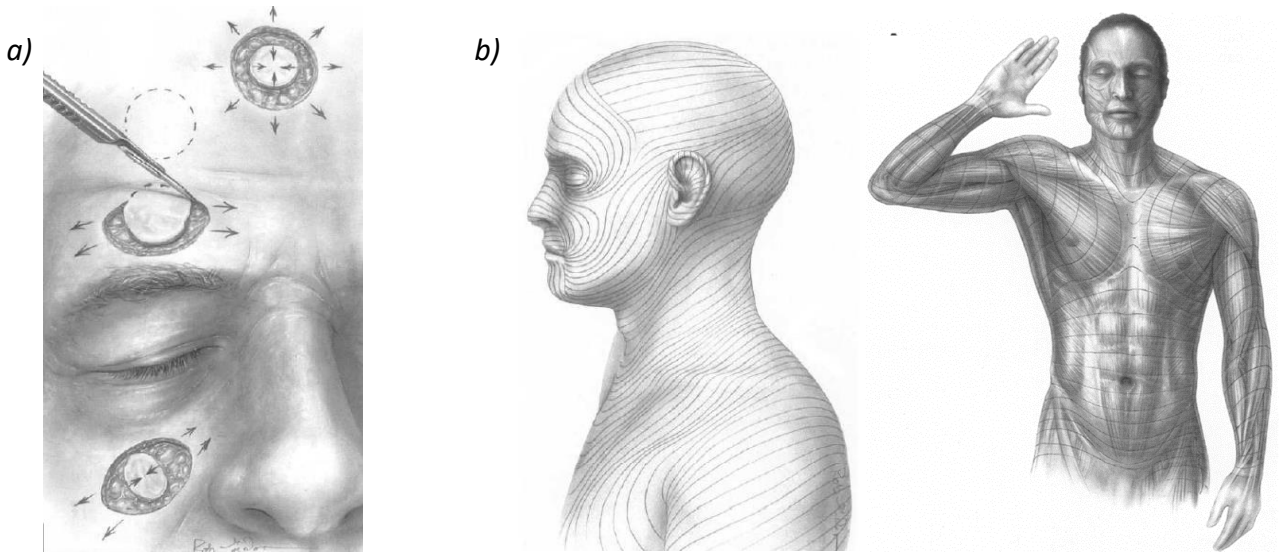

Figure 1.26: The state of skin pre-tension. a) Evolution of the shape of circular incisions made on the face. b) Schematic representation of the Langer Lines on the upper body and anterior trunk of a male – [Waldorf et al., 2002]

Langer lines are the visual representation of collagen fibres that lie in the dermis. These lines have a preferred direction parallel to the skin surface, indicating the dominant direction in which the collagen fibres tend to orient themselves [Holzapfel, 2000]. They are longitudinal in the face and limbs while they show circular patterns in the neck and trunk [Langer, 1978a,b,c].

The pre-tension due to Langer's lines varies with age, morphology of the individual, body position and direction of the fibres. In the longitudinal direction of the Langer lines, the pre-tension is of the order of 24 kPa; it is of the order of 9.3 kPa in the direction transverse to them [Drobez *et al.*, 2013]; [De Jong, 1995].

Growing in a prestressed environment, the skin develops a natural microstructural anisotropy, which is reflected in its mechanical properties. The first *in vivo* tensile tests, carried out using an extensometer, revealed that the deformation properties of the skin are influenced by the orientation of the sample in relation to the Langer lines [Ridge *et al.*, 1966]. Other research has also shown a strong dependence of skin mechanical properties on their orientation with respect to these skin tension lines, the Langer lines [Ayadh *et al.*, 2023]; [Ni Annaidh *et al.*, 2019]; [Groves *et al.*, 2013]; [Liang *et al.*, 2010].

Histological studies have also established a significant correlation between the orientation of Langer lines and the preferential arrangement of collagen fibres in the dermis [Ni Annaidh *et al.*, 2012]; [Ridge *et al.*, 1966]. The effect of fibre orientation during loading has been observed by many authors [Wilkes *et al.*, 1973]; [Liu *et al.*, 2008]; [Noorlander *et al.*, 2002]. Elastin and collagen fibres at rest are therefore more tense in the natural direction of tension [Zahouani *et al.*, 2006]; this results in a difference in elongation potential (less important) and stiffness (more important) in this direction compared to the others. Indeed, the maximum extension of the skin is obtained perpendicular to the Langer lines while the Young's modulus and ultimate tensile strength are higher along these lines [Stark, 1977]; [Gibson *et al.*, 1969].

Figure 1.27 shows the superposition of two stress-strain curves from tensile tests performed in directions perpendicular to each other, which demonstrates the highly anisotropic mechanical behaviour of the skin.

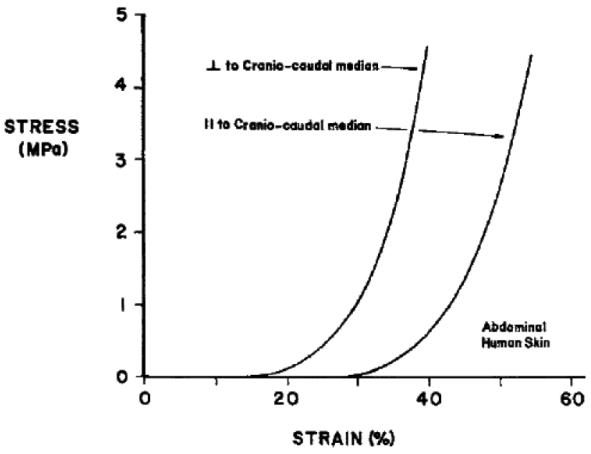

Figure 1.27: Stress-strain curves from abdominal skin tensile tests in mutually perpendicular directions (along and across the craniocaudal median) – [Daly, 1966]

Knowledge of the orientation of the langer lines is extremely important, especially for surgery. Indeed, the direction of the incisions is determined by the healing process. The surgeon prefers an incision parallel to the langer lines to a transverse incision (which would destroy the continuity of the collagen) in order to have better healing [Borges *et al.*, 1962]; [Tortora *et al.*, 2007]. It should be noted that wrinkles do not always correspond to Langer lines [Waldorf *et al.*, 2002].

1.3.5 Contribution of the different skin layers to the mechanical properties

The skin, a heterogeneous organ, is made up of three main layers with very different cellular composition and structure. Each skin component has a specific mechanical behaviour. Despite this complexity, the cohesion of the components and the perfect anatomical fit of the layers between them led some authors to consider the skin as a homogeneous material [Agache, 2000]. However, the individual behaviour of the different layers of the skin has been studied and most authors agree that the major mechanical constituent of the skin is the dermis [Diridollou *et al.*, 1998], [Silver *et al.*, 2001].

1.3.5.A The epidermis

The major mechanical role of the epidermis is that of the *stratum corneum*, whose hardness and high friction properties contribute greatly to the protection of the body. In terms of its contribution to the mechanical behaviour of the skin, the epidermis is of little importance. However, these mechanical properties are greatly influenced by environmental conditions.

Many investigations have been carried out concerning the *stratum corneum* and the effects of its hydration [Wildnauer *et al.*, 1971]; [Park *et al.*, 1972]; [De Rigal *et al.*, 1985]. The authors conclude that the higher the hydration level, the higher the elongation at break and the lower the Young's modulus of the *stratum corneum* (Figure 1.28a). The *stratum corneum* can therefore influence the total extensibility of the skin.

Temperature is also a factor influencing the mechanical properties of this layer. In the "physiological" temperature range: 30°C to 40°C, the Young's modulus of the *stratum corneum* falls sharply as the temperature increases, so that a "softening" of the *stratum corneum* is observed [Wilkes *et al.*, 1973] (Figure 1.28b).

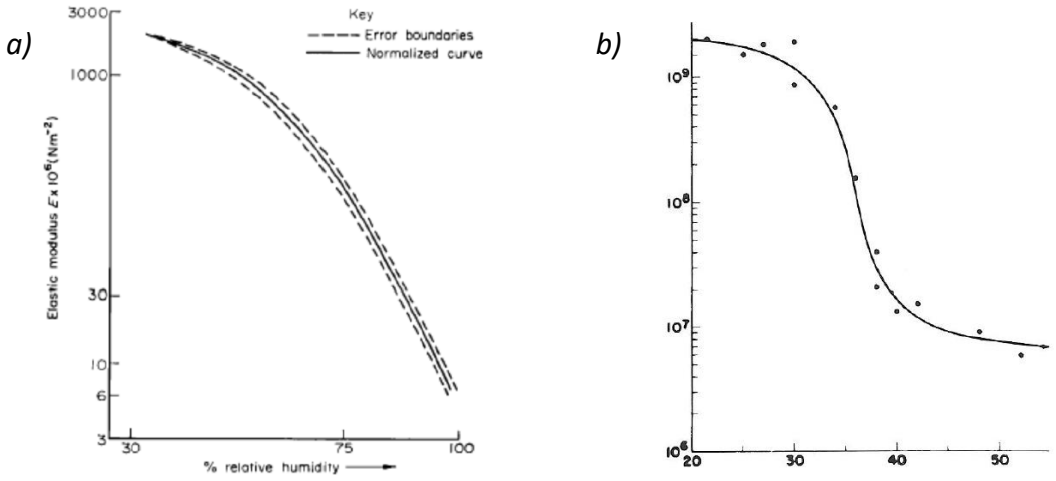

Figure 1.28: Variation of the Young's modulus (in Pa) of the stratum corneum as a function of environmental conditions. a) Variation of its relative hydration – [Park et al., 1972]. b) Variation of the temperature (in °C) – [Wilkes et al., 1973]

Thus, the mechanical properties of the epidermis are very variable according to environmental conditions, particularly those linked to its hydration and temperature. Finally, under fairly stable environmental conditions, studies agree that the influence of the epidermis on the overall

mechanical properties of the skin can be neglected as it only represents 10% of the total thickness of the skin [Silver *et al.*, 1992].

1.3.5.B The dermis

Most authors agree that the mechanical behaviour of the skin is mainly due to the dermis, and in particular to the collagen fibres which contribute strongly to the mechanical strength of the skin [Agache, 2000]; [Diridollou *et al.*, 1998]; [Dunn *et al.*, 1983]. Silver [Silver *et al.*, 2001] shows that the stiffness of total skin is equivalent to that of the fibres alone and Roeder [Roeder *et al.*, 2002] adds that the stress-strain curve of a reconstituted matrix of collagen fibres alone is similar to that of total skin.

The influence of the different components of the dermis on the overall behaviour can be studied using different treatments. Authors such as Yuan [Yuan *et al.*, 2000]; Black [Black *et al.*, 2005]; Jesudason [Jesudason *et al.*, 2007] have studied the effect of elastase and collagenase (destruction of elastin and collagen fibres) and have shown a decrease in the mechanical properties of the skin in both cases. These studies demonstrate the importance of the collagen fibre network but also that of elastin fibres despite their low proportion compared to that of collagen. Cavalcante [Cavalcante *et al.* 2005] also attributed to the proteoglycans of the ground substance a stabilising role in the collagen-elastin network. In addition to its viscous role, the ground substance therefore also plays a role in the structure of the skin itself.

It is therefore commonly accepted that the mechanical properties of the dermis depend mainly on the organisation of the collagen fibres but also on the network of elastin fibres, as well as on the viscosity of the ground substance [Lapière *et al.*, 1988]. More precisely, the deep dermis is very often considered as the strongest layer of the skin [Delalleau, 2007]; [Crichton *et al.*, 2011].

1.3.5.C The hypodermis

Some researchers have focused on the properties of the fatty layer, the hypodermis [Hendriks *et al.*, 2003]. For example, Gennisson [Gennisson *et al.*, 2004] found a shear modulus of 3 to 10 kPa by wave propagation.
Diridollou [Diridollou *et al.* 1998] showed that the influence of the hypodermis on the results is negligible due to its high deformation and low mechanical properties. Indeed, the hypodermis is a very loose tissue. Thus, most authors agree that the contribution of the hypodermis to the mechanical properties of the skin in tension is negligible [Silver *et al.*, 1992]; [Jacquemoud, 2007]; [Del Prete *et al.*, 2004].

As a result, the outermost layers (epidermis and hypodermis) do not contribute significantly to the mechanical properties of the skin. The dermis would thus be the main mechanical constituent of the skin.

1.3.6 Parameters affecting mechanical properties

The mechanical behaviour of the skin *in vivo* is influenced by different parameters such as the rate at which external stress is applied, the direction of the applied external mechanical stress, the anatomical location of the measurements or age.

In *ex vivo* tests, the wide variety of experimental protocols should further encourage caution when comparing two studies or matching the model to the experiment. Indeed, many additional variables can influence the results, such as:

- Sample preparation: tested just after excision, frozen, with layers or hairs removed.
- The method of hydration: immersed, sprayed, gel-coated, no hydration.
- The method of clamping: grips, clips with sandpaper, sewn with silk threads.
- Measurement parameters: pre-conditioning or not, strain rate, cycles, maximum stretch rate.

1.3.6.A Strain rate

Although Lanir [Lanir *et al.*, 1974] identified only a small variation in the mechanical properties of rabbit skin with strain rate, several other authors observed a significant influence of strain rate on the properties of connective tissues subjected to tension [Roeder *et al.*, 2002].

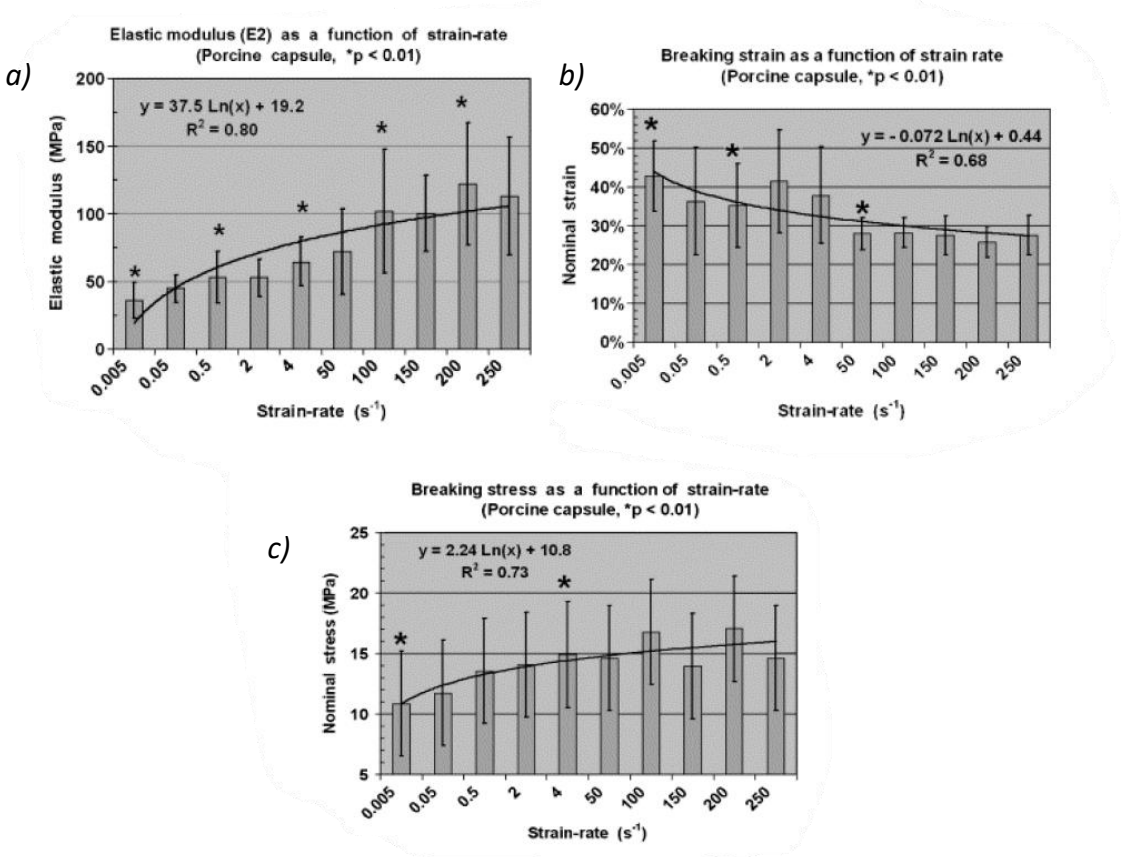

Figure 1.29: Effect of strain rate (0.005 to 250 s^{-1}) on the mechanical properties of a porcine kidney capsule. a) Effect on E_2 modulus of elasticity (last tensile phase). b) Effect on strain at break. c) Effect on stress at break – [Snedeker et al., 2005]

As shown in Figure 1.29, Snedeker [Snedeker *et al.*, 2005] observed an increase in both the elastic modulus E_2 and the stress at break with increasing strain rate; conversely, the strain at break decreases with increasing strain rate. These variations in mechanical properties are generally observed for speeds corresponding to quasi-static tests [Agache, 2000].

1.3.6.B Direction of loading

The marked mechanical anisotropy of the skin has an influence on the measured parameters. Yamada [Yamada, 1970] and Wijn [Wijn, 1980] have noticed different stress and strain values at failure in two perpendicular directions of loading (Figure 1.30). The different authors agree that the extensibility is lower and the stiffness higher in the directions where the skin is in a natural pre-tension state.

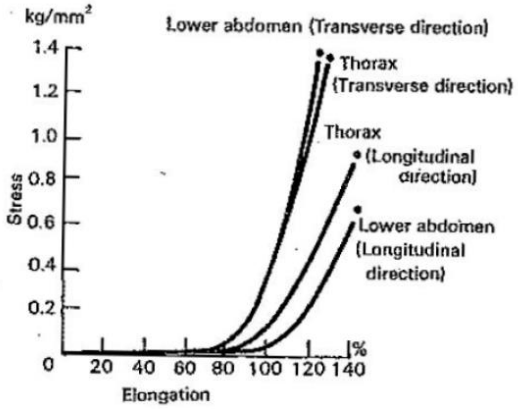

Figure 1.30: Stress-strain curves of human skin in tension in two perpendicular directions – [Yamada, 1970]

1.3.6.C Fibre density

The mechanical properties of the skin vary according to its location on the body [Yamada, 1970]. Indeed, the thicker the skin, the more fibres it will contain in the dermis, and the better the mechanical properties. For example, thick skin on the back will have a higher stress at break than thin skin on the eyelids. A high density of collagen fibres will therefore provide high strength to the skin as shown in Figure 1.31 [Vitellaro *et al.*, 1994]; [Roeder *et al.*, 2002].

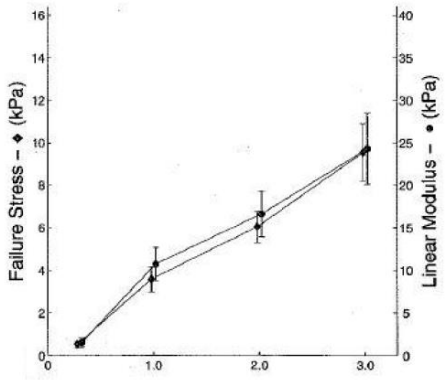

Figure 1.31: Evolution of the stress at break as a function of the collagen concentration of a collagen fibre network reconstituted from calf skin – [Roeder et al., 2002]

1.3.6.D Age

Studies of ageing show that various degradation mechanisms modify the microstructure of the skin over the years [Frances *et al.*, 1990]. In the dermis, there is a change in the activity of the fibroblasts which synthesise fewer fibres and which, as they age, produce more and more enzymes which destroy the fibres [Robert *et al.*, 2009]. In addition, the dermis decreases in thickness: -30% at 50 years of age and -50% at 80 years of age. These phenomena are mainly responsible for the decrease in the quantities of collagen and elastin fibres essentially after the age of 30 [Vitellaro *et al.*, 1994]; [Belkoff *et al.*, 1991]. Finally, Agache [Agache, 2000] observed a decrease in the level of proteoglycans in the ground substance making it more fluid.

These microstructural modifications concerning the fibres and the ground substance seem to be at the origin of the variations observed in the mechanical properties of the skin on a macroscopic scale. Indeed, the skin loses elasticity [Finlay, 1970]; [Agache *et al.*, 1980]. Strain levels for the same stress decrease, i.e. the length of the first tensile phase is reduced with age [Daly *et al.*, 1979]; [Gniadecka *et al.*, 1994]. As for the fracture characteristics, their values decrease with age in terms of stress and strain [Yamada, 1970].

1.3.7 Synthesis of the mechanical properties of the skin

Human skin, as seen by a mechanic, can be likened to a multi-layered composite material. Each of these layers, due to its own composition and thickness, ensures a different mechanical function. However, when the skin is subjected to tensile stress, only the dermis provides significant resistance thanks to its complex fibrous structure. The dermis is in fact classified as a dense connective tissue, and is therefore made up of a ground substance within which two networks of fibres are interwoven: collagen and elastin. It is mainly these fibres that ensure the skin's resistance to traction and their diversity means that the skin's behaviour is relatively complex. Due to the important role played by the dermis and in correlation with its microstructure, it follows that human skin has a complex anisotropic, non-linear, viscoelastic and pretensioned mechanical behaviour *in vivo*.

Under tensile load, the overall response of the skin is characterised by a stress-strain curve that could be described as bilinear in the elastic domain (or even hyperelastic), where each phase is interpreted by the role played by each of the families of fibres. Indeed, elastin fibres provide the elasticity to the skin at the beginning of traction and are responsible for its low elastic modulus during the first phase of traction, whereas collagen fibres resist large deformations after having unfolded and reoriented themselves in the direction of traction. The stiffer collagen fibres contribute to the high elastic modulus of the skin in the second tensile phase.

Studies on human skin show very scattered results concerning its mechanical properties. A summary of the literature data concerning the values of the elastic modulus or Young's modulus obtained in experimental tensile studies on skin is presented in Table 1.3. This table illustrates the diversity of modulus values measured on the skin, with a variation of 3 orders of magnitude. The diversity of

the types of loading, the intensity of the applied force, the rheological models developed and the anatomical sites may explain the large differences observed. In addition to these differences in protocol and experimentalist, there is a variation in mechanical properties within the same study, depending on a multitude of parameters, either related to the characteristics of the subject (age, sex, environment), or related to the sample taken (site, direction). Most of these parameters affecting the mechanical properties of the skin are often related to its structure and more precisely to the properties of its fibre network: preferred orientation and density of the fibres.

Finally, the mechanisms of connective tissue degradation are responsible for structural modifications on a microscopic scale (at the level of the ground substance and the fibre network of the dermis), which lead to variations in the mechanical properties of the skin on a macroscopic scale. Thus, the properties of human skin would be defined as "optimal" until about age 30 [Vitellaro *et al.*, 1994]; [Yamada, 1970], at which age degradation begins.

Table 1.3: Mechanical properties of the skin obtained in tensile studies from the literature.

Skin type	Elastic modules			References
	E_1	E_2	E_{global}	
Ex vivo pig skin			15 MPa	[Ankersen *et al.*, 1999]
Ex vivo human skin	< 7 kPa	510 kPa		[Agache, 2000]
Ex vivo rat skin			14 - 36 MPa	[Belkoff *et al.*, 1991]
Ex vivo pig skin (longitudinal axis / transversal axis of the body)	0,.0 - 1.25 MPa / 1.15 - 1.8 MPa	35.5 - 37.9 MPa / 70 - 118 MPa		[Brèque, 2002]
In vivo human skin - forearm	0.42 MPa	0.75 MPa		[Clark *et al.*, 1996]
Ex vivo human skin - abdomen	5 kPa			[Daly, 1982]
Ex vivo human skin - abdomen			30 MPa	[Daly *et al.*, 1979]
In vivo human skin			0.35 - 0.5 MPa	[Delalleau *et al.*, 2008a]
In vivo human skin	0.06 - 0.09 MPa	0.22 - 0.28 MPa		[Delalleau, 2007]
Ex vivo mouse skin	1.7 - 2.1 MPa	1.5 MPa		[Del Prete *et al.*, 2004]
Ex vivo human skin - back			99 MPa	[Gallagher *et al.*, 2012]
Ex vivo human skin (forehead, forearm, temporoparietal, neck)			0.3 - 1.3 Mpa	[Griffin *et al.*, 2017]
Ex vivo human skin - forehead	6 MPa	20 MPa		[Jacquemoud, 2007]
Ex vivo human skin - forehead (longitudinal axis / transversal axis)			E// = 14 MPa E⊥ = 140 MPa	[Jacquemoud *et al.*, 2007]
In vivo human skin - arm			1 - 10 MPa	[Jacquet *et al.*, 2008]
In vivo human skin - forearm (longitudinal / transversal axis)			E// = 0.65 MPa E⊥ = 1.30 MPa	[Khatyr *et al.*, 2004]
In vivo human skin - calf (longitudinal / transverse axis)			E// = 20 MPa E⊥ = 4,6 MPa	[Manschot *et al.*, 1986]
Ex vivo human skin - middle of the back (parallel / perpendicular / at 45° to the Langer lines)	0.9 - 1.3 Mpa		60 - 120 Mpa	[Ni Annaidh *et al.*, 2012]
Ex vivo human skin - abdomen			70 -220 MPa	[Ottenio *et al.*, 2015]
Ex vivo human skin - child/adult			3 / 20 MPa	[Rolhaüser, 1950]
Ex vivo human skin 23 / 87 years old	2.1 / 0.6 MPa	41 / 15 MPa		[Silver *et al.*, 2002]
Ex vivo human skin	0.1 MPa	20 MPa		[Silver *et al.*, 2001]
Ex vivo human skin			6 - 35 MPa	[Silver *et al.*, 1992]

1.4 Techniques for characterising human skin

Biomechanical analysis of the skin is fundamental to quantify and qualify the behaviour of a living tissue. It is an essential element to facilitate the development of tissue engineering and the development of certain care devices.

Mechanical testing is used to characterise the mechanical properties of skin tissue. Most researchers have used and are using standard mechanical characterisation techniques such as *ex vivo* traction or *in vivo* torsion, but many other techniques exist.

In addition to these mechanical techniques, known as direct techniques, there are also indirect techniques to examine the internal structure of the skin tissue. Indeed, with the help of evolving technology, new rigorous imaging techniques are available that provide additional characterisation for studying human skin. These imaging techniques allow to obtain observations on tissues in a non-invasive, deep and very precise way. In order to obtain a complete characterisation of the skin, a combination of a mechanical and an imaging technique may also be possible.

The most commonly used mechanical and imaging techniques in the literature for biomechanical characterisation of human skin are presented in this Section.

1.4.1 Direct techniques

Measuring the mechanical properties of the skin is generally of threefold interest [Tran, 2007]:

- to obtain a description of the natural history of the skin over the years, in particular during growth and ageing phases.
- to have a method of objective evaluation of the effect of certain medical or cosmetic products
- to observe and quantify skin pathologies that can lead to an alteration in mechanical properties, such as scleroderma, collagenosis or hyperkeratosis for example.

The importance in dermatology and cosmetology of describing or measuring the mechanical behaviour of the skin has led to the development of numerous measurement methods and equipment [Payne, 1991]. The most commonly used techniques in the literature are traction, torsion, suction and indentation [Pierard, 1999]; [Groves, 2011]. The tests can be performed in-plane, such as torsion and tensile tests, or perpendicular to the skin surface, such as suction and indentation tests, and provide access to several types of parameters. Tests performed in the surface plane of the skin rely mainly on the properties of the epidermis and upper dermis, while for tests performed perpendicular to the surface, all skin layers contribute to the measured mechanical properties [Groves, 2011].

Finally, some of the techniques mentioned above have led to commercialised devices. All these techniques for characterising the mechanical properties of human skin will be presented in this Section. Before that, a presentation of the general conditions of measurement on the skin is made to clearly identify the constraints and the difficulty of carrying out measurements on skin tissue.

1.4.1.A General information on measurement conditions

The mechanical characterisation of the skin can be carried out according to three approaches, depending on the state of the tissue at the time of testing:

***+ In vivo* (Latin: "within the living").** This term refers to research or examinations carried out on a living organism. Clinical trials are a form of *in vivo* research, in this case on humans. It is the most realistic of all living conditions, but also the most experimentally complex. In addition, numerous regulations must be respected [ANSM, 2013]. The measurement must be non-invasive and non-destructive for the living organism, which imposes work at low or medium deformations. The *in vivo* tests evaluate the properties of the skin in its natural state of pre-stress and hydration. The experiments were mainly performed on humans.

+ *Ex vivo* (Latin: "outside the living"). This expression means that the operations are performed outside the living organism. In general, the piece of tissue is taken from a living subject or cadaver, and then a suitable geometrical cut is made to obtain the desired test piece in order to perform the tests under controlled conditions. *Ex vivo* testing has the advantage of allowing the exploration of a wide range of parameters. Skin can be isolated from fat, muscle and bone to characterise only its properties, not a set of tissues. The same is true for skin layers, which can also be isolated for independent testing. While with *in vivo* analysis only the upper layers of the skin are accessible, *ex vivo* analysis allows the entire depth of the tissue to be tested. In addition, the mechanisms of rupture can be assessed by destructive tests that are not available *in vivo*. Finally, another key advantage of *ex vivo* testing is that samples can be modified or attacked with chemicals. This method can be used to vary the proportions of collagen [Del Prete *et al.*, 2004], elastin [Oxlund *et al.*, 1988] and proteoglycans [Eshel *et al.*, 2001] within the dermis. Finally, *ex vivo* results can also be used as a database to compare real tissues and their tissue engineered mimics.

Although they allow a control of the experimental conditions, several factors influence the *ex vivo* state. Indeed, these tests isolate the tissue from its natural environment, which facilitates the identification of skin properties, but removes the natural pre-stress and control of hydration. In addition, tissue preparation is an inevitable source of damage: from extraction to potential preparation, the tissue may deteriorate (e.g. loss of ground substance during ablation [Daly, 1966]). This inevitably results in different mechanical characteristics from those measured by *in vivo* analysis. It should be noted that freezing has often been used as a method of optimal conditioning of *ex vivo* skin for experimental purposes [Gahagnon, 2009]; [Moon *et al.*, 2006]

***+ In vitro* (Latin: "in the glass").** Like the *ex vivo* test, the *in vitro* test is conducted using components of an organism that have been isolated from their usual biological environment. The test is carried out under artificial conditions or in culture (e.g. cell culture). *In vitro* tests generally involve cell lines, proteins, and reconstituted models of human epidermis, for example. Although they allow individual parameters to be studied, *in vitro* test conditions are far from the real conditions present in a living organism.

While *in vitro* and *ex vivo* tests can use "conventional" devices, *in vivo* tests generally require specific devices depending on the objectives.

1.4.1.B Solicitations parallel to the surface

In this Section, mechanical stresses are applied in the plane of the skin. These tests correspond to an application of tensile and shear stresses to all skin layers.

i) Ex vivo tensile test

Three types of skin tensile tests are found in the literature: uniaxial tensile [Jansen *et al.*, 1958], biaxial tensile [Lanir *et al.*, 1974] and multiaxial tensile [Reihsner *et al.*, 1995].

The uniaxial skin tensile test is a standard tensile test: the skin is stretched parallel to its surface with a constant stretching speed. This test consists in establishing the relationship between the elongation resulting from a relative displacement of its two ends at a constant speed and the force required to obtain this elongation.

Tensile tests have been widely used to identify the mechanical parameters of the skin [Edwards *et al.*, 1995]. In particular, they allow the study of the viscoelastic mechanical behaviour and anisotropy of the skin. They are mainly carried out on skin samples taken from cadavers or from post-operative waste. Conventional (dumbbell-shaped) tensile specimens are most often used [Belkoff *et al.*, 1991]; [Brèque, 2002]; [Ni Annaidh *et al.*, 2012]; [Yamada, 1970]. Soft tissue attachment systems are designed to fit small sample sizes and hold the tissue without alteration. The most common solutions are systems of sandpaper-covered plates or equivalent that are clamped onto the skin sample [Mansour *et al.*, 1993]. On the same principle, protocols use cyanoacrylate glue to fix the sample to jaws [Gerin, 2012]; [Barbenel *et al.*, 1977]. A diagram of tensile tests is shown in Figure 1.32.

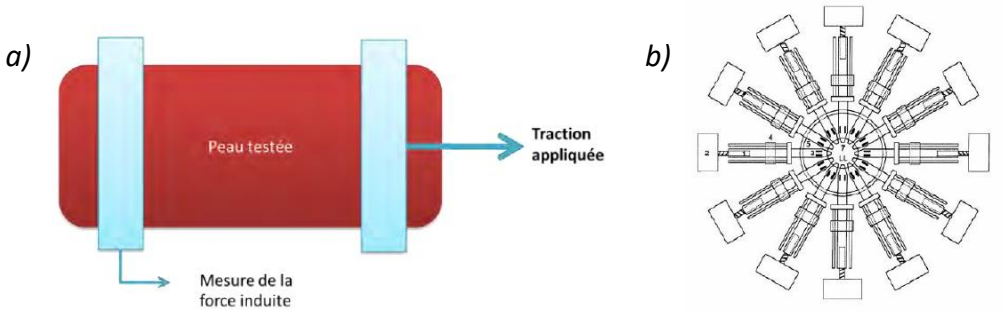

Figure 1.32 : Schematic of ex vivo tensile tests. a) Uni-axial tensile – [Pan et al., 1998]. b) Multi-axial tensile with 12 axes – [Reihsner et al., 1995]

In the literature, many tensile tests have been performed on different sites of the human body to study the mechanical properties of skin tissue. Some of the studies include: [Daly, 1982]; [Dunn *et al.*, 1983]; [Manschot *et al.*, 1986]; [Mansour *et al.*, 1993]; [Meijer *et al.*, 1999]; [Sacks, 2000]; [Zeng *et al.*, 2001]; [Del Prete *et al.*, 2004] and [Gahagnon, 2009].

These tests provide a standard mechanical assessment that is easy to implement. They are also easily transposable to reconstructed skins. However, this mechanical test requires the *ex vivo* collection of skin fragments. This implies numerous difficulties related to the sampling (delicate cutting, difficult calibration of the skin, taking into account pre-tension constraints, retraction of the specimen), and to the preservation (management of dehydration) of *ex vivo* skin samples [Dellaleau, 2007].

ii) Extensometry test

The extensometry test, also known as the extension test, is an *in vivo* tensile test. It involves tensile loading of the skin with two pads attached, usually one movable and one fixed or both movable pads moving in opposite directions (Figure 1.33). The device is equipped with a force transducer to measure the force induced by the tissue following the application of the stretch and an optical system to visualise the displacement of the tissue. Adhesion must be perfect between the pads and the skin surface; generally, a cyanoacrylate glue is used to ensure this fixation. Other authors [Vescovo *et al.*, 2002]; [Khatyr *et al.*, 2004] use suction gluing of the pads. Several research devices have been developed but only one device performing these extension tests has been commercialised: the *Extensometer®* (Cutech).

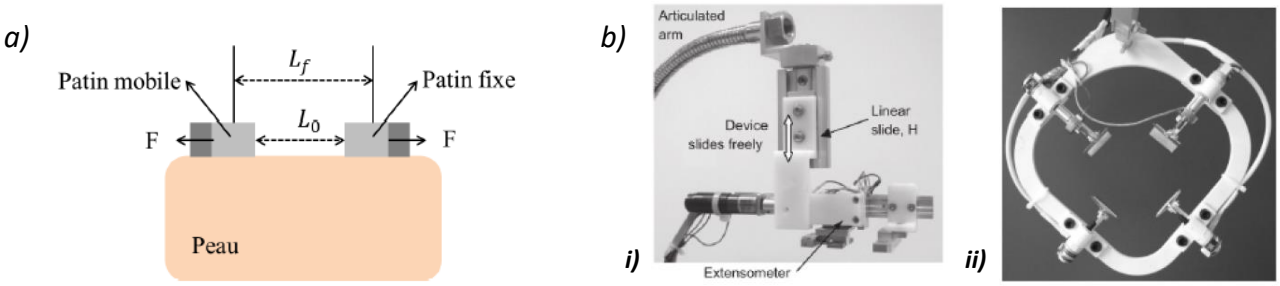

Figure 1.33: Extension tests. a) Schematic diagram of the test principle (L_o = initial pad spacing, L_f = final spacing) – [Azzez, 2019]. b) Extensometers used in vivo: i) uni-axial extensometer – [Lim et al., 2008]. ii) biaxial extensometer – [Capek et al., 2010]

It is a directional test that quantifies the anisotropy of the skin, characterises its elasticity and identifies its natural tension lines. However, the skin extension test is not a standard tensile test in which the experimental conditions are well defined. The test is performed under ill-defined initial and boundary conditions that depend on the anatomical area of the subject's skin. Indeed, during an extension test, the zone of the skin loaded between the pads (called the useful zone) is difficult to define in geometry and dimensions. In fact, not only is the useful zone loaded, but also the entire zone peripheral to the useful loading zone, both in terms of surface and thickness [Jacquet *et al.*, 2008]. Depending on the anatomy and the location of the test, it is difficult to delimit this peripheral zone whose response to the load may be unknown.

Numerous investigations using the extension test have been carried out to determine the mechanical properties of the skin, including the studies of different teams. [Evans *et al.*, 1967]; [Gibson *et al.*, 1969]; [Hutton *et al.*, 1975]; [Barbenel *et al.*, 1977]; [Gunner *et al.*, 1979]; [Leveque *et al.*, 1980]; [Barnhill et al, 1984]; [Diridollou, 1994]; [Asserin, 1996]; [Marcellier *et al.*, 2001]; [Vescovo *et al.*, 2002]; [Alexander *et al.*, 2006]; [Jacquemoud, 2007] and [Delalleau *et al.*, 2008a].

The advantage of this test is that it is directional and therefore allows for an in-depth study of the anisotropy of the skin tissue. Furthermore, it is performed in the plane of the skin and does not stress the underlying structures. However, the studies conducted show that the area around the pads has a significant influence on the measurements. The provision of follower pads, additional pads that protect the measurement area from peripheral forces, may be a possible solution to minimise this effect [Lim *et al.*, 2008].

iii) Torsion test

The torsion test involves the application of shear to the skin surface. A torsion is applied to a ring of skin placed between a central disc (movable to induce the torsion) and another peripheral disc (immovable to isolate the area of skin to be studied). The two discs are bonded to the skin, usually with a double-sided adhesive [Agache, 2000], and a constant torque is imposed on the central disc (Figure 1.34). The measured deformation is the angle of rotation of the skin enclosed between the two discs. The angle of rotation or twist of the skin is thus measured as a function of time and torque. It depends on the elasticity and viscosity of the skin, two parameters obtained with this test.

The most commonly used torsion device, or twistometer, in clinical and research settings is the *Dermal Torque Meter®* (DIA-Stron). The *DTM* is used to assess the suppleness and firmness of the skin mainly in the field of cosmetics by observing the return of the skin to its mechanical equilibrium state. It should be noted that particular attention must be paid to its handling during the test since this device is hand-held.

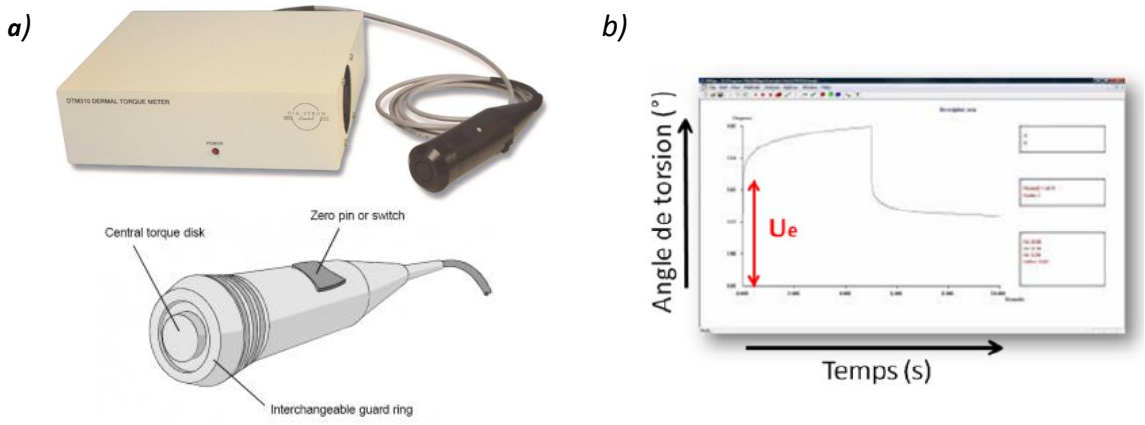

Figure 1.34: Torsion tests: torsion device (DTM). a) Device and probe. b) Torsion curve obtained – [Chartier, 2017]

The mechanical loading of the different skin layers depends on the applied torque and the width of the skin ring under test. The use of discs of different diameters allows the depth of loading to be varied and therefore the behaviour of one skin layer to be studied preferentially to another [De Rigal *et al.*, 1985].

Several researchers have been interested in *in vivo* torsion testing. [Daly, 1966]; [Finlay, 1970]; [Sanders, 1973]; [Leveque *et al.*, 1980]; [Agache *et al.*, 1980]; [Auber *et al.*, 1985]; [Escoffier *et al.*, 1989]; [Edwards *et al.*, 1995] and [Delalleau, 2007].

Torsion tests have several advantages. Firstly, they are simple in design and can be performed *in vivo*. They stress the skin in a tangential plane, minimising the influence of underlying structures. Finally, these tests allow the calculation of the shear modulus and the elasticity modulus of the skin. However, the torsion test is axisymmetric and therefore does not allow the study of the anisotropy of the skin [Vescovo *et al.*, 2002] whose effect is averaged [Hendriks, 2005]. Another disadvantage of this device is that it can only be used in reasonable deformation domains (the measurement frame should not exceed 10° of angle variation) because, beyond that, the analytical formulations become complex [Delalleau, 2007].

1.4.1.C Solicitations perpendicular to the surface

In this Part, mechanical stresses are applied perpendicular to the skin surface. These tests stress all layers of the skin by compression or suction.

i) *Suction test*

The suction test consists in applying, perpendicular to the skin and for a few seconds, a vacuum within a suction chamber glued to the skin surface. The skin deforms due to the decrease in pressure inside the chamber. It will form a hemispherical cap, the deflection of which is measured as a function of time and applied vacuum (Figure 1.35). Once the vacuum is removed, the deflection is measured until the skin returns to its original state. A typical test involves the near-instantaneous application of a vacuum and then maintaining it for a specified time (similar to a creep test). Optical or ultrasonic imaging techniques are used in conjunction with suction tests to visualise and measure the movement of the skin [Agache, 2000].

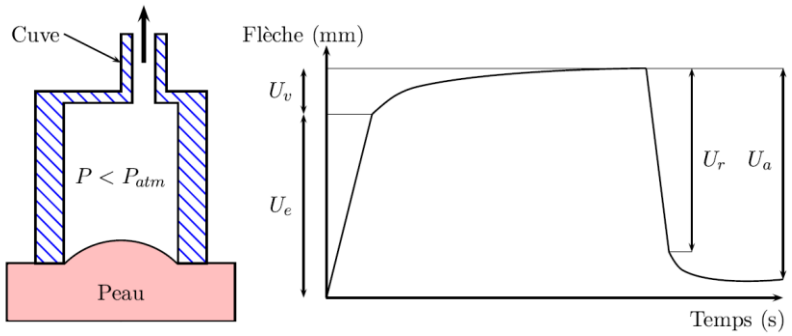

Figure 1.35: Schematic diagram and typical suction test curve – [Agache et al., 1980]

Ratios of characteristic displacement amplitudes during the suction and relaxation phases are used to obtain the mechanical parameters of the skin. As shown in Figure 1.35, some parameters can be measured directly, namely: U_e (the instantaneous extensibility), U_v (the skin creep, viscous contribution), U_r (the instantaneous elastic return) and U_a (the total return). These parameters vary according to the vacuum which depends on the suction device.

Several suction devices are commonly used by researchers and clinicians, including the *Dermaflex®* (Cortex Technology) and the *Cutometer®* (Courage & Khazaka) which use an optical system for skin surface elevation measurements [Hendriks, 2005].

In a suction test, the size of the chamber and the applied vacuum are two important factors in measuring the behavioural parameters of the stressed skin. The use of different opening diameters allows the different skin layers to be mechanically stressed. As the aperture diameter increases, the deeper layers are stressed during suction [Hendriks *et al.*, 2006]; [Delalleau, 2007]; [Hendricks *et al.*, 2003].

[Grahame *et al.*, 1969]; [Cook *et al.*, 1977]; [Alexander *et al.*, 1977]; [Diridollou *et al.*, 1994, 1998, 2000, 2001]; [Dobrev, 2000]; [Vogt *et al.*, 2003]; [Dobrev, 2005]; [Gniadecka *et al.*, 2006]; [Stroumza *et al.*, 2015] et [Rosado *et al.*, 2015] were interested in the suction test.

Suction tests have the advantage that they can be performed *in vivo*. They are therefore easily implemented and allow the measurement of many parameters. However, the interpretation of the results is complicated [Khatyr *et al.*, 2004].

ii) Indentation test

Among the various methods of mechanical testing, indentation testing is one of the most widely used techniques for determining the mechanical behaviour of skin *in vivo*. It consists of applying a load (pressure force) to the skin through an indenter and measuring the indentation it produces on the tissue surface. The load is applied perpendicular to the skin surface. The depth of penetration under the applied load is measured and allows the determination of the viscoelastic properties of the skin. These tests can be carried out in the quasi-static regime, with imposed load, with imposed penetration, under harmonic stress, with or without contact. In addition, they are often coupled with imaging methods (magnetic resonance imaging in particular) which allow the identification of the deformed skin strata and thus to deduce their contribution to the overall mechanical behaviour.

The diagram and a typical indentation test curve are shown in Figure 1.36. In this Figure, the first part [OA] corresponds to the load of the indenter and the second part [AB] corresponds to the discharge. The difference in the areas under the curves corresponds to the dissipation of the material. Finally, the part [BC] corresponds to the adhesion between the indenter and the material.

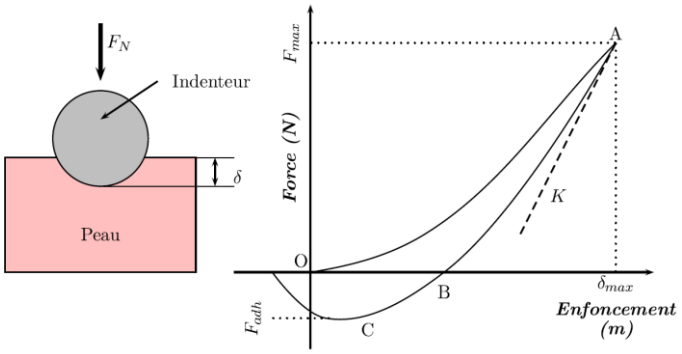

Figure 1.36: Diagram of the principle and typical curve of an indentation test – [Boyer, 2010]

The important parameters during an indentation test are: the indentation load, the indentation depth, the indenter geometry, and the indenter radius. The variation of these parameters allows the mechanical loading of the different skin layers.

Numerous works using the indentation test have been carried out to determine the mechanical properties of the skin. [Shade, 1912]; [Kirk *et al.*, 1949, 1962]; [Dikstein *et al.*, 1979, 1983, 2006]; [Lanir *et al.*, 1990, 1993]; [Zheng *et al.*, 1996,1999]; [Pailler-Mattei et al, 2006, 2008]; [Jachowicz *et al.*, 2007]; [Tran, 2007]; [Boyer *et al.*, 2009, 2012]; [Zahouani *et al.*, 2009, 2011] and [Kearney *et al.*, 2016].

These tests thus provide access to numerous parameters allowing in-depth characterisation of the skin tissue. The particularity of these tests is that they allow to study the behaviour of the skin by compressibility, whereas the other tests stress the skin by extensibility. They are relatively old and have the advantage of many years of theoretical studies, particularly those developed for the characterisation of the hardness of steels. However, characterisation by indentation of thin tissues

is extremely delicate. The penetration depths and the diameter of the indenters must be small in order to limit the contribution of subcutaneous structures [Delalleau, 2007].

iii) Ballistometry test

The ballistometry test consists in measuring the successive rebounds of a mass of very low weight falling on the skin (Figure 1.37). The mass impacting the skin will then oscillate and the movement of the skin is measured until it returns to equilibrium using an optical sensor. The energy applied by the mass to the skin is controllable in order to stress the different layers of the skin. This simple device, which allows *in vivo* measurement of skin properties, is widely marketed: the *Ballistometer®* (Monaderme) is an example.

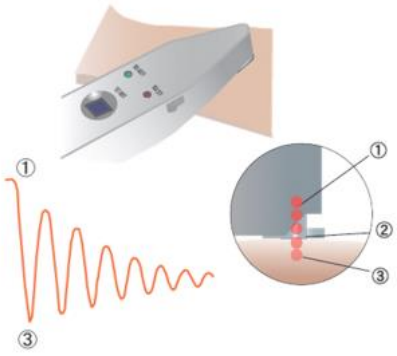

Figure 1.37: Diagram of a ballistometer – [Du Pont De Romemont, 2014]

During impact, the elastic components of the skin store the kinetic energy released by the falling mass. The consequence of the release of this energy is the rebound. The energy loss is related to the viscosity of the tissue, resulting in a smaller rebound [Tosti *et al.*, 1977]. The fundamental parameter of this test is the coefficient of restitution. This method has been used in studies of the mechanical properties of stratum corneum and skin: [Fthenakis *et al.*, 1991]; [Jemec *et al.*, 2001] and [Hargens, 2006].

The ballistometry test is simple, it does not require attachment to the tissue and the evaluation of the curves is straightforward. However, the interpretation of the results and the identification of the mechanical parameters are very difficult because this method involves the underlying tissues in a dynamic way.

1.4.1.D Summary of direct techniques

The mechanical tests most commonly used to characterise the mechanical properties of the skin fall into two main categories: *ex vivo* tests and *in vivo* tests. *Ex vivo* tests are mostly uni-axial, biaxial or multiaxial tensile tests performed on skin taken from a body. *In vivo* tests are various and differ according to the type of loading and the way it is applied. These *in vivo* tests are also divided into two categories: (i) to apply a load in the plane of the skin, such as extensometry and torsion, and (ii) to apply a load perpendicular to the skin surface, such as suction, indentation or ballistometry.

In the literature, numerous studies on the skin are carried out using various mechanical measurement systems. Table 1.4 illustrates the variety of Young's modulus and shear modulus values measured on the skin using these direct techniques (with the exception of the tensile and extensional test results presented in Part 1.3.7). Few means of comparison between these different methods are available as each test is independent and each makes different assumptions in order to analyse the results.

The different mechanical tests discussed all provide relevant information characterising the behaviour of the skin and their interest lies in the need to multiply the type of loading to take into account the structural complexity of the tissue. In fact, each of them gives the skin's response to a type of stress and characterises a particular feature of its behaviour under mechanical stress. The skin extension test, for example, is a directional test with which anisotropy is addressed. It appears as the test without coupling of loads and thus allows direct interpretation of the stress-strain curves.

Table 1.4: Mechanical properties of human skin in vivo obtained in torsion, suction, and indentation studies from the literature.

Methods	Location	Elastic modules	References
Torsion	dorsal forearm (<30 years / > 30 years)	0,42 / 0,85 MPa	[Agache *et al.,* 1980]
	ventral forearm	1,12 MPa	[Escoffier *et al.,* 1989]
	forearm / arm / thigh / shin	G = 0,98 / 0,58 / 0,84 / 1,33 MPa	[Grebenyuk *et al.,* 1994]
	forearm	0,02 - 0,1 MPa	[Sanders, 1973]
Suction	cheek	130 - 260 kPa	[Barel *et al.,* 2006]
	forearm	0,13 - 0,26 MPa	[Barel *et al.,* 1998]
	forearm	130 kPa	[Diridollou *et al.,* 2000]
	ventral forearm	0,20 - 1,45 MPa	[Hendriks, 2005]
	forearm	56 kPa	[Hendriks *et al.,* 2003]
	palm / forearm	25 kPa / 100 kPa	[Liang *et al.,* 2010]
Indentation	male thigh / male forearm / female forearm	2 / 1,5 / 1,1 kPa	[Bader *et al.,* 1983]
	forearm	4,75 - 17,99 kPa	[Boyer *et al.,* 2012]
	forearm	13,2 - 33,4 kPa	[Boyer *et al.,* 2009]
	forearm	5,1 - 13,3 kPa	[Boyer *et al.,* 2007]
	ventral forearm	0,1 - 2,4 MPa	[Khaothong, 2010]
	shin	10,4 - 89,4 kPa	[Zheng *et al.,* 1999]

1.4.2 Indirect techniques

When describing a tissue, either for its characterisation or to diagnose a pathology, the examination of the internal structure is valuable. Imaging techniques are complementary tools to direct mechanical techniques and provide an in-depth view of the skin tissue. The main imaging techniques to study the skin are MRI, ultrasound, Optical Coherence Tomography and confocal microscopy. These techniques have two important parameters: resolution and depth of penetration.

The general principle, performance, interest and applications of the main human skin imaging techniques are briefly presented in this Section. Some of them allow *in vivo* imaging, while others require cutting the tissue, some are destructive, others not.

1.4.2.A Non-optical imaging

These imaging techniques are commonly used in *in vivo* imaging for diagnostic purposes such as ultrasound (using sound waves) and magnetic resonance imaging (MRI, using magnetic fields and radio waves). They are non-invasive and fairly easy to use, although they require special equipment. The images cover a wide spatial field of view, but have low resolution (≈ 0.1 mm at best) and are sometimes difficult to interpret. In contrast, there is another non-optical imaging technique that is much more accurate but requires skin sampling: electron microscopy.

i) *Ultrasound imaging*

Ultrasound has been used in obstetrics and cardiology for many years. The principle of ultrasound imaging is based on the propagation of mechanical waves in biological tissues and the detection of the amplitude and phase of echoes backscattered by internal tissue structures. The presentation of the echo amplitudes in intensity in the image allows the construction of an anatomical section in a plane. This real-time, non-invasive and non-ionising method is relatively easy to implement and low cost.

The resolution of the ultrasound image is dependent on the ultrasound frequency, the higher the frequency the better. *In vivo* skin tissue has been explored at high frequencies between 20 and 150 MHz corresponding to axial resolutions of 30 to 150 µm. However, the higher the frequency, the greater the attenuation of ultrasound in the tissue. Penetration depths into the skin tissue are therefore several millimetres at high frequencies and over 1 cm at 20 MHz.

This ultrasound imaging technique, used by some authors including [Alexander *et al.*, 1979]; [Turnbull *et al.*, 1995]; [Serup *et al.*, 2006], therefore allows the skin structure to be visualised and its thickness to be measured. Morphological ultrasound images are obtained by analysing the echoes reflected from the tissue (Figure 1.38). The *Dermcup®* (Atys Medical) or the *Vevo® 2100* (VisualSonics) are examples of ultrasound scanners on the market.

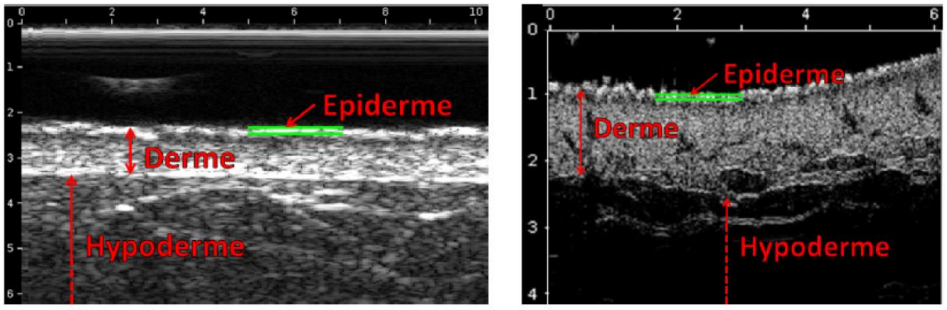

Figure 1.38: 20 MHz (a) and 50 MHz (b) ultrasound images of human skin in vivo (forearm) – [Chartier, 2017]

The multiple advantages of this technique are thus apparent: simplicity, rapidity of execution and total safety due to its non-invasive nature. The disadvantages are rare and we will rather talk about the limits of the examination: a low contrast of the images and a weak depth of penetration.

ii) Magnetic Resonance Imaging (MRI)

Magnetic Resonance Imaging is based on the coupling between the magnetic moment of the nucleus of atoms and the external magnetic field (the principle of nuclear magnetic resonance). It uses the properties of the body's hydrogen nuclei (very present in water-rich soft tissues [Richard *et al.*, 1993]) to emit a signal when, after being placed in a magnetic field and excited by a radio frequency wave, they return to their equilibrium state. The signal emitted during this relaxation phenomenon is the source of the image.

This *in vivo* examination is non-invasive, non-irradiating and repeatable, and allows a three-dimensional analysis of the organs. For the study of the skin, specific antennas with a resolution fifty times higher than that of traditional MRI have been developed. MRI can reach voxels[12] of 40 x 40 x 300 µm^3 resolution [El Gammal *et al.*, 1996]. As shown in Figure 1.39, MRI of the skin allows good differentiation of skin layers. This medical imaging method allows to understand certain skin pathologies and also to visualise their evolution.

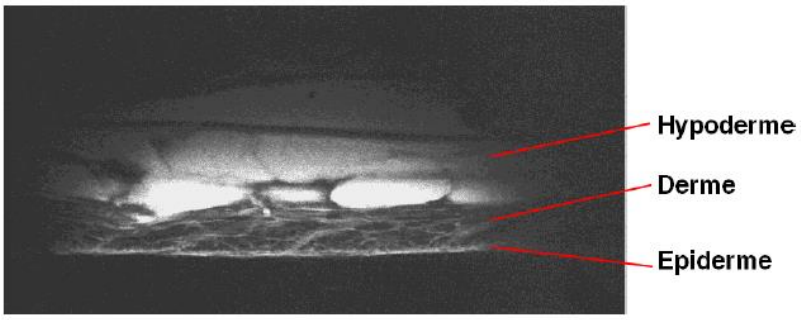

Figure 1.39: MRI image of human skin in vivo (calf) – [Ginefri et al., 2001]

MRI gives high quality images (high resolution and high contrast) while having a high penetration depth (several millimetres). The only drawback is that this advanced technique is quite expensive.

[12] **Voxel:** A unit of graphic information that defines a point in three-dimensional space. The voxel is to 3D what the pixel is to 2D.

iii) Scanning Electron Microscopy (SEM)

Another imaging technique is available to study the architecture of the skin: scanning electron microscopy (SEM). Electron microscopy gives access to very small scales with very good resolution, in the nanometre range or less, over a small field of view. It requires careful preparation of the sample in thin sections, which must be resistant to both vacuum and electron beams. SEM images are shown in Figure 1.40. SEM has been applied to the study of fibre reorganisation in a skin tensile test by Brown [Brown, 1973] and later by Belkoff [Belkoff *et al.*, 1991]. The disadvantage of this method is that it is destructive.

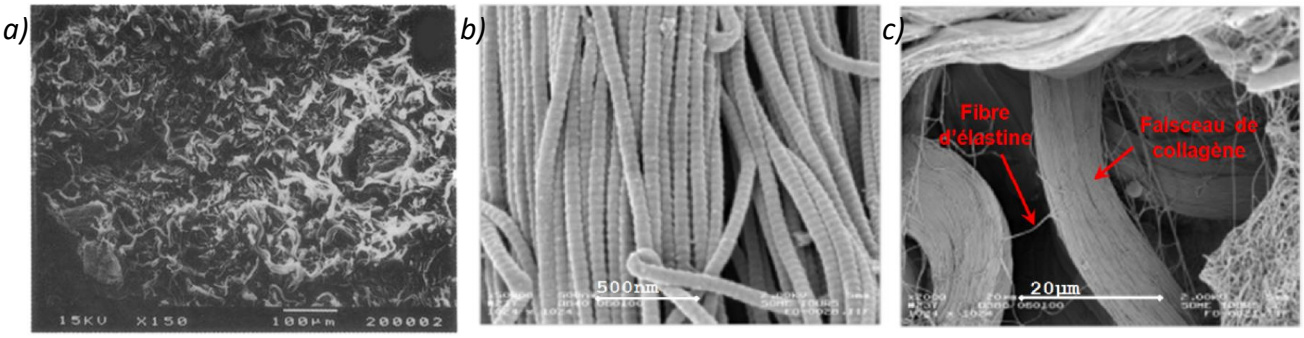

Figure 1.40: Scanning electron microscopy images. a) Rat skin dermis (x 150) – [Belkoff et al., 1991]. b) Collagen fibres from the abdominal dermis (x 50,000) and c) Collagen bundles in the presence of elastin fibres (x 2000) – [Lebertre, 2001]

1.4.2.B Elastography

Elastography is the coupling of an ultrasound imaging system with a mechanical system to explore biological tissue. The tissue under study is stressed in various ways in order to propagate movements or deformations, which are measured by ultrasound. Elastography is therefore a non-invasive way of assessing the elasticity of soft tissues. Two elastography techniques, differentiated by the mode of mechanical stimulation, allow the quantitative measurement of tissue elasticity: dynamic elastography and quasi-static elastography.

i) *Dynamic Elastography*

Dynamic elastography is based on the analysis of mechanical vibrations of the skin in which shear waves are generated [Agache 2000]. It is the mechanical stress on the surface of the tissue that generates low frequency shear waves in the skin. This dynamic stress can be generated by means of an external vibrator such as a vibrating pot [Catheline, 1998] or by focusing an ultrasound beam [Bercoff *et al.*, 2003]; [Sugimoto, 1990].

Ultrasound imaging allows the measurement of movements induced by internal vibrations from the frequency distortions of the acoustic signals. It allows the mapping of an elastogram which corresponds to the displacements of the medium or the deformations induced by the shear wave as a function of time. This signal can be traced back to a qualitative parameter (mapping of soft and hard zones) or quantitative parameter (shear modulus).

Authors such as [Lerner *et al.*, 1987]; [Gennisson *et al.*, 2004]; [Zhang *et al.*, 2011] or [Nguyen, 2012] have used this technique to study the skin.

ii) Quasi-static elastography

Quasi-static elastography consists of carrying out an ultrasound analysis of the medium under consideration, then applying an external static stress such as compression, depression or stretching [Gahagnon, 2009] to this medium, and finally comparing the different elastograms obtained [Xu *et al.*, 2008]. This tissue elasticity imaging technique was developed by Ophir [Ophir *et al.*, 1991] and has been used by many authors such as [Gennisson *et al.*, 2003, 2004]; [Prevorovsky *et al.*, 2007]; [Gahagnon, 2009]; [Gaspari *et al.*, 2009]. The acquisition of ultrasound images allows the study of the rigidity of the medium (Figure 1.41).

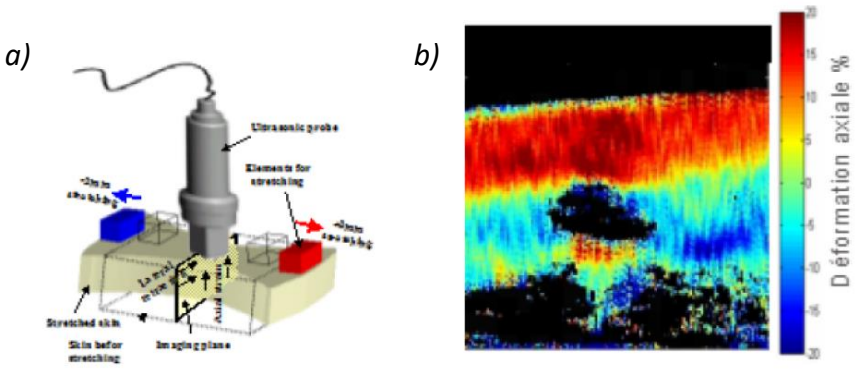

Figure 1.41: Quasi-static elastography technique. a) Measuring device. b) Axial deformation image – [Mofid et al., 2006]

1.4.2.C Optical imaging

Optical imaging is based on the principle of optical backscatter (reflectance) of the observed structures. Two main imaging techniques using reflected light to observe skin tissue are mentioned: optical coherence tomography and confocal microscopy.

Optical imaging techniques have several advantages: relatively large fields of view, good resolutions, light sample preparation and reasonably short imaging times. Depending on the technique used, lateral resolution can be as high as 0.2 to 0.5 µm. These advantages make optical imaging ideal for microscopic observations of tissue in mechanical testing.

i) *Optical Coherence Tomography (OCT)*

Optical Coherence Tomography (OCT) was developed in the early 1990s for the medical community [Huang *et al.*] This biomedical optical imaging technique provides high resolution and tomographic imaging of the cross-section of the system under study. Its operation can be compared to that of ultrasound, but using electromagnetic waves in the infrared range instead of ultrasound waves. The measurement is based on the principle of the Michelson interferometer to analyse the delay between two beams of coherent light: a first laser beam makes a reference path by projecting onto

a plane mirror, and a second one by projecting onto the explored tissue. The coherence of these waves is then compared and an image of the explored tissue is produced.

OCT offers a high spatial resolution of between 1 and 15 µm, twice as accurate as standard ultrasound [Gambichler *et al.*, 2007]. The penetration depth of OCT is determined by optical scattering, approximately 2-3 mm into the tissue. It is a future technology as tissue is imaged *in situ* and in real time without excision [Fujimoto, 2003]. The images acquired, Figure 1.42, are the two-dimensional cross-sections that show the tissue microstructure of the sample.

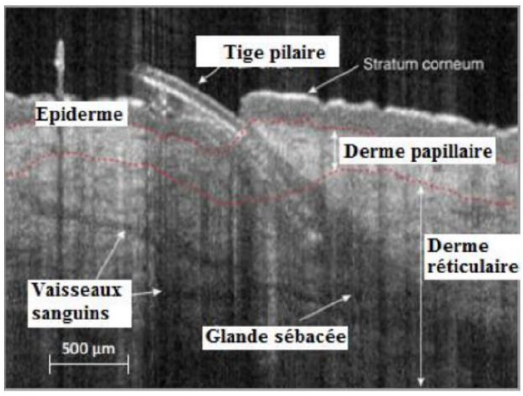

Figure 1.42: Optical Coherence Tomography image of the skin in vivo (forearm) – [Greaves et al., 2013]

OCT imaging, used by some authors such as Fujimoto [Fujimoto *et al.*, 1995] and Bordenave [Bordenave *et al.*, 2002], has many advantages: no sample preparation, micrometric resolution, 3D imaging possible and very short imaging time. However, this imaging technique requires a tissue with optical interfaces (different refractive indices), and its main drawback is the total absence of imaging specificity.

ii) Confocal microscopy

Confocal Microscopy is a very advanced technology in optical microscopy. The application to skin characterisation only appeared in the 1990s [New *et al.*, 1991]. It is built on a standard fluorescence microscope that provides the optics, to which a special laser beam processing system is added. This microscopy allows to obtain horizontal histological sections (confocal images parallel to the skin surface) of the epidermis and dermis of the skin by keeping only the fluorescence information located in this plane.

This *in vivo* imaging method is the only one to offer cell size resolution. Indeed, the lateral resolution of the images is between 0.5 µm and 1 µm and the distance between sections varies from 2 to 5 µm. Very thin sections are thus obtained, giving access to information at the dimensions of the cell. This imaging allows, for example, the evolution of keratinocytes in each layer of the epidermis to be observed with precision (Figure 1.43). It has a limited depth of exploration between 250 and 300 µm in the skin [Nehal *et al.*, 2008], allowing only the visualisation of the epidermis, the papillary dermis and the upper part of the reticular dermis.

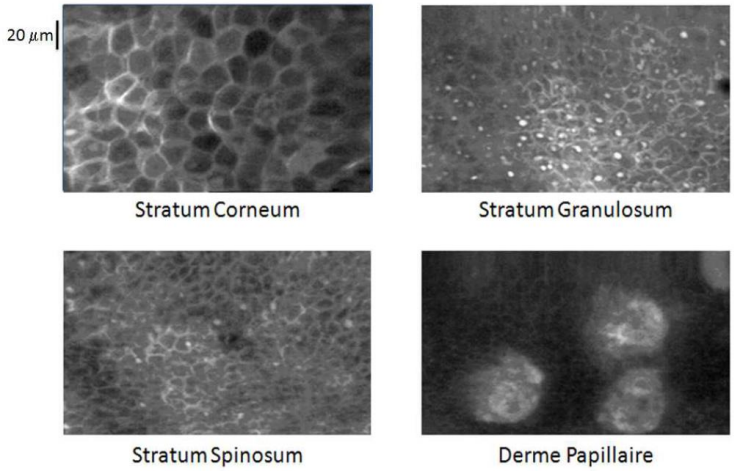

Figure 1.43: Confocal microscopy images of different skin layers – [Chartier, 2017]

Authors such as [Brakenhoff, 1979]; [Pawley, 1990]; [Matsumoto, 1993] and [Stevens *et al.*, 1994] have used this imaging technique to visualise the skin. This imaging technique, commonly used to image biological tissues, has two advantages: its high resolution and its direct three-dimensional observation of the skin *in vivo* without damaging it. In addition, it allows for temporal data acquisition, facilitating the complete observation of biological structures undergoing deformation over time.

iii) Histological section

One of the most common ways of examining the microstructure of a tissue is to perform a histological section. A biopsy of the tissue is embedded in paraffin, and very thin slices of the tissue are cut out (a few micrometres thick). The sections are then deparaffinised, stained with a selected dye specific to the components of interest, and observed under a light microscope. One of the most common stains for skin is *H&E* (haematoxylin and eosin), in which cell nuclei are stained purple and proteins (such as collagen) are stained pink. Figure 1.44 shows a histological section of skin stained with *H&E*. It is also possible to stain proteins, carbohydrates or lipids with specific antibodies: this technique is called immunohistochemistry.

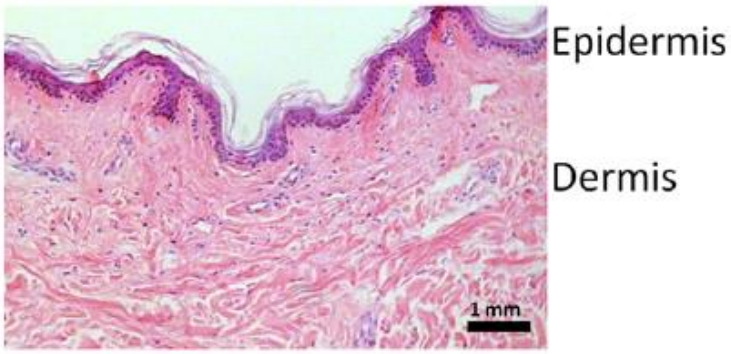

Figure 1.44: Vertical histological section of skin stained with H&E – [Lynch, 2015]

Histological analyses allow accurate and relatively immediate identification of the components of a sample, as they are stained in relation to their nature. However, these analyses are highly invasive and inherently destructive.

1.4.2.D Summary of indirect techniques

Indirect imaging methods are techniques with many advantages: most are non-invasive and allow rapid characterisation of the interior of tissues. However, their use is qualitative as only the observation of the internal microstructure of the tissue is feasible. Their application on human skin *in vivo* must take into account the dimensional aspect of this organ. Indeed, an optimal compromise must be found between resolution and depth of observation.

1.4.3 Summary of characterisation techniques

The interest in dermatology and cosmetology in describing or measuring the mechanical behaviour of the skin has led to the development of numerous measurement methods. We can distinguish, among others, traction, indentation, torsion, suction or ballistometry. Most of these techniques have resulted in commercially available devices.

However, these methods are difficult to evaluate and compare because each test is independent and each makes different assumptions in order to obtain results. There is no universal standardisation between laboratories, but each has its own standardised methods. Furthermore, the mechanical properties determined are greatly influenced by the diversity of the types of loading, the intensity of the force applied, the influence of the environment and the anatomical sites characterised. This helps to explain the differences observed in the value of the modulus of elasticity of the skin.

In addition to these mechanical exploration techniques, high-resolution imaging methods are used to map the internal microstructure of the tissue. Magnetic resonance imaging, optical coherence tomography, confocal microscopy and ultrasound are the most commonly used imaging techniques to image the skin tissue in depth.

These two approaches, mechanical and imaging, are often complementary: the elastography technique based on the coupling between an imaging module and a mechanical stress measuring system is a good example.

Methods for determining the mechanical properties of skin tissue require numerous simplifications and assumptions. In order to obtain a characterisation of the mechanical behaviour of the skin that is as close as possible to reality, the authors resort to the development of numerical or analytical models that can be optimised with the help of optimisation algorithms in relation to the experimental results.

1.5 Modelling the mechanical behaviour of human skin

In biomechanics, the mechanical characterisation of biological materials is always difficult. *In vivo*, it is impossible to isolate tissues for testing, while *ex vivo*, it is often impossible to keep tissues in the living state [Fung, 1993]. It is therefore necessary to use a modelling technique to seek for a good approximation of the mechanical behaviour of skin tissue (Figure 1.45).

The skin has a very complex structure: multilayered with a multitude of cells and components. As presented in Part 1.3, a complete description of the mechanical behaviour of the skin requires an anisotropic, viscoelastic and non-linear model. Modelling such behaviour is very complicated and simplifications are often necessary to achieve an efficient model. For this reason, several more or less simplified analytical and numerical models can be found in the literature to approximate reality as closely as possible [Yazdi *et al., 2022*]. Most often, the models describe the mechanical behaviour of the dermis since it is the main mechanical component of the skin. Most models also neglect long-term changes and remodelling as well as degradation mechanisms that may be physically relevant in clinical procedures.

Analytical modelling gives exact mathematical solutions by accepting simplifying assumptions about boundary conditions, geometry, and material behaviour. [Danielson, 1973]; [Khatyr *et al.*, 2006] and [Diridollou *et al.*, 2000].

Numerical modelling is based on the Finite Element (FE) Method to determine the mechanical properties of soft tissue [Flynn *et al.*, 1998]. This modelling technique requires few simplifying assumptions about the behaviour and constitution of materials. The accuracy of the results of the FE modelling technique depends on the size of the elements. [Larrabee *et al.*, 1986a,b,c]; [Bischoff *et al.*, 2000]; [Hendriks *et al.*, 2003]; [Khatyr *et al.*, 2006]; [Delalleau *et al.*, 2006]; [Xing *et al.*, 2006].

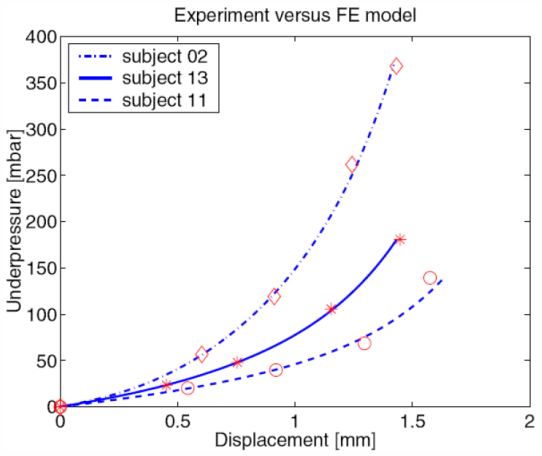

Figure 1.45: Finite Element modelling of human skin – [Hendriks et al., 2003]

1.5.1 Phenomenological and microstructural models

Mainly two approaches have been adopted in the scientific community to model the mechanical behaviour of the skin: the phenomenological approach and the structural approach.

The phenomenological approach describes the overall mechanical behaviour of the material; the parameters identified with this model have no biological significance. On the contrary, the structural approach allows to predict and explain the mechanical behaviour of the material based on its microstructure and the interaction between its different components. The identified parameters describe the mechanical behaviour of each component of the material and their combination allows to describe its global behaviour.

Phenomenological and structural models are classified into elastic (time independent) and viscoelastic (time dependent) models.

1.5.1.A Phenomenological models

The identification of a strain energy function is the most widely used method to characterise the complex mechanical properties of the skin and identify a constitutive equation. The elastic potential energy can be expressed with a scalar-valued strain energy function *W* such that:

$$S = \frac{\partial W}{\partial F}(F) \quad (1.1)$$

where *S* is the nominal stress tensor and *F* is the strain gradient tensor. The simplest deformation energy function is the neo-Hookean:

$$W = \frac{\mu}{2}(I_1 - 3) \quad (1.2)$$

where I_1 is the first invariant of the Cauchy-Green deformation tensor and μ is the shear modulus. It involves a single parameter and provides a simple model for non-linear deformation.

Through their pioneering experimental work on skin, Lanir and Fung were the first to demonstrate both the highly nonlinear elasticity of skin and the preconditioning effect [Lanir *et al.*, 1974]. To model the stress-strain relationship, he developed a two-parameter strain energy function that is still widely used today [Tong *et al.*, 1976]. Many other strain energy functions have been developed to improve the data and in particular to extend the models to large strains. A comprehensive review of strain energy functions used to describe the non-linear elasticity of rubbery materials can be found in [De Pascalis, 2010]. An example of mechanical modelling with different strain energy functions is shown in Figure 1.46.

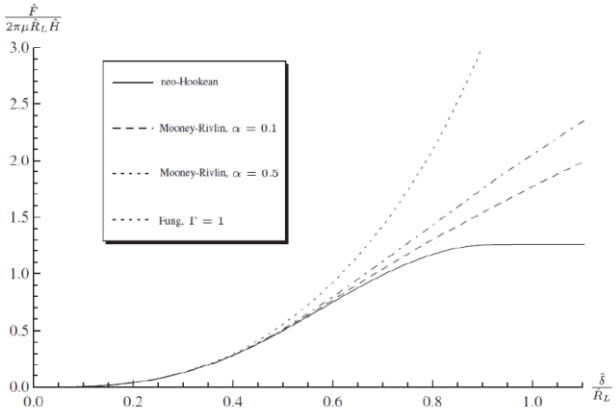

Figure 1.46: Hyperelastic models: force/indentation curves for a spherical indenter on a flat membrane, modelled using three strain energy functions: neo-Hookean, Mooney-Rivlin and Fung – [Pearce et al., 2011]

Phenomenological models are commonly used to describe the mechanical behaviour of soft collagenous tissues: many Finite Element modelling software packages are available. They generally fit well with data from simple experiments, but the parameters are difficult to interpret physically. For this reason, microstructural models have been developed using new data on the microstructural architecture of soft tissues.

1.5.1.B Microstructural models

Microstructural models are based on the classical interpretation of the non-linear stress-strain curve of the skin. This interpretation is supported by early observations by Brown [Brown, 1973] and later by Belkoff [Belkoff *et al.*, 1991]. In these studies, scanning electron microscopy was used to image different skin samples at various strains. The progressive alignment of collagen fibres was observed (Figure 1.47) and can therefore be modelled.

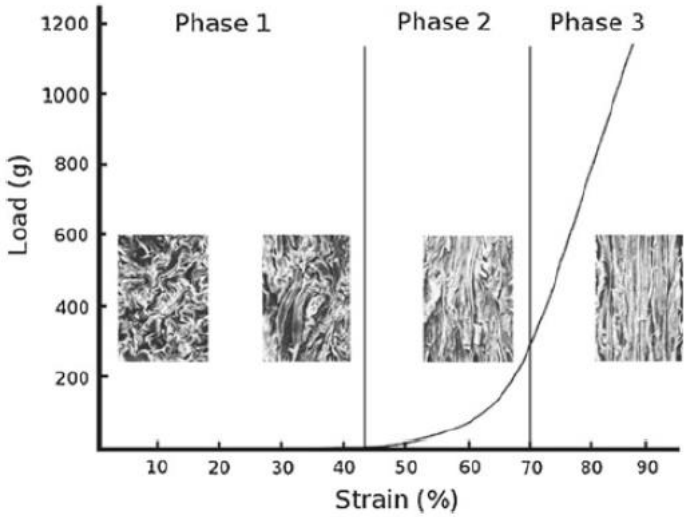

Figure 1.47: Stress-strain curve for skin, with samples observed by scanning electron microscopy at different strain levels – [Brown, 1973]

Microstructural models therefore require microstructural observations by any given method. The knowledge of the properties of the basic components as well as the microstructure of the skin tissue will allow to model the skin tissue. These formulations are certainly closer to physical reality but require the identification of a large number of parameters which is often difficult due to the limited experimental data.

1.5.2 Elastic and hyperelastic models

Skin, like all soft tissues, exhibits a non-linear hyperelastic behaviour. Following these observations and based on the shape of the experimental stress-strain curve, Tong and Fung [Tong *et al.*, 1976] proposed a biphasic law of the exponential type, which will be widely adopted thereafter to model the behaviour of soft biological tissues in tension. This law, which is considered as the reference, allows to correctly describe the first elastic phase of the behaviour of human skin [Jacquemoud, 2007].

Like Tong and Fung, the first models proposed for hyperelastic behaviour, namely [Ridge *et al.*, 1966], [Lanir, 1983] and [Fung, 1993], consist of formulating a pseudo-strain energy function based on work done on polymers.

Subsequently, Larrabee developed numerical FE models to describe the elastic behaviour of skin [Larrabee *et al.*, 1986a,b,c]. Since then, there has been a proliferation of finite element models modelling the elastic behaviour of skin tissue. For example, some authors have developed elastic models, such as [Bischoff *et al.*, 2000]; [Billiar *et al.*, 2000]; [Delalleau *et al.*, 2006, 2008a,b]; [Khatyr *et al.*, 2006]; [Abellan *et al.*, 2013]; [Boyer *et al.*, 2013] or [Hara *et al.*, 2013].

Other authors such as [Veronda *et al.*, 1970]; [Ogden, 1972]; [Holzapfel *et al.*, 2000]; [Bischoff *et al.*, 2002]; [Hendriks *et al.*, 2003, 2006]; [Gasser *et al.*, 2006]; [Groves *et al.*, 2013] whereas [Iivarinen *et al.*, 2013] have developed numerical models to describe the hyperelastic behaviour.

1.5.3 Viscoelastic models

The viscoelastic models developed are based on two phenomenological models: Maxwell models and generalised Kelvin-Voigt models.

Decreamer [Decreamer *et al.*, 1980] and Sanjeevi [Sanjeevi, 1982] were the first to propose numerical models of the skin to describe its viscoelastic behaviour. Subsequently, other authors such as [Potts *et al.*, 1983]; [Dunn *et al.*, 1983]; [Holzapfel *et al.*, 2000]; [Khatyr *et al.*, 2004]; [Flynn *et al.*, 2011] or [Amaied *et al.*, 2015] also developed viscoelastic numerical models.

1.5.4 Summary on the modelling of the mechanical behaviour of the skin

In this Section, we have reported some examples of phenomenological models developed in the literature to predict the mechanical behaviour of skin. Biomechanical modelling of the skin allows, for example, the prediction of its mechanical behaviour for surgical planning or grafting of a skin substitute. It can also be used to improve diagnostic techniques for skin diseases.

Several models of skin mechanical behaviour have been proposed in the literature. However, none of these models is fully satisfactory to simulate the mechanical behaviour of skin due to the complexity of the material structure, the experimental conditions (initial and boundary conditions), the interaction between the different skin constituents, and finally the mechanical behaviour itself (non-linear, anisotropic, time-dependent and assumed to be in the natural state).

From a biomechanical point of view, the properties of the tissues will be known if their constitutive equations are known. On the other hand, these equations are only determined by experimentation [Fung, 1993]. Therefore, testing is really necessary to identify parameters of the physical or mathematical model.

1.6 General conclusion of the literature review

This literature review enabled the study of the physiology of the heaviest and most extensive organ of the human body: the skin. Skin anatomy has shown that this tissue has a complex structure made up of multiple elements. The skin is composed of three layers: epidermis, dermis, and hypodermis. This anatomical organisation confers functions that are essential to the body's survival. The skin is the human body's envelope, the body's first protective barrier. Its main function is therefore to protect the human body from multiple external aggressions. In addition to this main function, the skin is home to many vital functions such as thermal regulation and sensory function.

The mechanical properties of this tissue are therefore essential for it to perform all these functions. The skin has complex mechanical properties (viscoelasticity, non-linearity, and anisotropy) which make this tissue highly resistant but also flexible. The dermis, made up of collagen and elastin fibres, is the main structure of the skin that controls its mechanical properties. In terms of skin characterisation, direct mechanical techniques can be used. These biomechanical analyses are fundamental for quantifying, qualifying, and modelling the behaviour of the tissue when it is deformed. Indirect imaging techniques can also be used to better observe the internal structure of this organ.

Chapter 2.

Materials and Methods

This Chapter is devoted to the presentation and description of the development and evolution of a new device. The diversity of the instrumentation development work carried out during the thesis will be described. Only the key elements in the evolution of the equipment are presented in this Chapter.

The device is protected by a French Patent filed in 2020, which benefits from an international extension since 2022 [Derail *et al.*, 2022].

The first part of the Chapter is devoted to the equipment used in our research: the technology developed, which is the focus of this PhD work. The methods developed and used to characterise the mechanical properties of human skin with this specific equipment will then be described. Finally, the human skin explants used in this research will be presented.

2.1 Development of an original equipment for measuring the mechanical properties of skin

2.1.1 Initial state: Principle and description of the device

This work is based on an original equipment that is currently being developed in the laboratory (Figure 2.1). The present PhD work consists in testing, consolidating, and developing it. This Section consists in describing the specific device in its initial state.

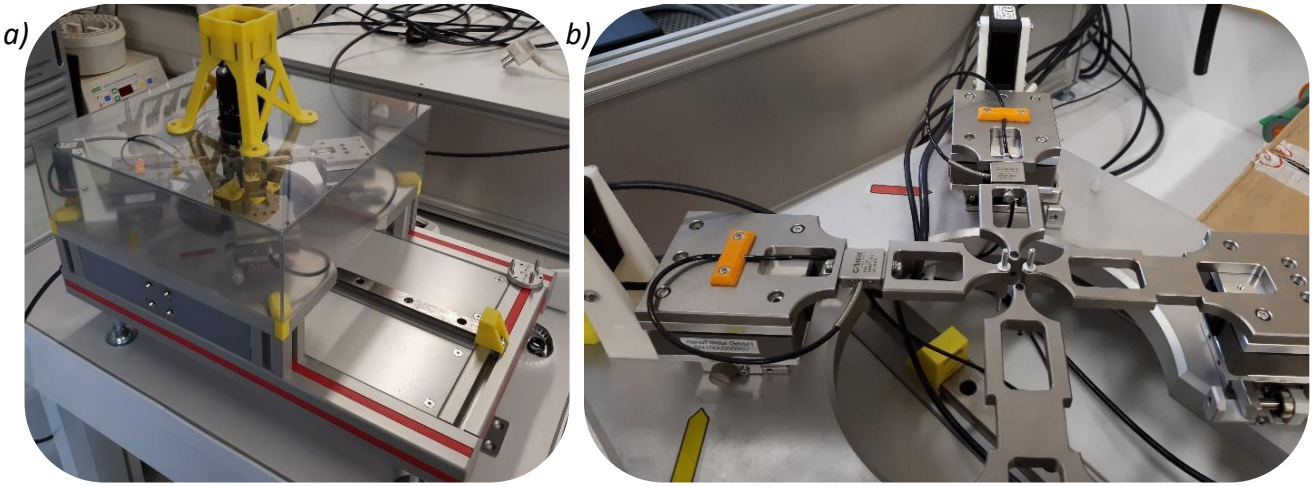

Figure 2.1: Photos of the device in its initial state. a) Whole device with camera. b) Core of the "mechanical testing" area.

2.1.1.A Introduction

As the patent indicates, the device is a system for measuring the mechanical properties of a skin sample [Derail *et al.*, 2022]. The skin sample may be of human or animal origin, *ex vivo* or *in vitro*. It should be noted that the sample can also be any type of biological soft tissue. By "mechanical properties" we mean the physical parameters that can be defined from the deformation of the skin subjected to mechanical stress. By analysing the mechanical responses to the imposed deformation, it is possible to determine the elastic, viscoelastic and plastic properties of the skin.

2.1.1.B Principle of the equipment

Initially, this device was designed to characterise the mechanical properties of an *ex vivo* skin sample held in a fixed position on a nutritional medium that maintains the mechanical properties of the skin sample in physiological like conditions for at least seven days.

The principle is based on the application of a specific and controlled mechanical stress to the skin sample. These mechanical stresses are applied in the form of traction in different directions in the plane of the skin and, eventually, at different frequencies or at different traction speeds. The mechanical responses of the stressed skin are then measured by various sensors.

2.1.1.C Description of the device

As shown in Figure 2.2, this equipment includes four **mechanical loading modules** (part assemblies n°20, 40, 70, 80) which are each capable of applying a tensile force in a direction parallel to the skin surface (allowing two uniaxial tensile tests to be performed simultaneously). The mechanical loading modules work in pairs: in Figure 2.2, module 20 and module 40 are arranged opposite to each other and exert tractions along a common axis (BB') in opposite directions. The same applies to modules 70 and 80. The two measurement axes (AA') and (BB') intersect at a point located precisely at the centre of the base opening (part n°100).

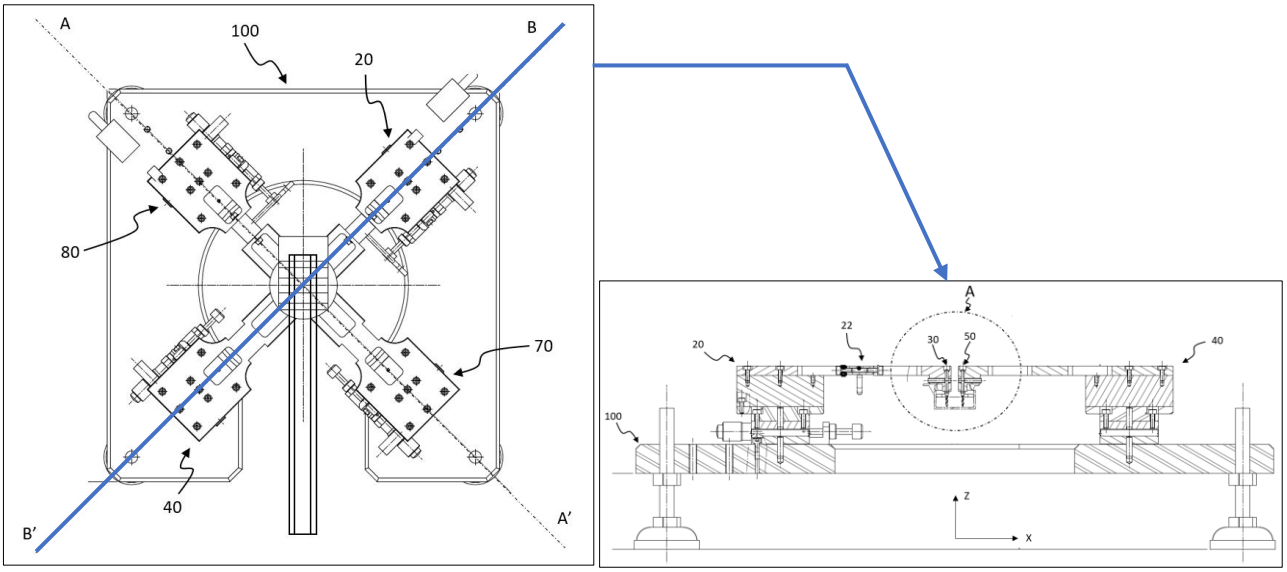

Figure 2.2: Schematic top view of the device with a cross-section view along axis (BB').

The mechanical loading modules are supported by this base designed to be placed and stabilised (by a suction cup effect) on a horizontal table surface. The centre of the base is equipped with a circular opening to allow the **sample holder**, in which the skin is positioned, to move to the test area. The sample holder, mounted on a mobile plate that slides on a rail, allows the skin to be moved both horizontally and vertically. To carry out the tests, the skin sample is therefore placed in the centre of the base opening, under the four mechanical loading modules.

The mechanical loading modules are described in more detail below. Only the measurement axis (BB') is described; the second is structurally identical to the first.

As shown in Figure 2.3, the 1st mechanical loading module (part assembly n°20) includes a **translation arm**, known simply as the "instrument arm" (part n°21 in stainless steel), connected to (i) a **traction element** (part n°30), also known as a fixing head or **stud** (visible in Figure 2.6), which is intended to be fixed to the skin sample during the traction test, and to (ii) a **displacement system** (part assembly n°24), which consists of a **piezoelectric nano-positioning table** and a manual **micrometric displacement table**, suitable for moving this arm.

The 2nd mechanical loading module (part assembly n°40) is almost identical; only a force sensor is added and inserted into the translation arm (part n°22).

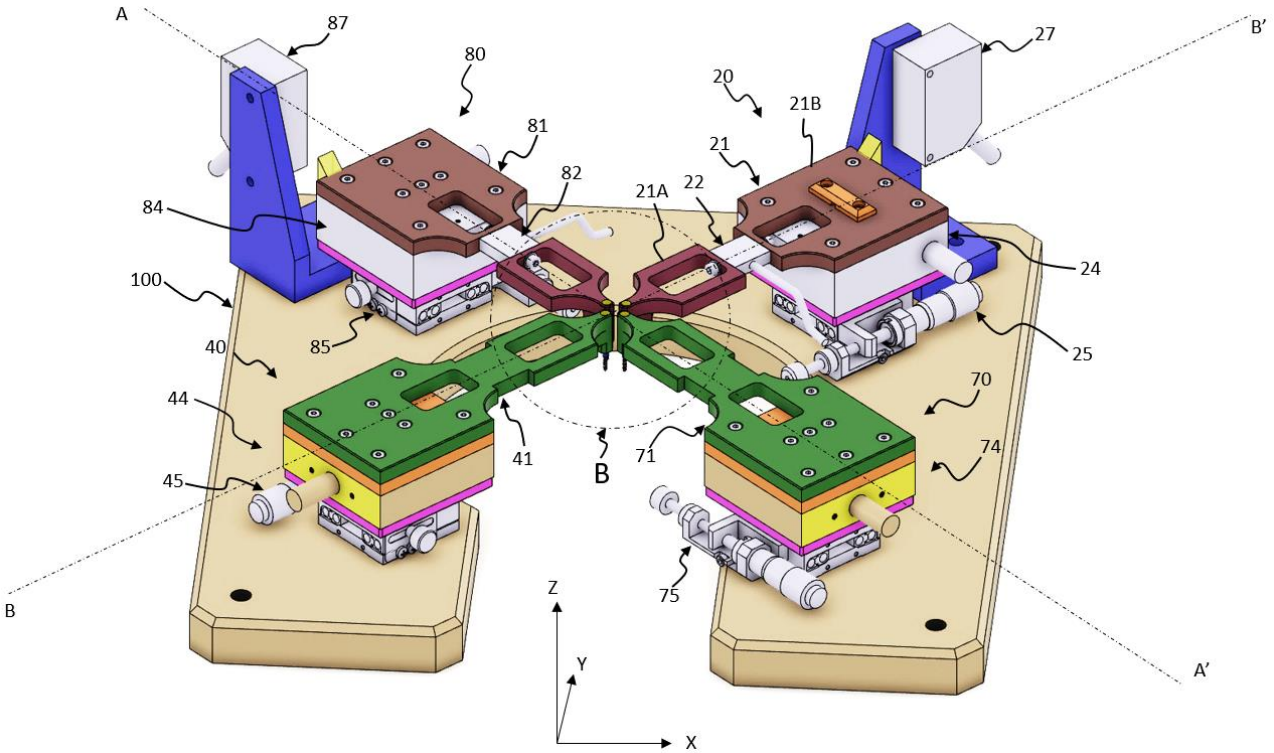

Figure 2.3: Perspective view of the device.

The displacement systems (part assemblies n°24 and 44) will move the arms, which will also move the studs along the axis (BB'). These 2 synchronised movements will induce a deformation of the skin sample and have the function of exerting an opposing traction force along the common axis (BB').

The four arms are therefore attached to a mobile part of the piezoelectric nano-positioning table. These piezoelectric actuators enable the deformation of the sample to be controlled by axial displacement of the arm. By applying a specific voltage to the piezoelectric material, it deforms and causes the arms movement. The piezoelectric material converts the energy it receives into a physical phenomenon. The maximum displacement of the piezoelectric actuator is 600 µm. The piezoelectric nano-positioning tables are aligned and synchronised so that the arm movements are synchronised.

In this configuration, the tensile force exerted by the opposing displacements of the piezoelectric tables has the same value at any point on the displacement axis. This means that only one **force sensor** is required to measure the tensile force per axis of displacement between the two aligned nano-positioning tables. For example, in Figure 2.3, only the first n°20 module and the fourth n°80 module are equipped with such a tensile force sensor. More specifically, the force sensor (part n°22) is arranged at a translation arm (part n°21) which comprises a first part (21A) and a second part (21B). The two parts are connected together via this sensor. The opposite translation arm is formed from a single piece (part n°41).

The manual micrometric displacement table (parts n°25 and 45) enables the position of the translation arm to be adjusted manually before the start of the tensile test. In this way, it is possible to adjust the distance between two fastening heads carried by the translation arms.

The piezoelectric nano-positioning table and the micrometric displacement table are positioned relative to each other in order to have the same axis of displacement. The piezoelectric nano-positioning table is fixed to a movable part of the manual micrometric displacement table. The micrometric displacement table itself is fixed to the base.

The device also includes a **position measurement sensor** (part n°27) per axis of movement. For example, in Figure 2.3, only the first module 20 and the fourth module 80 are equipped with such a sensor (parts n°27 and 87), which measures the actual position of the moving part of the piezoelectric displacement table in the reference system associated with the base.

Figure 2.4 shows the displacement of one of the fixation heads from an initial position L_0 to a position L_1. This displacement exerts a tensile force on the skin, generating a deformation or extension of the skin that is represented by the distance ΔL travelled by the fixation head. The displacement of the skin is measured by the laser position sensor, which is projected and aligned with the axis of the translation arm that moves the stud. The position sensor is used to measure the position of the stud in relation to a given reference position. It can therefore be used to determine the skin deformation caused by the traction applied by the stud from the resting position.

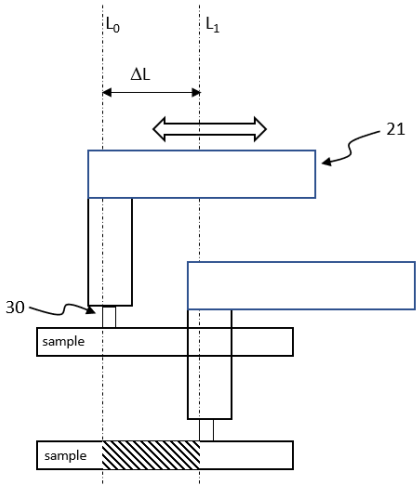

Figure 2.4: Schematic representation of the translation of one of the two studs in a direction parallel to the surface of the skin, causing deformation of the skin by axial displacement.

The traction element, or stud, is oriented in the vertical direction, normal to the surface of the skin. It is a straight cylindrical object with a flat end, designed to be attached to the skin surface during operation of the measuring device. As shown in Figure 2.5, the stu

a) b)

(part n°21, 22) until their annular bearing surface is in contact wi they are fixed using clamping screws (parts n°29, 49). They are rer the arm. The system for positioning the studs is quick and preci surface of the skin using a cyanoacrylate glue. This method of at that does not cause any slippage (unlike jaws). The studs glued t Once the mechanical tests have been completed, the studs mus unscrewing the clamping screws.

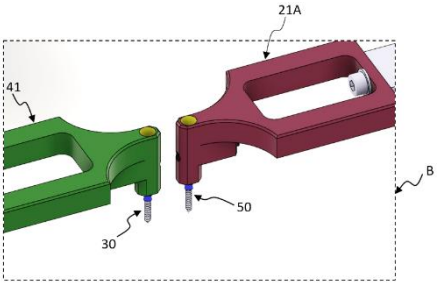

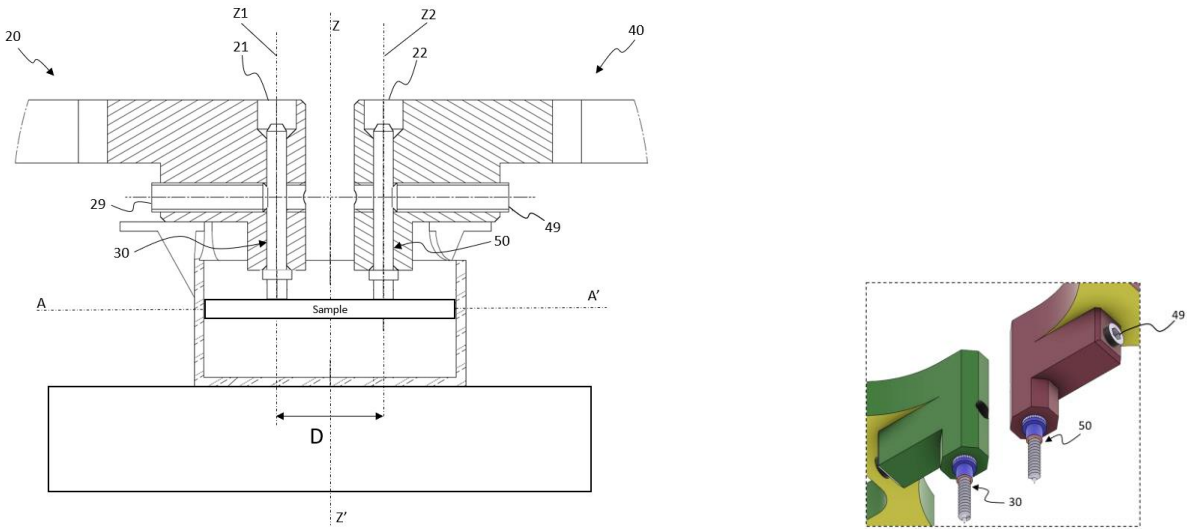

Figure 2.5: a) Enlarged view of an area (A) in Figure 2.2. b) Enlarged perspective views of zone (B) in Figure 2.3.

Note: two possible forms of stud were initially considered (Figure 2.6). The first (A) has the form of a rod with a thread for screwing into the skin. The second (B) has the form of a cylindrical body, the base of which is provided with a layer of adhesive enabling its fixation to the surface of the skin. The second form of construction was chosen for adhesion to the skin. In fact, piercing the skin to fix the solution studs (A) can cause severe damage to the skin and can also lead to an undesirable degradation of the mechanical properties of the skin between two experiments.
However, there are two disadvantages to stick the studs onto the surface of the skin:

- the use of adhesives for anchoring may damage the surface layer of the skin when the studs are removed,
- the anchoring points may not be strong enough leading to a risk of displacement between the stud and the measurement zone, resulting in erroneous measurements.

As we will see later, none of these disadvantages occurred.

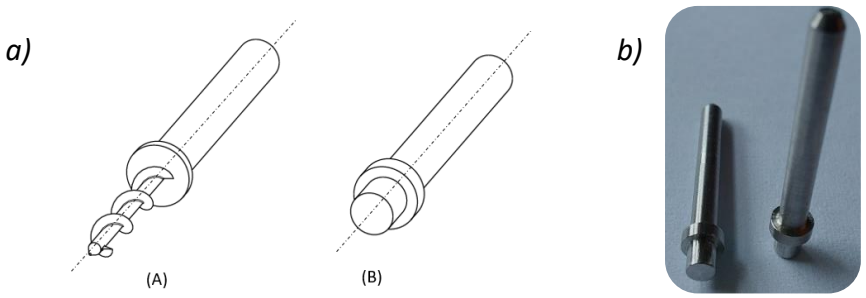

Figure 2.6: a) Perspective view of a stud according to two examples of the invention. b) Picture of the machined stainless-steel stud.

The measuring device also includes an **imaging equipment** configured to observe and record the area of deformation of the skin surface caused by the movement of the studs. The optical axis of the imaging system is oriented in a direction normal to the skin surface. The imaging equipment is currently a colour camera with adaptable magnifications, but could also be a more precise microscopy device.

2.1.1.D Conclusion

Figure 2.7 shows a schematic representation of the system, comprising the measuring device and a **control and calculation unit** for the displacement devices. This unit includes a control program (LabVIEW® program), which controls the displacement components (piezoelectric displacement tables) of the measuring device in order to move the translation arms. The traction force sensors, position measurement sensors and imaging equipment are also connected to this unit.

The control unit is configured to control the movement of the translation arm in a sinusoidal, triangular, or rectangular manner, by varying various parameters such as the loading frequency and the deformation of the sample. The load frequency can vary between 0.1 mHz and 1 Hz and the sample deformation can vary between 0.001% and 10%. All the signals measured by the sensors are then processed in this unit to calculate the mechanical properties of the skin, in particular to plot stress as a function of deformation.

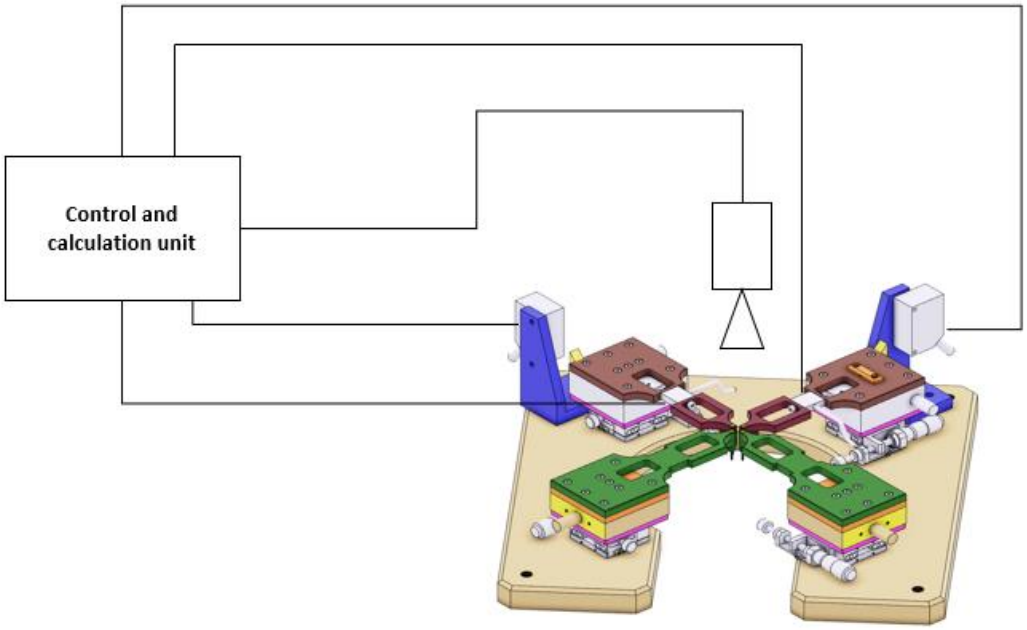

Figure 2.7: System for measuring mechanical properties, comprising the measuring device connected to a control and calculation unit.

2.1.2 Main improvements to the device

The initial state of the equipment presented above is an initial prototype of the device. Initial tests on different types of material have enabled this first prototype to evolve, to be developed and improved further, prior to testing on human skin. Several modifications were made to the equipment to enable full mechanical tests to be carried out on human skin explants. The main modifications are presented in this Section (minor modifications are presented in Appendix 1).

Note: in order to properly develop the device, and with the aim of limiting expenses, a single loading axis was mainly developed and improved during this work. This loading axis will be named the X-axis in the rest of the described research. In the future, when biaxial stresses will be required, the second Y-axis will also need to be developed.

2.1.2.A Force measurements improvement

Changes have been made to the force sensors and their power conditioners to improve the accuracy and quality of force measurements.

i) *Force sensor power conditioners improvement*

Signal conditioning is a data acquisition process. A power conditioner is an electronic circuit for processing the signal from a sensor. Its role is to amplify and condition the measured signal, translating it into a value that can be processed (e.g. voltage or current). The power conditioner intervenes between the sensor and the data acquisition system. It helps to provide accurate measurements, which are essential for data acquisition.

When carrying out dynamic tests at high frequencies, the system must be able to collect data quickly so as not to lose any information. It was therefore necessary to change the power conditioners for the force sensors in order to obtain continuity in the data captured by these sensors (no delay in force measurement).

ii) Force sensor improvement

Force sensors measure the tensile force exerted by the arms of the instrument on the skin sample. These are S-type transducers that are stretched or compressed when a force is applied. Strain gauges are placed exactly where the deflection occurs, to detect this change in shape. By placing a strain gauge at each crucial point, the gauges will generate a change in resistance. Using electronics, this change in resistance is translated into a change in weight (g/kg) or force (N). These sensors are therefore suitable for tension and compression applications.

The accuracy of the force sensor is defined by its measurement range. For materials like skin, which is a soft tissue, we need to be very accurate at low forces. A change of force sensor was therefore necessary to improve accuracy. A sensor with small dimensions that fits in well with the equipment and has a measurement range of up to 4.4 N was chosen (Figure 2.8a). This small measurement range means that the data is highly accurate, with a measurement uncertainty of 1.8 mN (0.04% of

the measurement range). This change of sensor, on the X-axis of measurement developed, allows to be very precise in the range of skin elasticity.

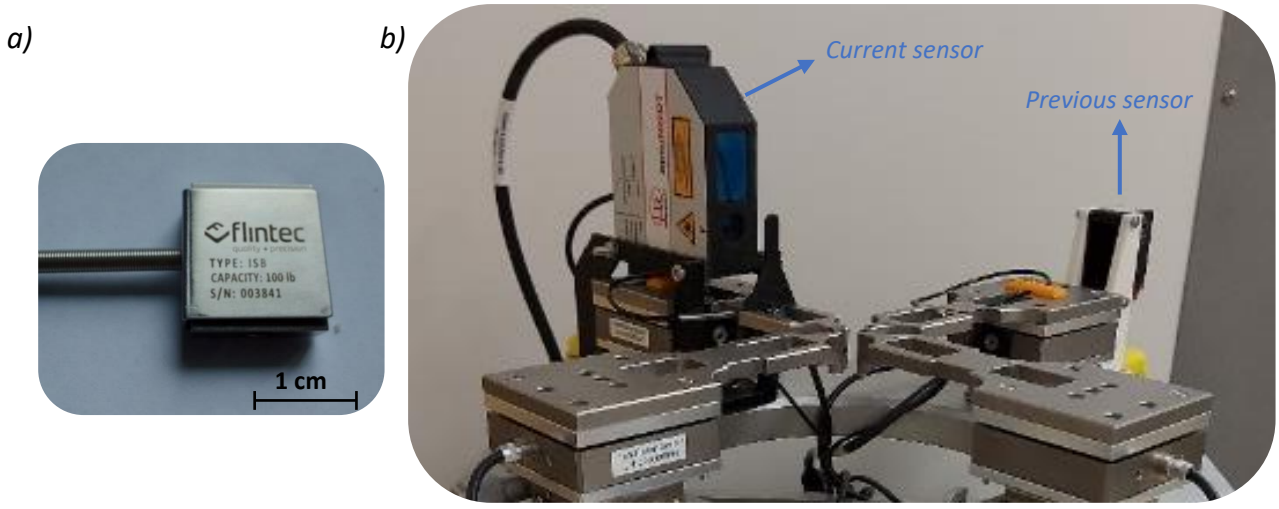

Figure 2.8: Measurement improvement. a) Photo of a miniature S-type force sensor used in our device. b) Photo of the current device configuration with a new position sensor.

2.1.2.B Position measurement improvement

The aim here is to improve the accuracy and quality of the position measurements used to calculate the displacement of the arms and, ultimately, the deformation of the skin sample.

The position sensor is an extremely compact laser triangulation sensor with an integrated controller. Laser triangulation sensors use a laser diode to project a visible spot of light onto the surface of the object to be measured. The light reflected from the spot is received by a sensor element via a receiver optic. A variation in the distance of the object from the sensor varies the angle at which the sensor receives the light. These are high-performance sensors that provide accurate measurement results at a high measurement frequency.

The accuracy of the position sensor is defined by its measuring range. In order to stress the skin at low strain rates, we decided to change the position sensor by choosing a compact sensor with a reduced measurement range. A high-precision laser triangulation sensor with a measurement range of 2 mm and a resolution of 0.03 µm was chosen (Figure 2.8b). This change of sensor, on the X-axis of measurement developed, allows to be very precise for small deformations.

Note: compared with the previous position sensor, which used a laser pointed at the back of the arm of the instrument, the new sensor uses a laser positioned above the arm, targeting a specially designed part located in the middle of the arm, just after the force sensor (Figure 2.8b). This means that the deformation measured is solely attributable to the deformation of the sample, unlike the previous positioning which had to take into account the intrinsic deformation of the force sensor under stress (device's notion of complacency).

2.1.2.C Vertical force sensors addition

To improve the reproducibility of the experiments, it was necessary to install a system to measure and control the compression force on the skin sample during the tests. This is an important parameter which has a major influence on the results (see later in Part 3.5).

To achieve this, we have imagined a special shape of the instrument's arms so that a force sensor could be inserted in a vertical position. This sensor, placed on a vertical axis above the sample, will allow direct measurement of the compression force of the studs on the sample. The force sensor chosen is identical to the horizontal force sensors used in the equipment, because they are accurate and small. It is a vertical force sensor measuring forces of [0 - 4.4] N with an uncertainty of 1.8 mN.

A major prototyping work was carried out on the arms. After defining the various parameters of the specifications, 3D modelling (using CATIA software) enables an initial study of the desired end product, which is the first stage in the manufacturing process. Once the industrial design has been produced, the prototype is made using the 3D printing technique, which is one of the additive manufacturing methods. This involves producing 3D prototypes using a printer. Once the prototype has been validated, the final machining and design of the parts can begin. The different stages of rapid prototyping are shown in Figure 2.9 below.

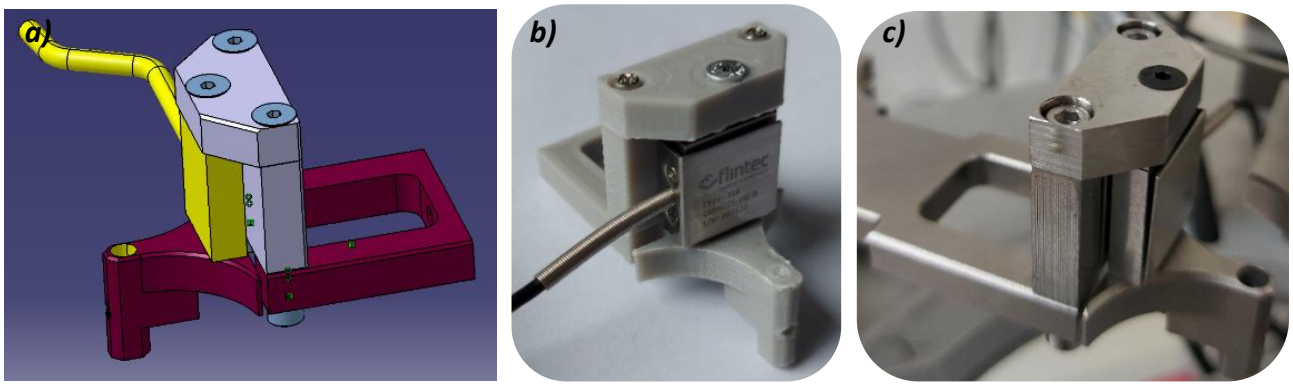

Figure 2.9: Prototyping of new arms with a vertical force sensor. a) Part designed in CATIA. b) 3D printed part. c) Machined part.

The disadvantage of adding these sensors is that they can induce an error in horizontal force measurements, since they can deform slightly under high stress, which can cause the arm to bend (vertical sensor is stressed in a direction other than its measurement direction). To avoid this, the vertical force sensors were placed on the Y-axis so as not to interfere with measurements on the X-axis.

In this configuration, the force sensors in a vertical position enable the pressure of the device's studs on the skin to be measured, and subsequently controlled. This notion of pressure is important as it has a major influence on the results. This modification to the arms resulted in a clear improvement in the reproducibility of the experiments (see later in Part 3.3).

2.1.2.D Sample holder improvement

To improve the reproducibility of the experiments, a specific sample holder, with a motorised sample holder with automatic vertical translation, has been designed.

The vertical movements of the sample holder were carried out manually, using a thumbwheel, which made it impossible to be precise when bringing the skin into contact with the device's studs. The new motorised vertical platform is a device that provides automated height adjustment with high precision: 50 µm accuracy (Figure 2.10). Levelling the skin explant on the device's studs will be done autonomously, without operator intervention. This change has also improved the reproducibility of the experiments (see later in Part 3.3).

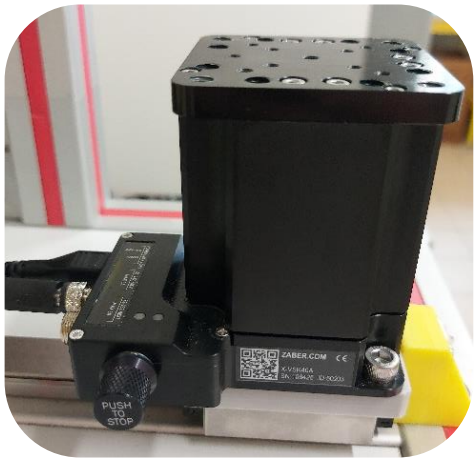

Figure 2.10: Specific support with integrated motor controllers and encoders.

2.1.2.E Programming updates and additions

Each structural or instrumental modification, as well as each addition of a component, entails numerous modifications to the software programming. The objective here is to develop the LabVIEW® control program for the technology's control and calculation unit, taking into account the technological modifications. This program controls and receives information from all of the equipment's various sensors and means of movement.

Firstly, the programming has been completed and enriched by adding various mechanical tests. The tensile test uses an added triangular signal, while the stress relaxation test uses an added square signal. These tests complete the dynamic tests already available, which use a sinusoidal signal (Figure 2.11). Other test possibilities, such as being able to pre-tension the sample before the mechanical tests, have been added. The addition of vertical force transducers and the ability to measure and control the pressure of the device's studs on the sample led to a significant change in the programming. Eventually, the final results were optimised in order to select the parameters needed to calculate the viscoelastic characteristics of the skin.

All these modifications and updates, such as the acquisition of new data, the control of new components, the addition of new test parameters, as well as the various adaptations of the test

procedures over time, have led to the final version of the programme. This latest version enables the operator to carry out mechanical tests in a reproducible way. Indeed, the operator using the device will follow a well-defined procedure via the programming software interface, which enables the connection of the various components, the final performance of the mechanical tests, through all the stages of sample preparation and test parameterisation. The procedure for carrying out the mechanical tests will be described later in Part 2.2.1. The software interface for this latest version of the programme is shown in Appendix 2.

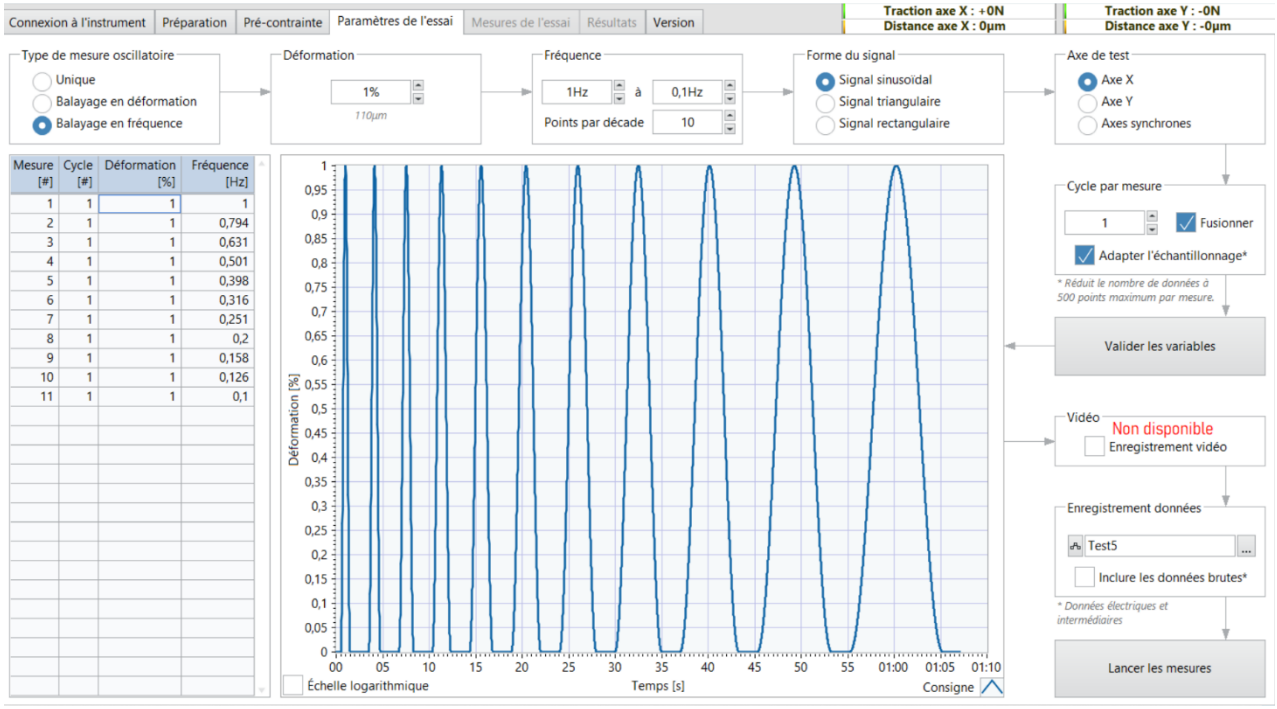

Figure 2.11: Example of a page from the software interface used to set up a mechanical test.

2.1.2.F Adaptation of the device to human skin explants

The ultimate objective of developing this innovative equipment is to characterise the mechanical properties of human skin. It was therefore necessary to adapt the device to human skin explants. As described in detail later in Part 2.3, these skin explants were provided by the Eurofins BIO-EC laboratory.

In order to create supports for the skin samples, it was essential to use prototyping and 3D printing techniques. 3D printing technique, also known as Additive Manufacturing (AM), involves building the final object by depositing layers of material one on top of the other. To print the parts, we used the molten wire deposition method, known as FDM (Fused Deposition Modeling), with PLA or ABS as printing material. To create the parts, we use PLA or ABS as the printing material. The printer used has a resolution of 0.2 mm in height and 0.4 mm in width.

Figure 2.12 shows, for example, the 3D printed parts that will be attached to the motorised sample holder in order to collect the various skin explants. The aim is for the equipment to be adaptable to the different types of skin explants in the Eurofins BIO-EC laboratory.

These printed parts are not involved in the mechanical stretching of the skin, but are rigid enough to be used as support parts or parts to complete and embellish the device. It is also interesting to note that 3D printing is a highly effective and inexpensive method of prototyping parts before ordering metal parts.

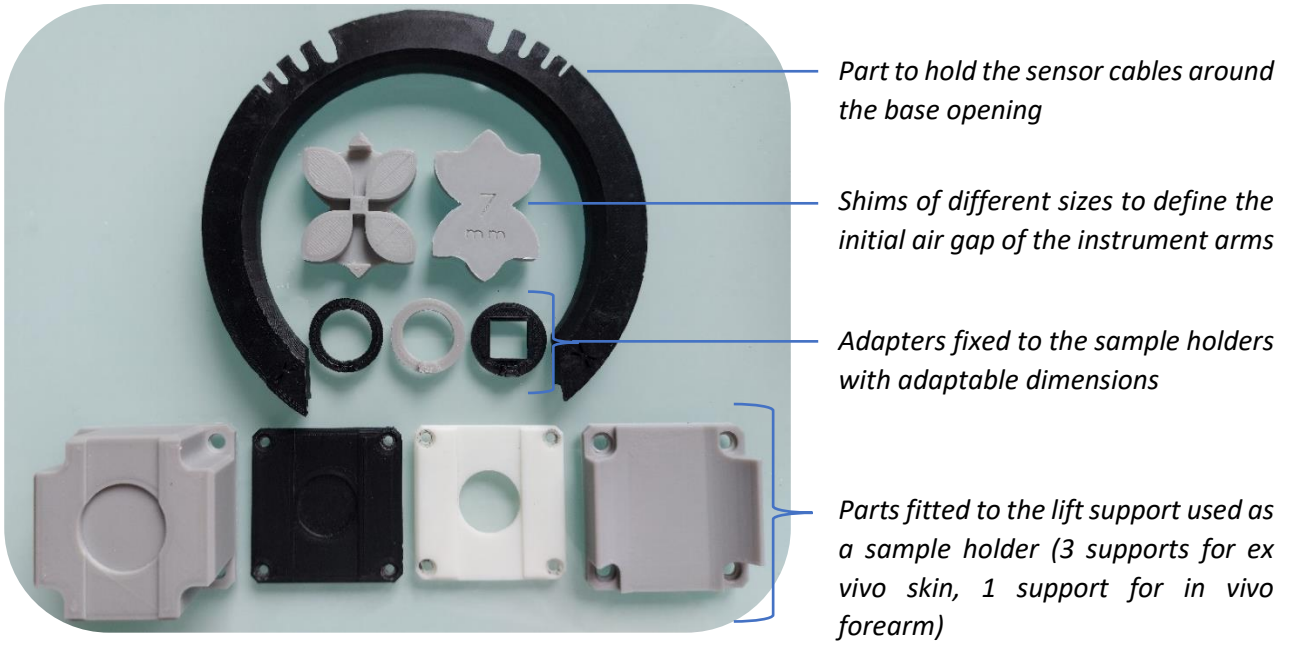

Figure 2.12: Photo of different 3D printed parts to adapt to different types of human skin samples.

2.1.3 Final state of the device

The ongoing development has enabled us to achieve the current version of this device (final state valid within the framework of this thesis). This final version of the device meets the objective of accurately characterising the viscoelastic properties of skin. Figure 2.13 shows a photo of the latest version of the device.

As a reminder, the four mechanical loading modules are arranged around the centre of the device and each configured to exert a tensile force in a radial direction parallel to the surface of the skin sample. The translation arms are aligned in pairs and the axial displacement devices are synchronised to simultaneously displace two traction elements along the common axis.

Each mechanical loading module comprises a translation arm connected:

- on the one hand to the traction elements: the studs
- and on the other hand, to a translational displacement system capable of displacing this arm: a piezoelectric nano-positioning table fixed to a manual micrometric displacement table.

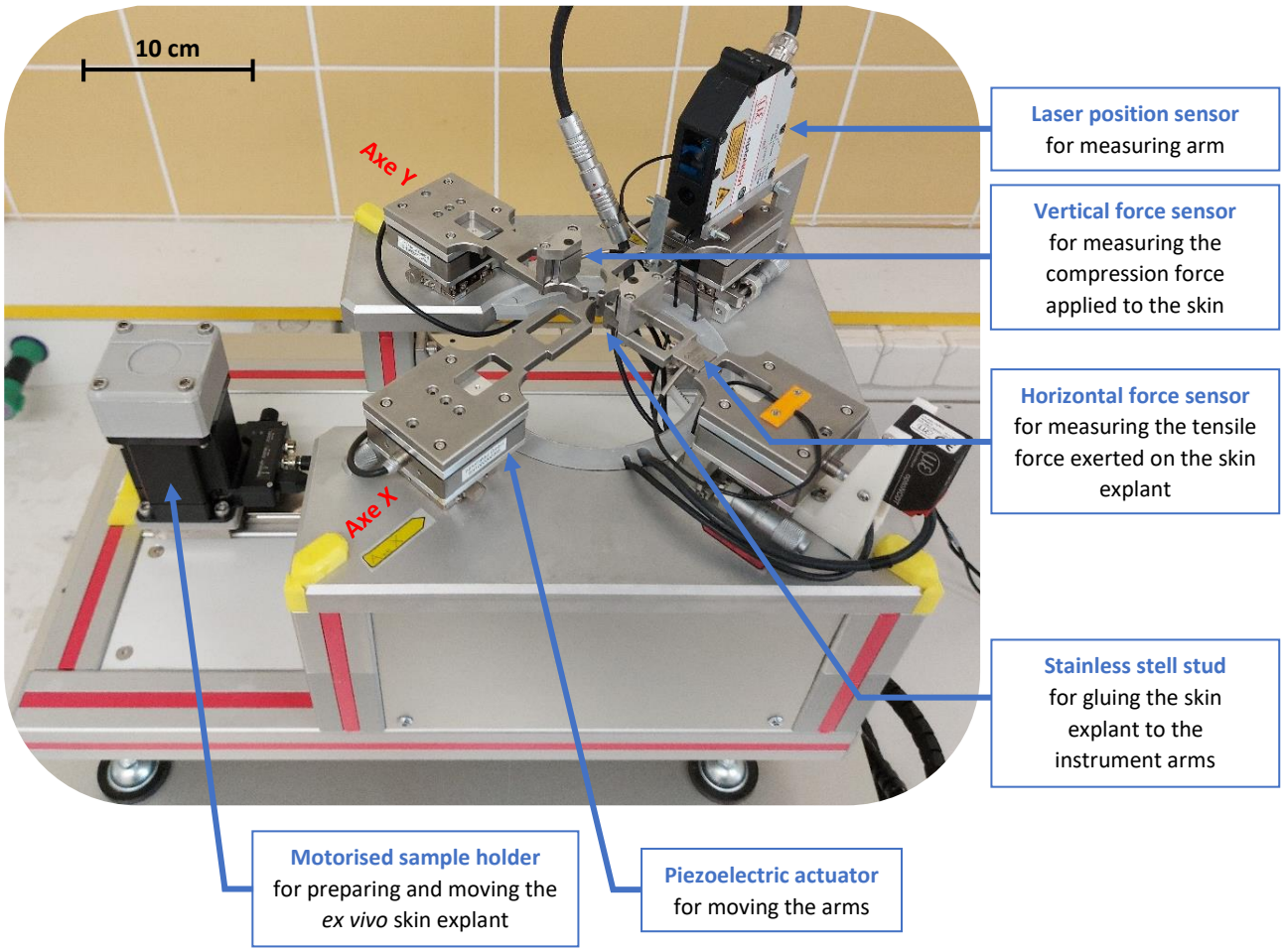

Figure 2.13: Photo and description of the final version of the device.

The X-axis is equipped with two highly accurate sensors: a position sensor that accurately measures the position of a translation arm during its movement, and a tensile force sensor that measures the force exerted by the studs. The sensors on this axis have been improved to offer greater precision. This is why this axis will be used to assess the mechanical properties of the skin.
The Y load axis is equipped with three types of sensors: a position measurement sensor, a horizontal force, and a vertical force sensor capable of measuring the compression force exerted by the studs. In this work, this axis will be used for placing the skin sample on the device, using the vertical force sensors.

The motorised sample holder is positioned on a mobile plate that allows the skin sample to be moved around the measurement zone, under the four mechanical loading modules. The sample holder has a number of templates for centring the sample and adapting it to the different skins used. A camera is also configured to observe and record the deformation zone of the skin surface. Finally,

a control and calculation unit has been developed to control the displacement means and receive the measured signals in order to calculate the mechanical properties of the skin. Various types of tests, including quasi-static tests and dynamic tests, enable the mechanical properties of the skin to be comprehensively evaluated.
The connectivity of all the components of the equipment, in terms of power and data, is presented in the form of diagrams in Appendix 3.

By controlling the displacement arms over a precise range of frequencies, it is possible to measure the mechanical properties of the skin over a wide range of loading times in order to characterise the overall behaviour of the skin. In contrast to the speed-controlled loadings normally used to analyse the mechanical properties of biological tissue, we are proposing a measurement system based on loadings over a range of frequencies, enabling to determine the complex modulus of the skin as a function of different frequencies in a single measurement phase. This type of measurement provides information on the viscoelasticity of the skin: the real part of the complex module characterises the elastic properties whereas its imaginary part characterises the dissipation properties (Figure 2.14).

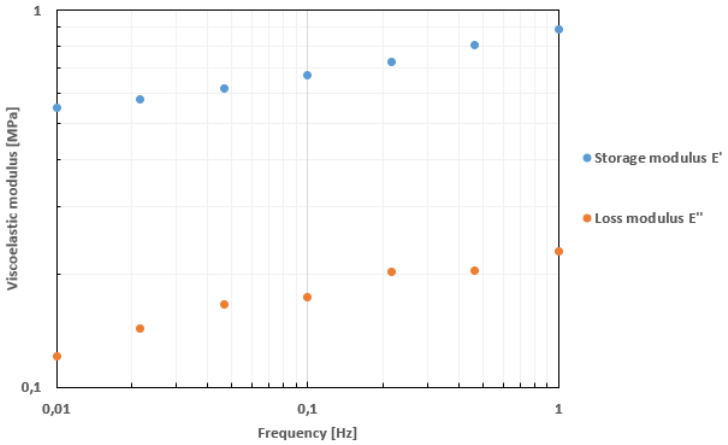

Figure 2.14: Example of the evolution of the complex modulus measured for a sample of pigskin as a function of the test frequency (Parameter: strain = 10%).

2.1.4 Experimental validation of the device using different materials

As human skin is a precious material that is difficult to obtain (because it is not widely available), we chose to carry out experimental tests on other types of material before carrying out the tests on skin in the Eurofins Bio-EC laboratory. A preliminary step was to calibrate our instrumentation using a reference material. We then carried out tests on elastic and viscoelastic materials.

2.1.4.A Tests on tension springs

The first important point, before testing different types of material with this newly developed equipment, is to validate the instrument's physical measurements by carrying out tests on a material with known mechanical properties. We therefore decided to choose a very small, rigid material: tension springs (Figure 2.15).

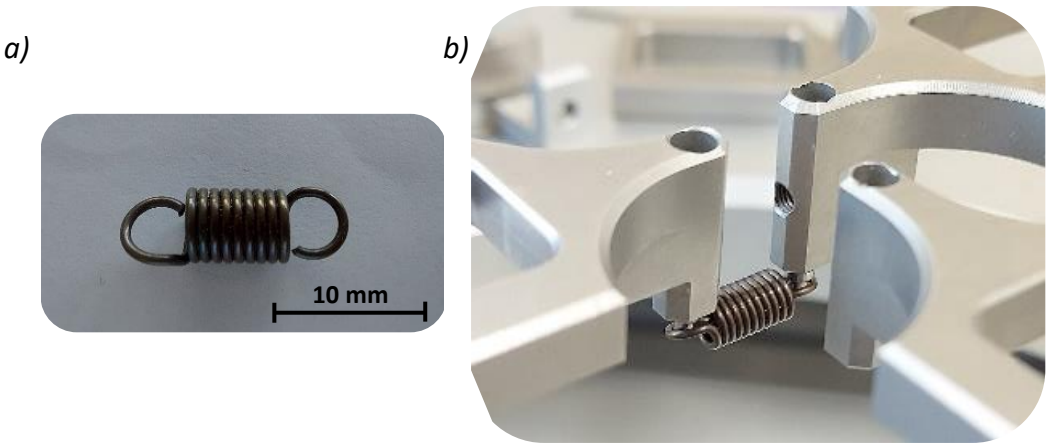

Figure 2.15: a) Tension spring used to calibrate our instrumentation. b) Spring set up for a test.

These steel tension springs were purchased from "*Sodemann ressort*" and comply with current DIN standards (DIN 17223). When a spring is stretched, it accumulates force. This force is released when the spring returns to its original length. Springs are elastic materials, which means that 100% of the energy accumulated by the spring is released. The elongation of the spring, noted *x*, is proportional to the force F_{ext} to which it is subjected, according to the following formula:

$$F_{ext} = k \,.\, x \quad (2.1)$$

where *k* is the constant of proportionality known as the "stiffness constant" of the spring and expressed in $N.m^{-1}$. The value of *k* therefore characterises the spring by defining its stiffness.

In order to obtain a certified value for this stiffness constant for the springs we own, they were sent to a certified centre: the *Centre technique des industries mécaniques* (CETIM). CETIM measured the spring stiffness in tension so that we could calibrate our device. This calibration stage enables the value measured by our device undergoing calibration to be compared with a reference or standard of known and high accuracy.

To measure the spring stiffness constant, quasi-static simple tensile tests were carried out. The spring constant of 3.88 $N.mm^{-1}$, as measured by CETIM, must therefore be measured as well using our device. For installation, the spring is held in place by the loops at the ends, which are hooked

onto the studs (Figure 2.15b). The results obtained with our device, shown in Figure 2.16, demonstrate the ability of our equipment to reliably measure the spring stiffness constant. These measurements validate the fact that the force and position sensors are well calibrated. This allows us to scientifically validate the data obtained with our device.

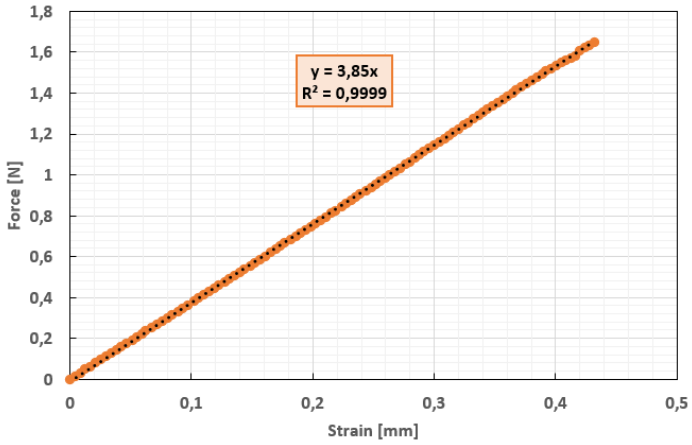

Figure 2.16: Tensile test results with a spring. Measurement of the spring stiffness constant: k = [3.85 ± 0.05] N.mm^{-1}.

2.1.4.B Tests on elastic materials

Tests on elastic materials were then carried out to examine and confirm the purely elastic behaviour of this type of material. We therefore carried out tests on elastic bands.

Regarding the installation of the elastic samples on our device, Figure 2.17 shows that the studs of the translation arms were glued to the elastics.

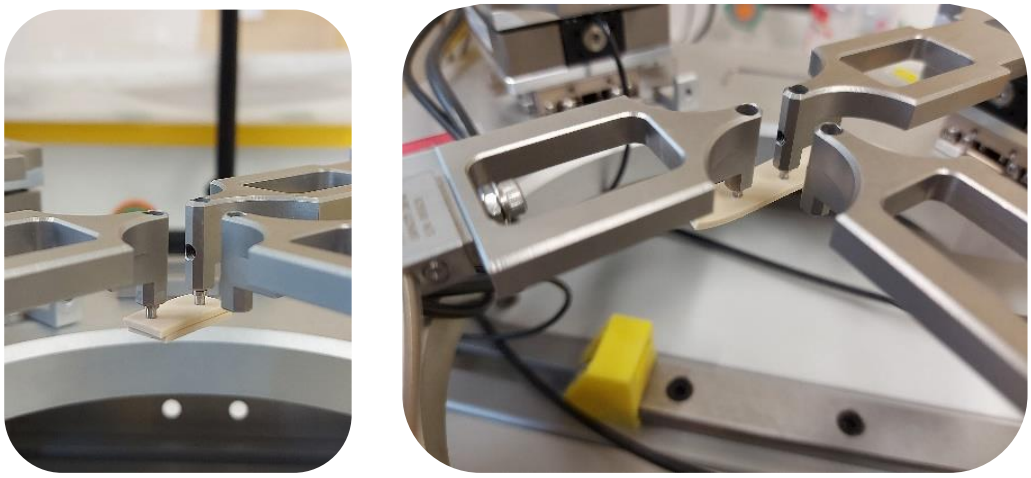

Figure 2.17: Mechanical test on an elastic band.

An elastic material, as its name suggests, is characterised by 100% elasticity. This means that all the energy accumulated during deformation is fully restored when the deformation ceases.

On a graph, this can be seen as follows:

- The "force versus deformation" curve is linear in the case of simple traction.
- There is no shift in phase between the sinusoids of the force curve and the deformation curve during dynamic tests.

The results obtained with the elastic bands, illustrated in Figure 2.18, confirm their purely elastic behaviour. In other words, there is no phase shift between the two curves during the dynamic tests and the force response of the material is linear with the strain imposed in simple tension.

The measurements carried out on elastic materials enable us to experimentally validate the data obtained using our device. A further step can be reached by carrying out the following tests on viscoelastic materials.

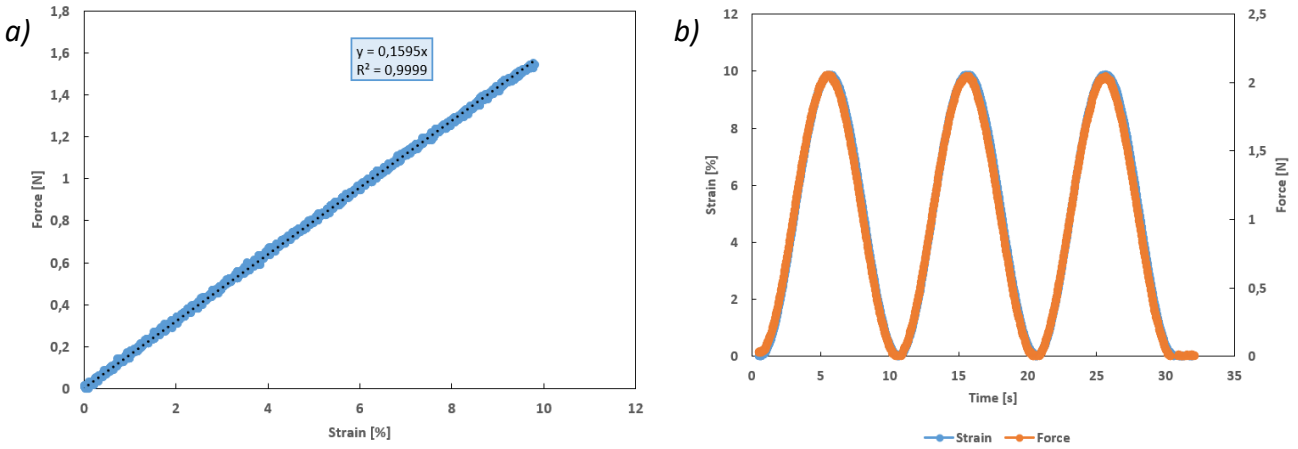

Figure 2.18: Results of mechanical tests with elastics. a) Simple traction (speed = 1 mm.min-1). b) Dynamic tests (f = 0.1 Hz - strain = 10%).

2.1.4.C Tests on viscoelastic materials

To complete and finalise our experimental validation, we carried out tests on viscoelastic materials whose mechanical behaviour is very similar to that of human skin [Brèque, 2002]; [Convelbo, 2017]. Indeed, first tests were carried out on biological materials: pig skin and pig pericardium.

These models are considered equivalent to human skin. Porcine skin and pericardium, the envelope of the heart, are viscoelastic connective tissues with mechanical properties similar to those of human skin. Their microstructures are virtually identical, with the presence of networks of collagen and elastin fibres [Le Bras, 2012].

The biological tissues used were obtained from a local butcher. They were frozen at -24°C for preservation and thawed 30 minutes before testing. Samples were taken by making incisions in the skin. With regard to the positioning of these samples in our equipment, Figure 2.19 shows that the ends of the translation arms, i.e. the studs, are glued to the tissue.

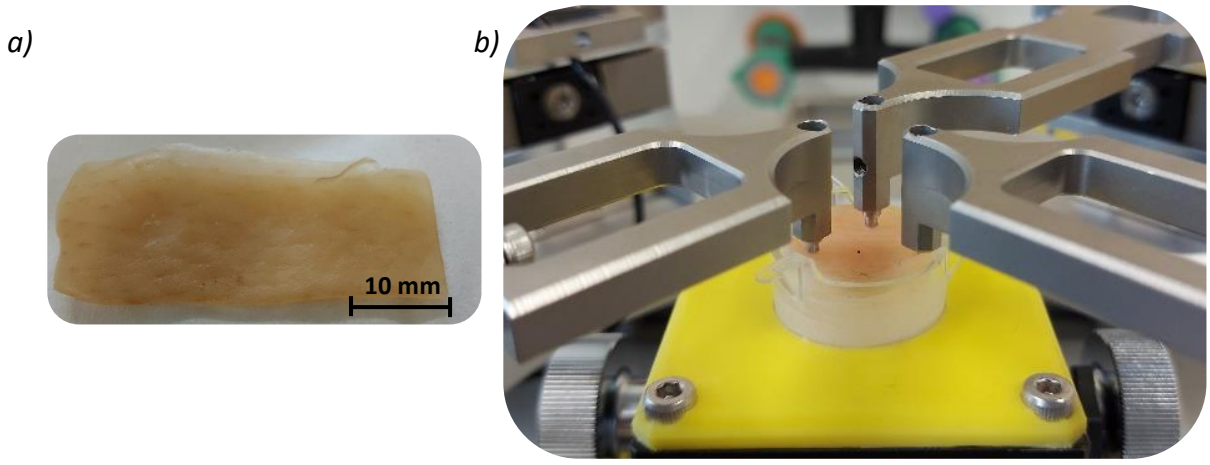

Figure 2.19: Preliminary tests on a viscoelastic material. a) Photo of a sample of pig skin. b) Photo of a test on pig skin under experimental conditions close to future conditions with ex vivo skins.

The skin and pericardium, as soft tissues, exhibit viscoelastic properties. A viscoelastic material combines both elastic and viscous characteristics. On a graph, this can be seen as follows:

- The "force versus strain" curve presents a non-linear domain in the case of simple tension,
- There is a shift in phase between the sinusoids of the force curve and the deformation curve in dynamic tests.

The results obtained with pigskin, shown in Figure 2.20, confirm the viscoelastic behaviour of pigskin. In other words, there is a phase shift between the two curves during the dynamic tests and the force response of the material is not linear with the deformation imposed in simple tension.

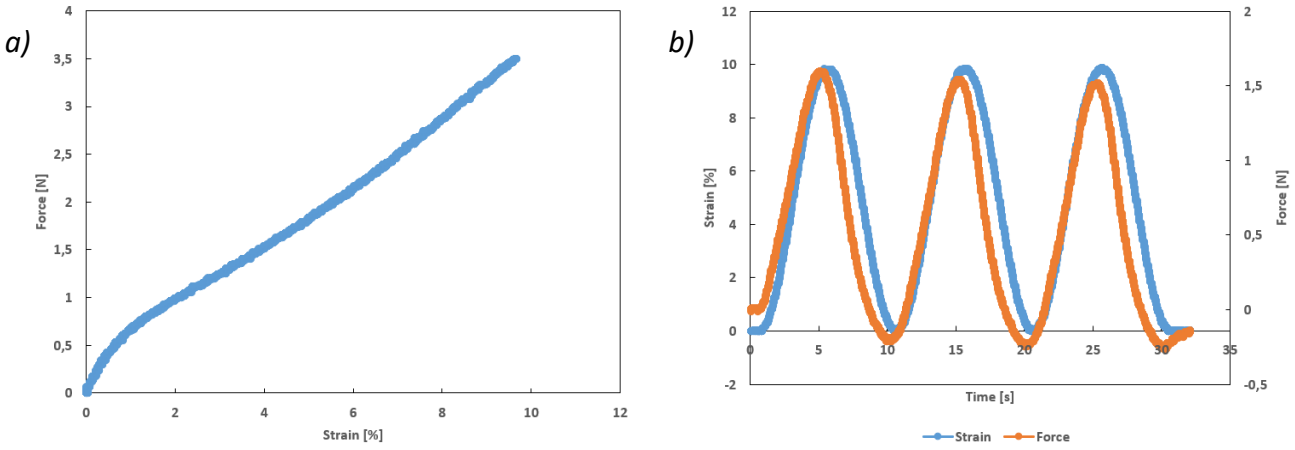

Figure 2.20: Results of mechanical tests on a sample of pigskin. a) Simple traction (speed = 1 mm.min^{-1}). b) Dynamic tests (f = 0.1 Hz - strain = 10%).

These tests have enabled us to validate the data obtained using our device on a material that is very close to human skin. The device is therefore ready to characterise the mechanical behaviour of real samples of human skin.

2.1.5 Conclusion on the development of the equipment

The development described all along this part proceeded continuously over the first two years of the thesis, leading to a final version of the device (Figure 2.21b) capable of accurately characterising the mechanical properties of soft tissue, in our case the human skin. This so-called 'final' version, described in Part 2.1.3, marks the end of the technological development, as we decided to temporarily put this development on hold in order to focus on characterising the properties of human skin in different situation. Of course, there is still room for improvement and development for the instrumentation, as indicated in the "Conclusion and prospects" Section.

This development process was achieved through preliminary tests on different types of materials (Part 2.1.4), as well as initial tests on human skin carried out at the Eurofins BIO-EC laboratory. The device was first calibrated using calibrated tension springs. The measurement approaches and techniques were then validated on elastic and viscoelastic materials before being applied to human skin.

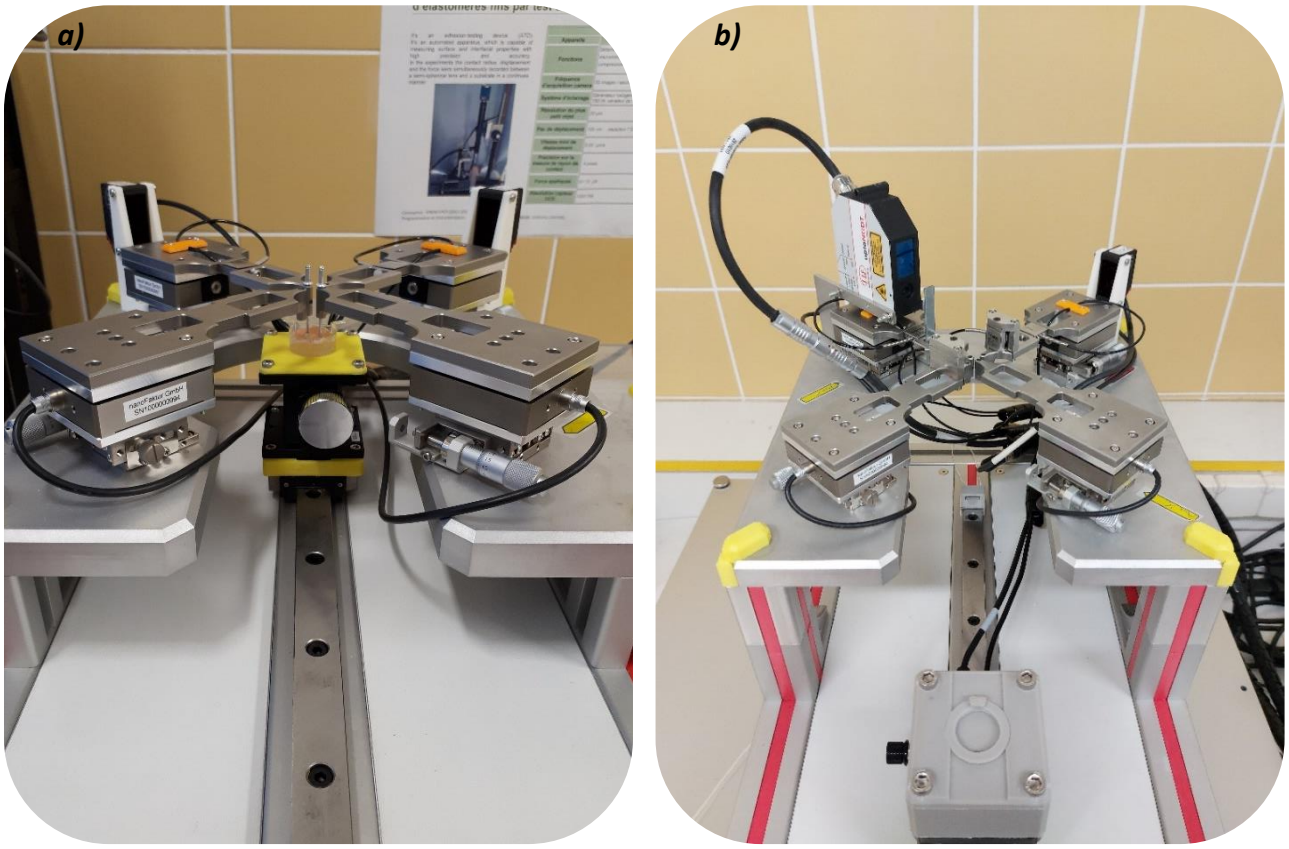

Figure 2.21: Photo of the initial (a) and final (b) versions of the device.

2.2 Methods

2.2.1 Test protocol

The entire procedure for performing a test on a skin explant is described in detail in Appendix 2. This Appendix presents the different pages of the software interface that allow the operator to follow a well-defined path to carry out a mechanical test on a skin explant. The main steps of this procedure are described below.

2.2.1.A Settings and initial conditions before starting the test procedure

Before preparing the skin samples and even before switching on the device, there are a few actions that need to be carried out, in particular the adjustment and initial preparation of the arms of the equipment.

First of all, it is necessary to check and, if necessary, adjust the horizontality of the studs on the four arms. Next, the manual adjustment of the air gap between the studs for the 0% deformation must be carried out using the manual micrometric displacement table. Fine adjustment of the centre-to-centre spacing of the studs is checked using standard length shims.

To perform a uniaxial tension-compression test, a dimensional requirement must be satisfied [Standard ISO 6721-1]. There must be a certain distance between the attachment points on the skin in order to not cause changes in the stress field during tension. A dimensionless parameter, denoted F_C, must be as close as possible to 1, or in any case greater than 0.97, in order to load the sample in almost pure tension-compression. This parameter depends on the geometry of the sample:

$$F_c = \frac{1}{1 + 2.(\frac{S_E}{S_L})^2} \quad (2.2)$$

with S_E the excited cross-section ($S_E = e.l$) and S_L the unstressed lateral surface of the skin sample ($S_L = 2.L.(l+e)$). In our case, the thickness e of the various skins is approximately 3 mm, the width l of the skin subjected to tensile stress is approximated by the width of the device studs, i.e. 2 mm, and the length L of the sample is the initial air gap of the studs. To meet this dimensional requirement, $F_C > 0.97$, L must be larger than 5 mm. During the tests, this criterion was satisfied by setting the initial air gap at 7 mm. This is the largest possible distance between the studs, taking into account the dimensions of Eurofins BIO-EC skin explants, which generally have a diameter of 12 mm.

Particular attention must also be paid to the conditions under which the tests were carried out, and in particular the temperature (T °C) and the percentage of relative humidity (%RH) during the tests. All tests on human skin took place in a closed manipulation room in the Eurofins BIO-EC laboratory. They were carried out under the same experimental conditions, paying particular attention to these two parameters. A box measuring temperature and humidity was placed in the device room. For all the different series of tests, the average temperature was 25°C and the average relative humidity was 45% RH.

2.2.1.B Device connection and preparation of ex vivo human skin explants

Once the initial conditions have been met, the operator can power up the device and open the "Mécapeau" software on the computer dedicated to this device (Appendix 2).

Human skin explants can then be prepared for testing. These human skin explants, which come from the Eurofins BIO-EC Laboratory, are presented and described in detail later in Part 2.3. These explants are removed from an incubator where they were maintained in survival under specific environmental and culture conditions. They are then placed on a special support supplied by Eurofins BIO-EC (white support visible in Figure 2.22) which allows the explants to be maintained 'fed' during the experimental phase of mechanical testing.

Note: the support on which the sample rests, and where it will slide, is smooth but has holes so that the skin is in contact with the nutritional medium. Friction forces are therefore likely to be present during the mechanical tests. These forces were not measured; they were considered to be constant for all the skin explants analysed.

2.2.1.C Placement of the explant

The skin is first placed on the motorised sample holder, which is then positioned in the centre of the device.

The end of the two studs of the X measurement axis is then glued using a liquid cyanoacrylate adhesive. The sample holder rises automatically to bring the skin into contact with the glued studs, and stops when the compression force entered in the software and measured on the Y-axis studs is reached (Figure 2.22a&b).
Once the adhesive has dried and solidified in a few minutes, the mechanical tests can be carried out.

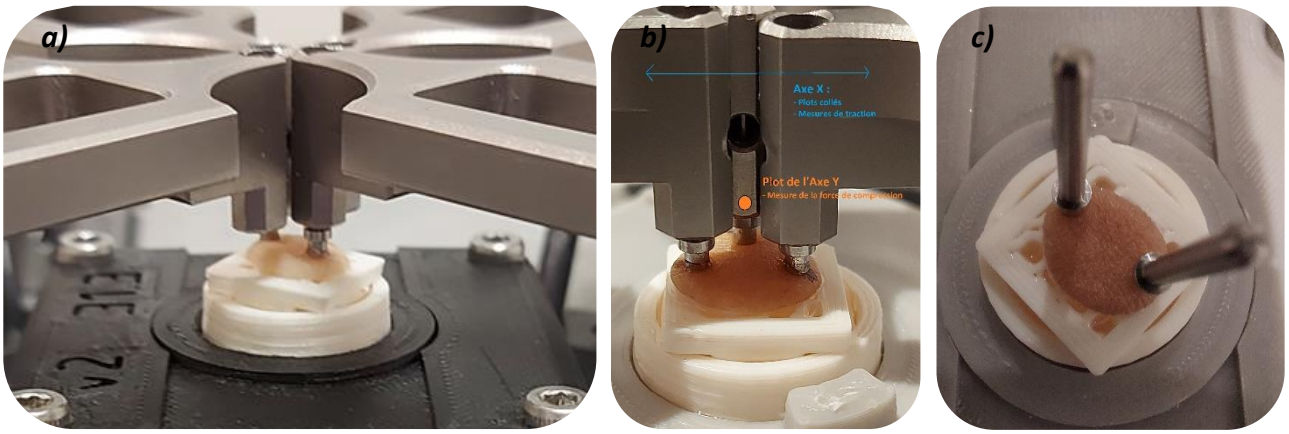

Figure 2.22: Photo of the measurement area showing the X-axis studs bonded to the skin sample. a) Enlarged view. b) Zoomed view of the skin explant: bonded X-axis studs inducing traction and Y-axis stud measuring compression force. c) View of the sample at the end of the tests when the studs are detached from the arms.

Positioning the studs is an important step, as it determines how well the mechanical tests are carried out. Precise positioning of the skin guarantees reproducible measurements. In fact, it is essential to

carry out this stage in the same way for each test in order to avoid any initial errors. The addition of the vertical force sensors and the motorised lift support has made it possible to automate this sample positioning procedure, making it highly reproducible.

2.2.1.D End of tests

Once the mechanical tests have been completed, the lift support is lowered to its initial position with the studs still glued to the surface of the skin (Figure 2.22c). The studs are then removed and peeled off by inducing a slight flexion in the skin at the adhesive point. It is important to note that all of the glue remains on the studs and no treatment is required to remove the glue from the skin. Visually, the skin does not appear damaged, although it is certain that this gluing step removes some layers of the stratum corneum at the gluing point. At the end of the tests, the explant is placed back in the incubator.

Important note:
A reference point or pen mark should be made on the skin at the bond points to ensure that future tests on the explant will be carried out at the same precise location. It is crucial to identify this bonding area on the skin so that the studs can be repositioned in the same place at a later time.

The disadvantage of this method is that, between two tests spaced out over time, the studs must be removed and repositioned, which can lead to inaccuracies in the location of the area studied and potentially affect the reproducibility of the tests.

2.2.2 The different types of mechanical tests possible

As a reminder, this device enables to carry out mechanical tests on the skin by imposing different constraints. These different types of constraints are induced by the displacement of the moving part of the piezoelectric nano-positioning tables on each arm. These tables are set for a maximum displacement of 550 µm. This means that on a measurement axis where two piezoelectric tables are aligned, the maximum deformation applied to the sample is 1.1 mm. The device can therefore be used to perform the following tests.

2.2.2.A Dynamic tests

The innovative aspect of this device is the fact that we can carry out dynamic tests: spectromechanical analyses (for polymer materials, this is known as Dynamic Mechanical Analysis). Dynamic Mechanical Analysis (DMA) is a method for measuring the viscoelasticity of materials.

In dynamic mechanical analysis, the sample is subjected to oscillatory deformation. In our case, sinusoidal deformations are repeatedly applied to the material at a specific frequency. The resulting force of the material is then measured. In the dynamic regime, the mechanical properties of a material depend on the deformation and the excitation frequency. Two dynamic mechanical tests are used to characterise a material:

- Strain sweep test (Figure 2.23a). The strain sweep or amplitude sweep is the first test to be carried out. It determines the linear viscoelastic range (LVE range) of the material. In the LVE range, the viscoelastic moduli are constant, so the structure of the sample is not damaged by the applied deformation. For this type of test, the amplitude of deformation increases logarithmically and the frequency of the sinusoids is constant. In our case, the deformation can vary from 0.1% to more than 10% during the test; the frequency used is often around 1 Hz.
- Frequency sweep test (Figure 2.23b). Frequency scanning is used to study the short- and long-term behaviour of the material. The high-frequency data represents the short-term behaviour of the sample, where the local displacements of the polymer chains are analysed. On the other hand, at low frequencies, the data reflect the long-term behaviour of the sample, where the global displacements of the polymer chains are taken into account. For this type of test, the frequency decreases logarithmically and the deformation of the sinusoids is constant. In our case, the frequency can vary from 10 mHz to 1 Hz during the test; the deformation used should, if possible, fall within the LVE range defined above.

These two dynamic tests will provide information about the viscoelastic moduli of the studied material.

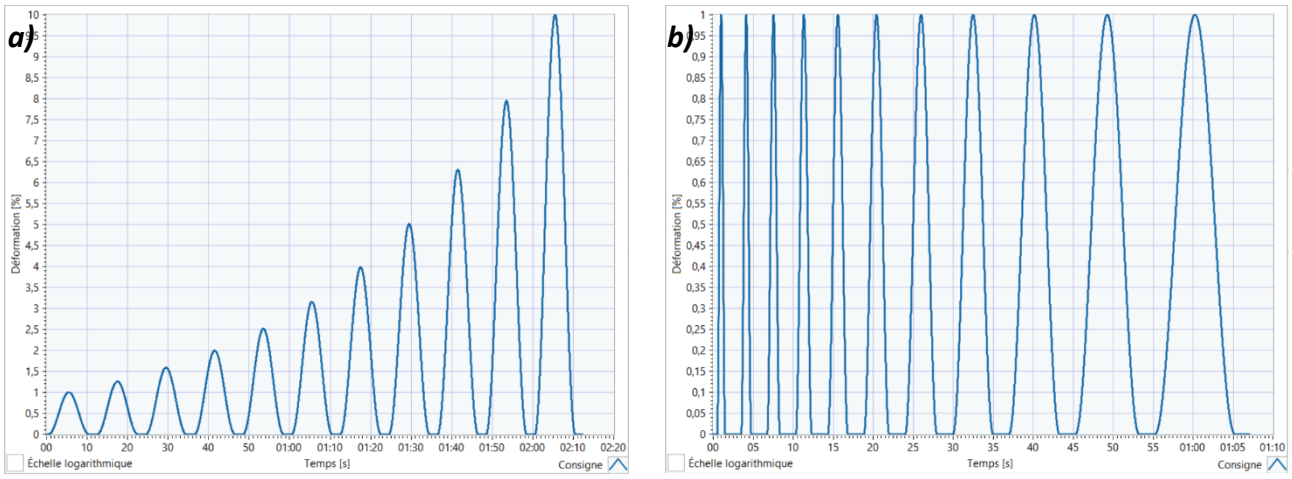

Figure 2.23: Dynamic mechanical tests: imposed strain sinusoids. a) Strain sweep (Parameters: strain = 1 to 10% - frequency = 0.1 Hz). b) Frequency sweep (Parameters: f = 1 to 0.1 Hz - strain = 1%).

Another type of dynamic mechanical test consists of stressing the material by imposing load-unload cycles (Figure 2.24). The amplitude of deformation and the test speed are kept constant. These cycles enable to evaluate the hysteresis phenomenon of a material.

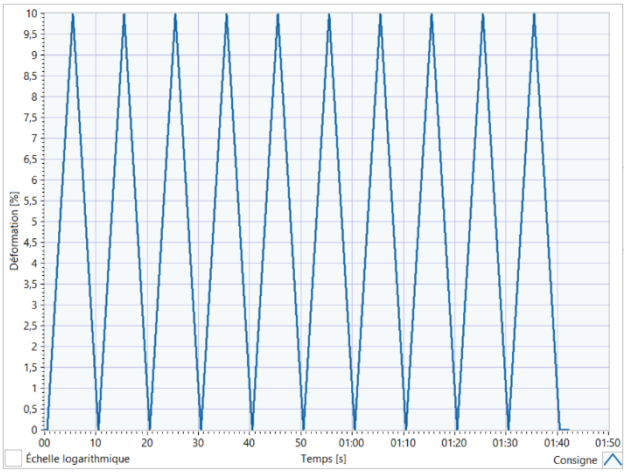

Figure 2.24: Dynamic mechanical testing: loading-unloading cycles (Parameters: strain = 10% - f = 0.1 Hz)

2.2.2.B Quasi-static tests

The device can also be used to carry out quasi-static tests, often called static tests. In this type of test, a very slow deformation is applied to the material, allowing dynamic effects to be neglected. The resulting force of the material is then measured.

i) *Tensile test*

The tensile test consists in applying a linear and constant deformation to the material (Figure 2.25a). The strain is applied progressively and constantly, at a low strain rate. Similar speeds to those used during tests on a conventional tensile testing machine were used here, generally around 1 mm per minute.

These tests are used to characterise the strength of the material and its behaviour to large deformations under tensile stress. Tensile tests provide information about the elastic behaviour of the material.

ii) Stress relaxation test

The last tests that can be carried out with the device are stress relaxation tests (Figure 2.25b). Like the dynamic techniques, this test is used to analyse the viscoelasticity of a material. In a relaxation test, a constant instantaneous strain is applied to the sample over a period of time. The resulting stress is monitored as a function of time.

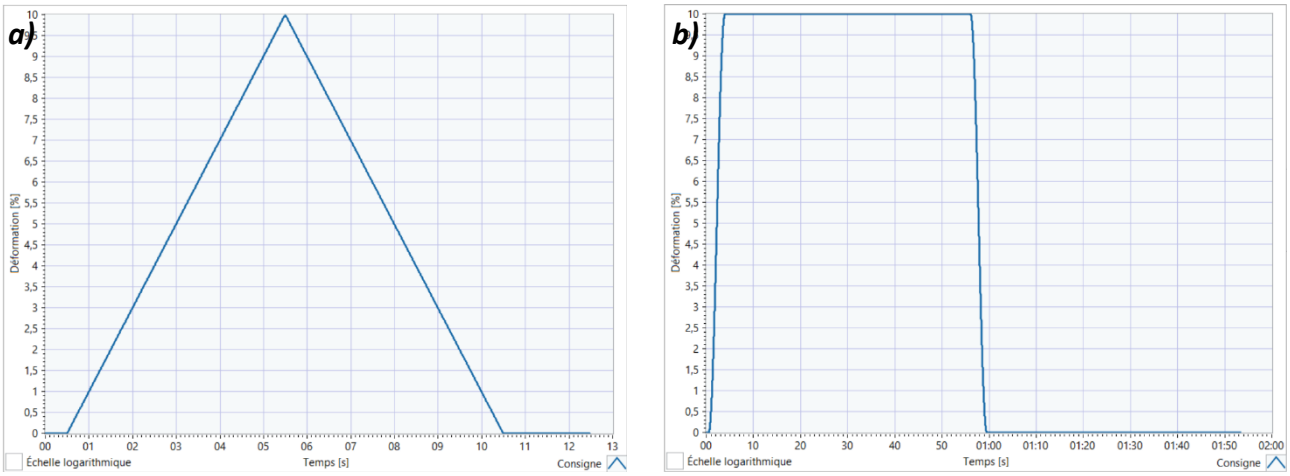

Figure 2.25: Static mechanical tests. a) Simple traction: linear ramp of imposed strain (Parameters: strain = 10% - speed = 6 mm.min^{-1}). b) Stress relaxation: strain kept constant (Parameters: strain = 10% - time = 60s).

Note: definition of mechanical terms

- Elasticity: it is the physical property of a solid material to deform when forces are applied and to return to its original shape once the applied forces have been removed. Elastic deformation is reversible. The elasticity of a material therefore reflects its ability to conserve and restore energy after deformation.

- Viscosity: it is the property of resistance to uniform flow without turbulence occurring in the mass of a material. A viscous product is one with a high resistance to flow. The viscosity of a material therefore reflects its ability to dissipate energy.

- Viscoelasticity: it is the property of materials that exhibit a combination of elastic and viscous properties when subjected to deformation. Viscoelasticity is characterised by a rheological behaviour that is intermediate between:

  + on the one hand, that of an elastic solid, represented by the spring.

  + on the other hand, that of a Newtonian viscous liquid.

- Stiffness: it is the main characteristic that indicates the resistance to elastic deformation of a material such as skin. In other words, it is the ability of an object to resist to deformation when an external stress is applied. Elastic moduli such as Young's modulus represent the stiffness of the material; the higher the modulus, the stiffer the material.

In terms of vocabulary, a biomechanist will use the terms elasticity, viscoelasticity, and stiffness to describe the mechanical behaviour of human skin under stress. Conversely, for a doctor or clinician, terms such as firmness are used to refer to the toned texture of the skin (notion of "sensation"). Skin firmness can be translated as its ability to resist pressure and stretching. Skin firmness is intimately linked to its viscoelastic properties.

2.2.3 Methods for analysing results

The various mechanical tests presented above are used to probe the elastic and viscoelastic properties of different materials, particularly skin. This Section is now devoted to a description of the various methods used to analyse the results.

2.2.3.A Parameters used to calculate the elastic and viscoelastic moduli

The raw results measured by the equipment, in response to the movements of the piezoelectric nano-positioning tables that cause the sample to deform, are force in Newtons (N) and sample deformation in millimetres (mm).

However, in materials resistance science, it is generally preferable to use mechanical stresses to represent and analyse the results of mechanical tests. The mechanical tensile stress σ is the tensile force F divided by the tensile area S:

$$\sigma = \frac{F}{S} \quad (2.3)$$

Stress is the same as pressure; the unit of measurement is the $N.m^{-2}$ = Pa (pascal).

In our situation, we know precisely the value of the force applied to the sample because it is measured by a force sensor. However, the surface or section stressed during the tests is not exactly known because our samples are circular biopsies of human skin, for which there is no reference or standard allowing this type of experiment to be carried out.
The skin explants supplied by Eurofins BIO-EC are generally very thin, with a thickness of between 2 and 3 mm. We therefore assume that the entire thickness of the explant is subjected to a tensile force. The thickness of the skin, measured for each explant as described in Appendix 2, will therefore be taken into account in our calculations.
Regarding the width subjected to tensile stress, we make an approximation using the width of the instrument's studs, which is 2 mm (Figure 2.26b). In fact, the actual width subjected to tension is at least equal to the width of the studs used to stretch the skin.
We are making a strong assumption here by saying that everything happens as it would on a rectangular sample. We therefore calculated our moduli on the assumption that most of the mechanical forces between the two studs came from what happens between the width of the two studs and the thickness of the skin (to our knowledge, no rectangular skin explant suitable for mechanical testing currently exists on the market ; and given the small size of the explants, it was not possible to cut strips of 2 mm in width).

We carried out several tests to analyse the surface of the sample under tensile loading using the camera located above the test zone (Figure 2.26a). The aim was to identify the stress field of our system. The images, analysed using the *ImageJ* software, show different results in terms of the width subjected to tension depending on the material studied. For example, an elastic seems to be stressed over a width of 10 mm, whereas only 4 mm of width seems to be stressed in the case of pigskin. These results show that the width subjected to tension depends on the material used, its structural organisation and its internal cohesion. In order to ensure that the entire cross-section

subject to tension is taken into account, we chose a constant width of 2 mm (corresponding to the width of the studs) for the modulus calculations on human skin explants.

These initial calculations allow us to obtain stress-strain curves, from which we can determine the viscoelastic moduli of the skin.

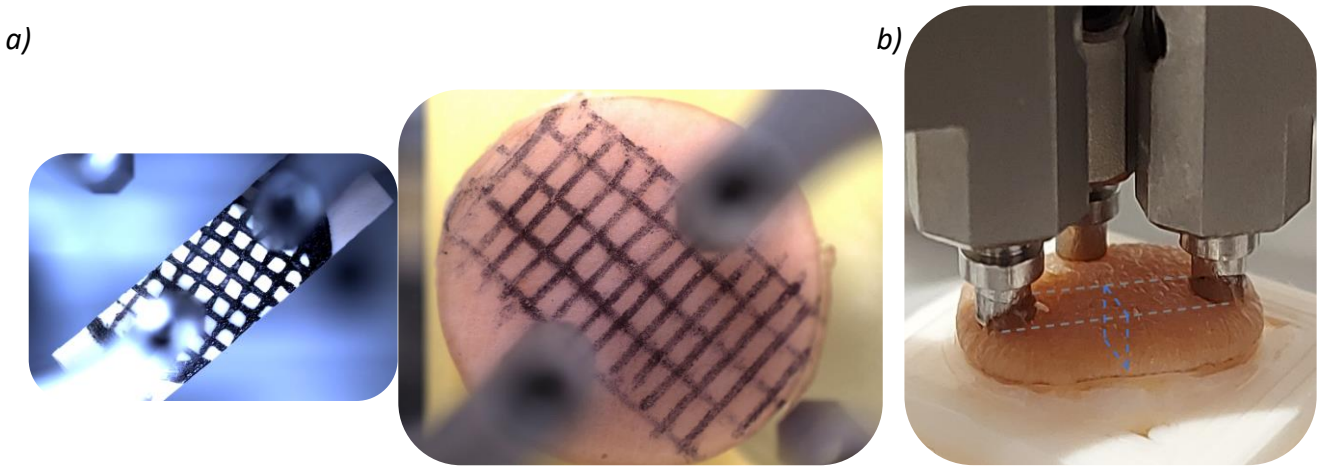

Figure 2.26: a) Analysis of the surface of the sample under stress using the camera and an ink grid (elastic band and pigskin). b) Section stressed in tension (human skin).

2.2.3.B Dynamic tests

The dynamic test method consists of applying a small sinusoidal deformation to the material and measuring the resulting sinusoidal force (Figure 2.27a).

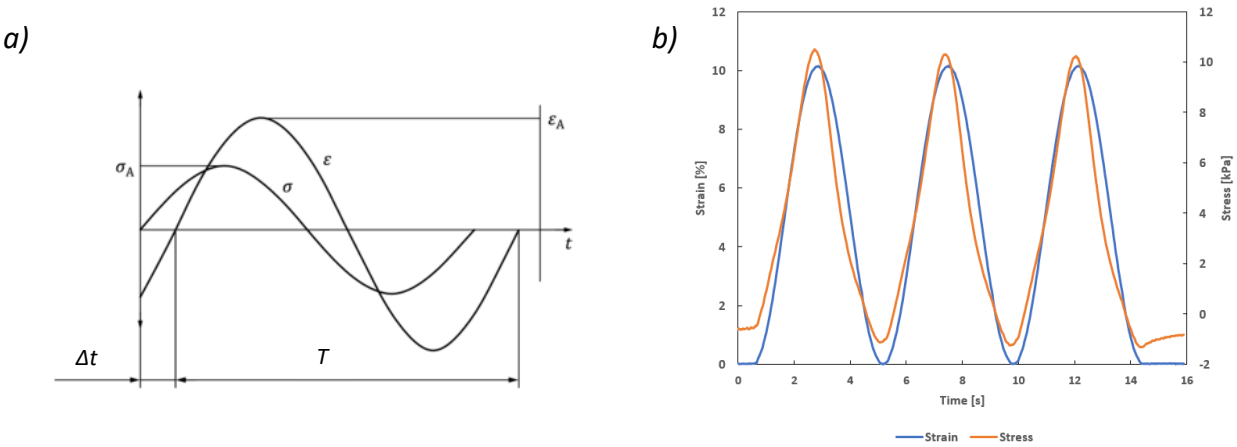

Figure 2.27: Dynamic tests: stress-strain curves as a function of time for a viscoelastic material. Theoretical curve (a) and experimental curve on human skin (b).

Using the values for the amplitude of the strain curve, the amplitude of the stress curve and the phase shift between these two curves, it is possible to calculate the viscoelastic moduli of the skin (E' and E''). It should be noted that, due to the complex mechanical behaviour of the skin, the force sinusoids measured do not correspond perfectly to perfect sinusoids (Figure 2.27b). The phase shift is therefore measured between the peak of the two curves.

In the dynamic mechanical measurement, the applied sinusoidal strain signal can be written as:

$$\varepsilon(t) = \varepsilon_0 . \sin(\omega t) \quad \text{or in complex notation} \quad \varepsilon^*(t) = \varepsilon_0 e^{i\omega t} \qquad (2.4)$$

with ε_0 the amplitude of the deformation cycle, $\omega = 2\pi f$ the pulsation in rad/s, and *t* the time. The stress response signal of a viscoelastic material is out of phase because it dissipates part of the energy as it deforms:

$$\sigma(t) = \sigma_0 . \sin(\omega t + \delta) \quad \text{or in complex notation} \quad \sigma^*(t) = \sigma_0 e^{i(\omega t+\delta)} \qquad (2.5)$$

with σ_0 the amplitude of the stress cycle and δ the phase shift. The ratio of the stress and the associated strain, for given experimental conditions, defines the complex modulus of elasticity ***E**** of the material for these same conditions, which can be written in the following form:

$$E^*(\omega) = \frac{\sigma^*(t)}{\varepsilon^*(t)} = \frac{\sigma_0 e^{i(\omega t+\delta)}}{\varepsilon_0 e^{i\omega t}} = \frac{\sigma_0}{\varepsilon_0} e^{i\delta} \quad \text{or} \quad E^*(\omega) = \frac{\sigma_0}{\varepsilon_0} . (\cos\delta + i . \sin\delta) \qquad (2.6)$$

The complex modulus is written symbolically as:

$$E^* = E' + iE'' \qquad (2.7)$$

The real component of the complex modulus is the conservation modulus:

$$E' = |E^*| . \cos\delta = \frac{\sigma_0}{\varepsilon_0} . \cos\delta \qquad (2.8)$$

The **conservation modulus E'** represents the rigidity and **elastic component** of the material. It expresses its capacity to store the mechanical energy of the stress and to release it in full in the form of elastic deformation (notion of reversibility).

The imaginary component of the complex modulus is the loss modulus:

$$E'' = |E^*| . \sin\delta = \frac{\sigma_0}{\varepsilon_0} . \sin\delta \qquad (2.9)$$

The **loss modulus E''** represents the **viscous component** of the material. Viscosity reflects its ability to dissipate mechanical energy (irreversibly lost in the form of heat). This phenomenon is associated with the friction of chains of molecules and their flow.

The modulus (in the mathematical sense) of the complex number ***E**** is:

$$|E^*| = \sqrt{E'^2 + E''^2} = \frac{\sigma_0}{\varepsilon_0} \qquad (2.10)$$

The calculation of these moduli allows an in-depth energy analysis of the skin sample. To interpret the results, the viscoelastic moduli are plotted as a function of the different frequencies or deformations of the mechanical test (Figure 2.28).

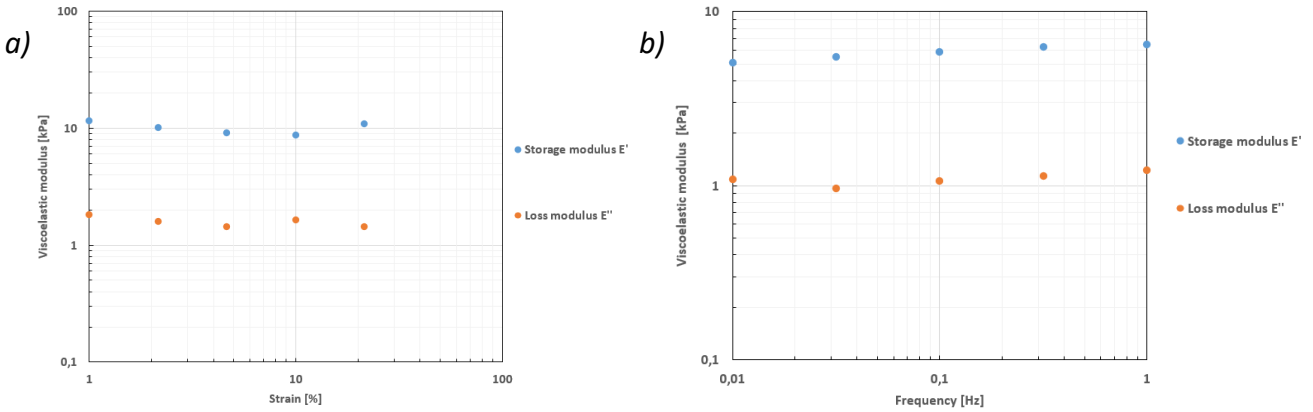

Figure 2.28: Dynamic tests on a skin explant. a) Strain sweep test (frequency = 0.1 Hz). b) Frequency sweep test (strain = 10%)

The phase shift between the measured stress and the imposed sinusoidal deformation is characterised by an angle called the "loss angle" or "phase angle", which quantifies the more or less viscous nature of the material for the imposed conditions. This angle reflects the energy dissipated by the material at pulsation ω. It measures the damping during dynamic deformation, i.e. the capacity of the viscoelastic material to dissipate mechanical energy as heat. The higher the phase angle is, the greater the vibration damping is.

The tangent of the angle δ represents the damping or loss factor of the material. For a viscoelastic solid ($E'(\omega) > E''(\omega)$), the phase shift δ is less than $\pi/4$ (Figure 2.29). The loss factor is the ratio of the energy dissipated by damping within the material to the elastic energy conserved and then restored during a sinusoidal deformation cycle:

$$\tan\delta = \frac{E''}{E'} \quad (2.11)$$

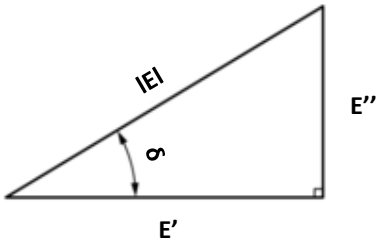

Figure 2.29: Relationship between the storage modulus E', the loss modulus E'', the phase angle δ and the magnitude |E| of the complex modulus E.*

During the dynamic mechanical loading-unloading test, the data is represented in a graph showing the relationship between stress and strain (Figure 2.30). By running a load-unload cycle, the hysteresis phenomenon of the material can be evaluated. The different cycles are then superimposed to assess the stability of the material's mechanical behaviour.

For each cycle, the energy E during loading and unloading is calculated using the trapezoidal method and the following equation:

$$\mathrm{E} = \int_0^{\varepsilon_{max}} \sigma . d\varepsilon \quad (2.12)$$

The difference in energy between the loading and unloading cycles gives the energy dissipated by the material. This enables to quantify the energy losses associated with the viscoelastic properties of the material.

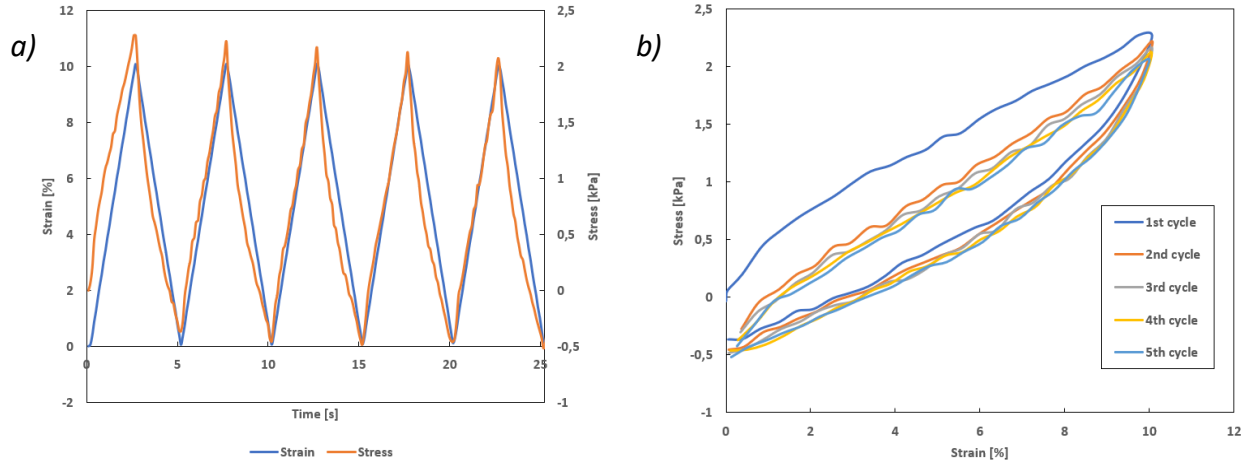

Figure 2.30: Dynamic load-unload test on a skin explant: stress-strain curves as a function of time (a) and as a function of the measured cycle (b). Parameters: strain = 10% - f = 0.2 Hz.

2.2.3.C Quasi-static tests

i) *Tensile test*

The tensile test consists of applying a constant deformation to the material. It is used to analyse the elastic, or even hyperelastic, behaviour of the material at large strains. During this mechanical test, the data is represented in a graph showing the relationship between stress and strain (Figure 2.31).

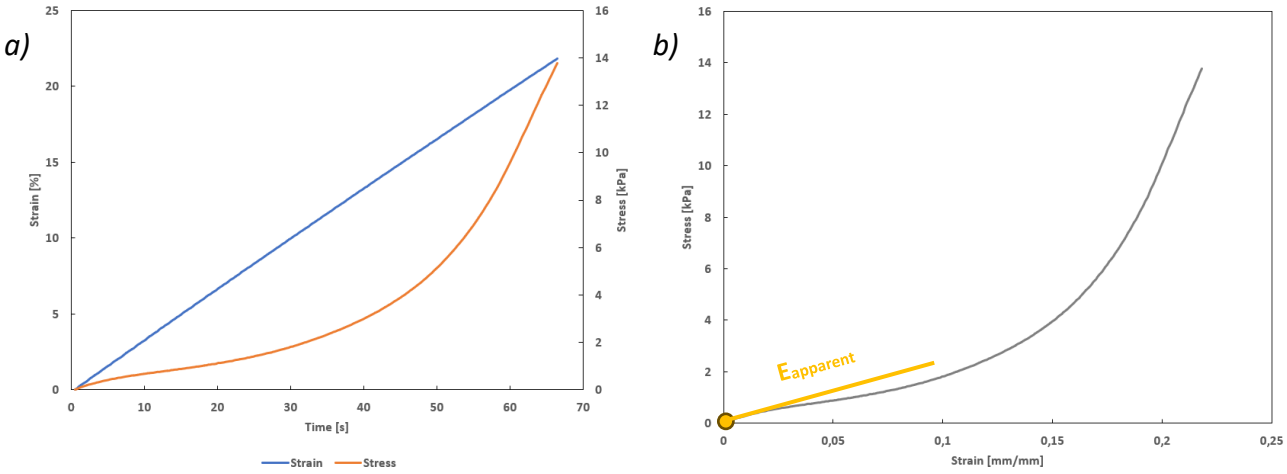

Figure 2.31: Tensile test on a skin explant. a) Raw curves: stress and strain as a function of time. b) Stress versus strain graph. Parameters: strain = 22% - speed = 1mm.min^{-1}.

From the stress-strain graph, it is possible to calculate the elastic modulus of the skin, also known as Young's modulus (E). This modulus is an essential parameter for characterising different types of

material. Using this modulus, it is possible to compare the rigidity of the skin with that of other materials.
The modulus of elasticity is the constant that links the tensile stress and the start of deformation of an elastic material. Graphically, Young's modulus corresponds to the initial slope of the stress-strain curve (Figure 2.31). The ratio between the tensile stress applied to a material and the resulting deformation is constant, as long as this deformation remains small and the material's elastic limit is not reached. This law of elasticity is known as the Hooke's law:

$$\sigma = E.\varepsilon \quad (2.13)$$

where σ is the stress (in Pa), E is Young's modulus (in Pa), and ε is the relative elongation or strain (dimensionless: $\varepsilon = \frac{l-l_0}{l_0}$).

In our case, Young's modulus is said to be "apparent" because the skin can deform beyond a proportional limit. The calculated value may therefore not represent the real modulus of elasticity in the material's elastic domain.

ii) Stress relaxation test

The stress relaxation test is used to analyse the viscoelastic behaviour of a material. When the material's rate of deformation is kept constant, due to its viscoelastic nature, it will dissipate energy to gradually return to a more stable state. Graphically, the material's stress will decrease over time until it reaches a plateau: this is the stress relaxation phenomenon (Figure 2.32a). The curve can be used to measure the dissipative and elastic components of the mechanical behaviour of human skin. In addition, we can define the tensile relaxation modulus E(t), visible in Figure 2.32b. This modulus is the ratio of the stress at time *t* to the constant strain:

$$E(t) = \frac{\sigma(t)}{\varepsilon_0} \quad (2.14)$$

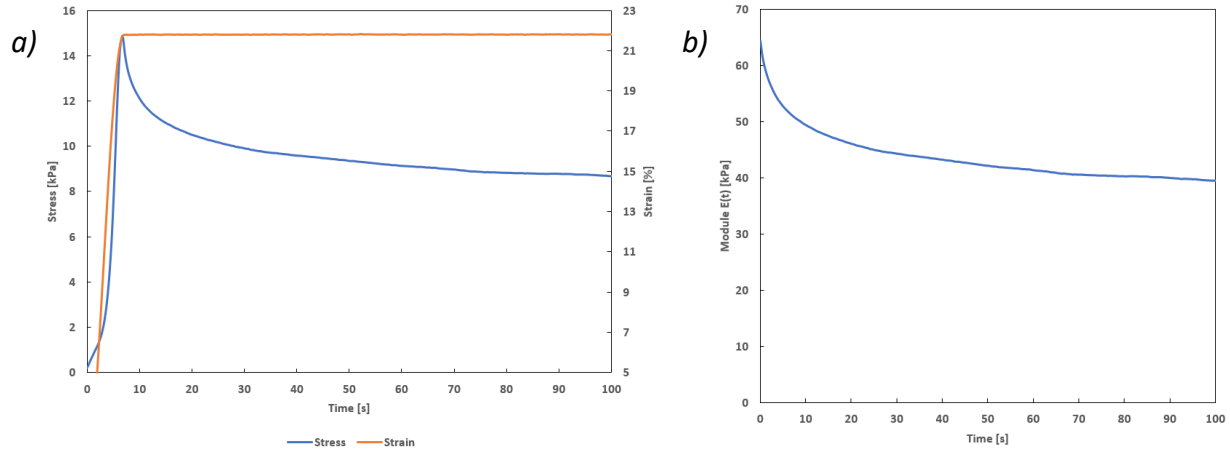

Figure 2.32: Stress relaxation test on a skin explant. a) Stress and strain as a function of time (raw curve). b) Relaxation modulus E(t). Parameter: strain = 22%.

2.2.4 Conclusion on methods

The development of this new device also requires new test procedures to be implemented, as no similar apparatus currently exists. An optimal protocol, described in Part 2.2.1 and more specifically in Appendix 2, has been developed for carrying out mechanical tests. This protocol allows the operator to follow a precise procedure when preparing the sample, thus ensuring reproducibility, and limiting sample placement errors.

Preliminary tests were carried out on pig skin and pericardium prior to testing on human skin. These tests were used to analyse the mechanical results obtained in order to highlight the most relevant parameters to be measured on human skin. These essential parameters should make possible to detect the effects of stress on skin viscoelasticity.

2.3 Human skin

2.3.1 Ethics: human skin models as an alternative to animal experimentation

For decades, the pharmaceutical, cosmetics and chemical industries have used animal experimentation to provide adequate documentation on the safety and toxicity of their products. This animal experimentation has been widely used to carry out toxicity tests and to develop new pharmaceutical or cosmetic products. However, growing awareness of the plight of laboratory animals (animal testing is increasingly frowned upon by the general public) has encouraged legislators to restrict the use of animals in experimental procedures. Indeed, animal testing of cosmetic products and their ingredients was banned in Europe in 2009, and a ban on the sale of cosmetics tested on animals has been implemented in 2013 [Regulations CE n°1223/2009].

This change in regulations forced scientists to find alternatives to assess the efficacy and toxicity of their products, without resorting to animal testing. This has led to the development of methods, with more in-depth *in vitro* studies and human skin models which are now an accepted alternative.

This alternative method has been developed by Eurofins BIO-EC, among others, to avoid animal testing and allow industries to test the effects of their products on human skin. The method uses an *ex vivo* human skin model. *Ex vivo* skin models appear to be a relevant solution for testing the efficacy of cosmetic products, but also for gaining a better understanding of skin ageing and of various pathological conditions [Lebonvallet *et al.*, 2010]. In fact, it is an ideal model, known as organotypic, because the 3D organisation and the functions of the skin are retained. It is the closest alternative to the *in vivo* clinical trial currently available on the market.

2.3.2 *Ex vivo* explants

The human skin explants used in this work come from the Eurofins BIO-EC laboratory. This laboratory is a private research centre specialising in studies on the efficacy of cosmetic and dermatological products. Eurofins BIO-EC collects human skin samples (real human tissue) from reconstructive plastic surgery from clinics and hospitals. Skin samples are collected immediately after surgery with the consent of voluntary donors. All donors expressly agree to donate excess tissue after the operation to help science progress while preserving the welfare of the animals.

They have developed an *ex vivo* model based on keeping human skin explants alive for 10 to 12 days. It is a model that provides relevant answers for cosmetic and dermatological objectification. Indeed, this model allows:

- To replace *in vivo* animal experiments for skin toxicity and efficacy tests;
- To benefit from samples with properties very close to the real physiology of the skin, with the entire cell population and their communications remaining active. The skin retains its normal morphology, structure, and metabolism. This is an essential factor for estimating the response of human skin to certain products;
- To observe the effects of cosmetic products or external stress (exposure to UV rays or pollutants, chemical aggression, wounds, etc.) on the skin prior to *in vivo* studies (on volunteers).

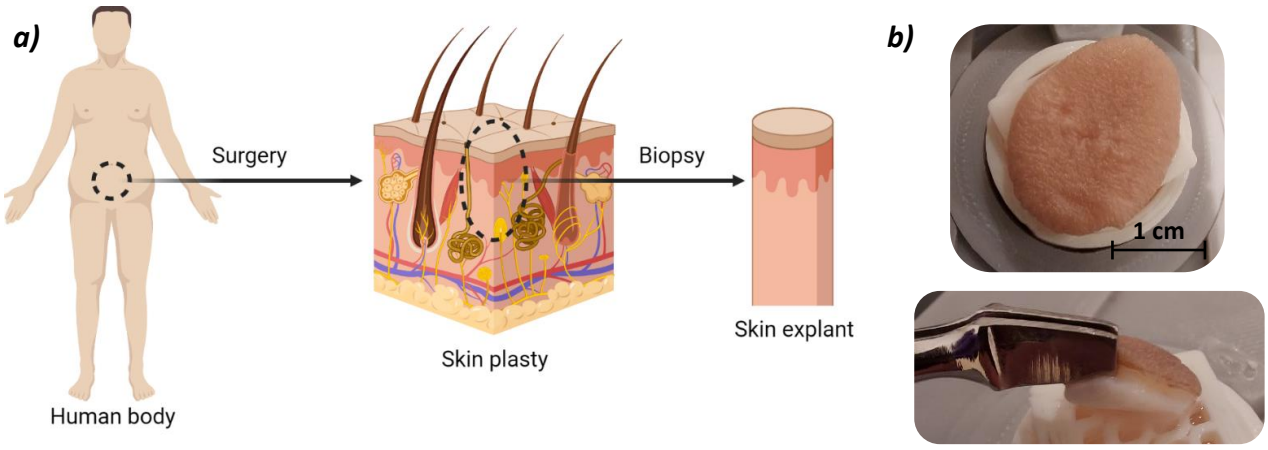

Figure 2.33: Ex vivo skin explant. a) Schematic illustration of the origin of the skin. b) Photos of a skin explant.

Explants, also called organ-cultured skin or skin organ, are small skin samples taken from humans after surgical interventions (mainly in the abdomen), according to legal restrictions (Figure 2.33). These are therefore round skin biopsies of human origin, prepared from surgical skin residues, also known as skin plasty, donated by adult donors with their consent and collected in compliance with all applicable regulations. The diameter of the explants can vary from 12 to more than 40 mm; this diameter is defined by the operator, according to the studies to be carried out, who uses a punch to cut the skin plasty. The thickness of the explants varies from 2 to 3 mm, depending on their morphology.

After decontamination, re-sizing, and fat cell removal (de-hypodermisation: only the dermis and epidermis are preserved), the skin explant is deposited on a specific appropriate culture medium. Thus, it can be studied over the course of a few days; we therefore speak of "*ex vivo*" skin, which is kept alive like "*in vivo*" skin.

Skin explants from Eurofins BIO-EC company may be kept alive from 10 to 12 days thanks to the culture medium. Explants are deposited at the air-liquid interface; air exposure is helpful to maintain the structural integrity of the skin and to allow complete differentiation of the epidermis. Explants are placed on a stainless-steel grid, with the epidermal side upward, that is bathed in the culture medium; explants are nourished by diffusion via the grid (Figure 2.34). The media use by Eurofins BIO-EC laboratory to make skin explant cultures is kept secret. These explants are cultivated inside an incubator at 37°C with 5% of CO_2 and 95-98% of humidity.

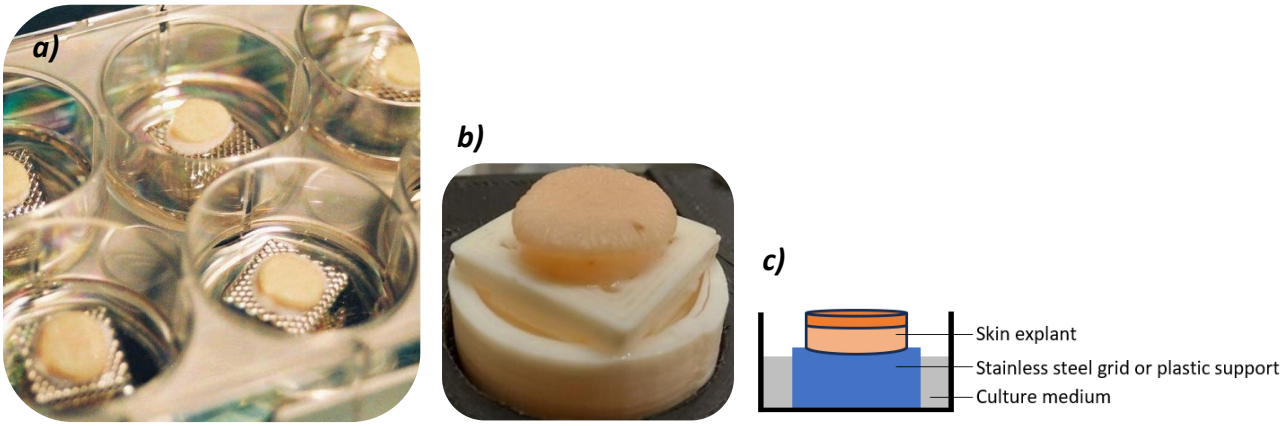

Figure 2.34: Ex vivo skin explant from BIO-EC company - a) Embedded in multi-well culture plates, then placed in an incubator for survival. b) Placed on a support to carry out the tests. c) Schematic explanation of culture supports.

For mechanical testing, the human skin explants are first removed from the incubator where they were placed in contact with the culture medium on metal grids in Petri dishes (Figure 2.34a). They were then placed on a specific support supplied by Eurofins BIO-EC, comprising a plastic grid to support the skin and a tank filled with culture medium (Figure 2.34b). Thanks to capillary action, the dermis of the skin explant is in contact with and hydrated by the nutrient culture medium. The skin explant can remain in this configuration for about an hour before it dries out or degrades.

When using these explants, there is a large variability in skin type that is representative of living beings. Explants are representative of the donor age and life habits (sun exposure, injury, care, allergies, medication, or smoking), they have therefore all the characteristics of their donor. Donors are generally aged between 18 and 70, and most are women.

The main limitation, which is just as important for preparing and carrying out tests, is that this 'skin' material utilisation depends on surgical operations. These surgical procedures are not performed on a daily basis, which limits the number of experiments that can be carried out on the skin *ex vivo*.

Despite their limitations, skin explants are a very convenient model to investigate the effects of environmental stress, ageing and skin diseases.

Note: to ensure donor confidentiality and research safety, hospitals and clinics provide the following information on human skin samples: donor age, donor sex, known skin diseases and conditions, drugs used (corticosteroids, steroids, topical antibiotics, immunosuppressive or immunomodulating agents).

2.4 General conclusion on materials and methods

This Chapter presents the different materials used and the different methods developed for this research work.

We have developed an innovative measuring device capable of assessing the mechanical properties of skin *ex vivo* that is accurate, economical (in terms of skin) and easy to use. The measuring device developed is capable of performing tensile mechanical stresses parallel to the surface of the skin and of performing accurate and reproducible measurements of mechanical properties. The device is now protected by a patent [Derail *et al.*, 2022].

This device is particularly well suited to monitor changes in the mechanical properties of a skin sample *ex vivo* over a period of several days, and to establishing a link with any changes in the skin's mechanical properties induced by an external stress. Maintaining the skin *ex vivo* on a nutritional medium allows the skin to retain its mechanical properties. Skin samples are taken from a living body and kept alive for the duration of the measurements.

Our device enables the mechanical properties of a skin sample to be fully characterised using various types of mechanical test (detailed in Part 2.2.2):

- Dynamic tests that apply sinusoidal deformations to the skin.
- Quasi-static tests which apply linear or stationary deformations to the skin.

The evolution, through instrumental development work, of the equipment over the course of my thesis was an important and necessary step in achieving robust instrumentation. Indeed, this ongoing development of the equipment, described in Part 2.1, has enabled us to obtain a reliable and reproducible device for measuring the mechanical properties of a skin sample. This device enables to carry out different types of uniaxial mechanical tests on the skin in a highly reproducible way, while being able to visualise the behaviour of the skin under these mechanical stresses. The final equipment used in further research to characterise the mechanical properties of various skins is therefore that presented in Part 2.1.3.

Chapter 3.

Preliminary studies on human skin and method validation

This Chapter is dedicated to the presentation and description of the various preliminary studies carried out on skin before being able to fully and accurately characterise the skin explants in physiological-like conditions. The first objective was to validate the experimental methods described in Chapter 2. The second objective was to optimise the system for future mechanical characterisations by carrying out the first tests on *ex vivo* skin explants.

These tests on human skin samples represent the first attempts to characterise living tissues using our device. The aim is to definitively adapt the equipment to this type of explant. To do this, several controllable parameters must be tested in order to reach the optimum technological configuration and measurement methods for characterising *ex vivo* human skin explants as accurately as possible. The robustness of the equipment and test method employed is therefore demonstrated in this Chapter.

This Chapter deals with the concepts of preconditioning, repeatability, reproducibility, strain rate, compression force, pre-tension, and skin anisotropy.

3.1 Notion of skin preconditioning

3.1.1 Skin preconditioning and the Mullins effect

Due to the structural composition of biological soft tissues, their intrinsic viscoelastic behaviour produces uneven mechanical results when the tissue is subjected to repeated mechanical loading [Liu *et al.,* 2008].

In fact, if a tissue is stressed to measure a load-strain curve, left to relax, and then stressed a second time following the same procedure, the curves will not overlap [Fung, 1993]. During the first consecutive tests, a shift in the stress-strain curves is observed. If the test is repeated indefinitely, the difference between successive cycles is decreased, and eventually disappears. The sample has been preconditioned. The reason why preconditioning occurs in a sample is that the internal structure of the tissue changes with the stress. By repeating cycles, a steady state is eventually reached from which no further changes will occur unless the cycling routine is changed. If the upper limits of cycling are changed, the internal structure changes again and the sample must be preconditioned again.

Preconditioning is therefore considered as a necessary step to overcome the effects of soft tissue manipulation and establish a reproducible set of experiments [Liu *et al.,* 2008]. Such a procedure allows the tissues to reorganise themselves in order to adapt gradually to the load and therefore to obtain more consistent data during mechanical testing.

Uniaxial cyclic loading has been used to demonstrate the preconditioning effect in various soft tissues [Giles *et al.,* 2007]. Although preconditioning is an accepted aspect of mechanical testing of soft tissues, there is no consistent preconditioning protocol. Typically, multiple loading cycles are performed until repeatable data are obtained.

This effect seems close to the Mullins effect observed in elastomers. Rubber-like materials exhibit an appreciable change in their mechanical properties resulting from the first extension. The Mullins effect is a softening that occurs during the first deformation. Figure 3.1 shows that if cyclic loading is applied to an initially non-prestressed rubber, a decrease in stiffness is observed during the first few cycles. Theories to explain the Mullins effect include bond ruptures, molecule slipping, filler-cluster rupture, chain disentanglement, chain retraction, and network rearrangement [Diani *et al.,* 2009].

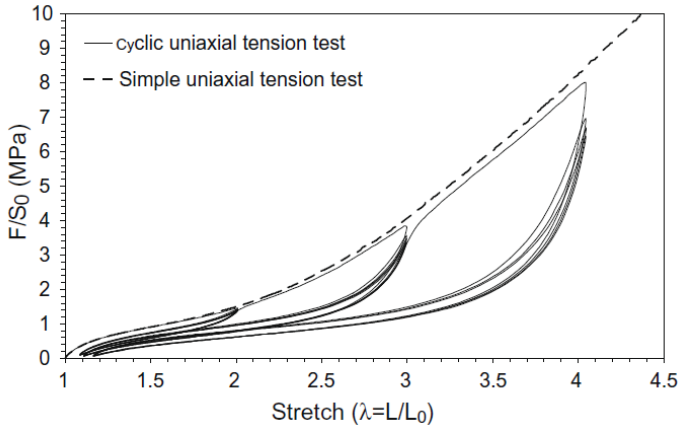

Figure 3.1: Stress-strain curves of a 50 phr carbon-black filled styrene-butadiene rubber (SBR) submitted to a simple uniaxial tension and to a cyclic uniaxial tension with increasing maximum stretch every 5 cycles. Under cyclic loading, after the first extension, a loss of stiffness is observed for subsequent extensions (lower resultant stress for the same applied strain) [Diani et al., 2009].

Figure 3.2 illustrates a typical change between stress-strain curves during skin preconditioning. Ten load-unload cycles were therefore imposed on the skin explant before each series of tests. The displacement speed is 10 mm min^{-1} and the deformation is 10%.

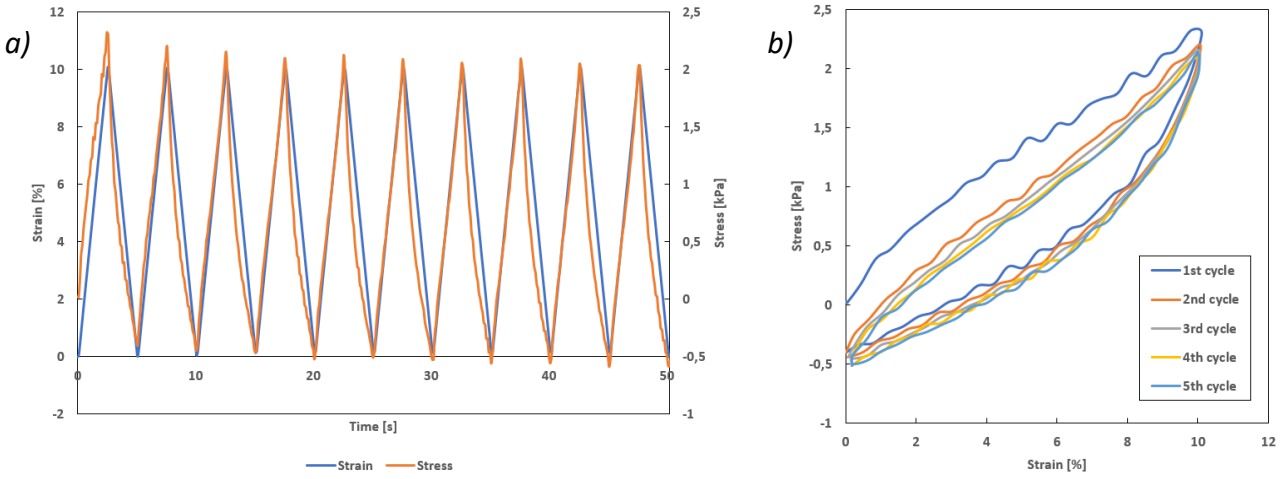

Figure 3.2: Preconditioning experiment on a human skin explant showing the Mullins effect, carried out using our instrumentation. a) 10 loading-unloading cycles. b) Superimposed stress-strain curves showing stabilisation of the mechanical properties of the skin from the 3rd/4th cycle.

During the preconditioning cycles, a decrease in stress at a given strain was observed for the first successive loadings. However, this decrease is significant between the first two loading-unloading cycles, and the curves stabilise after about three to four cycles. In general, the skin explants used required between three and ten cycles of uniaxial tensile stress before reaching the preconditioned state.

Conclusions: due to the viscoelasticity of the skin, preconditioning is important to study the mechanical behaviour of the skin. Each characterised skin explant was therefore subjected to these ten loading cycles in order to precondition the sample before carrying out the full tests. No more than ten loading cycles were necessary to stabilise the mechanical behaviour of the skin and avoid what we call the Mullins effect.
For larger deformations, measurements are also taken from the 3rd test to avoid this effect.

3.1.2 Skin loading history and test programme

It is important to pay attention to the mechanical liabilities of the skin during testing. A soft tissue is a viscoelastic material. Since the time dependence is an essential characteristic of tissue response, it is important to create a well specified loading history for data acquisition. Indeed, the mechanical properties of the skin explant are influenced by its loading history [Fung, 1993]; [Edsberg *et al.,* 1999].

This is why, for each explant, a test programme is defined beforehand in order to be able to compare the different results correctly over several days of measurements or on several explants. The aim applies to the different skin explants to be subjected to the same stresses with the same relaxation times between consecutive tests. As a result, comparison of the mechanical properties of the different skin samples will be accurate.

Here is an example of a complete series of tests that can be carried out on a skin explant in this precise order: loading-unloading cycles, strain sweep, frequency sweep, simple traction, and stress relaxation. Dynamic tests at low strains are performed first, followed by quasi-static tests at high strains. All the tests are carried out in the same way and in a well-defined order to enable reliable analysis and comparison of the mechanical properties of the different explants of a study.

3.2 Test repeatability[13]

Before carrying out various in-depth studies on human skin explants, we need to ensure that the tests carried out with our new equipment are repeatable.

In our case, the method consists of placing a skin explant, following the procedure described in Part 2.2.1, and performing a mechanical test on the same skin explant several times in a row. This means that the same skin sample is analysed by the same operator, using the same measurement procedure and method, all in the shortest possible time. Figure 3.3 shows the repeatability results of a simple tensile test and a dynamic test.

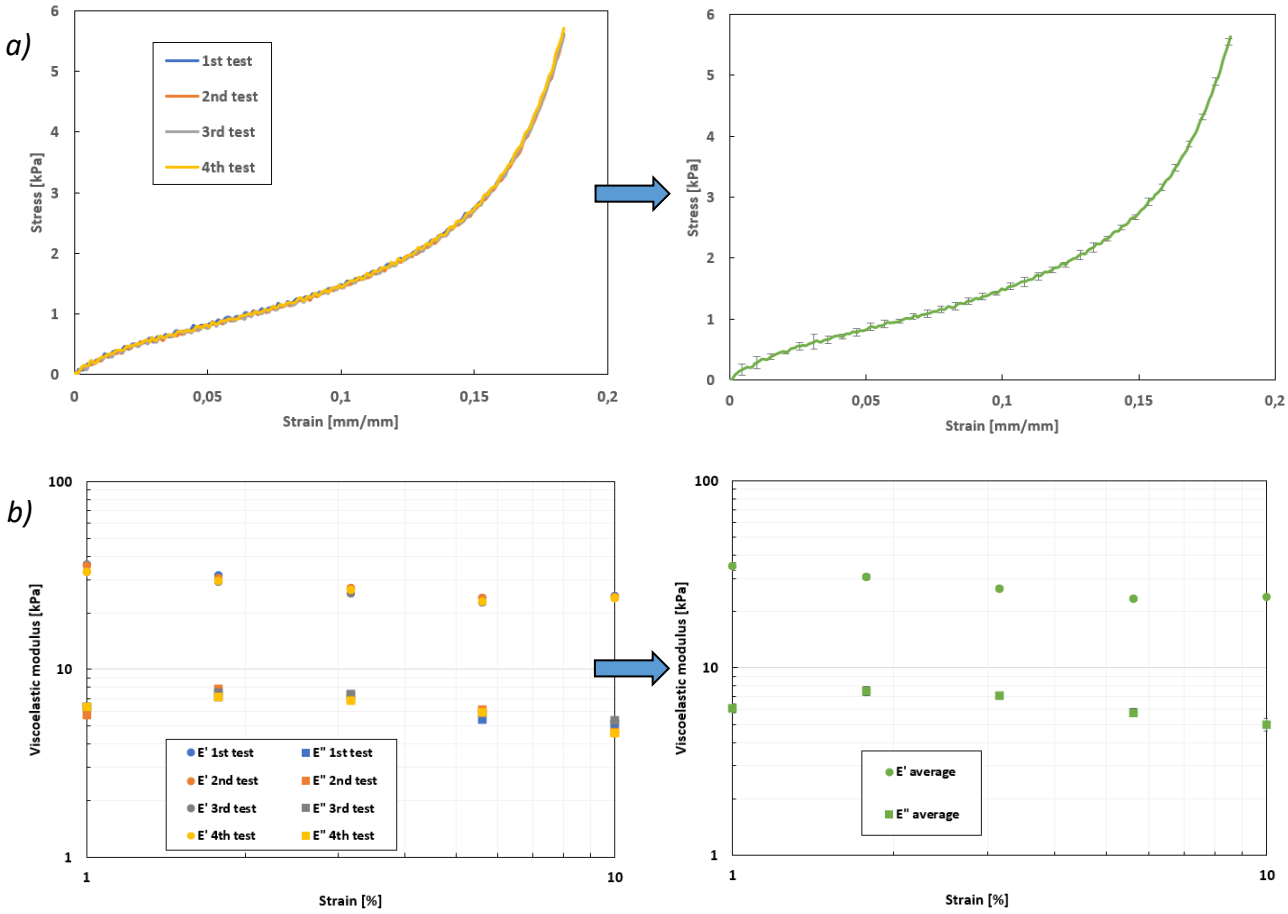

Figure 3.3: Repeatability of tests on a human skin explant. a) Tensile test (speed = 10 mm.min^{-1}): 4 tests + average curve with standard deviation. b) Dynamic test (strain sweep at 0.5 Hz): 4 tests + average curve with standard deviation.

To check the repeatability, the mechanical tests were carried out four times consecutively. As observed in Figure 3.3, the curves for the quasi-static and dynamic tests are superimposed, demonstrating that the tests carried out with this device are repeatable in these two loading modes.

[13] **Repeatability:** it is the ability of a device to produce homogeneous results (precision) during repeated tests using the same method on similar sample. A measurement is considered to have good repeatability if the values obtained remain stable when the experimental conditions remain unchanged. In simple terms, repeatability can be defined as the dispersion of measurements when nothing changes, in other words the "background noise" of the measurement.

This repeatability of the mechanical tests is attributable to the quality of the instrumentation and the initial pre-conditioning of the skin, which stabilised the mechanical properties of the explant beforehand.
These tests also showed that the skin explants did not deteriorate at strain levels below 20%.

3.3 Test reproducibility[14]

Before carrying out various in-depth studies on human skin explants, we also need to ensure that the tests carried out with the new device are reproducible.

The reproducibility of a measurement is essential for the scientific validation of an experiment. This notion of reproducibility is of great importance for our studies, because when we carry out experiments at different times on a skin explant, for example to monitor its mechanical properties over time or to subject it to stress, we have to remove the explant and place it back in an incubator for preservation between experiments. This process of removal and reinstallation of the sample can lead to errors during mechanical testing.

In our case, the method consists in placing a skin explant (see Part 2.2.1), carrying out a mechanical test prior to its removal; the whole process is repeated several times consecutively. Figure 3.4 shows the reproducibility results of a simple tensile test and of a dynamic test.

[14] **Reproducibility:** it is the ability of an instrument to provide repeated results, regardless of the operator performing the test (operator variation) or the time of the test. It is therefore the ability of an instrument or method, used by several operators, to reproduce consistently the same measurement on the same sample, under the same conditions. Reproducibility, like repeatability, are two components of precision in a measurement system. Repeatability assesses the variability inherent to the measurement itself, whereas reproducibility assesses the impact of variations caused by external factors. A measurement is considered reproducible when the values obtained show little variation.

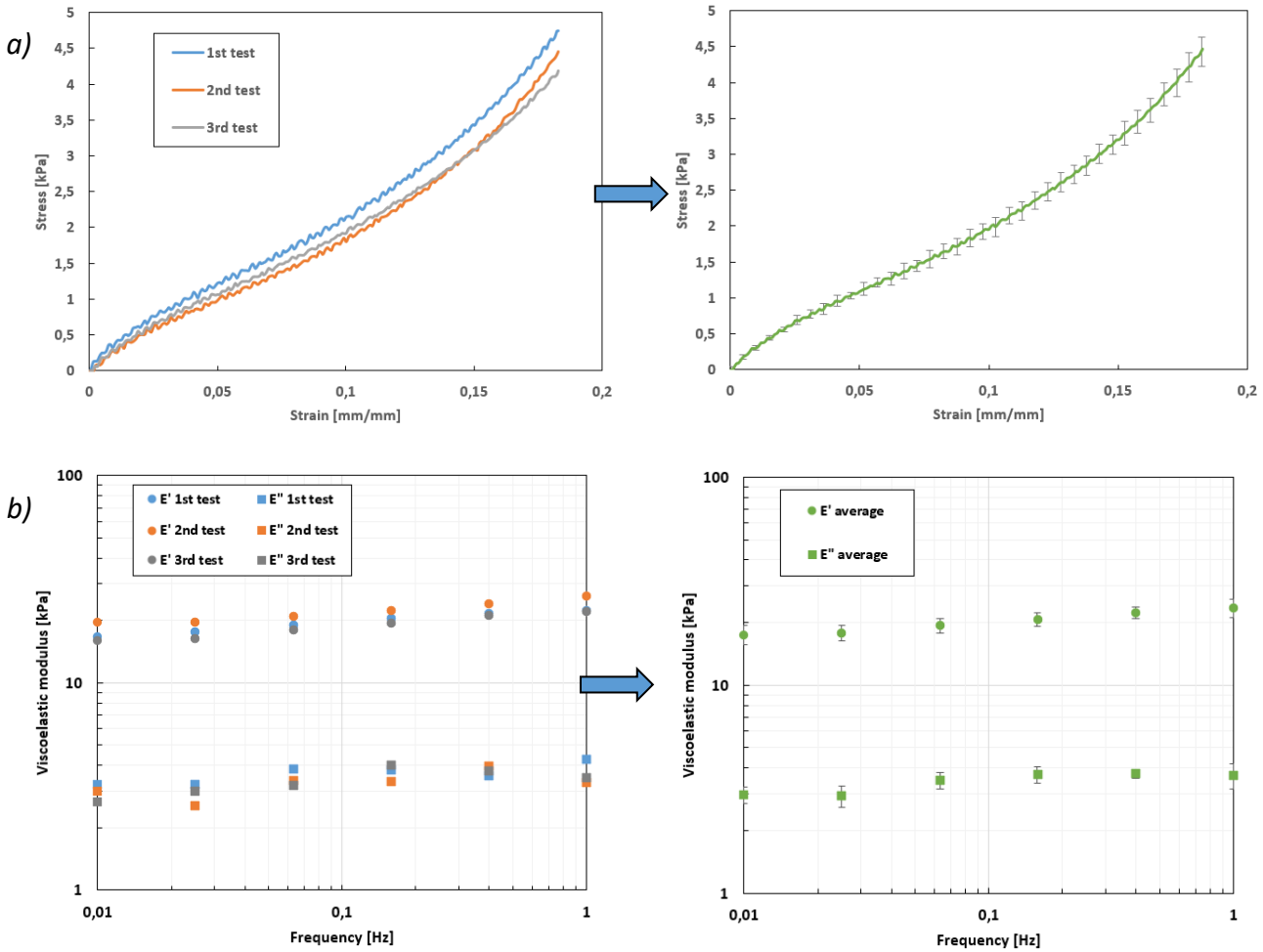

Figure 3.4: Reproducibility of tests on human skin explants. a) Reproducibility in tensile test (speed = 10 mm.min^{-1}): 3 tests + average curve with standard deviation. b) Example of reproducibility of a dynamic test (frequency sweep at 10%): 3 tests + average curve with standard deviation.

To check the reproducibility of the tests, the mechanical tests were therefore carried out several times consecutively, placing back the skin explant for each test. The curves for the quasi-static and dynamic tests show only slight variations. We estimate less than **5% variation in simple tensile stress measurements and less than 10% variation in dynamic modulus measurements**, demonstrating that the tests carried out with this equipment are reproducible. This reproducibility of the mechanical tests is attributable to the quality of the instrumentation and the method developed for placing the skin explant in the equipment. It indicates that the procedure for placing the skin in the device is reproducible.

It should be noted that the addition of the vertical force sensors, which allows for the control of the bonding pressure (see later Part 3.5), and of the motorised lifting support have helped to improve the reproducibility of the tests. However, there is always the possibility of an error occurring when positioning the skin (see Figure 3.5b). For future in-depth studies, it should be kept in mind that possible errors could influence the characterisation results.

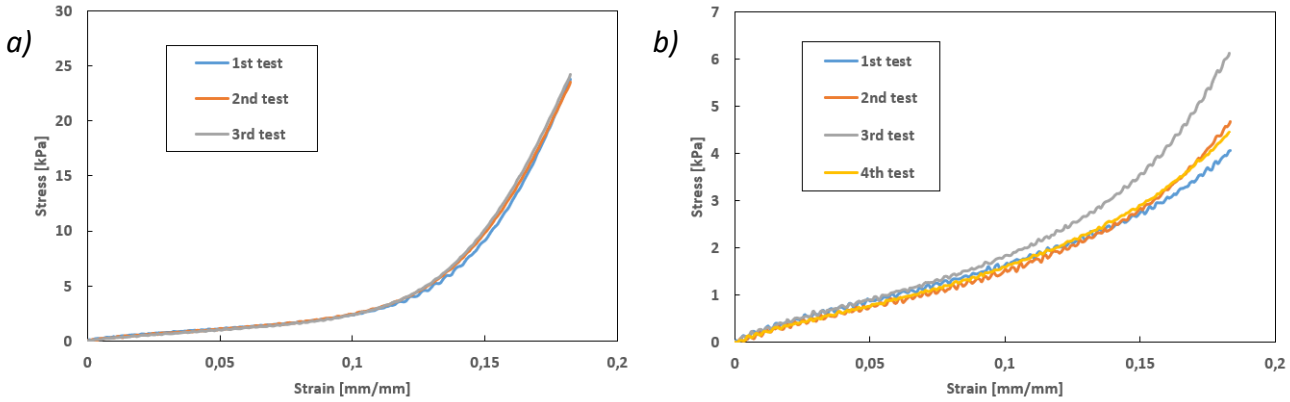

Figure 3.5: Other examples of the reproducibility of tensile tests on two human skin explants (speed = 10 mm.min^{-1}). a) Experiment with very good reproducibility. b) Experiment with poorer reproducibility: error in the positioning of the skin for test no. 3, which does not follow the general trend in mechanical properties.

3.4 Study of the effect of strain rate

Because of its composition and viscoelastic characteristics, the mechanical properties of the skin show a sensitivity, a dependence, on the speed at which the skin is stressed, i.e., the mechanical stretching rate during tests.

Strain rate is an important parameter influencing mechanical testing of soft tissues. For example, studies by Shergold [Shergold *et al.,* 2006] and Zhou [Zhou *et al.,* 2010] examined the mechanical responses of pig skin over a wide range of strain rates, revealing that pig skin becomes stiffer and stronger as the strain rate increases. Several researchers have observed this significant influence of strain rate on the properties of human tissues under tension [Ottenio *et al.,* 2015]; [Snedeker *et al.,* 2005]. They observed that the apparent modulus of elasticity and the stress at break increase as the strain rate increases. This leads to an increase in the stiffness of the human skin tissue when subjected to higher strain rates. It is therefore clear that the strain rate has a significant effect on the mechanical properties of skin [Roeder *et al.,* 2002]; [Arumugam *et al.,* 1994].

The aim of this preliminary study was to examine the influence of strain rate on the mechanical behaviour of *ex vivo* human skin explants. To do this, identical mechanical tests were carried out on the same skin explant, but at different strain rates. The results of a single tensile test with different strain rates are shown in Figure 3.6.

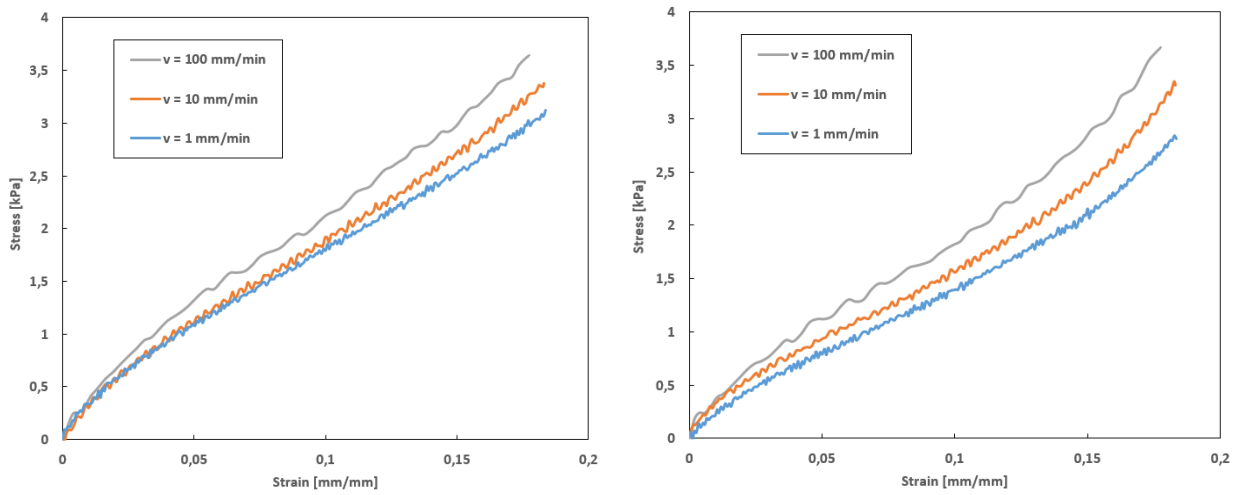

Figure 3.6: Influence of strain rate on the mechanical elongation behaviour of the explant. Tensile tests on 2 human skin explants (right and left graphics - speed = 1, 10 and 100 mm.min^{-1}).

The tensile tests were carried out on two different explants, using three strain rates achievable with our equipment: 1 mm min^{-1}, 10 mm min^{-1} and 100 mm min^{-1} (i.e., with an initial air gap of 6 mm for these tests: 3×10^{-3} s^{-1}, 3×10^{-2} s^{-1} et 0.3 s^{-1}). Figure 3.6 shows that the skin is sensitive to the strain rate, which is consistent with the reported results [Zhou *et al.,* 2010]; [Ottenio *et al.,* 2015]. Indeed, it shows that with an increased loading rate, the stress-strain curve shows a tendency towards hardening. For the second explant, the apparent modulus at maximum strain varied from 23 kPa for a strain rate of 1 mm min^{-1} to 34 kPa for a strain rate of 100 mm min^{-1}. This mechanical parameter increased with increasing strain rate.

At a lower deformation speed, the protein fibre bundles have enough time to reorganise and slide over each other when the load is applied. On the contrary, at a higher strain rate, the fibre bundles do not have time to reorganise, and the total skin strength is the summation of the strength of the collagen fibres and of the collagen-glycosaminoglycan matrix interactions [Dombi *et al.,* 1993].

The difference between the curves can be observed at low and high strains, implying that the two important components of the skin, elastin (responsible for the low-strain response) and collagen (responsible for the high-strain response), are strain-rate dependent materials [Zhou *et al.,* 2010]. Their stiffness increases with strain rate.

Conclusions: the stress-strain response of the skin is sensitive to the strain rate, a characteristic of viscoelastic materials. For the rest of the studies, the speed or frequency of the various mechanical tests will be kept constant when characterising different explants in order to be able to compare the results accurately.

3.5 Study on the effect of compression force on the skin

During the bonding stage of the studs to the human skin explant, a vertical force is applied to the sample at the level of the studs. This compressive force is induced by the studs as they come into contact with the skin. As shown in Figure 3.7, several compressive forces can be applied by the studs to the skin surface. This is an important parameter in our instrumentation because it influences the mechanical properties of the tissue, as we will see in this Section.

a) b)

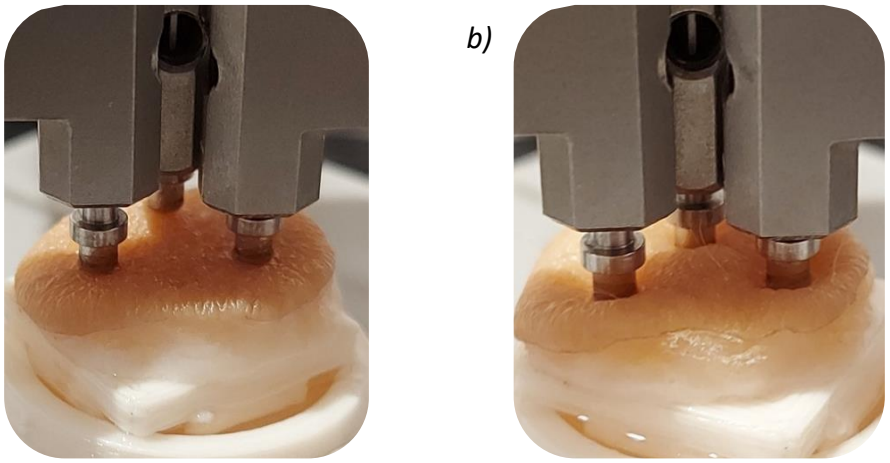

Figure 3.7: Photographs of the instrument's studs glued to the skin surface, showing different normal forces applied to the same skin explant: 3 mN (a) and 23 mN (b). The difference between the 2 pressures applied to the skin is clearly visible.

When a material is subjected to compression, it contracts in volume. The forces of compression exert pressure on the material, increasing its density. During this process, the relative positions of the atoms and molecules in the object change.

By applying a compressive stress to the material (a transverse pressure on its structure), its axial tensile properties might increase. Studies, such as that by Chowdhury [Chowdhury *et al.,* 2023], show that transverse pressure has a significant effect on the tensile properties of polymeric materials by strengthening intermolecular interactions. The higher the compression, the higher the tensile strength. Applying pressure to the material can also reduce the mobility of molecular chains, thereby limiting deformation in response to an applied load [Mears *et al.,* 1969].

The aim of this preliminary study was to examine how the compression force exerted by the studs on the sample influences the mechanical behaviour of the skin during tensile testing. To this end, the same skin explant was used. The studs were initially bonded to the skin with the lowest possible transverse force. A mechanical test was then carried out in this configuration. The motorised lifting support was then raised so that the studs glued to the skin exert a greater compressive force. Each time the sample support was raised, the compression force measured on the skin increased, and a mechanical test was carried out. The outcomes of this test, carried out at different compressions on the same skin explant, are shown in Figure 3.8.

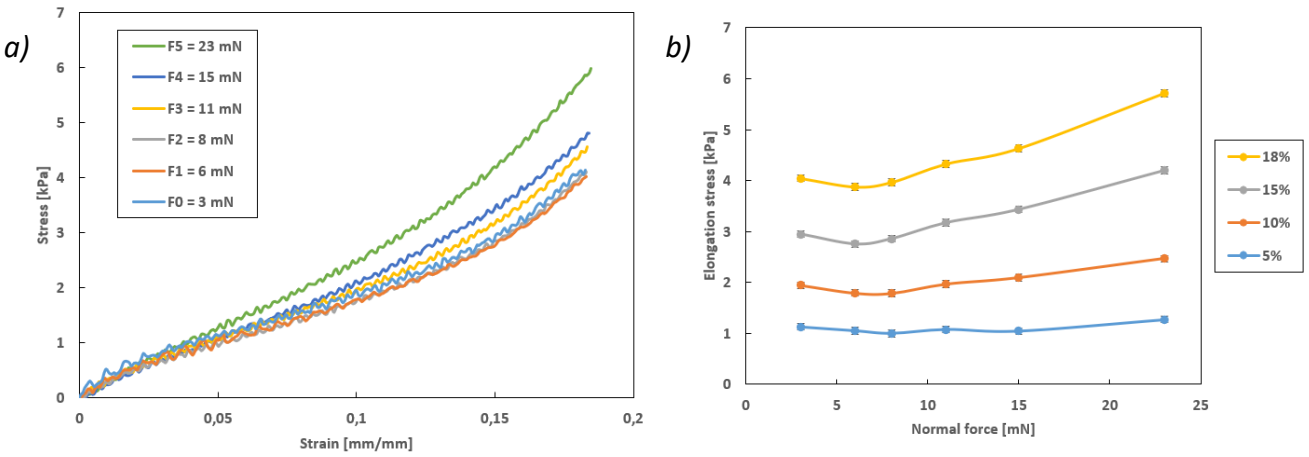

Figure 3.8: Influence of the compression force of the studs on the mechanical behaviour of the skin in elongation. a) Tensile tests on an explant of human skin (speed = 10 mm.min^{-1}) with different normal forces. b) Elongation stresses measured, for a given deformation, as a function of the normal force imposed.

Figure 3.8 illustrates the impact of the transverse compression force exerted by the studs on the mechanical properties of the explant during extension. The greater the compression force of the studs, the more the explant is constrained in the stud bonding zone, and the greater the forces required to stretch it. By compressing the skin perpendicular to its direction of tension, the different fibre networks responsible for its mechanical properties are compressed (Figure 3.9). These fibre networks are thus pre-stressed and tightened, and therefore require more force to be stretched horizontally.

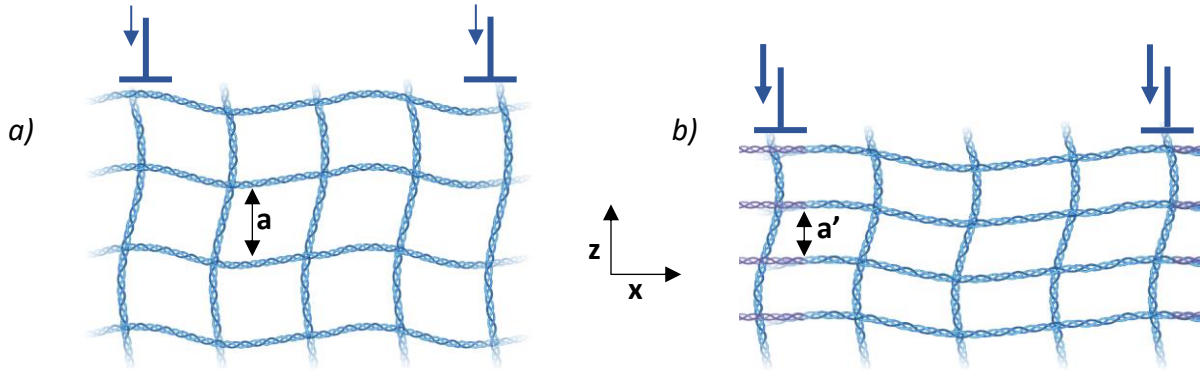

Figure 3.9: Attempt at a schematic representation of a dermal network of collagen fibres, vertical section view (Parameter a = lattice height / a > a'). a) Network under low normal force of compression; fairly loose network. b) Network under high normal force of compression; tightened and compressed network under the studs.

The mechanical behaviour of the skin, as a function of this parameter, is quite similar for other explants, as shown in Figure 3.10. This Figure clearly shows that in order to stretch the explant to a certain deformation, a greater force is required when the explant is strongly compressed transversely by the studs.

In addition, a high compression force from the studs will induce internal stresses in the skin prior to the experiment, which will modify the stress field in the skin. This will have an impact on the response of the material during extension.

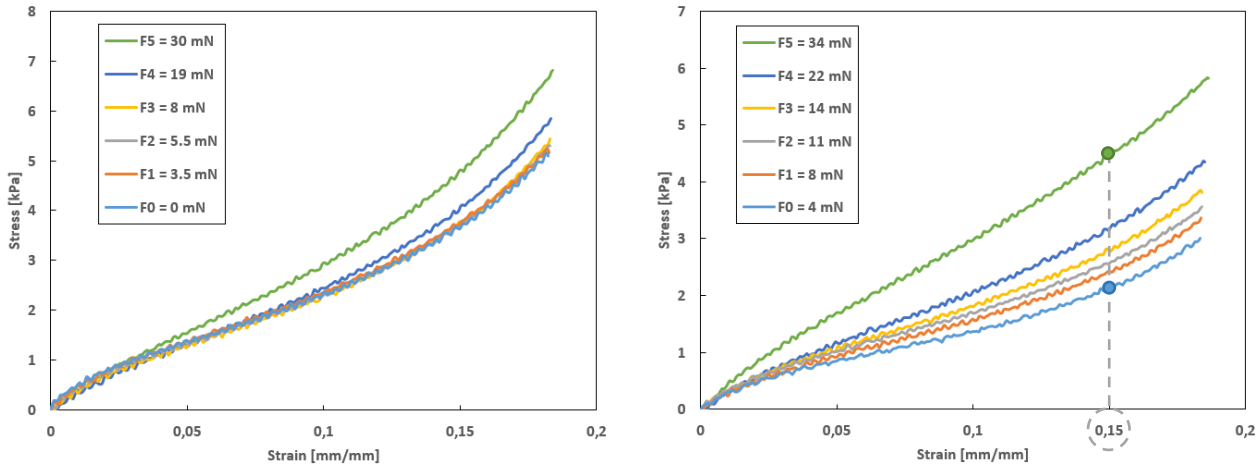

Figure 3.10: Tensile tests on 2 human skin explants (right and left graphics - speed = 10 mm.min^{-1}) with different normal forces.

Conclusions: it is essential to control the compressive force exerted by the studs on the skin in our test procedure. This force, which is orthogonal to the direction of skin extension, causes variations in the stress field within the skin sample, thereby modifying its mechanical properties.

The addition of vertical force transducers and a motorised lift support enabled us to measure and control this compressive force on the skin explant. This measurement, carried out prior to the tests, enabled us to control the procedure for gluing the studs to the skin in order to ensure reproducibility at this stage. When the studs are glued to the skin sample, the motorised lifting support raises the skin until it reaches the glued studs, using a compression force defined by the operator.

As a consequence, for each explant in each study, an identical compression force is applied so that the results can be analysed and compared appropriately. After examining the results of this pre-study, a compression force of between 5 and 10 mN was chosen for subsequent measurements on skin explants. This range of compression force minimises the influence of studs bonding on the mechanical properties of the skin, highly appropriate for further investigations (Figure 3.8b).

3.6 Study on the pre-tension state of the skin

The skin explant is a practical and versatile model because it contains all skin cell types and preserves the structure and physiology of *in vivo* human skin. However, one drawback of this type of *ex vivo* skin explant is that tissue contraction and tension are lacking [Lebonvallet *et al.,* 2010].

Explants are skin samples taken from humans after surgery. Like most biological soft tissues, skin is under an inherent residual stress [Ni Annaidh *et al.,* 2019]. Skin excisions are usually followed by skin retraction, shrinkage of explants [Ridge and Wright, 1966]; [Cox, 1941]; [Jansen *et al.,* 1958].

This phenomenon is due to the release of residual stresses of the skin. The amount of retraction of the explant is a measure of the intrinsic tension of the explant, its pre-tensioned state. Excising the skin results in a loss of the skin's natural pre-tension state *in vivo*.

As recalled in Part 1.3.4, Langer was the first to study this phenomenon by excising circular pieces of skin and observing the changes in shape and size of these pieces and the holes on the body [Langer 1978a]; [Langer 1978b]. The difference in size between the explant and the hole indicates the level of skin tension. Variations in skin tension in different directions result in a non-uniform change in the size of the hole and the removed skin. Skin retraction is generally, if it is non-uniform, highest in the direction of the Langer's lines.

When excising skin samples from the body, the shrinkage of explants is generally between 5 and 15%, but can be as high as 40% depending on the direction of measurement on the explant (parallel or perpendicular to Langer's lines) and the part of the body from which the skin was removed [Ridge and Wright, 1966].

One of the main consequences is that the results of *in vivo* and *ex vivo* mechanical tests differ, due to the loss of skin tension in *ex vivo* skin explants (see later in Part 4.2). The aim here was thus to study the skin tension of the *ex vivo* explants and to determine whether it is necessary to ensure natural *in vivo* pre-tension of the skin during testing.

In our case, the method consisted in applying different levels of pre-tension to the same skin explant before carrying out the mechanical tests. As shown in Figure 3.11, several tensions could be applied by the studs on the skin.

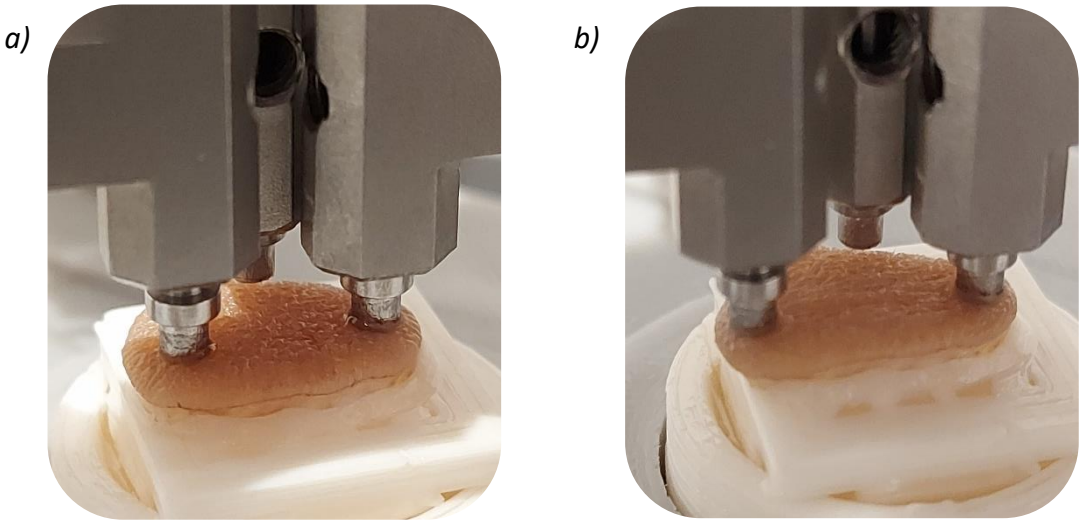

Figure 3.11: Photographs of a skin explant in the device before mechanical testing, showing that pre-tension can be applied to the explant. a) No initial pre-tension. b) Initial pre-tension (30% extension).

The skin explant was positioned (see Part 2.2.1) and remained there for the whole duration of the study. The first mechanical test was therefore carried out with the studs glued to the skin with a certain initial air gap. At the end of this test, a pre-tension was applied to the skin by moving back the two opposite arms using the manual micrometric displacement table. The mechanical test was then repeated with this initial pre-tension.

Several initial deformations, used as a pre-tension in our study, were carried out. A time of 60 seconds was observed between the end of manual deformation and the start of the test. This time was kept constant so that the explant benefits from the same level of relaxation for all the tests. This allows the skin to relax long enough to stabilise its mechanical behaviour. Figure 3.12 shows the results of this study for two different explants.

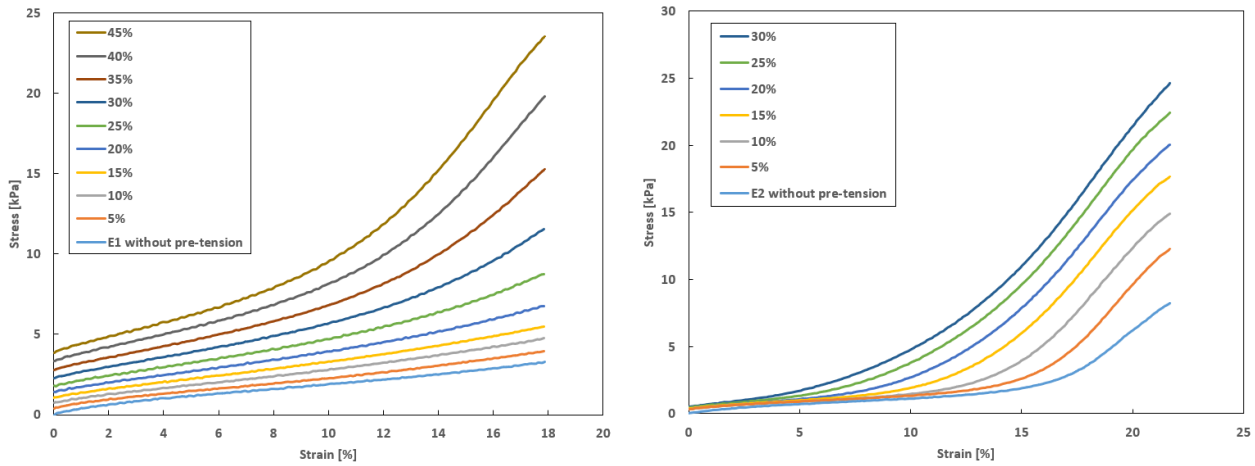

Figure 3.12: Influence of explant pre-tension on its mechanical behaviour in elongation. Tensile tests on 2 human skin explants (right and left graphics - speed = 10 mm.min^{-1}) with different initial pre-tensions.

These mechanical tests show the impact of pre-tensioning the explant on the mechanical properties. To compensate for the *in vivo* tension of the skin, the explants were stretched to deformations of up to 30% before the mechanical tests. The mechanical behaviour of a pre-stretched explant is therefore very different from that of a sample without pre-stretching. As the pre-tension increases, the skin is initially stretched, resulting in an increase in the stresses measured during deformation.

For example, with an initial pre-tension of 30%, the mechanical test stretches an explant that is already under tension. The dermal fibre network is therefore subjected to greater stress because it is already under tension, which increases the mechanical properties of the explant (Figure 3.13). On the other hand, without pre-tensioning, the mechanical test stretches an explant whose dermal fibre network is rather relaxed, which leads to lower mechanical properties.

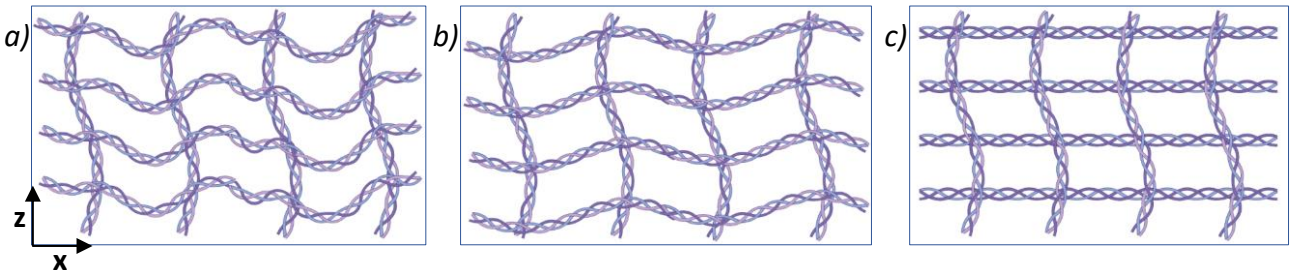

Figure 3.13: Attempt at a schematic representation of a dermal network of collagen fibres, vertical section view. a) Network without pre-tension; fairly loose network. b) Network with low pre-tension; the horizontal collagen fibres begin to reorganise along the direction of tension. c) Network with high pre-tension; the horizontal collagen fibres are aligned along the direction of tension.

The resulting characterisation of the stress-strain response, shown in Figure 3.12, indicates that the effect of pre-tensioning is to bring the stiffening part of the stress-strain curve to smaller strain levels. Indeed, it can be seen that the transition region between low stiffness and high stiffness

moves towards a region of lower stretch with increasing pre-tension. This indicates that the stiffness of elastin and collagen increases with pre-tension. The fact that the slope of the curves becomes steeper with increasing pre-tension indicates that the network of dermal fibres becomes increasingly rigid. Pre-tension will therefore stiffen the explant; the stress-strain curves are shifted on the vertical stress axis.

If we respect the initial deformation levels imposed by pre-tension of the skin, the graphs in Figure 3.12 would be represented as shown in Figure 3.14a. In fact, each mechanical test would start at its own strain level. It is clear from this graph that the mechanical behaviour of the explant will evolve progressively as a function of the initial pre-tension.

However, respecting the real initial deformations of the explant, the curves do not overlap. The skin, being a viscoelastic material, relaxes after the applied deformation.

It is the phenomenon of stress relaxation that is highlighted here when the skin is kept under tension. On the graph, the imposed deformation is correct, but the measured stress is not at the same level than the theoretical stress measured in the previous test. For example, the first test without pre-tension gives a stress of 1.1 kPa at 5% strain. At the end of the test, 5% strain is imposed on the explant, and the same test is performed again. The initial stress in this new test was not 1.1 kPa but 0.4 kPa, indicating stress relaxation. By adjusting the stresses, as shown in Figure 3.14b, we can find a reference curve which allows to characterise the skin explant at the greatest strains.

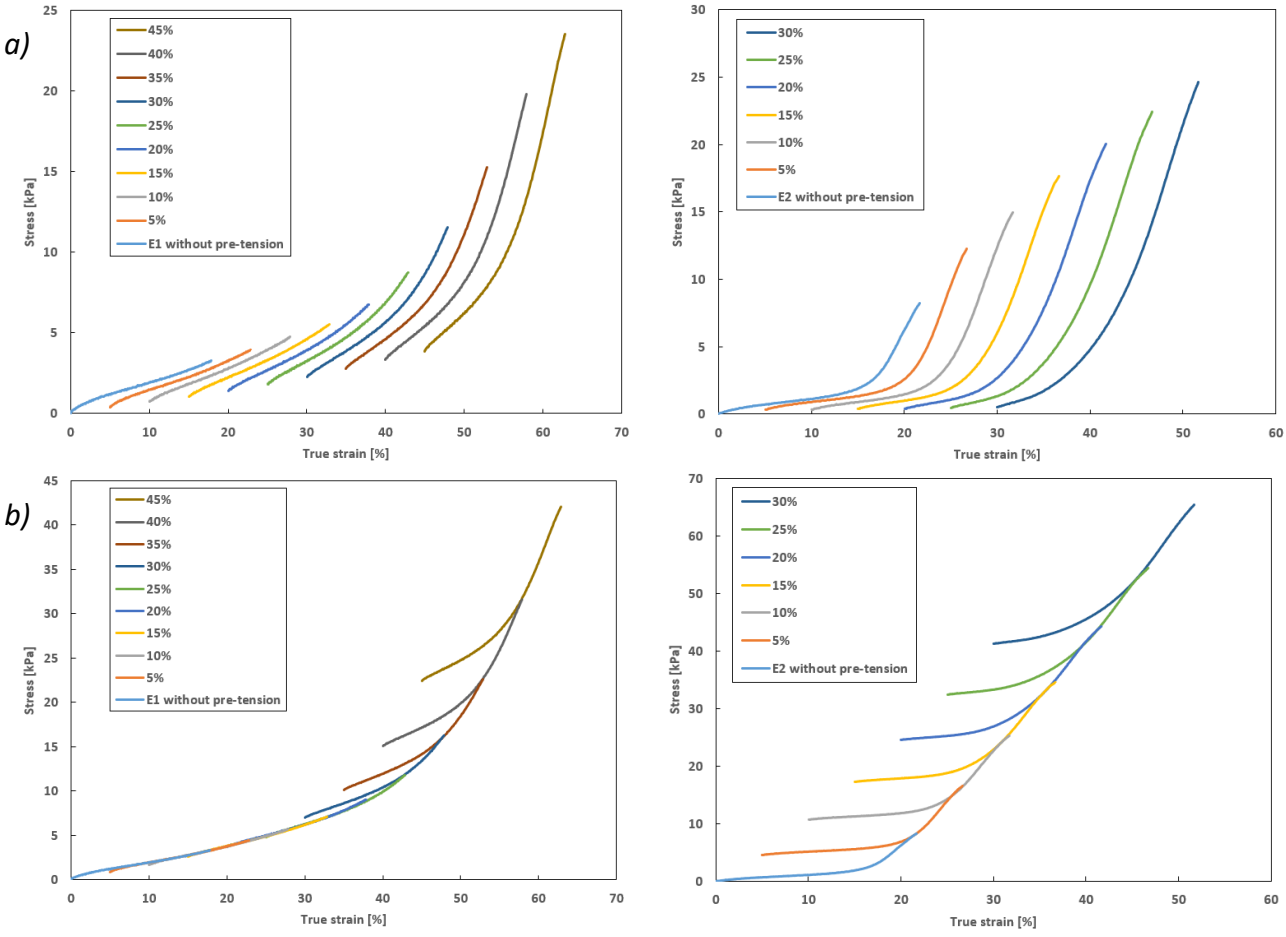

Figure 3.14: Tensile tests on 2 explants of human skin (speed = 10 mm.min^{-1}) with different initial pre-tensions. a) Graphs with initial deformations respected. b) Graphs with adjusted stresses.

Despite the phenomenon of stress relaxation when the skin is held under tension, this analysis allows to recover the bilinear, or J-shape, reference curve of the skin. The possible deformation that can be induced in the skin can therefore reach more than 50%. However, beyond this deformation, the system for attaching the sample shows its limits. Indeed, the glue point begins to detach and the studs come off the skin.

Remark: Use of the "Perfex vivo" system from Eurofins BIO-EC

With the aim of recovering the intrinsic tension of the skin *in vivo*, we also carried out tests with human skin explants attached to a support developed by Eurofins BIO-EC: the "Perfex vivo" support (Figure 3.15a). This support puts the skin explant under tension using a circular rubber seal. However, it has the disadvantage of not allowing the skin tension to be controlled. In fact, the circular seal is placed manually on the skin, which can lead to variations in explant tension. Tests carried out with the "Perfex vivo" support are therefore not reproducible, unless the circular seal is left on the explant throughout the study and the explant is fed continuously with a nutrient fluid circulation system.

Despite this drawback, the skin is stretched uniformly, unlike the unidirectional pre-tension applied by our equipment. This uniform tension will influence the results of the mechanical tests, as shown in Figure 3.15b. This Figure shows the comparison between a mechanical test carried out with the "Perfex vivo" support, which induces approximately 30% deformation of the explant, and the same mechanical test carried out with the device's pre-tension at 30% deformation.

a) *b)*

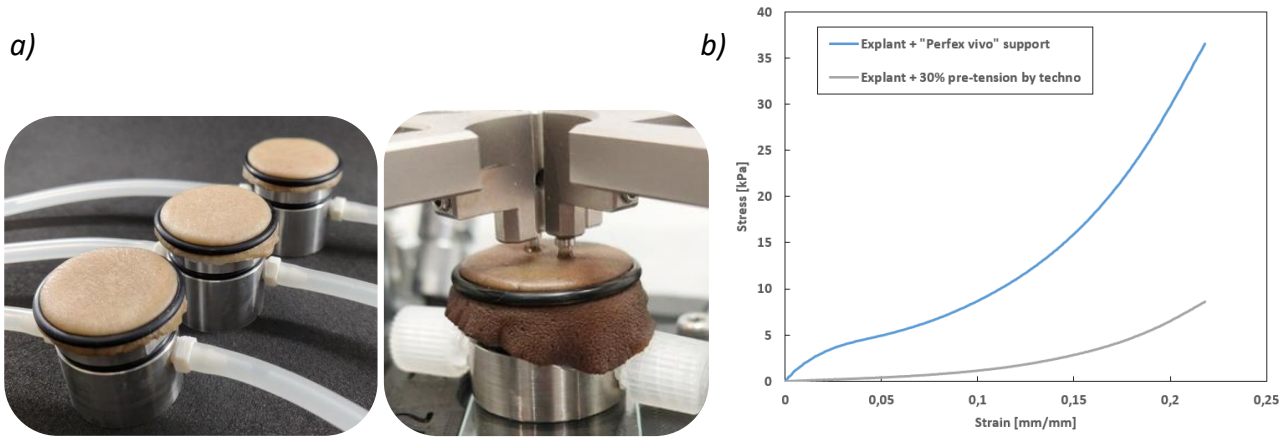

Figure 3.15: Tests with "Perfex vivo" support. a) Photographs of the support and the installation on the device. b) Comparison of a simple tensile test, on the same explant of human skin (speed=10mm.min^{-1}), with the "Perfex vivo" support and with a pre-tension generated by the equipment.

The mechanical behaviour of the skin is clearly superior when the entire explant is initially tensioned ("Perfex vivo" support). With this support, all the fibrous dermal networks of the explant are pre-tensioned before carrying out the mechanical test. These results therefore show that the area surrounding the test zone (between the two studs) has a significant influence on the mechanical properties of the explant. Although this zone is not directly stressed by the mechanical tests, as the skin is a highly cohesive material, it does have an impact on the study zone.

Another disadvantage of this support is that it can induce high tensions which can degrade the skin. During tests with the "Perfex vivo" support, we observed a very pronounced Mullins effect, which persisted over time, leading to a very long stabilisation of the mechanical behaviour of the explant.

Conclusions: although the *ex vivo* explant does not have the intrinsic tension of skin under *in vivo* conditions, we have chosen not to apply any pre-tension, for the majority of tests, to the explant prior to the mechanical tests. Mechanical characterisation will therefore be carried out directly on the *ex vivo* explants, with no initial pre-tension imposed. The skin is therefore characterised in its *ex vivo* state, i.e. in its state outside the human body.

The "Perfex vivo" support was not chosen because the tension of the explant is not controlled, which makes the tests non-reproducible. Similarly, the initial pre-tensioning of the explant, carried out by manually moving back the arms of the instrument, was not adopted because it leads to additional internal stresses which induce a stress relaxation phenomenon and a greater Mullins effect. This requires longer pre-conditioning of the explant, reducing the time needed to carry out the experiments. In addition, these initial tests show that pre-tensions of 5 to 15% deformation, enabling the *in vivo* tension of the skin to be restored, do not lead to significant variations in the mechanical properties of the explant.

However, these results encourage us to think about new types of sample attachment onto the device in order to propose characterisations with different types of pre-tension. This could be an avenue for future work.

3.7 Notion of skin anisotropy

As described in Part 1.3.4, skin anisotropy is an important property. The structural characteristics of the skin are not uniform in all directions, which confers different mechanical resistance depending on the axis of stress. This anisotropy seems to be linked to the preferential orientation of collagen fibres in the dermis [Ni Annaidh *et al.,* 2012]. The heterogeneous distribution of these fibres means that skin anisotropy is defined as directional variations in tissue organisation.

Thus, the mechanical behaviour of the skin depends mainly on the directionality and the arrangement of the collagen fibres present in the dermis [Liu *et al.,* 2008]. The orientation of the tension lines has a significant influence on the mechanical response of the skin. Tensile tests carried out on skin explants have revealed that the directions with the highest pre-tension, following the Langer lines, are also those with the greatest stiffness [Elouneg *et al.,* 2023]; [Ottenio *et al.,* 2015].

These different studies thus demonstrate that the anisotropic mechanical response of the skin is mainly attributable to the structural arrangement of the collagen fibres in the dermis (Figure 3.16).

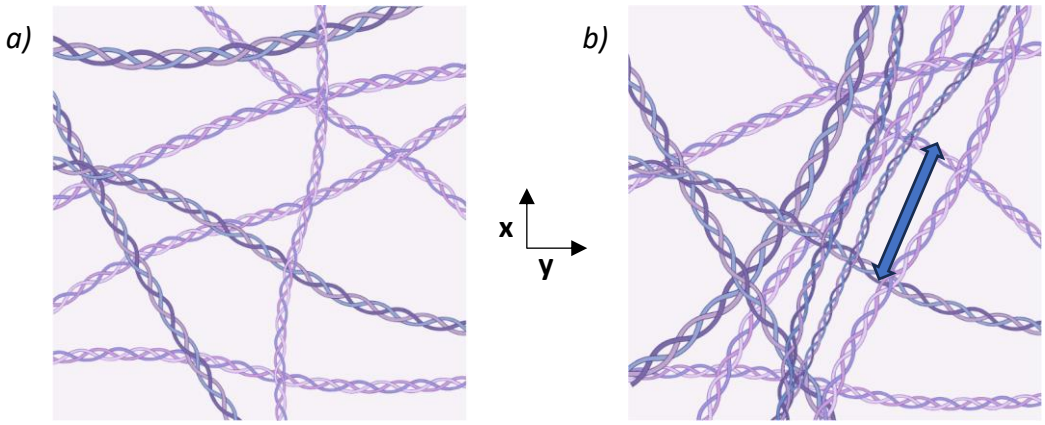

Figure 3.16: Schematic representation of a dermal network of collagen fibres, top view. a) Network with no preferential arrangement of fibres. b) Anisotropic network, with preferential direction of fibres (represented by a blue arrow), therefore exhibiting anisotropic mechanical behaviour.

The aim of this preliminary study was thus to examine the anisotropic mechanical behaviour of human skin explants *ex vivo*. To do this, several identical mechanical tests were carried out on the same skin explant, but in different directions. First, the explant is positioned and glued, then a mechanical test is performed in this first direction. Next, the explant is peeled off the studs, rotated through a 45° angle, repositioned, and glued back to perform the second mechanical test. This operation is repeated three times to characterise the skin in four different directions: 0°/180°; 45°/225°; 90°/270° and 135°/315°. Only four tests were carried out, representing mechanical properties in four different directions, on the same explant in order to limit the duration of the experiment (Figure 3.17).

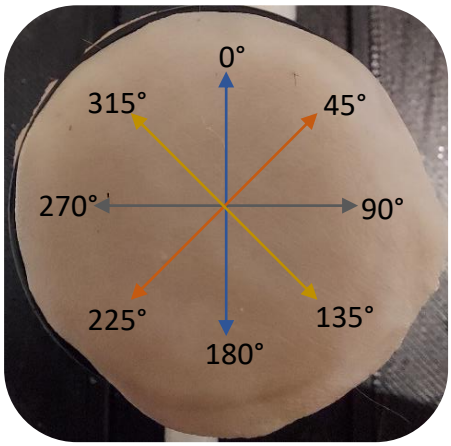

Figure 3.17: Representation of the four tests carried out on the same skin explant to study the mechanical anisotropy of the skin.

One of the advantages of our device is that it allows to carry out unidirectional tests. This mode of loading allows to take measurements in different possible directions in the plane of the skin, and therefore to study the anisotropic behaviour of the skin. This method seems to be ideal and reliable for characterising the anisotropy of the skin because the deformations are in the plane, corresponding to the alignment of the collagen fibres which are organised parallel to the surface of the skin. Figure 3.18 shows the results of this study for two different skin explants.

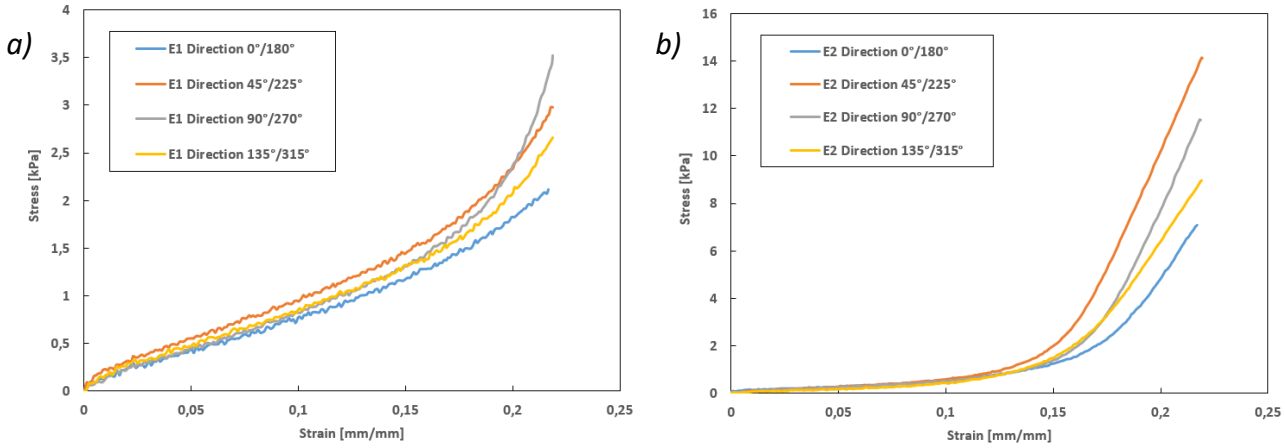

Figure 3.18: Mechanical anisotropy of human skin. Tensile tests on 2 human skin explants (speed = 10 mm.min^{-1}) in different directions.

Figure 3.18 illustrates that the mechanical properties of the explant vary according to the direction of loading. We observed these variations at high strains, greater than 15%. This tends to prove that this anisotropy is indeed the consequence of the preferred directions of the collagen fibre bundles which are stressed at high strains. Conversely, the elastic network of elastin fibres stressed at low strain appears to be isotropic, with mechanical properties that do not depend on the direction of testing.

At large strains, one direction seems to hold the highest mechanical properties in the explant. This direction of measurement can be associated with the direction of the lines of tension in the skin: the Langer lines. The collagen fibres would therefore have this preferred orientation within the explant, giving it superior mechanical properties in this specific direction. The results presented in Figure 3.18 can also be represented in a different form, as shown in Figure 3.19 by representing all the angles two by two on a spider web graph.

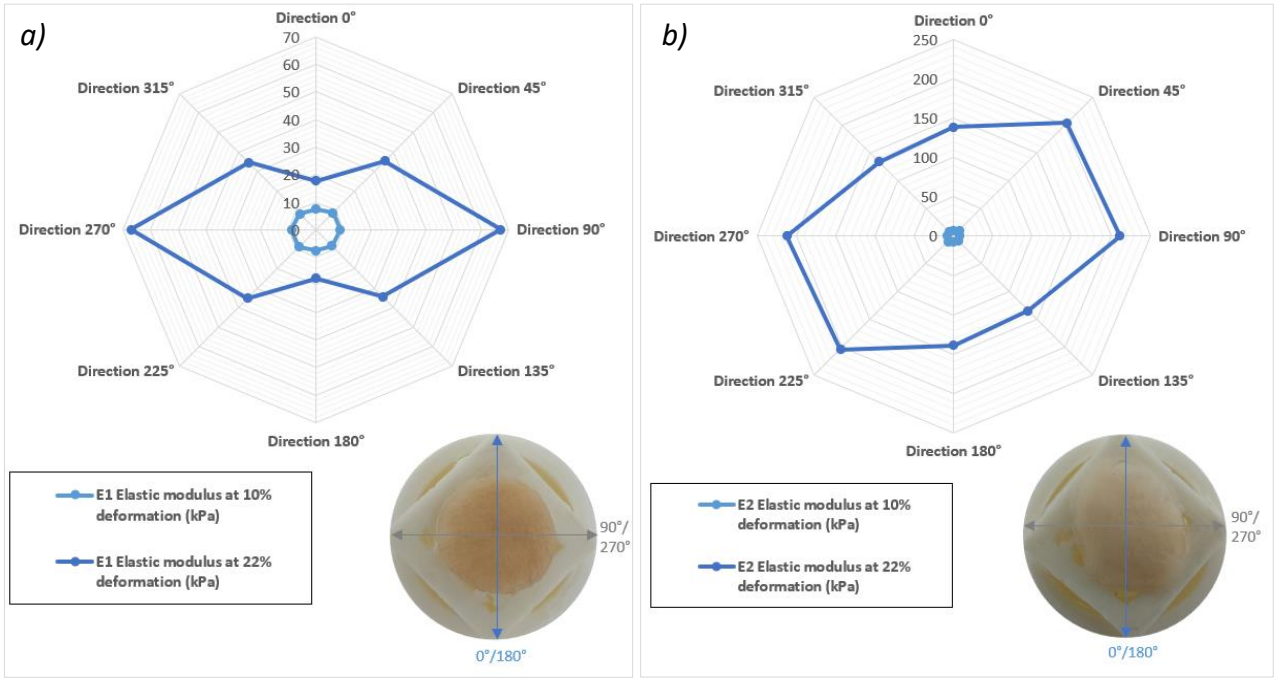

Figure 3.19: Mechanical anisotropy of human skin. Radar graph of the elastic moduli of the 2 explants.

This Figure clearly shows the mechanical anisotropy of the skins as a function of the direction of stress. It is also clear from this graph that the anisotropy is only marked at high deformations. These graphs highlight the preferred direction of the collagen fibres, which is in the 90°/270° direction for explant E_1 and in a direction close to 67°/247° for explant E_2.

It should also be noted here that explant E_2 is not circular. Indeed, as shown in Figure 1.26, due to the anisotropy of the skin, a circular explant taken from the human body can take on an oval shape once excised. This oval-shaped explant means that it comes from an area of high skin tension (the moduli of the oval explant E_2 are much higher than those of the round explant E_1). The skin, which is initially highly pre-tensioned *in vivo*, will relax more in the *ex vivo* state. According to Langer [Langer, 1978b], the direction of the smallest diameter of the explant (where there is the greatest retraction) is the preferred direction for the fibres. In fact, from a highly pre-stressed state, the collagen fibres will relax significantly. These analyses are confirmed by our study, since it is along the axis of this small ellipse, towards the 90°/270° direction, that we find the strongest mechanical moduli for explant E_2 (Figure 3.19.b). The fibres pre-oriented along this axis will therefore respond significantly and rapidly to the deformation of the explant. The results for skin tension and mechanical anisotropy are therefore consistent with those of Langer.

Conclusions: this study confirms that *ex vivo* human skin explants therefore have anisotropic mechanical properties. In fact, there is a wide variation in mechanical results within an explant, mainly due to this anisotropy.

In order to follow an explant in a consistent way throughout a study, it is essential to maintain the same direction of loading during the mechanical tests in order to measure the same mechanical properties each time. This parameter must be kept the same.

When comparing mechanical properties between two or more different explants, it is important to keep in mind their anisotropic behaviour (see later in Part 4.1.3). This will make it difficult to obtain an accurate and reliable comparison of their properties, as each explant has anisotropic mechanical properties that vary slightly depending on the direction of loading.

For the mechanical characterisations carried out in the following Chapter 4, the tests were always carried out in the direction of the long axis of the elliptical explants in order to have a more comfortable space for bonding the studs. For circular explants, the test axis was chosen randomly.

3.8 General conclusion of "Preliminary studies"

This Chapter presents the various preliminary studies carried out on the skin. The aim was, firstly, to validate the experimental test methods developed in Chapter 2 and, secondly, to optimise future mechanical characterisations by carrying out the first tests on skin explants *ex vivo*.

These initial tests on human skin explants enabled us to use our equipment on living tissues for the first time. To verify the reliability and accuracy of our equipment, we first carried out repeatability and reproducibility tests on the skin. These tests validated the methods we have developed for reliable and accurate characterisation of the mechanical properties of human skin.

As skin is viscoelastic, we paid particular attention to the pre-conditioning of the skin before the tests and to the rate of deformation during the tests. Subsequent studies on the effect of compression force and the pre-tension state of the skin highlighted the importance of measuring and controlling these two parameters before carrying out mechanical tests. Finally, the anisotropy of the skin's mechanical properties, an intrinsic property of the tissue described in Part 1.3.4, was confirmed and quantified in the last preliminary study.

Various controllable parameters were therefore tested in order to obtain the optimum technological configuration and measurement methods for characterising *ex vivo* human skin explants as accurately as possible. This Chapter highlights the reliability and robustness of the device and test method used to assess the mechanical properties of the skin. Indeed, our instrumentation is capable of accurate measurements in the specific environment in which it is used. The device gives close results even in the presence of slight variations in experimental conditions that may occur in the use of the procedure. In this way, our equipment can be used by any user while guaranteeing reproducible and consistent results.

After taking into account all the parameters studied in this Chapter, we are now ready to characterise the mechanical properties of a sample of human skin *ex vivo* in a complete and reproducible way using our device.

Chapter 4.

Characterisation of human skin mechanical properties

This Chapter presents the results of our experiments, which aimed at characterising the mechanical properties of *ex vivo* human skin explants using our equipment as described in Chapter 2.
We recalled as well in Chapter 1 that the overall viscoelastic properties of human skin play a key role in skin integrity, as they provide the skin tissue with the ability to remain intact. The central objective of this Chapter is to characterise the global rheological and mechanical behaviour of the human skin and its elasticity and dissipation properties, which can be different according to the load frequency.
Knowing the evolution of these two parameters of the rheological behaviour, a link will also be established between the mechanical properties and the structure of the skin. The deformation behaviour of the skin is closely linked to its mechanical properties, which are governed by the complex structure of the skin tissue, in particular the dermal layer and its fibre networks.

In this first part of the Chapter, the results of the characterisation of the mechanical properties of *ex vivo* human skin explants are presented. A large number of skin explants from a large number of donors were experimentally tested in order to obtain a broad characterisation of the mechanical properties. As introduced in Part 2.3, the skin explants characterised come from the Eurofins BIO-EC laboratory. All mechanical tests were carried out at a constant temperature, which is the ambient temperature in the test room (around 21°C).
A study of the viability of the skin explants over time was then carried out in order to monitor and evaluate the survival of the explants under *ex vivo* conditions.
Finally, a comparison of the mechanical properties of different types of explants with different characteristics have been carried out. In addition to the inter-donor variability of the mechanical characteristics of the explants, the notion of intra-donor variability will also be presented.

The main aim of this Chapter is to demonstrate the scientific contribution made by our device and to highlight the variety of tests that can be carried out using it.

Note on the identification of the samples:
In this Section, many explants were used so that they could be characterised using our equipment. To ensure clarity and traceability of the origin of the samples, as well as to maintain good organisation during the various experiments, a rigorous notation method was established to identify the samples precisely.
The explants are therefore named as follows: 'P2510-AB55'. The 'P' stands for 'skin plasty'; the first four digits correspond to the number allocated to the plasty received (Eurofins BIO-EC internal reference); the first letter corresponds to the anatomical site from which the plasty was taken ('A' for the abdomen area, the only area used for our explants); the second letter corresponds to the skin phototype ('B' for white skin and 'N' for black skin); and the last two digits correspond to the age of the donor.

4.1 Characterisation of *ex vivo* skin mechanical properties

A complete and detailed characterisation of the mechanical properties of different *ex vivo* skin explants is presented and described in this Section. The aim here is to characterise the typical mechanical behaviour of *ex vivo* skin explants.
The skin explants analysed are randomly selected. They come from different donors, all of whom are women, but of different ages and skin colours. The possible disparity in mechanical properties will therefore reflect the diversity of the explants due to the diversity of the donors (variability of living organisms).

The analyses presented in this Section will therefore enable to map the mechanical behaviour of different explants taken at random. Before presenting the results, a concise overview of the different skin explants used in these characterisations is provided in Figure 4.1.

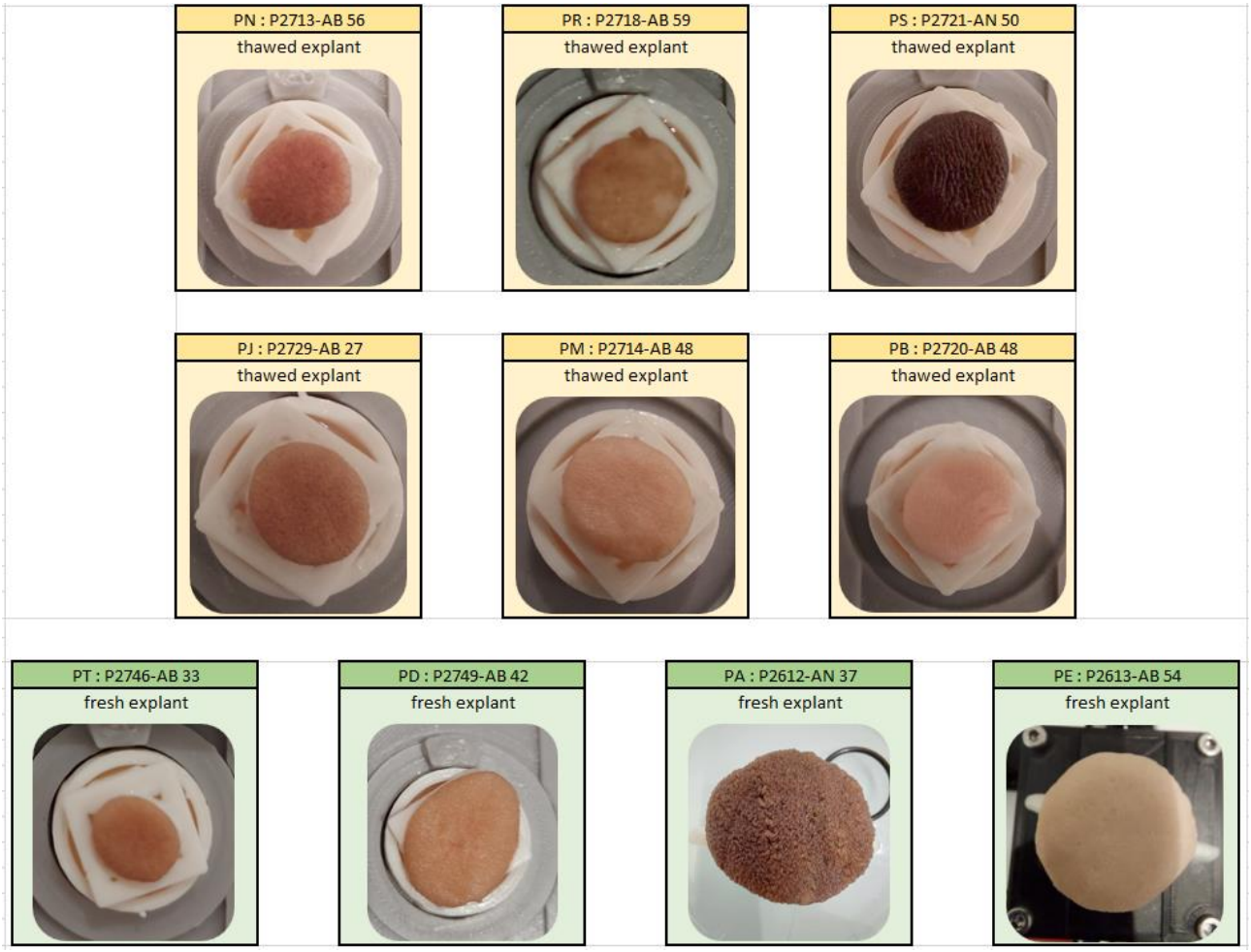

Figure 4.1: Brief presentation of the different skin explants characterised in this Section. To easily identify the different skins, the notation is simplified to 2 letters.

In order to keep the explants from fresh plasty for further studies on the effects of different stresses (see later in Chapter 5), most of these characterisation tests were performed on explants taken prior to the test campaigns, which were then frozen at -20°C for long-term preservation. Although this method could potentially have an impact on the properties of the skin (see later in Part 5.2), it enables the properties of the explants to be preserved and numerous tests to be carried out on a large number of skin samples.

The protocol for carrying out the tests on *ex vivo* human skin explants is presented in Part 2.2.1. In order to be characterised:

- Fresh skin explants, which are maintained in physiological like conditions, are removed from the incubator and positioned in the instrumentation. All mechanical tests are performed within a limited timeframe to ensure optimal survival of the explant and to quickly return it to the incubator. All tests are completed in approximately 30 minutes.
- The frozen skin explants are removed from the freezer and returned to their holder. Based on Eurofins BIO-EC's experience, a thawing time of 30 minutes at room temperature is required for the explant to regain its initial properties. The explant is then placed in the equipment to be characterised, and at the end of the series of tests, it is discarded as it is no longer usable.

Our equipment enables to carry out unidirectional tensile tests in the plane of the skin. When the skin explant is subjected to traction, it expands due to the elastic fibrous networks present in the dermis. Once the stress ends, the skin retracts with a viscoelastic return to its initial state.

It is important to note that in our case, we do not observe any significant extensions that would lead to plastic and irreversible deformation of the skin, at which the fibre networks would be broken (see Part 3.2).

4.1.1 Tensile test

The tensile test consists in deforming the sample at a constant tensile speed. It is used to characterise the relationship between stress and strain. Typical results of simple tensile tests on skin explants are shown in Figure 4.2. All the skin explants tested and characterised in this loading mode exhibit one of these four types of mechanical behaviour. These graphs are therefore representative of the tensile mechanical behaviour of *ex vivo* human skin explants.

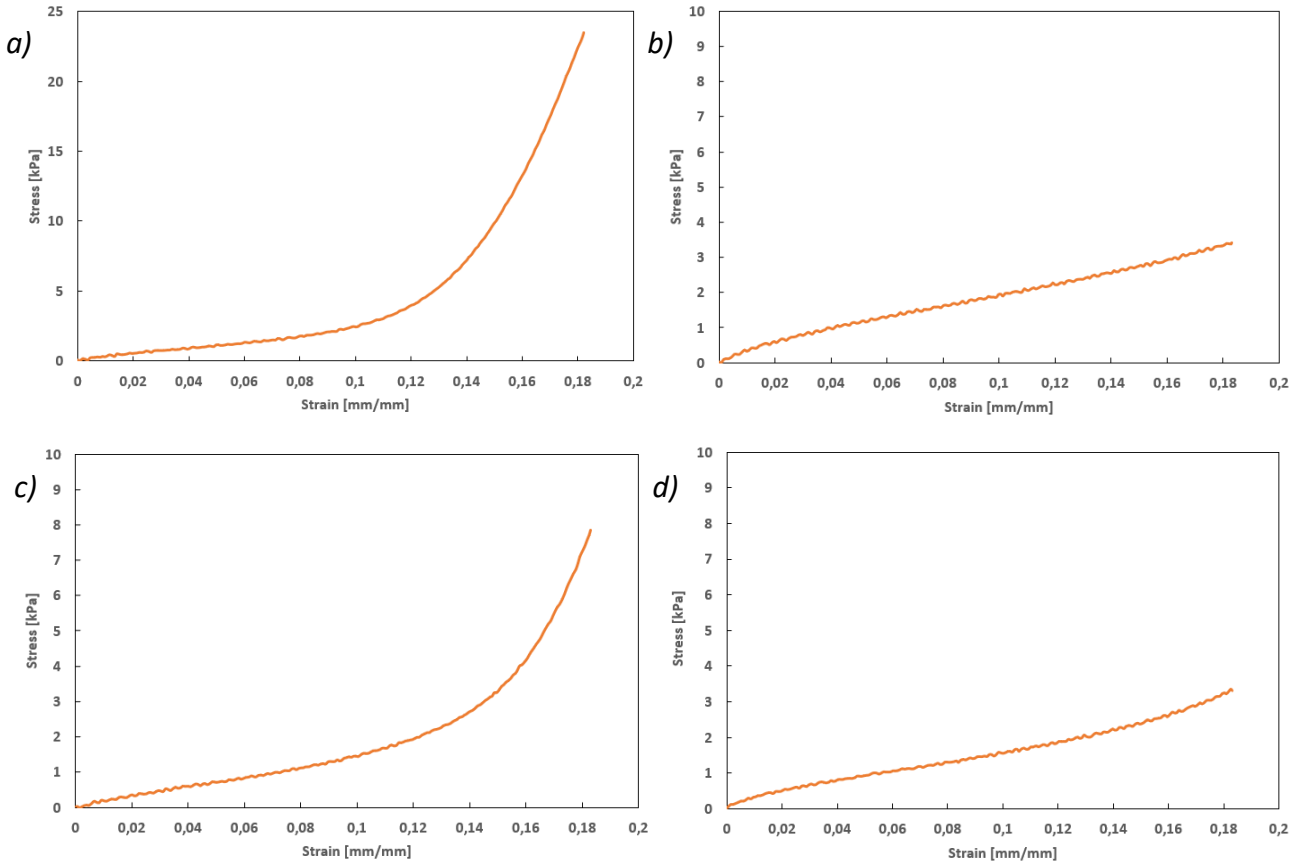

Figure 4.2: Stress - Strain curves for 4 human skin explants (speed = 10 mm.min^{-1}). Stress versus strain graphs. Explants PR (a), PJ (b), PB (c) and PM (d).

Simple tensile tests show differences in the elasticity of the skin explants. In this Figure, two types of mechanical behaviour can be distinguished for the skin explants under traction. The PJ and PM skin explants exhibit a quasi-linear elastic mechanical behaviour over the range of deformation imposed. In contrast, PR and PB skin explants have linear elastic mechanical behaviour for the lower deformations followed by a hardening phase. The behaviour of the PR skin explant can even be considered as bilinear over the range of imposed deformation. As described in Part 1.3.2, this form of curve, known as the J-shaped curve, is characteristic of the mechanical behaviour of the skin at large deformations [Holzapfel, 2000].
In fact, the characteristic curves for the PJ and PM skin explants only show the first part of the J-shaped curve at these percentages of deformation. If these explants were stretched even further, we would observe this stiffening phase in the mechanical behaviour of the skin. It can be seen that at the maximum deformations of the PM explant, this slight stiffening is observed, corresponding to the start of the second part of the J-shaped curve.

From a physiological point of view, this typical shape of the curve on human skin is due to the various forces generated by the deformation of the network of the elastin and collagen composing the dermis of the skin [Brown, 1973].
In the first region of skin stretch, a strong extension is observed under low loading. This initial linear rise in the curve is linked to the elastic network of elastin fibres in the dermis. During this phase, elastin fibres, which are highly extensible and easy to stretch, elongate. The collagen fibres, on the other hand, are coiled and wavy. The initially wavy collagen fibre bundles are then reoriented and

aligned along the loading axis. This is the transition phase when the skin's mechanical behaviour becomes stiffer: stress and rigidity increase. The last region is a new linear region corresponding to the stabilisation of stiffness. This region reflects the elastic modulus of the collagen fibres, which are aligned in the direction of traction and offer maximum resistance.
While elastin is primarily responsible for the skin's suppleness and resistance to small deformations, collagen is responsible for maintaining the skin at larger deformations [Silver *et al.*, 2003].

Analysis of the graphs in Figure 4.2 allows to measure the mechanical properties of the explants, and in particular to calculate the various mechanical parameters, which are presented in the following two figures.
Firstly, as shown in Figure 4.3, the different apparent moduli of elasticity are determined at different percentages of explant deformation: initially, at 5%, 10%, 15% and 18% (maximum deformation reached in our configuration).

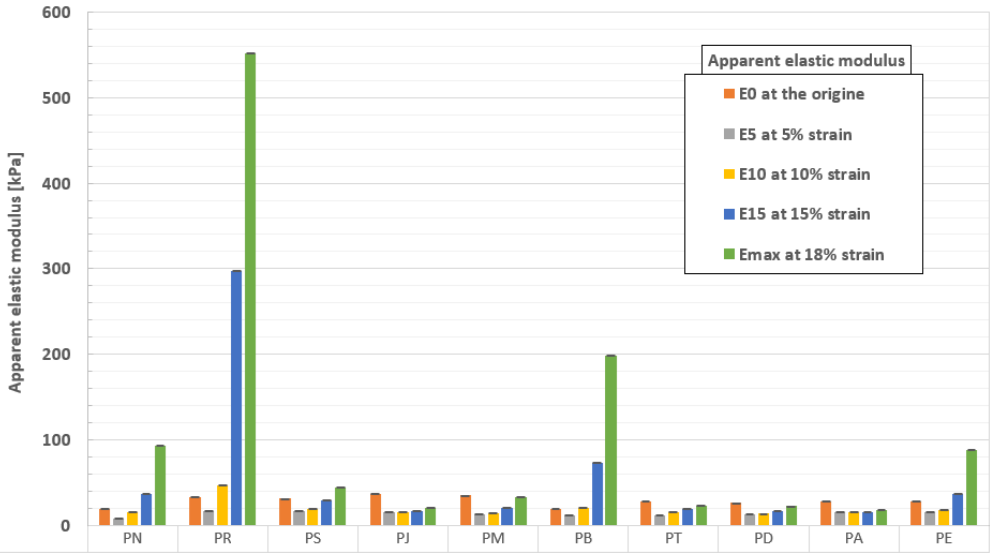

	PN	PR	PS	PJ	PM	PB	PT	PD	PA	PE
E0 at the origine	19,4	33,1	31,4	37,4	35,2	19,2	27,9	26,3	28,7	28,0
E5 at 5% strain	8,6	17,2	16,5	15,8	12,8	11,7	11,9	12,7	15,3	15,6
E10 at 10% strain	16,1	47,5	19,8	15,3	14,0	20,3	15,7	13,9	15,3	18,3
E15 at 15% strain	36,9	297,9	29,6	17,3	21,1	73,2	19,1	16,5	15,9	37,2
Emax at 18% strain	93,2	552,1	44,5	20,7	33,6	198,2	22,8	22,7	18,7	88,4

Figure 4.3: Results of mechanical tensile tests on human skin explants. Apparent moduli determined for each explant, at different percentages of deformation (with force sensor measurements uncertainties).

The tensile test is a reference test in mechanics for characterising a material because it allows its modulus of elasticity, or Young's modulus, to be measured. This modulus, measured at the origin of the stress-strain curves, is the modulus denoted E_0 in Figure 4.3. The apparent Young's moduli for the different skin explants used in our test campaign are between 15 and 40 kPa. The PB skin explant has the lowest apparent Young's modulus, equal to (19.2 ± 0.5) kPa. Conversely, the PJ skin explant has the highest apparent Young's modulus, equal to (37.4 ± 0.5) kPa.

All the different apparent moduli, measured for different strain percentages, represent the stiffness of the skin explants for these strain rates. The higher the moduli, the stiffer the skin explants, and the less they deform under stress.

For some skin samples, such as PS, PJ, PM, PT, PD and PA, the moduli are stable and increase progressively with deformation. This is characteristic of the linear elastic behaviour of the skin

explants (Figure 4.2.b). The moduli at different percentages of deformation for these skins are characteristic of the first part of the J-shaped curve: they range from 10 to 45 kPa.
For the other skin samples, such as PN, PR, PB and PE, the moduli increase rapidly with deformation, demonstrating the rapid stiffening of these explants. This is characteristic of the bilinear elastic behaviour of the skin explants (Figure 4.2.a). The moduli at maximum percent deformation of these skins are high and are characteristic of the beginning of the second part of the J-shaped curve: they are between 85 and 560 kPa. Due to the configuration of our equipment, which does not allow us to continue deformation beyond 18%, these moduli are calculated at the start of the second steeper part of the curves. If the deformation were higher, these moduli would certainly be higher.

In the following part (Part 4.1.1.B), all the values of these moduli measured with our instrumentation will be compared with the values of the moduli in the scientific literature.

Similarly, as shown in Figure 4.4, the different stresses reached during the tests are measured at the same percentages of explant deformation.

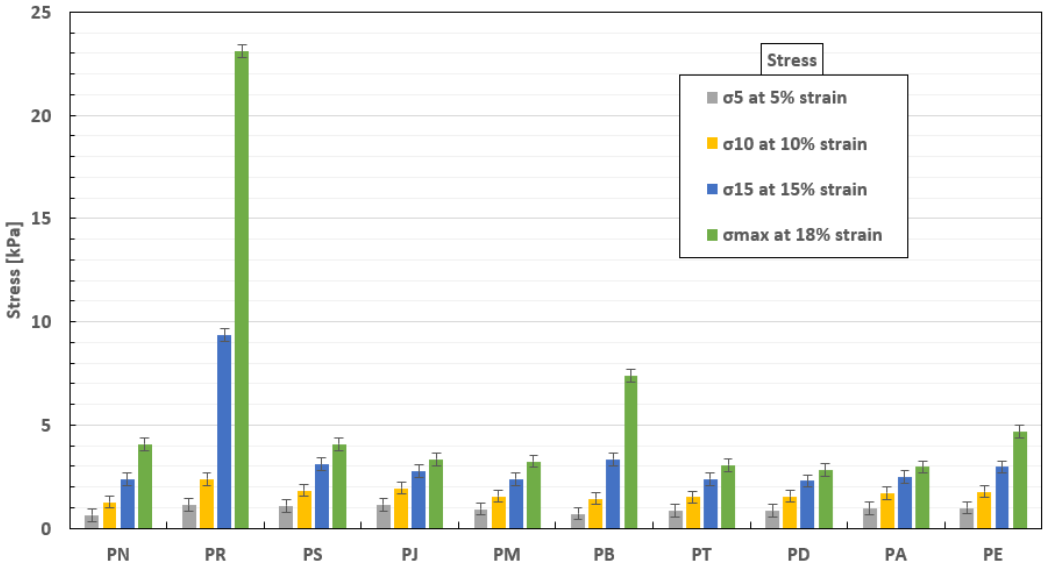

Figure 4.4: Results of mechanical tensile tests on human skin explants. Stresses measured for each explant, at different percentages of deformation (with force sensor measurement uncertainties).

The mechanical tensile test shows how, little by little, the structure of the skin will resist the deformation imposed. By measuring stresses at different rates of deformation, we can also demonstrate that two types of mechanical behaviour can be distinguished. For some skins, such as PS, PJ, PM, PT, PD and PA, we can note that the stresses increase proportionally with the deformation of the explant, which proves the linear elastic behaviour of the skin at large deformations. For other skins such as PN, PR, PB and PE, the stresses do not increase proportionally but rather exponentially with the deformation, demonstrating the bilinear elastic behaviour of the skin explants. This behaviour is shown graphically by a J-shaped stress-strain curve (Figure 4.2.a).

Conclusions:

The simple tensile test provides information on the elastic behaviour of the skin. As described in Chapter 1, this elasticity is due to the extension of the various elastin and collagen fibre networks in the skin. The stress-strain response of the skin at low rates of deformation is mainly due to the resistance of the elastin fibre network and the reorientation of collagen fibre bundles in the hydrated matrix. The stretching of the collagen fibres and their reorientation in the direction of the load are then recognised phenomena responsible for the non-linear tensile mechanical behaviour of the skin.

At deformations of up to 18%, two types of elastic mechanical behaviour are observed: linear elastic behaviour and bilinear elastic behaviour. These two observed mechanical behaviours will be explained later in Part 4.1.4. The tensile mechanical behaviour of human skin, shown in Figure 4.2.a, is similar to the mechanical behaviour of elastic rubber materials. Indeed, the J-shaped curve is similar to the "strain hardening" of rubbers. As with rubbery materials such as elastomers, the slope of the stress-strain curve increases with deformation, meaning that the skin becomes progressively more difficult to stretch. The skin therefore has a non-linear elastic behaviour, also known as hyperelastic, which is often modelled in the literature by hyperelastic behaviour models. During a mechanical test, the skin can undergo very large deformations without undergoing plastic deformation, and therefore return from its deformed configuration to its initial configuration.

The greater the first phase of skin extension (first part of the J-shaped curve), the more elastic the skin can be considered to be. PS, PJ, PM, PT, PD and PA skins therefore have high elasticity. These skin explants have apparent moduli and stresses that increase progressively with the rate of deformation. This results in skins that have a high capacity for extension under low load, while at the same time being able to deform reversibly.

4.1.2 Comparison of our results with those of the scientific literature

In this Section, a comparison is made between the elastic moduli measured with our instrumentation and those in the scientific literature (see Part 1.3). This confrontation of results allows to see where we are in the range of elasticity values of the skin, and to check that we are not disconnected from reality. Figure 4.5 shows this range of elastic moduli, which range from a few kilopascals to hundreds of megapascals.

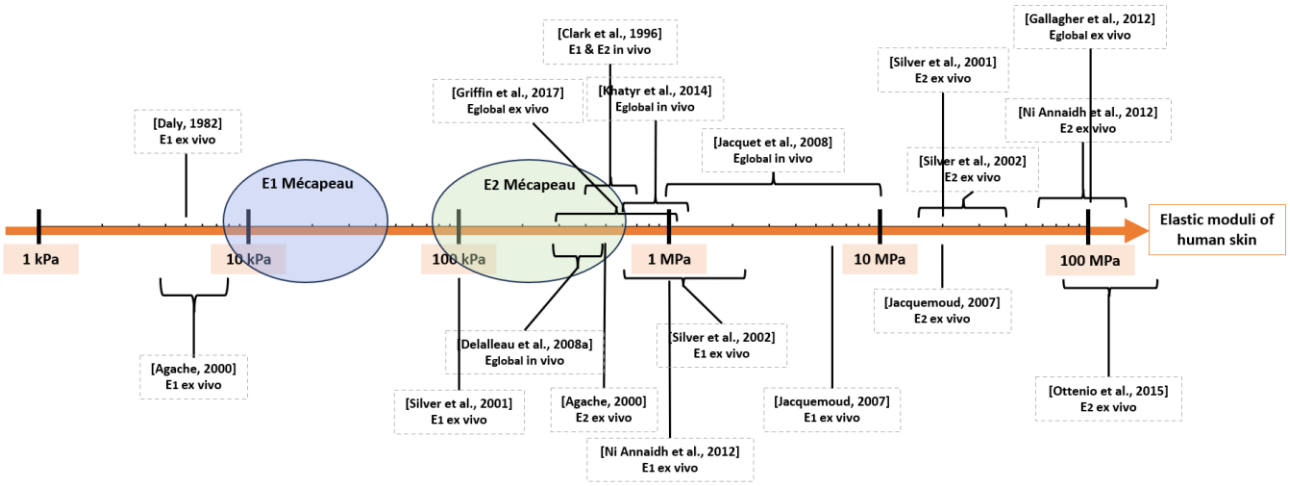

Figure 4.5: Frieze of the elastic moduli of human skin. Comparison of Mécapeau values with those in the scientific literature.

This Figure shows that our results are comparable with those in the literature. The apparent moduli of elasticity of the different skin samples we analysed were between 8 and 40 kPa in the first part of the extension and between 80 and 600 kPa in the second part of the extension (for samples revealing a bilinear behaviour). The literature study mentions moduli of between 5 kPa and 6 MPa in the first part of the extension and between 300 kPa and 150 MPa in the second part of the extension (see Table 1.3). The results of our study therefore appear to be consistent with the results of the literature. Compared with the data in the literature, which is quite broad, the results of our study fall within a rather low range of elastic moduli. Due to our method of attachment to the skin and our limited range of deformation, which means that we were able to avoid degrading the explants during the tests, we are in the low range of mechanical properties of human skin explants.

However, it is not easy to compare these results because many experimental parameters are involved. The mechanical properties of skin depend on a multitude of physico-chemical factors. Internal factors related to the material, such as its composition, structure, and anisotropy. But there are also external factors, such as the temperature, humidity, and atmosphere at the test site; the cutting and preparation of the explant; the type of test performed and the test parameters chosen, etc. Thus, the results of a mechanical measurement are highly dependent on the test conditions and are not easily comparable with other methods. Despite the differences between these numerous factors, which strongly influence the mechanical properties of the explants, this comparison of modules has been carried out.

4.1.3 Dynamic tests

Dynamic mechanical analysis (DMA) is a spectromechanical analysis dedicated to the measurement of the viscoelastic properties of materials. It allows to establish how the structure of the skin affects elasticity and energy dissipation. As the skin is a viscoelastic material, it has both elastic behaviour (like a solid) and viscous behaviour (like a liquid). Dynamic tests will therefore enable to quantify

the elastic and loss (viscous) properties of the skin according to the frequency (temperature kept constant).

In the dynamic regime, the mechanical properties of a material depend on the deformation and the excitation frequency. Two dynamic mechanical tests are used to characterise a material: the strain sweep test to define the linear domain and the frequency sweep test performed in the linear domain.

4.1.3.A Strain sweep test

The strain sweep test involves imposing sinusoidal deformations of increasing amplitude at a constant frequency and at a constant temperature. The sensitivity of the sensors requires to increase the strain range of these tests in order to maximise the measured torques. The strain sweep test is therefore carried out between 1% and 18% deformation. Typical results of this type of scan on skin explants are shown in Figure 4.6. All the skin explants tested and characterised in this loading mode show these types of mechanical behaviour. These graphs are therefore representative of the dynamic mechanical behaviour of *ex vivo* human skin explants.

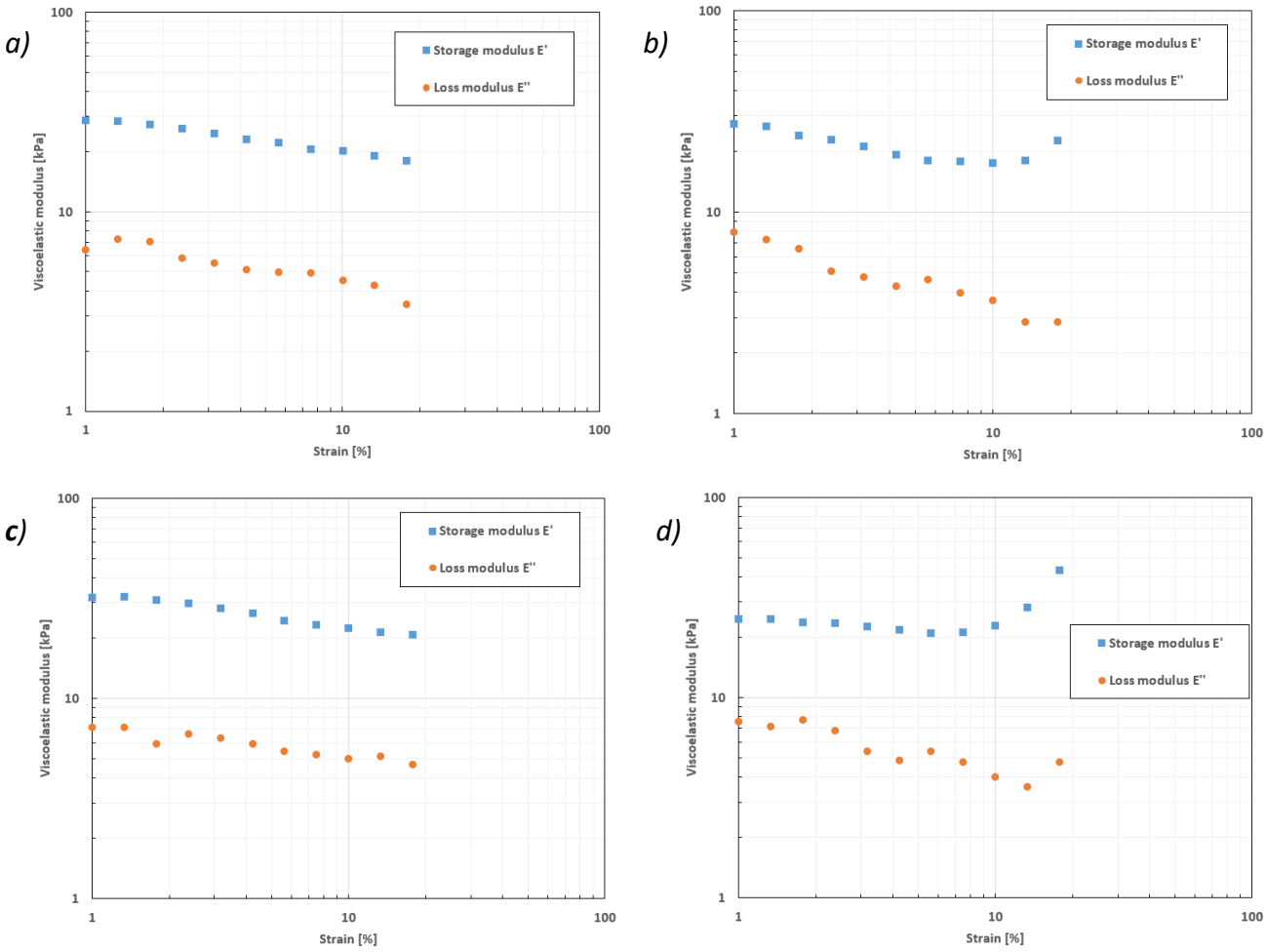

Figure 4.6: Strain sweep tests on 4 human skin explants (f = 0.5 Hz - T = T_{amb}). Graphs of viscoelastic moduli as a function of strain. Explants PD (a), PN (b), PM (c) and PB (d).

Firstly, it can be seen from all these graphs that the storage moduli E' are always greater than the loss moduli E''. This means that the skin is a material with an elasticity greater than its dissipation capacities.

This mechanical scanning deformation test is used to determine the linear viscoelastic domain (LVE domain) of the skin. For polymer materials, in the LVE range, the viscoelastic moduli are constant and independent of deformation. From a physical point of view, this implies that the condition of the observed system does not change during deformation: the effects of the orientation of macromolecular chains are negligible and do not modify the properties of the medium.
In Figure 4.6, between 1% and 18% strain, the general trend in viscoelastic moduli is a decrease with increasing strain. This means that as the elongation rate of the test increases, the global mechanical strength of the skin will decrease slightly. From these graphs, the linear viscoelastic domain of the skin does not appear to be present at these strain percentages. This linear domain should be present at strain rates below 1%. In fact, we can see that at around 1% strain, the viscoelastic moduli are almost constant. Above 2% strain, for all explants, the viscoelastic moduli slightly decrease with the strain rate.

This decrease in moduli may mean that the material is degrading for these deformations. This does not appear to be the case, as the explant retains its mechanical properties at the end of the tests. The most likely hypothesis is that the skin, being a soft organic material, adapts to the deformation imposed. During the first few stretches at a low rate of deformation, the fibre networks are initially stressed in the direction of stretching. During subsequent sinusoids, the fibres will gradually reposition themselves in the direction of load, releasing stresses and reducing the forces required to deform the skin.

From Figure 4.6, we can also note that for PN and PB skins, from 10% deformation, the storage modulus begins a phase of increase. This stiffening must be linked to the participation of collagen fibres in the overall mechanical strength of the skin. Indeed, according to the simple tensile tests (Figures 4.2 and 4.3), these two types of skin exhibit bilinear elastic behaviour with a J-shaped stress-strain curve.
The dynamic strain sweep tests therefore show differences in the viscoelasticity of the skin explants. As with the simple tensile tests, there are two types of dynamic mechanical behaviour for skin explants under extension. PD and PM skin explants exhibit the same dynamic mechanical behaviour over a wide range of deformations. PN and PB skin explants show the same general trend, but with more rigid storage moduli at large strains.

Analysis of the graphs in Figure 4.6 allows to measure the viscoelastic properties of all the explants, and in particular to calculate the modulus of elasticity, which are presented in the following Figure. Figure 4.7 shows the different storage modulus of the explants determined at different deformation percentages: 1%, 10% and 18% (possible deformations achievable with our equipment).

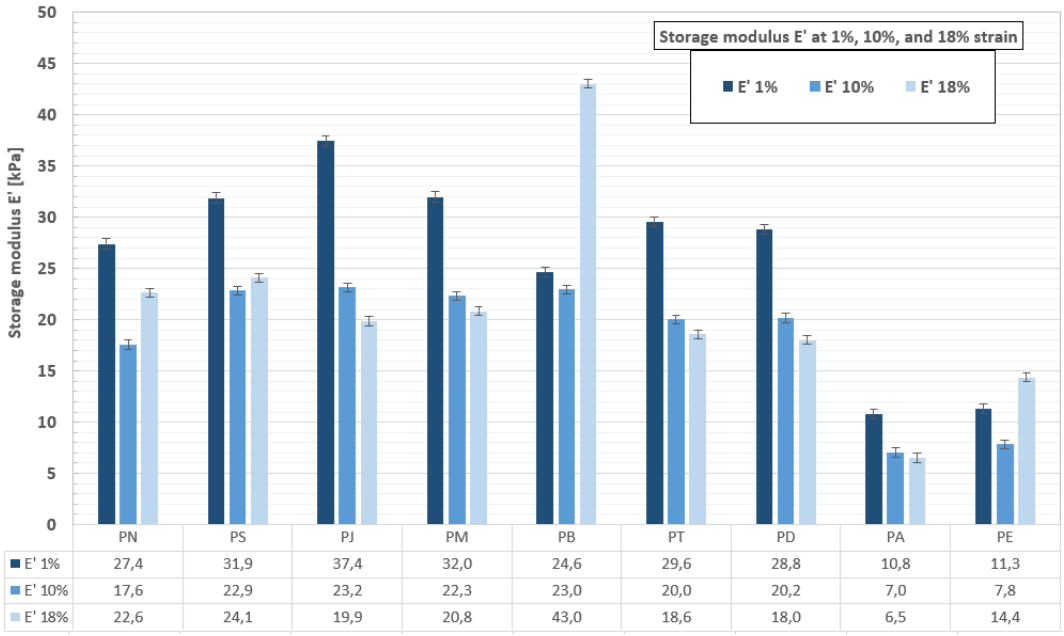

	PN	PS	PJ	PM	PB	PT	PD	PA	PE
E' 1%	27,4	31,9	37,4	32,0	24,6	29,6	28,8	10,8	11,3
E' 10%	17,6	22,9	23,2	22,3	23,0	20,0	20,2	7,0	7,8
E' 18%	22,6	24,1	19,9	20,8	43,0	18,6	18,0	6,5	14,4

Figure 4.7: Results of strain sweep tests on human skin explants. Storage modulus E' determined for each explant, at different percentages of deformation (Notes: without the PR test (not carried out) and with force sensor measurement uncertainties).

This graph clearly shows that, globally, the storage modulus E' decrease with the strain rate. As with the simple tensile tests, there are 2 different behaviours at high strains.
Contrary to the general trend of decreasing modules, PN, PB and PE skins experience an increase in their storage moduli at strains greater than 10%. For example, the storage modulus E' of the PB explant increases from (23.0 ± 0.5) kPa at 10% deformation to (43.0 ± 0.5) kPa at 18% deformation. Most of these skins also show this stiffening at high strains in simple tension. The two types of tests are therefore complementary and enable to highlight the mechanical contribution of the collagen fibre networks in resisting stretching.

Similarly, as shown in Figure 4.8, the loss factor of the explants was measured for the different strain rates.

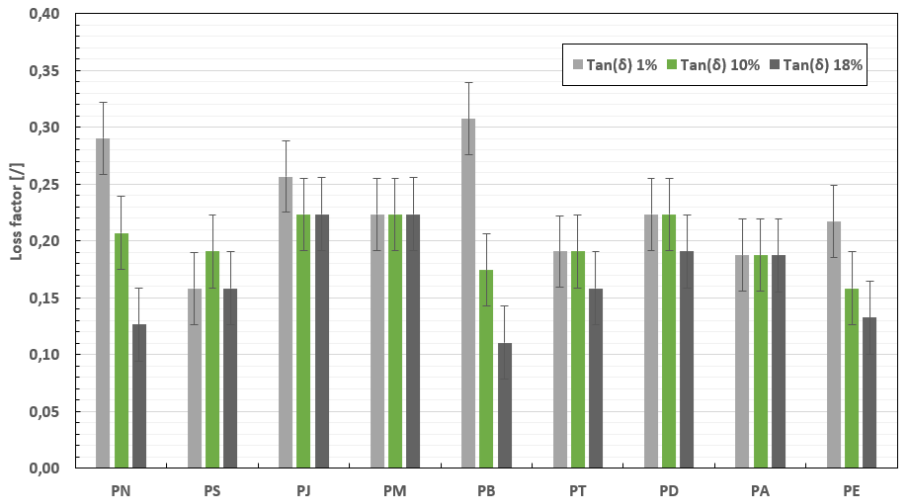

Figure 4.8: Results of strain sweep tests on human skin explants. Tangents δ measured for each explant, at different percentages of deformation (with force sensor measurement uncertainties).

The loss factor of the skin, named Tan(δ), quantifies the more or less viscous nature of the material for the conditions imposed, i.e., its capacity to dissipate energy. For all the explants, this factor is less than 1 (E' > E''). The loss factor for all the explants is between 0.10 and 0.30, demonstrating the preponderance of the elastic part in the mechanical behaviour of the skin (the closer the factor is to 0, the more elastic the material). The trend with deformation of the loss factor is stable for most skin samples investigated. It decreases for PN, PB and PE skins, which proves that the elasticity portion becomes more important for these skin explants as deformation increases.

Conclusions:

Strain sweep tests are dynamic tests that provide a complete energy analysis of human skin explants over a wide range of deformations. The viscoelastic behaviour of the skin is therefore clearly demonstrated with this mechanical test.

During stretching, the energy-conserving behaviour, represented by the conservation modulus E', is mainly due to the various fibre networks in the dermis, particularly elastin fibres at low deformations. The energy-dissipative behaviour, represented by the loss modulus E'', is probably due to the flow of fluid contained in the dermis' ground substance and to the sliding and reorganisation of the fibres, contributing to the dissipation of energy during deformation. The viscous aspect of the skin does not seem to be predominant at large deformations, at which the elastic component takes over the viscous component (involvement of collagen fibres, which are elastic and very rigid).

The dynamic results are consistent with the static results of the simple tensile tests. The linear viscoelastic domain of the skin determined in dynamics (constant viscoelastic moduli) as well as the linear elastic domain determined in traction (constant elastic modulus E_0), are found at deformations of less than 1%. The same applies to large deformations: a stiffening of the mechanical behaviour of the explants is visible in dynamics, with the storage modulus E' and in traction, with the apparent modulus of elasticity both increasing.

The fact that there is no marked linear viscoelastic domain in this range of deformation implies that the state of the observed system evolves slightly during deformation, certainly with changes in the localisation of the molecules and effects of the orientation of the macromolecular chains.

Note that the identification of the linear domain depends on the test frequency: an increase in this domain is visible as the frequency decreases. We could have reduced the frequency to try and find this linear domain, but as we had to carry out other tests on the explant and as we were working on a living material, we had to carry out each test relatively quickly.

4.1.3.B Frequency sweep test

The frequency sweep test consists of imposing sinusoidal deformations of constant amplitude and decreasing frequency on the material. This mechanical test is used to study the short- and long-term behaviour of the material properties. Typical results of this type of scan on skin explants are shown in Figure 4.9.

If possible, dynamic frequency sweep tests should be carried out in the linear domain. Therefore, the tests should be performed on the skin at a strain of less than 1%. However, given the sensitivity and the accuracy of the force sensors (accuracy of 1.8 mN which is not precise enough to make reliable measurements at less than 1% deformation), we decided to carry out these tests in the non-linear range of the skin: at 10% deformation. Measurement noise will be reduced and data accuracy will be much higher at this rate of deformation than at rates close to 1%. This deformation is therefore kept constant for all these tests.

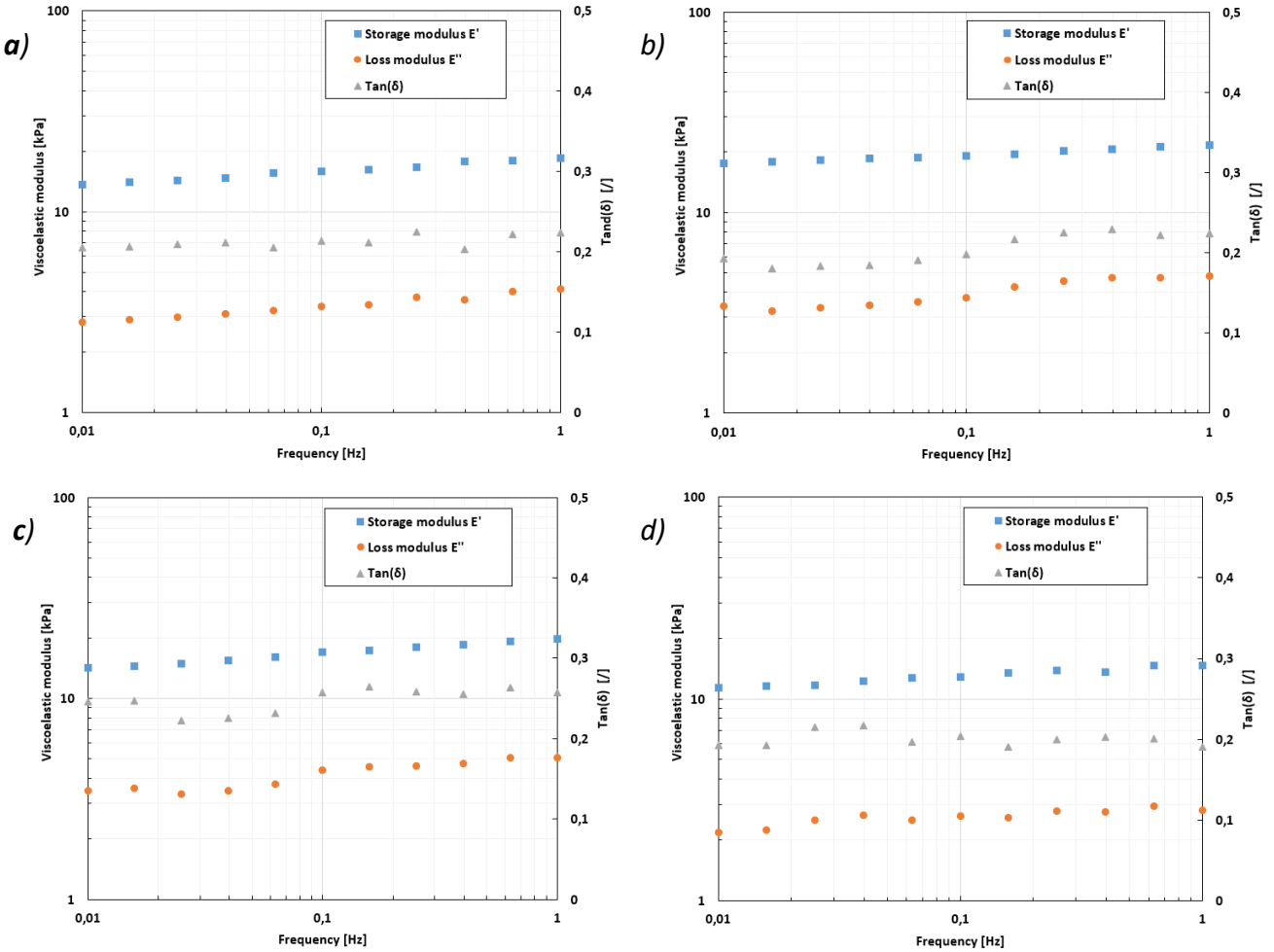

Figure 4.9: Results of frequency sweep tests on 4 human skin explants (strain = 10% - T = T_{amb}). Graphs of viscoelastic moduli, and loss factor, as a function of frequency. Explants PD (a), PJ (b), PM (c) and PN (d).

As with strain scanning, we can note that the storage modulus E' is greater than the loss modulus E'', whatever the frequency is, demonstrating the importance of the skin's elasticity properties.

In Figure 4.9, for all four explants, the storage modulus and the loss modulus increase with the frequency. The slope of the storage modules E' as a function of frequency is between 0.75 for PN skin and 1.30 for PM skin. The slope of the dissipation modules E'' as a function of frequency is between 0.14 for PN and 0.42 for PM.

This means that as the test frequency increases, the mechanical strength of the skin will also increase. Likewise, the higher the frequency, the faster the material must respond to deformation. The high-frequency data represents the short-term behaviour of the sample, where the local

displacements of the polymer chains are analysed. For these short loading times, little movement is possible within the material, the storage modulus is high and the skin behaves more rigidly.
Conversely, at low frequencies, the data reflect the long-term behaviour of the sample properties, where the global displacements of the polymer chains are taken into account. The lower the frequency, the greater the response time of the skin; the fibre networks are stressed on a larger scale. When the loading time is longer, the sample has more time to react to the deformation and local movements of the chain become possible. Viscoelastic moduli are lower due to the adaptation of the tissue, and in particular the fibre networks in the dermis, to relatively slow deformations.

Frequency sweep tests show little difference in terms of viscoelasticity of the skin explants. Unlike the tensile tests, only one type of dynamic mechanical behaviour can be distinguished in this loading mode, with the general trend of viscoelastic moduli increasing with frequency.

Analysis of the graphs in Figure 4.9 allows to measure the viscoelastic properties of all the explants, and in particular to calculate the modulus of elasticity, which are presented in the following figure. Figure 4.10 shows the different storage modulus of the explants determined at different test frequencies: 0.01Hz, 0.1Hz and 1Hz (frequencies achievable with our system).

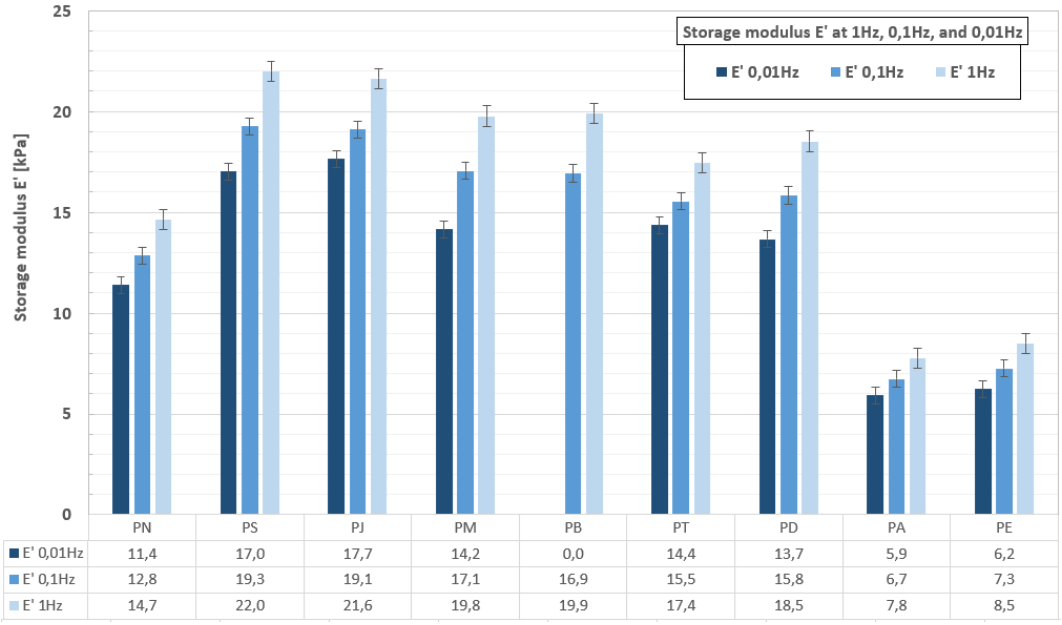

	PN	PS	PJ	PM	PB	PT	PD	PA	PE
E' 0,01Hz	11,4	17,0	17,7	14,2	0,0	14,4	13,7	5,9	6,2
E' 0,1Hz	12,8	19,3	19,1	17,1	16,9	15,5	15,8	6,7	7,3
E' 1Hz	14,7	22,0	21,6	19,8	19,9	17,4	18,5	7,8	8,5

Figure 4.10: Results of frequency sweep tests on human skin explants. Storage modulus E' determined for each explant, at different frequencies (Notes: without the PR test (not carried out) and with force sensor measurement uncertainties).

This graph clearly shows that the modulus of conservation E' increase with the frequency of loading. For all the skin samples, it is this single overall mechanical behaviour of stiffening with frequency that stands out in these analyses.
It can also be seen that the viscoelastic moduli are practically the same in strain sweep (Figure 4.7) and frequency sweep (Figure 4.10) when the test conditions are almost similar: same deformation rate of 10% and test frequency of 0.1 Hz for frequency sweep and 0.5 Hz for strain sweep. These two types of tests are therefore complementary and allow an overall energy analysis of the skin under two different types of dynamic loading.

Similarly, as shown in Figure 4.11, the loss factor of the explants was measured for different frequencies.

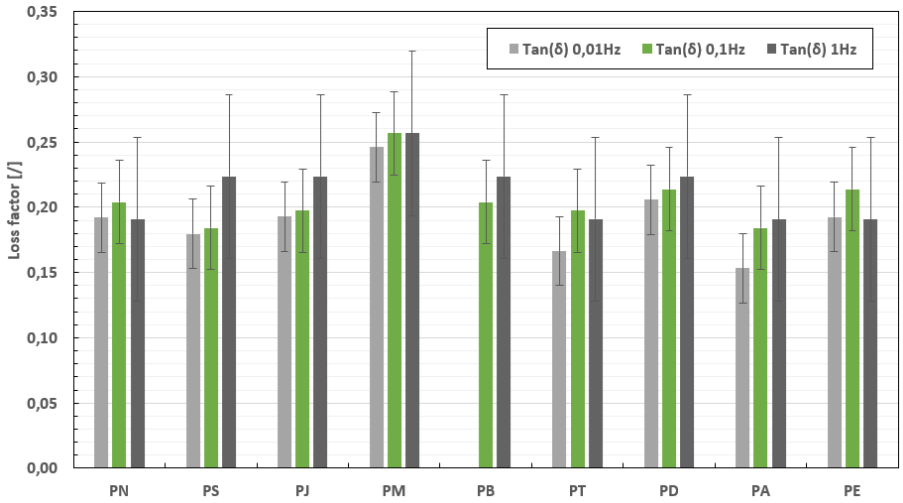

Figure 4.11: Results of frequency sweep tests on human skin explants. Tangents δ measured for each explant, at different frequencies (with force sensor measurement uncertainties).

For all the explants, the loss factor of the skin, named Tan(δ), seems to be constant at the different frequencies (the standard deviation being large compared to the results, this does not allow to affirm a possible increase in the loss factor with frequency). This means that the proportion of elasticity and viscosity remains relatively stable at the different test frequencies, as for an elastic network (like a gel). As the frequency increases, the elasticity part, and the loss one both increase in equal proportions.
It should also be noticed that this factor is less than 1, confirming that the skin is a solid viscoelastic material (E' > E''). The loss factor for all the explants is between 0.15 and 0.25, demonstrating the preponderance of the elastic part in the mechanical behaviour of the skin.

Conclusions:

Frequency sweep tests are dynamic tests that provide a complete energy analysis of human skin explants over a wide range of load frequencies. The viscoelastic behaviour of the skin is clearly demonstrated in this mechanical test.

As the frequency increases, the conservation modulus E', representing energy-conserving behaviour, and the modulus E'', representing energy-dissipative behaviour, increase slowly (see Figure 4.10). As the modulus E' increases with the frequency, the skin becomes stiffer.

It should also be noted that, even though the tests were not carried out in the linear viscoelastic domain of the skin, the results appear to be consistent and are similar to the results of DMA carried out on polymer materials (increase in the modulus E' with the excitation frequency) [Sangroniz *et al.*, 2023].

4.1.4 Loading-unloading cycles

This mechanical test involves stressing the material by imposing loading-unloading cycles. These cycles are used to assess the skin hysteresis phenomenon. Typical results of this cyclic loading-unloading test on skin explants are shown in Figure 4.12.
All the skin samples tested and characterised in this loading mode show this type of mechanical behaviour. These graphs are therefore representative of the mechanical behaviour of *ex vivo* human skin explants during loading and unloading.

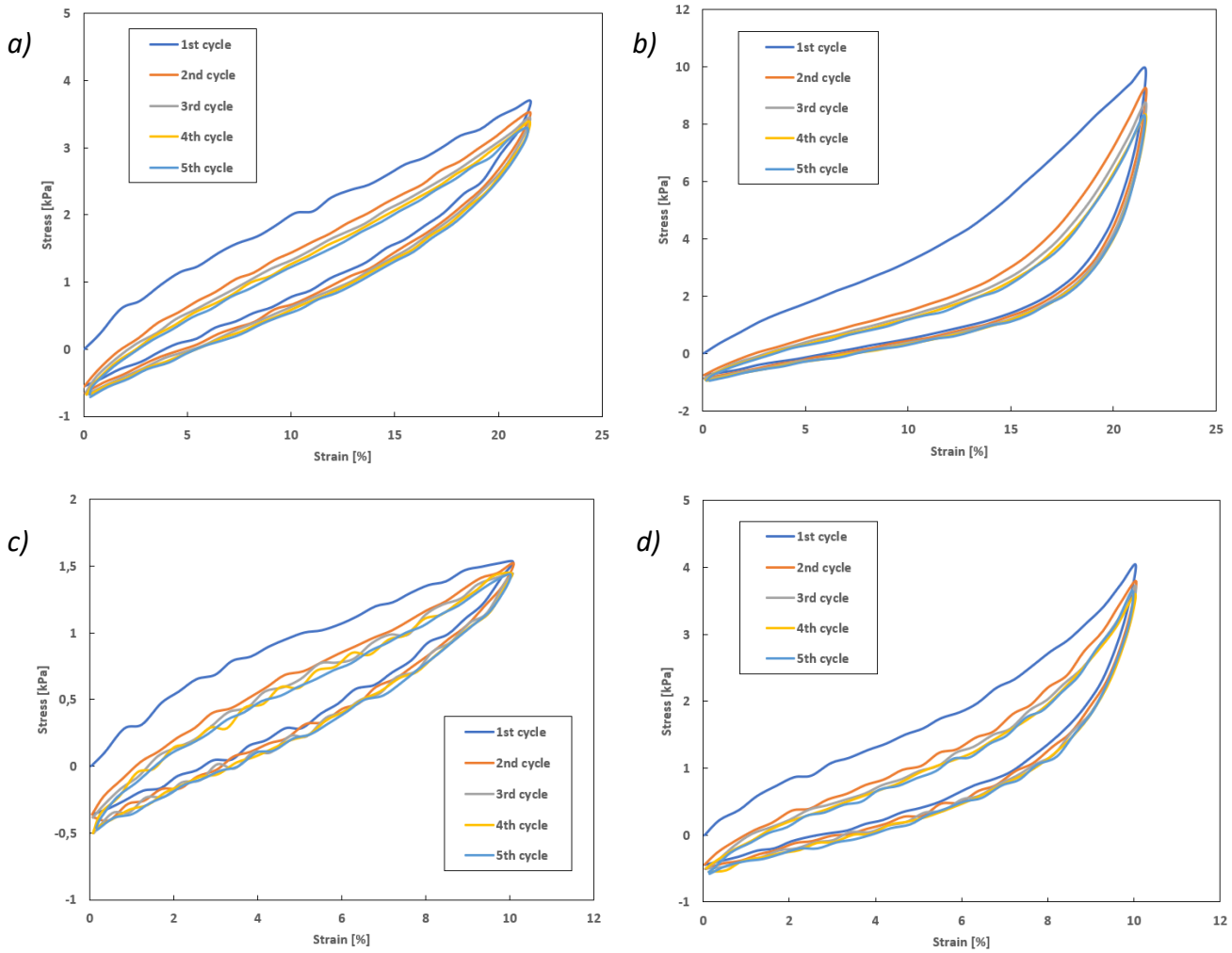

Figure 4.12: Results of cyclic mechanical loading-unloading tests on 4 human skin explants (def = 10% or 22% / speed = 10 mm.min^{-1}). Stress versus strain graphs. Explants PA (a), PE (b), PT (c) and PR (d).

These load-unload cycles make it possible, firstly, to evaluate and observe the stability of the mechanical behaviour of the skin and, secondly, to evaluate the phenomenon of hysteresis in the skin. Figure 4.12 shows for each skin the evolution of the dissipated energy as a function of the load-unload cycle, and gives examples of superimposed curves for five cycles.

Firstly, it can be noted that these graphs confirm the results of the preliminary study on the pre-conditioning of skin explants (see Part 3.1): the mechanical properties are stabilised at the 5th cycle. In fact, the stabilisation of the mechanical behaviour of the explants occurs during the first cycles, when the energy dissipated is reduced and stabilised.

The hysteresis phenomenon in skin explants is therefore represented by this difference between the effort measured during loading and the effort measured during unloading. The hysteresis cycle shows that the skin needs more force during an extension stress than during a contraction stress. When the skin is mechanically repositioned to its original position, it requires less force to relax. Energy is therefore dissipated between these two phases. The hysteresis phenomenon will be more or less marked but will always be present for skin explants, as for rubber [Diani *et al.*, 2009].

Analysis of the graphs in Figure 4.12 allows to measure the viscoelastic properties of all the explants, and in particular to calculate the mechanical energy dissipated during a loading-unloading cycle, which is presented in Figure 4.13 below. The dissipated energy is calculated at the 5th loading-unloading cycle so that the mechanical behaviour of the explants is stabilised (notion of pre-conditioning).

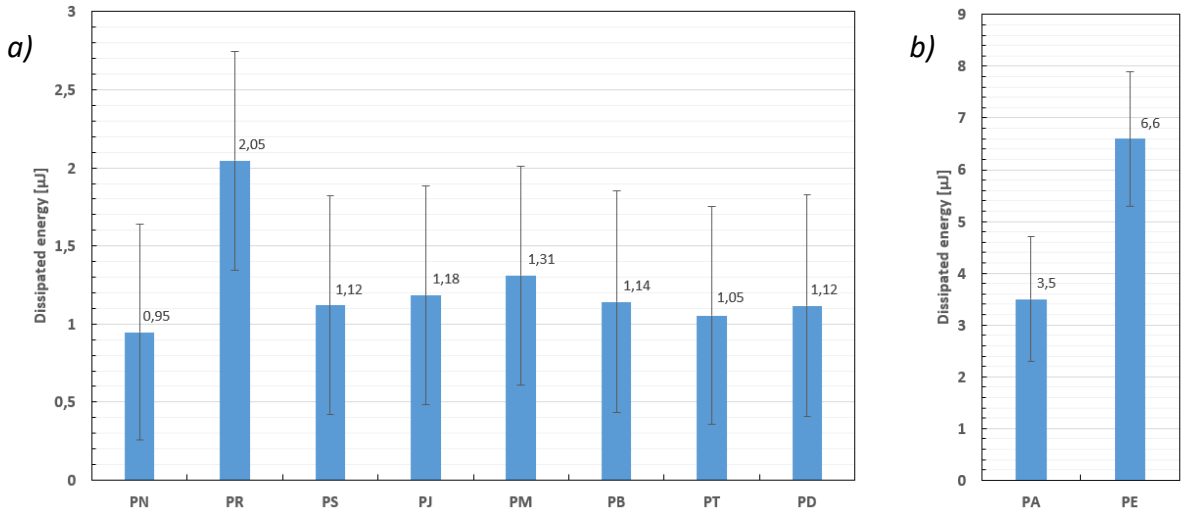

Figure 4.13: Results of cyclic mechanical loading-unloading tests on human skin explants. Mechanical energy dissipation during cycles, determined for each explant (with force sensor measurement uncertainties). a) Explants whose cycles reach 10% deformation. b) Explants whose cycles reach 22% deformation.

For cyclic loading of the skin, energy is dissipated in the form of heat. As described in Part 2.2.3, the amount of mechanical energy dissipated corresponds to the area between the loading phase and the unloading phase (Figure 4.12). It is the difference between the energy used during skin extension and the energy restored by skin relaxation.

For our skin explants, the energy dissipated during the cycles is between 1 and 7 µJ. The results in Figure 4.13 show that the skin explants PR, for a cyclic deformation of 10%, and PE, for a cyclic deformation of 22%, dissipate more energy during cycles than the other explants. A link can be made with the simple tensile tests because these two explants have a bilinear mechanical behaviour in extension. This mechanical behaviour allows the skin to respond to deformations with greater stress, which means that the skin stores more energy, some of which can potentially be dissipated. All the other explants dissipate roughly the same amount of energy during cycles.

Conclusions:

Under cyclic loading and unloading, viscoelastic materials such as skin exhibit hysteresis, which leads to dissipation of mechanical energy. The energy dissipated over a complete cycle is proportional to the area inside the hysteresis loop.

As seen in Part 3.1, from the second cycle onwards, the mechanical behaviour of the explant is more or less constant, before stabilising completely around the 5th cycle. This phenomenon is due to the viscoelastic behaviour of the skin, and can be linked to the friction forces between the fibres.
At relatively low strain rates (10% in our case), there is little difference in terms of energy dissipation. However, when strain rates are higher, and when the linear or bilinear mechanical behaviour of the skin in extension starts to become visible, differences are visible in terms of energy dissipation.

4.1.5 Stress relaxation test

The stress relaxation test consists of applying a constant instantaneous deformation to the material over a period of time and to subsequently measure the relaxation of the stress. It is used to characterise the viscoelasticity of the material. Typical results of this stress relaxation test on skin explants are shown in Figure 4.14. All the skin explants tested and characterised in this stress mode show this type of mechanical behaviour. These graphs are therefore representative of the mechanical behaviour of *ex vivo* human skin explants when they are maintained under constant tension.

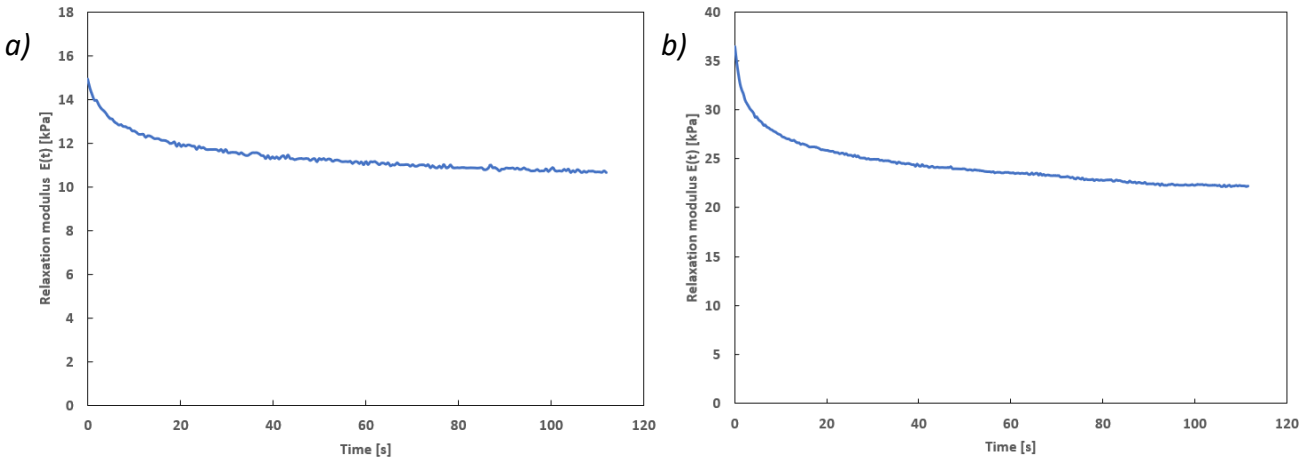

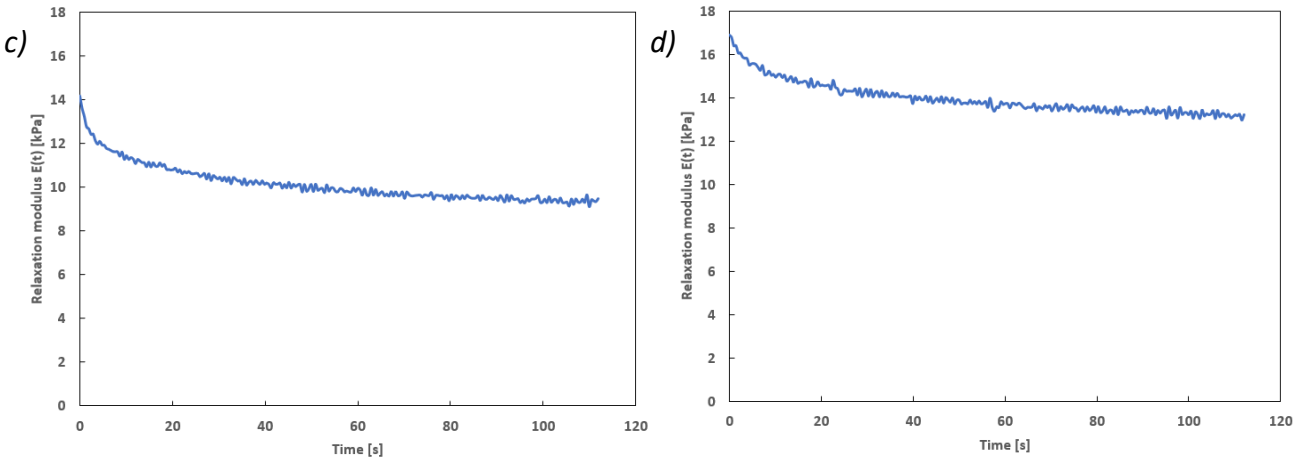

Figure 4.14: Results of mechanical stress relaxation tests on 4 human skin explants (Parameters: tension = approx. 2 min / strain = 18%). Graphs of relaxation modulus $\frac{\sigma(t)}{\varepsilon_0}$ as a function of time. Explants PA (a), PE (b), PM (c) and PJ (d).

When the deformation of the material is kept constant, due to its viscoelastic nature, the skin dissipates energy to gradually return to a more stable state. Figure 4.14 shows that the stress in the skin, linked to the relaxation modulus, will decrease over time until it reaches a plateau: this is the stress relaxation phenomenon.

Relaxation is a non-instantaneous property: it needs a certain amount of time that the stress reaches its final value. From the first few seconds of being held under tension, until around 30 seconds, the skin relaxes rapidly. The skin then relaxes slowly and progressively over time. We observe a relaxation of the effort, the stresses in the skin are eliminated, so that the skin gradually returns to a more stable state.

Analysis of the graphs in Figure 4.14 enables to measure the viscoelastic properties of all the explants, and in particular to calculate the relaxation rates, which are presented in Figure 4.15 below.

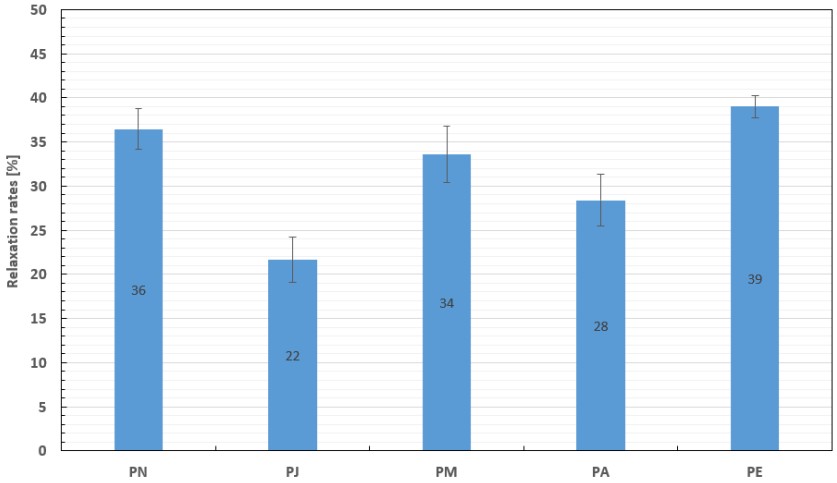

Figure 4.15: Results of mechanical stress relaxation tests on human skin explants. Relaxation rates, for 2 minutes of tension, determined for each explant (Notes: Only these five explants were characterised in this loading mode – Results with force sensor measurement uncertainties).

This graph clearly shows the differences in relaxation between the explants. For all the skin samples investigated, and within these precise test parameters (strain = 18% and time = 2 min), the relaxation rate was between 20 and 40%.
The PE, PN and PM skins showed the highest relaxation rates. A link can be made between these results and the results in simple tension: the PE and PN explants have a bilinear elastic behaviour in simple tension, and it is these two explants that relax the most mechanically when they are under tension. We can therefore assume that when the collagen fibres are stressed when the skin is held under tension, they will reorient themselves along the axis of tension but will also be able to relax and allow the explants to return to a more stable state of tension. The fibres slide in relation to each other in the matrix.

Relaxation involves the notions of resistance to flow and viscosity. The rate of relaxation can be correlated to the percentage of viscous dissipation within the material. The more the skin relaxes by releasing stress, the more energy will be dissipated.

Conclusions:

In contrast to dynamic loading, the mechanical test here consists of imposing a transient and static load on the explants. Due to its viscoelastic nature, the skin dissipates energy and gradually returns to a more stable state.

To provide a physical explanation for the phenomena observed, we can assume that macroscopic relaxation reflects microscopic changes in the configurations of the macromolecular chains that are the fibres in the material. Viscoelastic phenomena originate from the possibility of intra- or intermolecular movements of the chains to return to a position of statistical equilibrium.

4.1.6 Conclusion on the characterisation of *ex vivo* skin mechanical properties

This Section presented all the mechanical tests that can be carried out with our equipment. In addition to the classic tensile mechanical tests, widely used in the scientific literature, we have provided a new vision by measuring the overall rheological properties of the skin, and in particular by taking into account the dissipation parameters, which have been little or not reported in the literature. To the best of our knowledge this enables us to carry out an energy analysis that has never been reported.

Explants from different donors were characterised using our equipment. These explants have the intrinsic physiological characteristics of their donor, which means that each explant has its own mechanical behaviour. The results of the various mechanical tests on all the explants are summarised below.

Firstly, the tensile tests revealed two types of mechanical behaviour of the explants in extension: linear elastic behaviour and bilinear elastic behaviour (J-shaped stress-strain curve). This means that for deformation rates of less than 20%, some explants have a mechanical behaviour that stiffens

under the effect of extension. The PE, PB, PR and PN explants have this kind of bilinear mechanical behaviour. They deform little under stress and can be considered as rigid explants. It can also be concluded that they have a low capacity for elastic extension because the second part of the extension curve appears at relatively low deformations, between 10 and 15%. The other explants show a linear elastic mechanical behaviour. They therefore have a high capacity to deform under stress while returning to their initial configurations. These explants therefore have a large linear elastic range and can be considered highly elastic (but less rigid).

Next, mechanical tests using dynamic spectrometry were used to assess changes in the storage modulus E', representing the elastic part of the skin, and the loss modulus E'', representing the viscous part of the skin, over a wide range of deformations or frequencies. These tests demonstrate the viscoelastic behaviour of skin explants. In strain sweep, for all the explants, the two viscoelastic moduli decrease with increasing deformation rate. For the tested deformation range, there does not appear to be a linear viscoelastic domain. For explants with bilinear tensile behaviour, the conservation modulus at large deformations increases, demonstrating the stiffening effect of the skin. In frequency sweep, for all the explants, the two viscoelastic moduli increase with the test frequency. The faster the skin is stressed, the greater its mechanical response.

Finally, cyclic loading-unloading and stress-relaxation tests were used to assess the skin's energy-dissipative behaviour. The cyclic tests reveal the hysteresis phenomenon of the skin, with dissipation of mechanical energy between the loading and unloading phases. Stress relaxation tests highlight the dissipation of energy to gradually return to a more stable state when the skin is maintained under tension.

The results of these different tests are complementary and consistent. A skin like PE exhibit a bilinear elastic behaviour in simple tension. Dynamically, its storage modulus increases at large deformations, confirming the stiffening of the explant. This explant therefore stores more energy during deformation, which means that a large proportion of its energy is dissipated during stress relaxation and cyclic testing.

4.2 Study on the viability[15] of *ex vivo* skin explants

Introduction:

In general, skin explants removed during surgery or biopsies can maintain their integrity and functionality for a limited period of time, generally from a few hours to a few days, depending on storage and handling conditions. However, it should be noticed that the viability of skin explants gradually decreases over time, due to the deprivation of blood supply and the lack of interaction with body cells. Researchers working with *ex vivo* skin explants must carefully monitor their condition and functionality throughout the experiment.

Three techniques are commonly used to assess the quality and viability of skin explants: histological staining, assessment of cell proliferation and apoptosis, and cytotoxicity tests [Lebonvallet *et al.*, 2010]. However, to our knowledge, there is currently no technique for assessing the viability of explants in terms of their mechanical properties. To the best of our knowledge, no specific data on this subject has been reported in the public scientific literature. Consequently, to date, it has not been established whether ex-vivo skin explants retain their mechanical properties throughout their survival period.

In previous studies, the mechanical properties of *ex vivo* skin explants were determined at a given time, within a week of surgery. But do these properties vary over the course of the explant's survival? This Section will enable to answer this question and study the viability of the explants over time, in terms of their mechanical properties. The aim is to show that Eurofins BIO-EC skin explants are kept alive for more than 7 days. Ideally, the mechanical properties of the explants should be constant throughout their survival. Moreover, the same time is announced by other suppliers as *Genoskin* for example.

Methodology and results:

The day of the operation, when the skin is extracted from the donor patient, is known as D0. The skin is considered fresh because it has just left the living organism. The Eurofins BIO-EC laboratory recovers this skin plasty, treats it and prepares *ex vivo* skin explants. As described in Part 2.3, Eurofins BIO-EC has developed an *ex vivo* human skin model based on keeping explants alive for 10 to 12 days. In order to maintain the survival of the *ex vivo* skin explants, they will be placed under culture conditions in an incubator and in contact with a specific nutrient. The next day is considered to be D+1, the day after D+2, and so on.

Ideally, to accurately monitor its mechanical properties, the explant should be tested every day. However, it is very difficult to carry out daily monitoring of the explants, due to the many other parallel studies and weekends. In our study, the explants were monitored from day D+1 to day D+9, with several survival times between tests.

[15] By 'viability', we mean that the conservation technique enables the preservation of a normal morphology, structure, and metabolism. In fact, this technique enables us to work in conditions very close to the real skin physiology, with the entire cell population and their communications remaining active. Various companies have developed this type of technology in France (Eurofins BIO-EC, Genoskin).

Figure 4.16 shows the results of the study of the viability of skin explants *ex vivo*. This Figure shows the evolution of the mechanical properties of two explants over time.

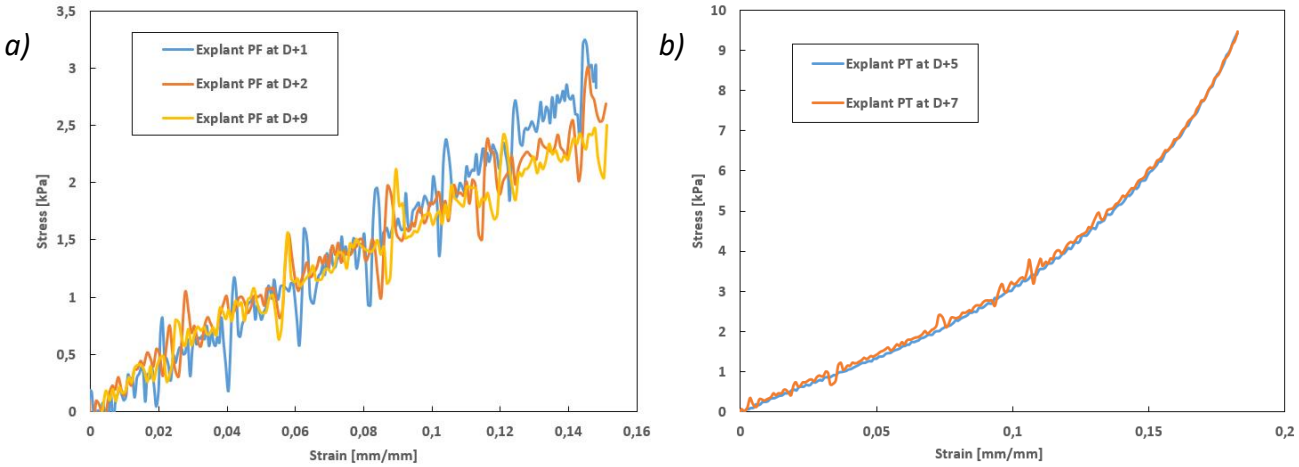

Figure 4.16: Study on the survival of skin explants over time - tensile tests. a) PF explant tested at D+1, D+2 and D+9 (explant from the first study at Eurofins BIO-EC: P1000-AB43). b) PT explant, tested at D+5 and D+7.

The study in Figure 4.16.a was carried out during the first experiments on human skin with the previous configuration of the equipment (see Part 2.1.1). The noise of the measurements is significant but this first test showed that after 9 days of survival, the skin explant had the same general mechanical behaviour.

As shown in Figure 4.16.b, these results were further confirmed with the new configuration of the equipment (see Part 2.1.3). The tensile mechanical properties are almost identical during the survival of this explant. At D+5 and D+7, the explant had the same elastic behaviour and the same apparent moduli of elasticity. Two days apart, an *ex vivo* explant can therefore retain its mechanical properties in extension.

In order to confirm these first results, a more detailed test, presented in Figure 4.17, was carried out on another skin explants, taking into account their viscoelastic properties.

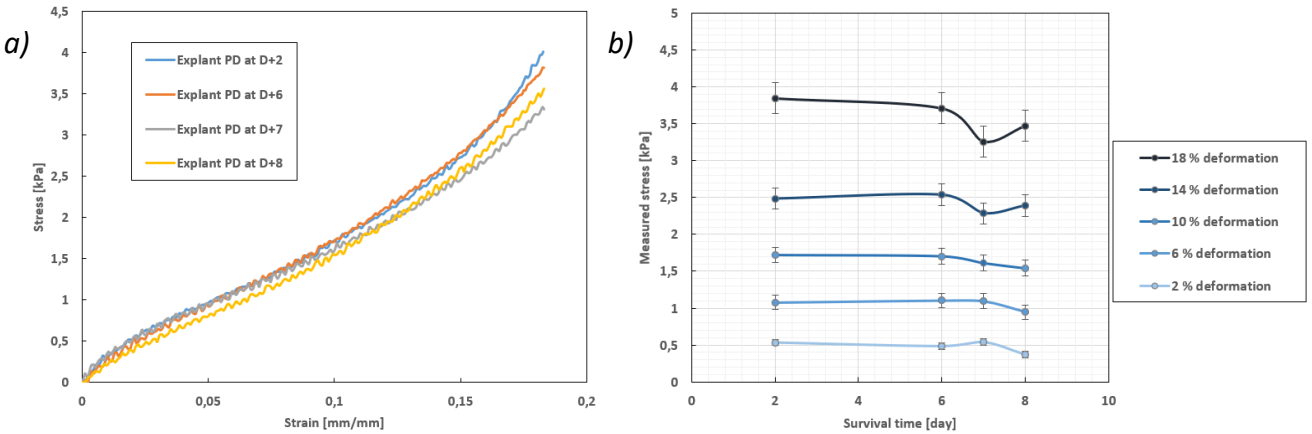

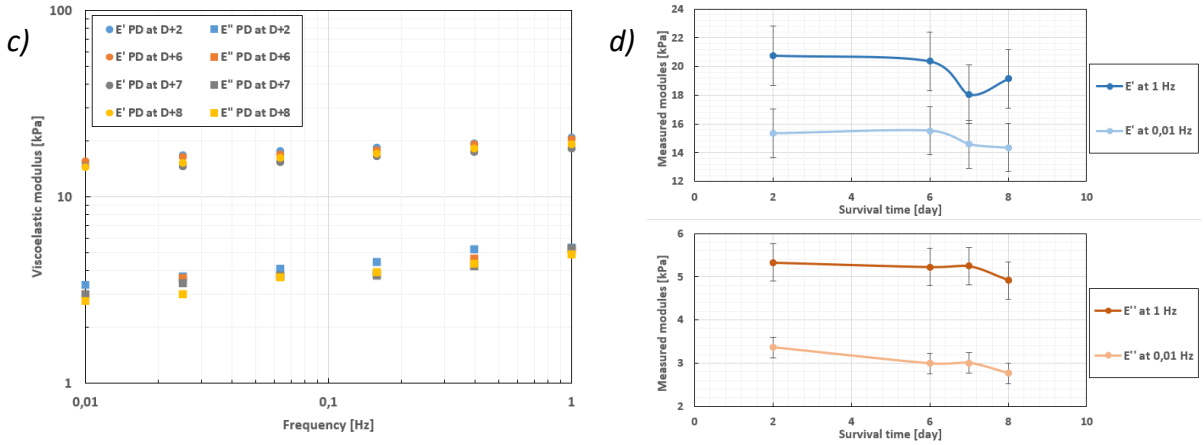

Figure 4.17: Study on the survival of a skin explant over time: PD explant, tested at D+2, D+6, D+7 and D+8. a) Tensile curves. b) Graph representing the value of the stress measured as a function of the survival time of the explant, and according to different percentages of deformation (Standard Deviation of the reproducibility tests). c) Frequency sweep curves (def = 10%). d) Graphs showing the values of viscoelastic moduli measured as a function of explant survival time, and at different frequencies (SD of reproducibility tests).

Firstly, Figure 4.17.a shows that the tensile mechanical properties are almost identical when the explant is kept for more than 7 days. The trend in the stress-strain curves is the same over time. The general elastic behaviour of the explant therefore remains the same; only a slight decrease in the measured stresses is visible, from (3.9 ± 0.3) kPa to (3.5 ± 0.3) kPa at 18% strain (Figure 4.17.b).

Dynamic analysis allows to observe variations in the viscoelastic properties of the explant over time (Figure 4.17.c). The tests show that these properties hardly change over time. Indeed, Figure 4.17.d, representing the evolution of the viscoelastic moduli over time, shows that they vary slightly, from (21 ± 2) kPa to (19 ± 2) kPa for the storage module E' at 1 Hz. There is a slight tendency for the moduli to decrease. This decrease in moduli does not seem significant given the standard deviation of the reproducibility tests carried out on explants. The skin therefore retains its elasticity as well as its viscosity. During the first 6 days of survival, the explant appears to have the same general viscoelastic behaviour. After one week of survival, a slight decrease in the mechanical properties of the explant was observed.

Conclusions:

This study enabled to examine the viability of the explants over time, in terms of their mechanical properties. According to our experiments based on the examination of three skin explants, the mechanical response of the skin, in traction and dynamics, is nearly identical over time. Indeed, there is no profound change in the elongation behaviour of the explant: the mechanical trend is the same.

Analysis of the viscoelastic moduli and stresses measured as a function of the explant's survival time shows that its viscoelastic properties vary very little. One week after surgery, the skin's properties remain almost unchanged. As shown in Figure 4.17, after approximately 7 days of survival, we observe a slight reduction in the mechanical properties of the explant.

For in-depth studies requiring daily monitoring, it can be cautiously assumed that the mechanical properties of explants kept alive are preserved over time. For a survival period of less than a week, the mechanical properties are correctly preserved. For a period of more than a week, there is a risk of a slight reduction in the mechanical properties of the explant.

Particular attention must be therefore paid to the survival time of the explant in the conditions of preservation established by Eurofins BIO-EC. As far as possible, in order to limit variations in mechanical properties, tests on fresh explants, which are maintained in physiological like conditions, should be carried out during the week following surgery. Tests carried out following surgery and over a two/three-day period can therefore be considered similar in terms of mechanical properties. This is a positive point which is important for the rest of our studies and in particular for monitoring stressed skin (Chapter 5).

4.3 Study of the variability of mechanical properties within the same plasty

In addition to the variability of living organisms, studied by exploring the mechanical properties of explants from different donors (Part 4.1.1), the mechanical properties of a single donor are studied here.

In this Section, several explants were taken from the same skin plasty (a single donor). The explants were removed from different parts of a plasty measuring approximately 20 cm^2. The aim is to test and compare these explants to see if they have the same mechanical properties.

Even though they come from the same donor, Figure 4.18 shows that it is possible for the mechanical properties of the explants to vary depending on where they are taken from within the plasty.

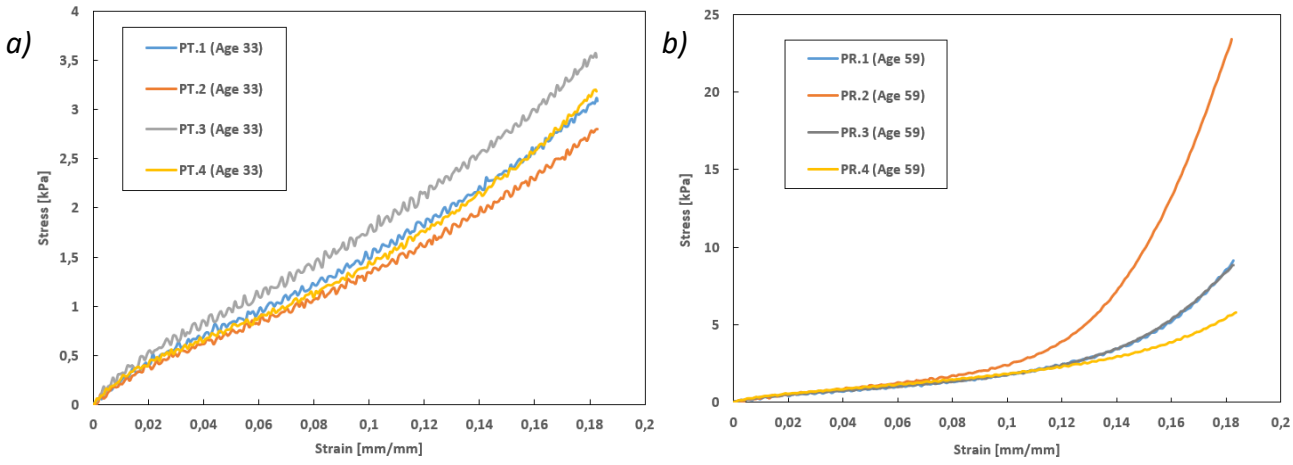

Figure 4.18: Results of tensile tests on 4 explants from the same human skin plasty (from the same donor). Intra-donor variation in mechanical properties. Skin PT (a) and skin PR (b).

For some skins, such as the PT skin in Figure 4.18.a, the mechanical tensile properties are relatively similar within the same plasty. In contrast, within the PR skin plasty, the explants may have different mechanical properties, as shown in Figure 4.18.b. The PR.1 and PR.3 explants have the same properties but their mechanical behaviour is different from that of the PR.2 or PR.4 explants. This is known as intra-donor variability, and also involves the notion of anisotropy (see Part 3.7). As the mechanical tests are unidirectional, the anisotropy of each explant is taken into account.

Conclusions:

Within the same skin plasty, which therefore comes from the abdomen of a single donor, the mechanical properties may differ. This is known as intra-donor variability.

The comparison of the mechanical results of different explants is therefore difficult to accurately interpret because of this intra-donor variability but also because of the anisotropy of the skin. Intra-donor variability, as well as the anisotropy of the mechanical properties of skin, which is an intrinsic skin property, can therefore significantly influence the mechanical properties of explants from the same donor.

This example therefore shows the potential difficulty of obtaining "average" mechanical properties that would be representative of the mechanical behaviour of a certain skin. Subject to the possible discrepancies observed in this study, a comparison of the mechanical properties of explants of different ages has been carried out in the following section.

4.4 Comparison of the mechanical properties of skin of different ages

As presented in Part 4.1.1, each explant has its own elongation behaviour and therefore its own mechanical properties. The fact that the mechanical results of the explants differ is due to the variability of the living organism. Because of their sex, age, origin and lifestyle, every human being has its own skin characteristics. The multitude of donors for our studies will give a multitude of results. Each donor's skin has its own mechanical characteristics.

One of the main factors affecting the mechanical properties of the explants is the age of the donors. Indeed, the advancement in time and the life history of the tissue influence its mechanical behaviour; behaviour linked to the structure of the skin and more specifically to the properties of its fibrous network (preferred orientation and density of the fibres).

The effect of ageing on the mechanical properties of the skin is described in detail in Part 1.2.2. Natural ageing is manifested by a reduction of the general metabolism, which leads to a decrease in synthesis and therefore in the density of the collagen and elastin proteins which compose the underlying skin fibre network. The skin's natural tension decreases and the fibres gradually follow

their preferred orientation, making the anisotropy more pronounced. This multitude of structural modifications manifests itself in a reduction in skin elasticity with age.

Methodology and results:

In this Section, mechanical tests on different explants from different donors are compared. The experimental conditions are controlled and kept constant for all the tests. More specifically, the preparation of the explants, the working environment and the mechanical test parameters are identical for all the tests.

As a reminder, all the *ex vivo* skin samples tested in this study came from female donors, none of whom had any skin disease. In addition, all these explants also come from the same area of the human body: the abdomen.
To carry out this comparative study, we therefore sought to isolate the main intrinsic factor in the skin that influences its mechanical behaviour: age. The aim here is to observe and evaluate the differences in mechanical properties of skin from donors of different ages.

The tested explants come from donors who are generally between 25 and 70 years old. To provide a framework for our analysis in this Section, in general and arbitrary terms, 'young' skins are considered to come from a donor aged between 25 and around 40; in contrast, 'old' skins are considered to come from a donor aged between around 55 and 70. When the mechanical tensile properties of all the explants tested previously are compared, we can note variable results as observed in Figure 4.19.

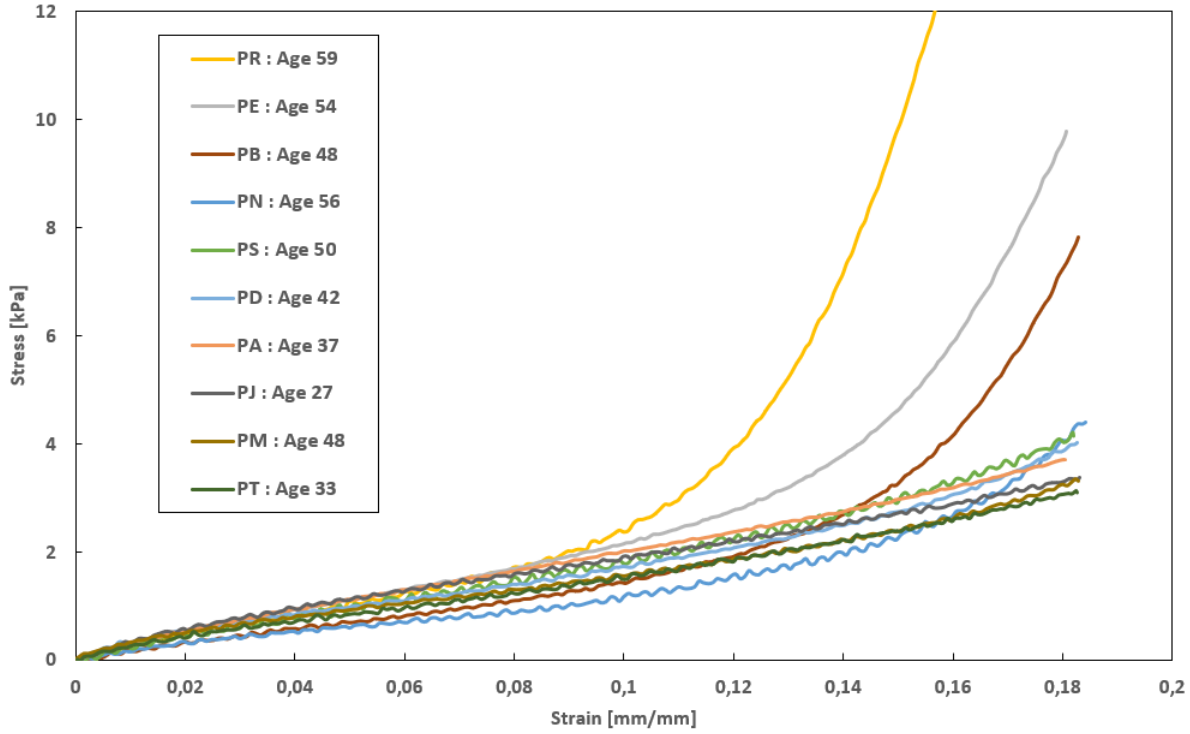

Figure 4.19: Results of tensile tests on all human skin explants (speed = 10 mm.min^{-1}). Stress versus strain graph.

From Figure 4.19, a trend in the mechanical behaviour of explants as a function of age emerges. In fact, the older the skin, the earlier the hardening phase in its behaviour (J-shaped curve) appears during deformation. In the limit of the window of the measured parameters, it can be noted that the skins showing bilinear elastic behaviour (PR, PE, PB and PN) are all older, around fifty to sixty years. Conversely, the younger skins (PA, PJ, and PT) reveal a linear elastic behaviour in tension. However, as the scientific literature shows, this stiffening of the mechanical behaviour of young skins is also present, but at higher levels of deformation (which our measuring device cannot achieve).

From Figure 4.19, we have tried to draw a master curve of the skin's mechanical tensile properties as a function of age (master curve as in Part 3.6). We want to demonstrate whether it is possible to construct a master curve that no longer takes age into account, with the aim of predicting the mechanical properties of human skin in the future and in the past as a function of its current mechanical behaviour. In this way, we propose a line of thought and a method of analysis based on the adjustment of the deformation and stresses of the curves as a function of age, with the aim of obtaining a master curve. The results of these different translations are shown in Figure 4.20.

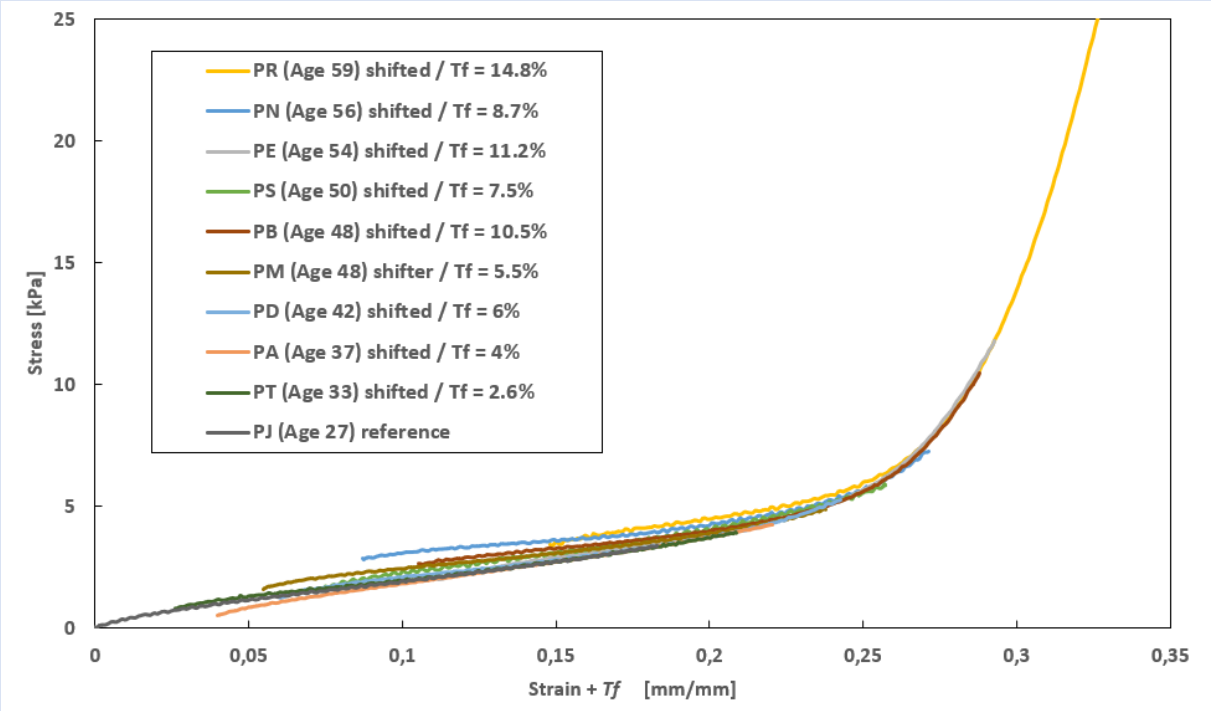

Figure 4.20: Translation of stress-strain curves of skins of different ages in order to establish a master curve (Tf = translation factor). Horizontal and vertical translation of curves having different mechanical behaviour.

The transition zone between the 2 linear behaviours of the tensile curves is taken into account as the reference zone for shifting the curves. The translated tests appear to form a general trend in the mechanical behaviour of the explants.

From this master curve, we extracted information on the strain translation factors, which we represented as a function of the age of the explants (Figure 4.21). This translation factor appears to follow a linear relationship with the age of the skin. The coefficient of determination of the trend curve is 0.96.

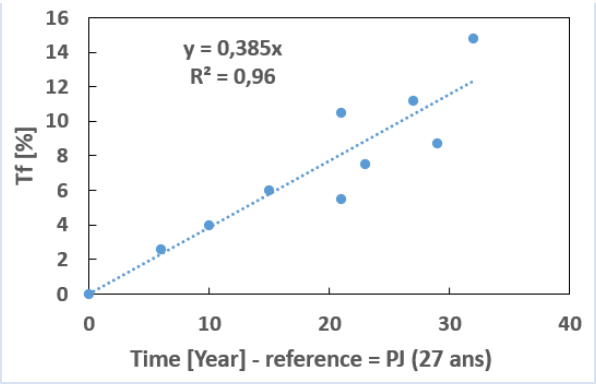

Figure 4.21: Strain translation factor Tf as a function of skin age (with 27-year-old PJ skin as the reference skin).

In conclusion, according to the analysis we propose, it seems possible to obtain a single curve to describe the mechanical tensile properties as a function of age. This approach should be analysed with caution, and should be consolidated with other results.

Comparing the mechanical results of different explants is difficult to interpret because of the anisotropy of the skin and the intra-donor variability (see Part 4.1.3). This anisotropy, an intrinsic property of the skin, is present in all explants and can cause its mechanical properties to vary significantly depending on the direction in which the test is applied (see Part 3.7). As a result, the mechanical test carried out and presented in Figure 4.19, which characterises an explant, may not be representative of the "average" mechanical properties of this explant. It is therefore difficult, using a single mechanical test, to differentiate clearly properties according to the age of the donor.

However, if we isolate 3 explants of different ages, we can distinguish a difference in terms of general mechanical behaviour. The results of mechanical tests on explants PN (56 years old), PM (48 years old) and PJ (27 years old) are shown in Figure 4.22 for comparison.

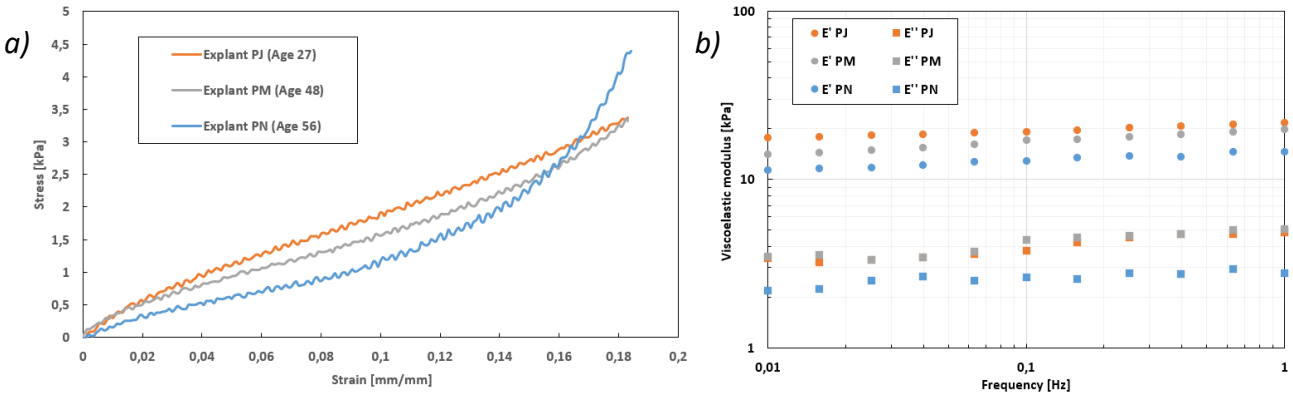

Figure 4.22: Results of tensile tests on 3 explants from 3 donors of different ages. Explant PN (56 years old) considered to be old; explant PJ (27 years old) considered to be young; explant PM (48 years old) from an intermediate age group. a) Simple traction (speed = 10 mm.min^{-1}). b) Frequency sweep (strain = 10%).

These explants were chosen because of the age of the donor but also because they reached a stress of around 4 kPa at maximum strain (Figure 4.22.a). In simple traction, "characteristic" curves can be obtained for these different age groups. In fact, three different paths are taken to reach this 4 kPa stress.

At this strain level, the PJ explant has linear elastic behaviour; the stress-strain curve is a straight line. For older skin such as PM, the stress-strain curve begins to bend. Finally, for an even older skin such as the PN explant, the stress-strain curve bends even more and becomes stiffer at large deformations. These trends were found for all the other explants of similar ages.

With age, the skin loses elasticity at low deformations and the natural tension of the skin decreases. Elastic moduli are lower and the range of linear elastic behaviour narrows. Bilinear elastic behaviour occurs earlier in the extension of the skin, demonstrating more pronounced anisotropy. From a physiological point of view, for aged skin, this implies that:

- the elastic fibre network is less able to resist deformation;
- the collagen fibres start to be stressed earlier, which reduces the skin's capacity for deformation.

The dynamic test confirms the loss of elasticity and also shows a loss of viscosity with age (Figure 4.22.b). Between these three explants, the storage modulus decreases as the age of the explant increases. The loss modulus also decreased with the oldest PN explant.

A comparison of all the biomechanical parameters measurable with our equipment on the PJ young skin explant and the PN aged skin explant is presented in Table 4.1. This comparison shows that the mechanical properties of each skin are different.

Table 4.1: Comparison of biomechanical parameters of young PJ skin and aged PN skin.

	Traction		Strain scanning		Frequency scanning		Hysteresis cycles	Stress relaxation
Explants	Young's modulus E0 (kPa)	Modulus at 18% deformation (kPa)	Viscoelastic modulus at 1% (kPa)	Viscoelastic modulus at 18% (kPa)	Viscoelastic modulus at 0,01 Hz (kPa)	Viscoelastic modulus at 1 Hz (kPa)	Dissipated energy (µJ)	Relaxation rate (%)
PJ (Age 27)	37.4 ± 0.5	20.7 ± 0.5	E' : 37.4 ± 0.5	E' : 19.9 ± 0.5	E' : 17.7 ± 0.5	E' : 21.6 ± 0.5	1.2 ± 0.7	22 ± 3
			E'' : 10 ± 2	E'' : 4.4 ± 0.7	E'' : 3.4 ± 0.5	E'' : 5 ± 2		
PN (Age 56)	19.4 ± 0.5	93.2 ± 0.5	E' : 27.4 ± 0.5	E' : 22.6 ± 0.5	E' : 11.4 ± 0.5	E' : 14.7 ± 0.5	0.9 ± 0.7	36 ± 3
			E'' : 8 ± 2	E'' : 2.9 ± 0.7	E'' : 2.2 ± 0.5	E'' : 3 ± 2		

This Table highlights the mechanical differences between an aged and a young explant. The PJ explant has higher Young's modulus and viscoelastic moduli, demonstrating the strong viscoelastic properties of a young skin. The elasticity and viscosity of young skin are therefore higher than those of old skin. The PN explant is more rigid to large deformations. When held under tension, young skin relaxes less than old skin, which also shows its good elasticity. Thanks to its greater elasticity, young skin is therefore firmer.

Conclusions:

Despite the inter- and intra-explant variability, this Section is devoted to comparing the mechanical properties of skins of different ages. According to the scientific literature, the age of the skin, which is an intrinsic parameter, greatly affects its mechanical properties.

Over the deformations studied, it can be assumed that young skin has higher viscoelastic properties than older skin. The mechanical behaviour is linear over these deformations. In fact, we strongly assume that young skin will experience its mechanical stiffening phase in extension (bilinear behaviour with a J-shaped curve) at higher strains. The more the skin is aged, the more this curve

hollows out at low deformations and the more rigid the skin becomes at high deformations. Older skin experiences a decrease of its mechanical properties at low strains and a rapid increase in explant stiffness, demonstrating reduced extension capacity with age.

The observed decreases in the extensibility of human skin with age are the result of changes and alterations in the dermal fibrous network. Whereas young skin has a random organisation of highly crimped collagen fibril bundles, older skin has compacted and straightened fibre bundles.
These mechanical results are consistent with the physiological studies from the literature (see Part 1.2.2), which show disorganised and weakened ECM, resulting in less dense and less elastic connective tissue for aged skin [Boisnic *et al.*, 2005]; [Ebling, 1982].

4.5 General conclusion on the mechanical properties of *ex vivo* skin explants

The mechanical properties of the skin must be known by the various practitioners so that they have all the knowledge they need to handle this organ. During surgical operations and manipulations, the skin can be subjected to high stresses under load, so it is important to find out its mechanical response during this process.
Our instrumentation enables to meet this need by assessing the viscoelastic properties of human skin. This device has been the subject of numerous studies, demonstrating its full potential and the diversity of tests that can be performed. It provides a comprehensive characterisation of human skin by carrying out quasi-static and dynamic tests, giving information about its elasticity and viscoelasticity. The various tests carried out using this device are complementary and provide an overall energy analysis of the skin under different types of mechanical stresses.

To provide a physical explanation of the phenomena observed, the macroscopic deformation of the skin is assumed to reflect microscopic changes in the configurations of the macromolecular chains in the material. From a physiological point of view, the elastic properties are due to the entanglements and chemical bridges that exist between the different protein chains within the extracellular matrix, which act as anchor points between which each portion of macromolecular chains behaves like a spring. The viscoelastic properties originate from the possibility of intra- or intermolecular movements of the macromolecules in the gel in relation to a position of statistical equilibrium.

In this Chapter, numerous skin explants were tested to characterise the mechanical properties of different donor skins. Due to the mechanical anisotropy of skin and the great variability of living organisms, many different mechanical results have been obtained on *ex vivo* skin explants from these different donors. The results obtained with our instrumentation on *ex vivo* skin explants are comparable with those in the scientific literature.

A study of the viability of the skin explants from Eurofins BIO-EC over time was then carried out in order to monitor and evaluate the time of survival of the explants under *ex vivo* conditions. It showed that *ex vivo* human skin explants retained their mechanical properties during the first week of culture. Analysis of the viscoelastic moduli and stresses measured as a function of the survival time of the explant shows that its viscoelastic properties vary very little. This is a positive point which is important for the continuation of our studies and in particular for monitoring stress on the skin (Chapter 5).
Finally, an intra- and inter-donor comparison of the mechanical properties of the explants was carried out. The comparison of skin from donors of different ages showed the impact of skin ageing on the mechanical behaviour of the skin. Younger skin has better viscoelastic properties than older skin. The observed decreases in skin mechanical properties with age are the result of changes and alterations in the dermal fibrous network.

The purpose of this device, discussed in the following Chapter 5, is to assess the effectiveness of a therapeutic treatment, whether topical or surgical, on the skin, with concrete measurements of certain skin properties such as elasticity or viscoelasticity.

Chapter 5.

Evaluation of the effect of stress on human skin mechanical properties

Ex vivo human skin explants are invaluable for many studies, particularly in the field of dermatological research and cutaneous toxicology. They provide close-to-reality models for exploring various aspects of skin biology and responses to treatments or environmental agents.

This Chapter is dedicated to the experimental characterisation of the mechanical properties of the skin under some specific stresses. The assessment of the effect of stress or the efficacy of therapeutic treatments on the mechanical properties of the skin *ex vivo* can be considered as the principal function of the instrumentation developed in the present project.

In this Chapter, we describe the exploration of the effects of specific stresses on the overall rheological properties on the basis of the instrumentation that we have developed and all the tests we have described previously. In particular, we will be analysing all the parameters measured, both those assessing elasticity and those measuring dissipation.

This Chapter therefore presents the experimental results of the characterisation of the mechanical properties of human skin explants that have been damaged or subjected to some aggressions. Firstly, skin lesions, i. e. stretch marks, will be studied on skin explants. Then, two stresses will be induced on healthy explants in order to assess the effect of these stresses on the skin. The first stress studied is the freezing of explants, a technique often used to preserve explants *ex vivo* over time. The second one was the introduction of proteolytic enzymes into contact with the explants; these enzymes mimic acceleration of the ageing of the skin explants. Finally, inhibitors of these enzymes will be tested to assess their effectiveness on the regeneration of mechanical properties of the skin. The variation in the mechanical properties of the skin *ex vivo* and the adaptation of the tissue will be correlated with these different stresses.

The main objective of this Chapter is to evaluate the effects of three specific stresses on the mechanical properties of human skin in order to propose an analysis of the evolution of the skin structure.

5.1 Study of the mechanical properties of a skin lesion: stretch marks

This first study is dedicated to the experimental characterisation of the mechanical properties of human skin explants with stretch marks. This type of skin lesion was chosen because it is regularly present on some of the Eurofins BIO-EC's skins, which, as a reminder, mainly come from the abdominal area.

5.1.1 Introduction and literature review on stretch marks

As introduced in Part 1.2.2.B, *Striae distensae* (SD), commonly known as stretch marks, are linear dermal scars accompanied by epidermal atrophy. These skin scars frequently appear during times of rapid tissue expansion, like during adolescence, because of obesity, or during pregnancy and in clinical situations associated with extensive use of corticosteroids. They are extremely common lesions that do not cause any significant medical problems, but are of cosmetic concern.
The pathophysiology is multifactorial with mechanical stretching of the skin being the most important. SD probably result from an initial inflammatory reaction that destroys collagen and elastic fibres, followed by the regeneration of these fibres in the direction imposed by the local mechanical forces. Therefore, the pathogenesis of *striae* is linked to changes in those structures that provide skin with its tensile strength and elasticity.

As shown in Figure 5.1 and described in the literature, SD appear macroscopically as parallel streaks (*striae*) aligned in a direction perpendicular to the direction of skin tension [Stamatas *et al.*, 2014]. In the early stage, SD appear and erythematous streaks form red-to-violaceous patches or plaques: these are *striae rubra*. Over time, they change into a chronic phase of hypopigmented, atrophic scars. Finally, they become white, depressed, and finely wrinkled: it is what we call *striae alba*.

Figure 5.1: Stretch mark. a) Photos of human skin explants with stretch marks (explants from Eurofins - BIO-EC). Stretch marks are visible as small, aligned striae that form an elongated damaged area (SD surrounded by orange ellipses and striae (streaks) indicated by black lines). b) Photo with striae markings; the blue arrow represents the direction of skin tension that caused the stretch mark.

The appearance of the epidermis around stretch marks is modified: the surface of SD skin is rougher and more anisotropic than that of normal skin. It could be inferred that the skin surface is elongated directionally along with the physical stretching of the inner structure as SD develop, forming bigger and longer blobs.

Ultrastructural analysis revealed alterations in the appearance of skin affected by striae compared with that of normal skin. Histologically, SD show variously a thin, flattened epidermis, fraying and separation of collagen bundles with dilatation of blood vessels, and separation or total absence of elastic fibres. SD exhibit abnormalities in the core components of skin that normally provide tensile strength and elasticity: collagen, elastin, and fibrillin (glycoprotein which surrounds elastin to form elastic fibres) [Sheu *et al.*, 1991]; [Arem *et al.*, 1980].

As Figure 5.2 shows, the dermal fibre networks are deeply modified, with a decrease in the elastin fibre network, the vertical fibrillin fibres adjacent to the dermal-epidermal junction (DEJ), and the collagen fibre network. This results in a looser and more floccular dermal matrix of striae [Watson *et al.*, 1998]. The very few elastic fibres are thinned and fragmented and the orientation of these fibres shows reorganisation in that they ran parallel to the DEJ [Pieraggi *et al.*, 1982]. There is also a reduction in the quantity of collagen. The collagen bundles were thin, short, separated by an abundant ground substance, and often parallel to the epidermis [Zheng *et al.*, 1985].

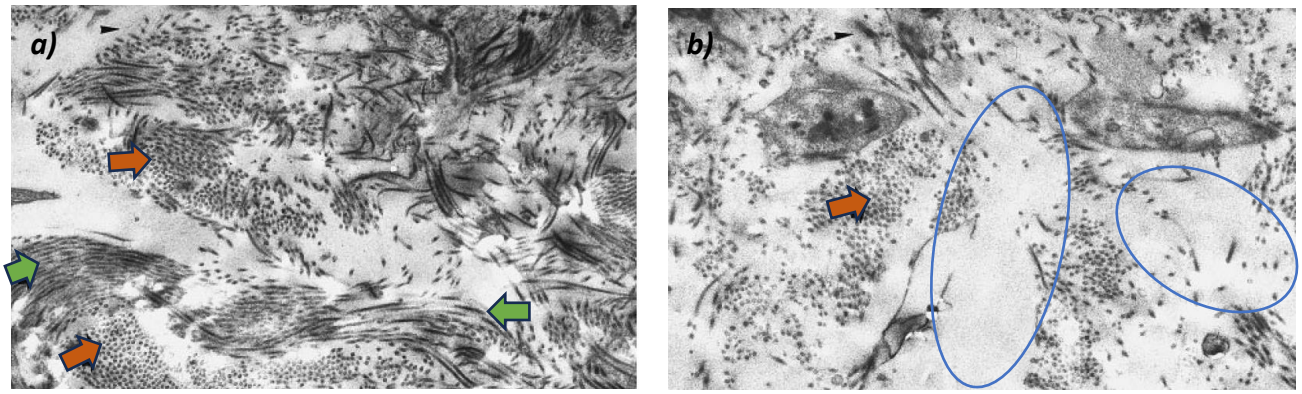

Figure 5.2: Transmission electron micrograph of the dermal matrix of normal skin (a) and SD (b) – Original magnification × 13,500. Normal skin has a highly organised extracellular matrix containing numerous collagen fibres, oriented in the plane of the image (green arrows) and perpendicular to this plane (orange arrows). In comparison, there is a reduction in the amount of fibres in the dermal matrix of stretch marks, with an increase in the amount of ground substance (blue ellipses). This highlights the redistribution of the observable components of the dermal matrix [Watson et al., 1998].

In general, in the SD area, there is therefore a striking decrease in elastin and collagen fibres and an increase in the level of proteoglycans. Excessive mechanical stretching of the skin determines the rupture of the fibres while the fibroblasts are unable to adequately repair the components of the extracellular matrix [Mitts *et al.*, 2005].

Striae bear a resemblance to other human scar models in which newly synthetised connective tissue has been reorganised by tension. Indeed, striae can be considered as a type of dermal scarring, where there is a collagen rupture and separation, and this gap is filled by newly synthetised collagen which then becomes aligned in response to local stress forces [Arem *et al.*, 1980]. Figure 5.3, taken from the study by Bertin [Bertin *et al.*, 2014], clearly shows the reorganisation of dermal fibres in the SD area.

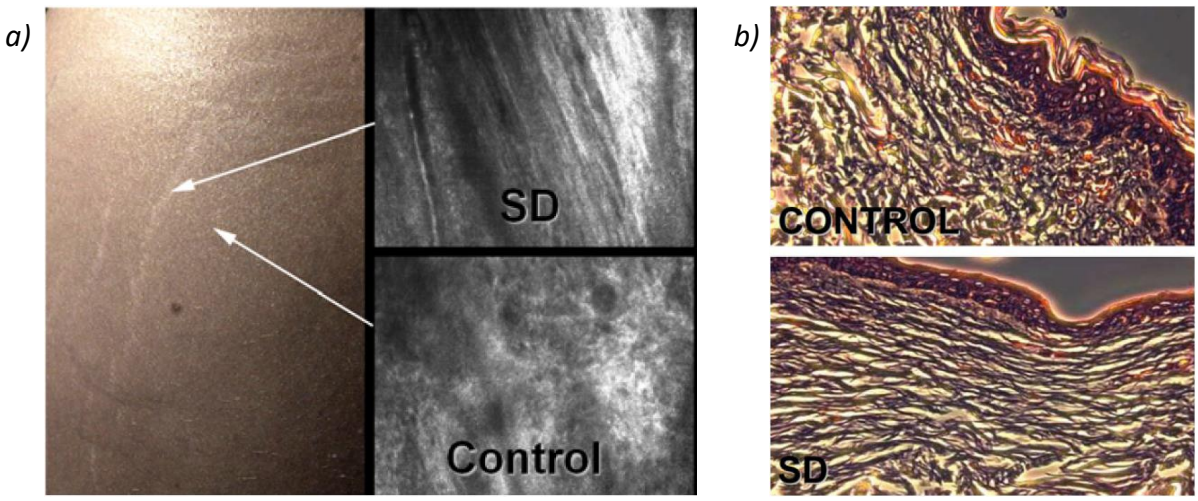

Figure 5.3: Microstructural analysis of SD [Bertin et al., 2014]. a) In vivo confocal imaging of a SD and adjacent skin. b) Haematoxylin and Eosin (H&E) staining of histological sections of abdominal SD and adjacent skin.

On these images, we can clearly observe that for normal skin, collagen bundles are arranged without any obvious preferred direction. In contrast, it was found that striae exhibited organised and parallel collagen bundles running in the direction of the presumed skin tension, perpendicular to the long axis of the lesions. Fibres are aligned parallel to the DEJ, and therefore parallel to the skin surface. The appearance of SD, both histologically and ultra structurally, suggests strongly that mechanical forces play an important role in their morphology [Arem *et al.*, 1980].

As the dermal structural properties are known to affect the skin biomechanical properties, measuring the properties of SD is highly valuable. Some authors have shown that SD lesions are less elastic and less deformable than normal skin. [Kim *et al.*, 2019] measured the viscoelasticity of SD using a Cutiscan® and found that they were less elongated by the negative pressure and less retracted when relaxed showing that they are therefore less viscoelastic than the normal skin area. Other viscoelasticity measurements were carried out using a Cutometer®. [Stamatas *et al.*, 2014] and [Pierard *et al.*, 1999] showed that SD were significantly less firm, less elastic, and less deformable than normal skin. It is assumed that in SD, the connective tissue shows weak resistance to tensile stress.

Given the way SD develop, in particular the alteration of the fibrous networks of the dermis and alignment to mechanical stretching, directionality or structural anisotropy is an important property of SD.

5.1.2 Methodology and presentation of the results

In this Section, we will describe the characterisation of the mechanical properties of stretch marked skin explants. The aim is to observe and evaluate possible differences in the mechanical properties of skin with stretch marks.

Ex vivo skin explants with stretch marks came from four different donors: PM (P2714-AB 48), PB (P2720-AB 48), PG (P2602-AB 55) and PF (P2604-AB 39). No information is available on the cause of these stretch marks on the abdominal skin of donors.
The surface of the explants was analysed to identify the defects that characterise stretch marks: aligned striae forming a slightly discoloured area. Because stretch marks are fine, linear lesions, we can mechanically load them both transversely and longitudinally.
We therefore propose, as shown in Figure 5.4, to carry out three tests on the same explant with a stretch mark, in three different directions on the skin:

- In a direction **parallel to the *striae*** of the stretch mark. This test is therefore performed along the transverse axis of the damaged area of skin. This is the **C test**;
- In a direction **perpendicular to the *striae*** of the stretch mark. This test is therefore performed along the longitudinal axis of the stretch mark. In fact, it is carried out in the area of damaged skin, this is the **B test**;
- In a neutral zone, out of the stretch mark zone, **healthy area** of the explant (part of the explant furthest from the stretch mark zone). This is the **A test**.

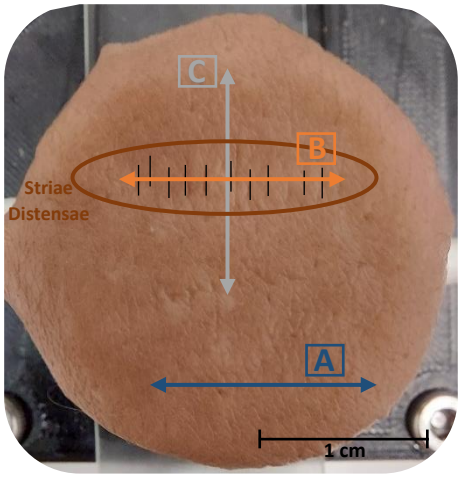

Figure 5.4: Study on stretch marks: representation of the 3 tests carried out on a human skin explant with a stretch mark. SD surrounded by an orange ellipse and striae (streaks) indicated by black lines.
Test A: neutral zone / Test B: perpendicular to striae (within the stretch mark area) / Test C: parallel to the striae (perpendicular to the stretch mark area).

To carry out these tests, the same stretch marked skin explant is first placed in the device (see Part 2.2.1) in one of the three test configurations (A, B or C). The mechanical tests are carried out, then the explant is removed before being immediately replaced and re-attached in the second test configuration. The procedure is identical for the third test configuration. These three areas of skin will therefore be fully and identically characterised (same tests and same parameters), by carrying out the various mechanical tests possible with our system. The different results are therefore comparable and representative of the mechanical properties of a stretch mark on the skin.

Figure 5.5 shows the first results of the mechanical tensile tests in the three test directions, for several skin explants presenting stretch marks zone. All the stretch mark skin explants characterised in this loading mode show this type of mechanical behaviour. These graphs are therefore representative of the mechanical behaviour in traction of this type of explant.

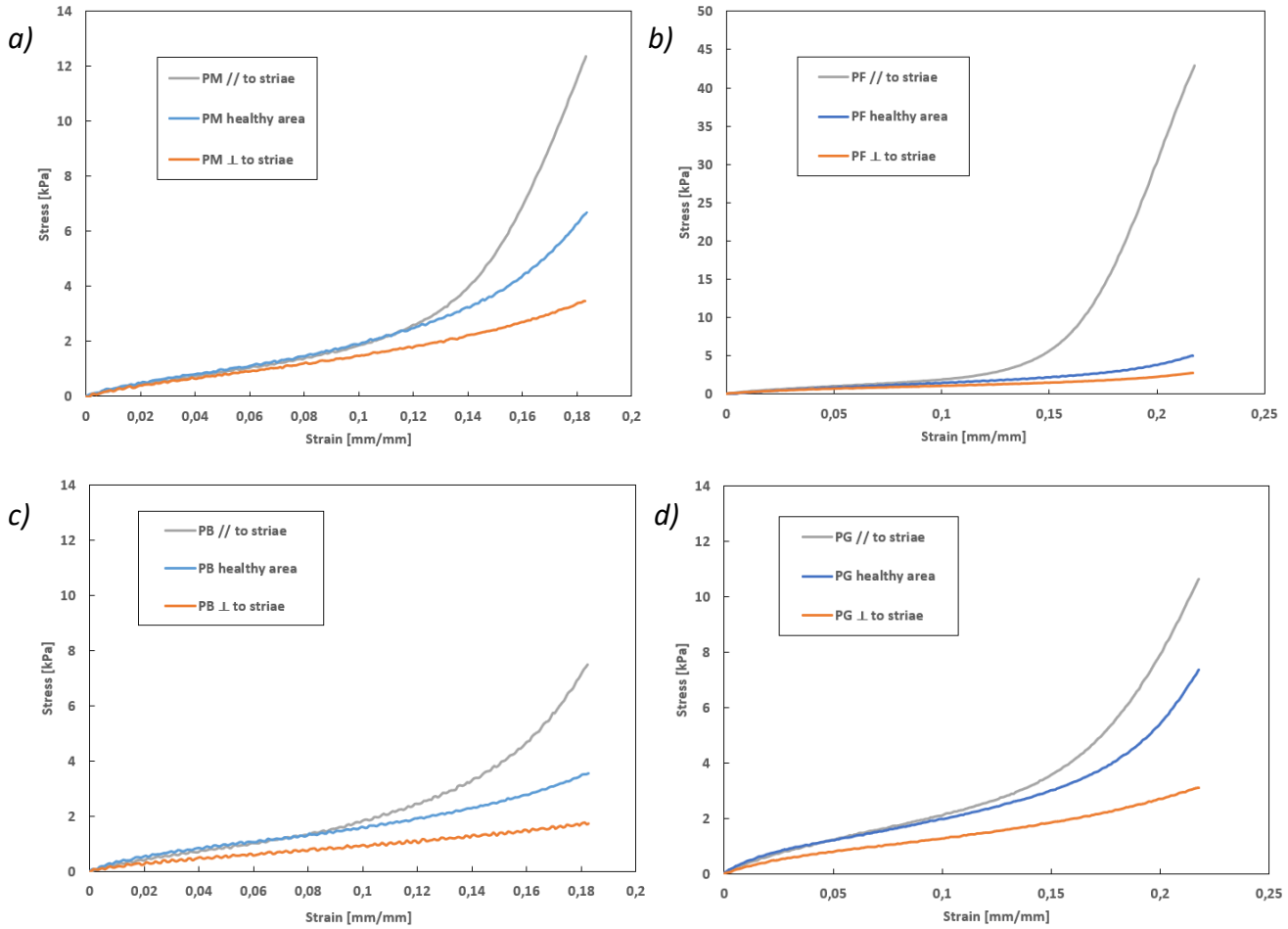

Figure 5.5: Study on stretch marks: tensile tests on 4 explants with stretch marks, in 3 directions of load (speed = 10 mm.min^{-1}). Stress versus strain graphs. Explants PM (a), PF (b), PB (c) and PG (d).

The tensile tests show differences in elasticity between the three directions in which the explants are loaded.

The tensile mechanical behaviour of the healthy zone of the explant, or stretch mark-free zone, is classic and typical of *ex vivo* human skin explants, as reported in Chapter 4. All four explants exhibit linear elastic mechanical behaviour for the lower deformation domain followed by the onset of the stiffening phase. This stiffening phase only occurs at strains greater than 15%. According to Figure 5.5, the mechanical behaviour in the healthy zone is different from that in the stretch zone and we observe that the tensile properties in the healthy zone are always between the tensile properties for tests performed parallel to the *striae* and the ones for tests performed perpendicular to the *striae*.

The mechanical behaviour in tension perpendicular to the *striae* (i.e., in the stretch mark), is the weakest. From the lower strains, the stresses and moduli measured are lower than those in the healthy zone. For example, the Young's modulus for PG skin is (42 ± 1) kPa in the healthy zone, and (26 ± 1) kPa perpendicular to the *striae*. The mechanical properties in the stretch mark area are therefore weaker and the skin's stiffening phase at large deformations is no longer visible. The skin in a stretch mark is therefore less rigid than healthy skin, and will tend to stretch easily with little resistance to deformation. This stretch mark area is therefore a damaged area with poorer mechanical properties.

The mechanical behaviour in tension parallel to the *striae* formed by the stretch mark (i.e., perpendicular to the stretch mark area), is the highest. At low percentages of deformation, the mechanical behaviour is the same as that of a healthy area of the explant. However, from around 10% deformation, the mechanical behaviour differs and rapidly becoming stiffer. The second phase of stiffening of the traction curves occurs earlier, and the stiffening of the explant is clearly marked. Skin subjected to loads parallel to the *striae* is therefore much more rigid than healthy skin. In this direction, the skin will strongly and rapidly resist the imposed deformations.

These three differences in mechanical properties clearly highlight the increased anisotropy created by stretch marks. The apparent elastic moduli, measured for two explants and summarised in Table 5.1, confirm the increased anisotropy of stretch marks.

To characterise in depth the mechanical difference, we have performed dynamic tests on the same samples. Figure 5.6 shows the results of dynamic strain sweep tests in the three test directions for explants with stretch marks. All the stretch marked skin explants characterised in this stress mode show this type of mechanical behaviour.

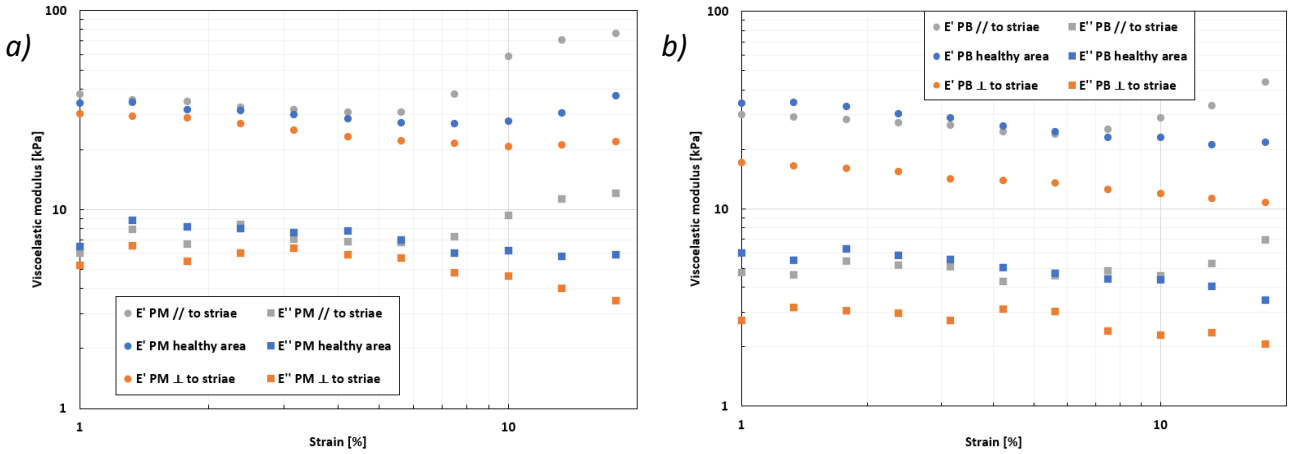

Figure 5.6: Study on stretch marks: strain sweep tests on 2 explants with stretch marks, in 3 load directions (f = 0.5 Hz). Graphs of viscoelastic moduli as a function of strain. Explants PM (a) and PB (b).

The strain sweep tests confirm differences in viscoelasticity between the three directions of loading. The viscoelastic behaviour of the healthy zone of the explants is classic and typical of *ex vivo* human skin explants, as reported in Chapter 4. Viscoelastic moduli decrease slightly with strain rate, and for some skins, like PM here, at large strains the storage modulus increases. According to Figure 5.6, the mechanical behaviour in the healthy zone is different from that in the stretch zone.

The viscoelastic behaviour in the stretch mark area is the weakest. Over the entire deformation range, the storage and dissipation moduli perpendicular to the *striae* are lower than those of the healthy zone. For example, for PB skin, these two modules are both approximately 50% lower than those of the healthy zone. The viscoelastic properties in this direction are therefore much weaker, confirming that this stretch mark zone is indeed an injured zone.
The viscoelastic behaviour parallel to the *striae* is similar to that of the healthy zone for low strains. However, at strains greater than around 5%, the behaviour differs by becoming stiffer: the viscoelastic moduli increase rapidly. The modulus of elasticity E' parallel to the *striae* of the PM skin

increases from (30.5 ± 0.5) kPa at 6% strain to (76 ± 0.5) kPa at maximum strain. As in traction, this stiffening phase occurs earlier than in healthy skin.

Figure 5.7 below shows the results of dynamic frequency sweep tests in the three test directions for explants with stretch marks. All the stretch marked skin explants characterised in this stress mode show this type of mechanical behaviour.

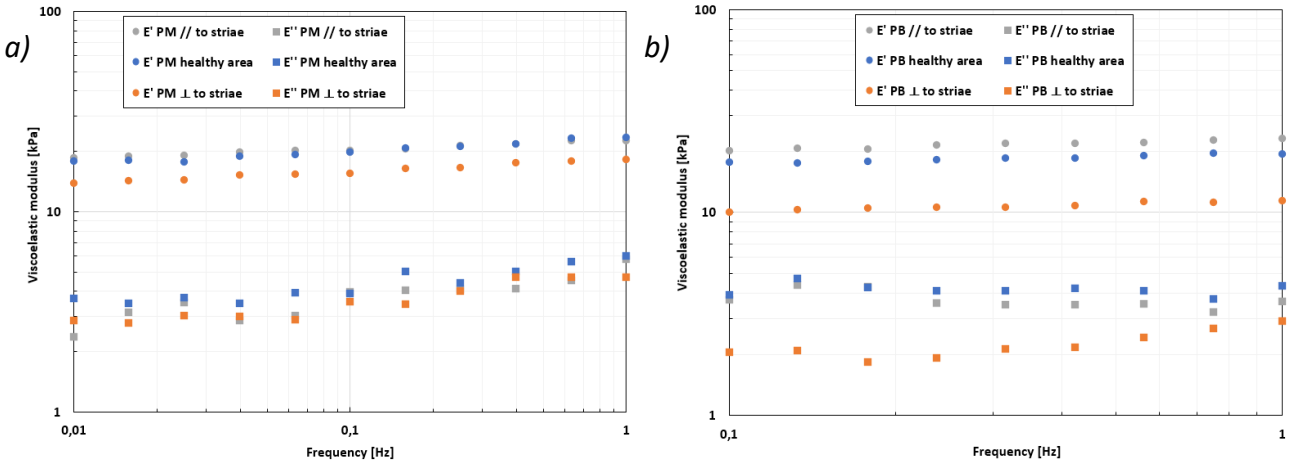

Figure 5.7: Study on stretch marks: frequency sweep tests on 2 explants with stretch marks, in 3 load directions (strain = 10%). Graphs of viscoelastic moduli as a function of frequency. Explants PM (a) and PB (b).

Note: these experiments were carried out at 10% strain for reasons of homogeneity of the load percentage with the tests on healthy skins. Experiments at 5% deformation, the limit of the "linear" domain (Figure 5.6), should have been carried out but were not possible due to lack of time.

As with the strain scans, the frequency sweep tests show differences in viscoelasticity between the three directions of loading of the explants.
The viscoelastic behaviour of the healthy zone of the explants is classic and typical of *ex vivo* human skin explants, as reported in Chapter 4. The viscoelastic moduli slightly increase with test frequency. According to Figure 5.7, we confirm that the mechanical behaviour in the healthy zone is different from that in the stretch zone.

Over the entire frequency range, the storage and dissipation moduli measured perpendicular to the *striae* are significantly lower than those of the healthy zone. Over this frequency range, the moduli of elasticity E' of the two skins are about 20% lower for PM and 40% lower for PB than for the healthy zone. Conversely, the viscoelastic behaviour parallel to the *striae* is fairly similar to that of the healthy zone: the viscoelastic moduli are almost the same.

The differences in viscoelastic properties, demonstrated by the two previous dynamic tests, also highlight the loss of elasticity in the stretch mark zone and the reinforcement of the anisotropy created by the stretch marks whatever the frequency is. The moduli of elasticity and dissipation, measured for two explants and summarised in Table 5.1, confirm this analysis.

Eventually, we have explored the viscoelastic behaviour with cycling tests reported in Figure 5.8 in the three test directions for explants with stretch marks. All the stretch mark skin explants characterised in this loading mode show this type of mechanical behaviour.

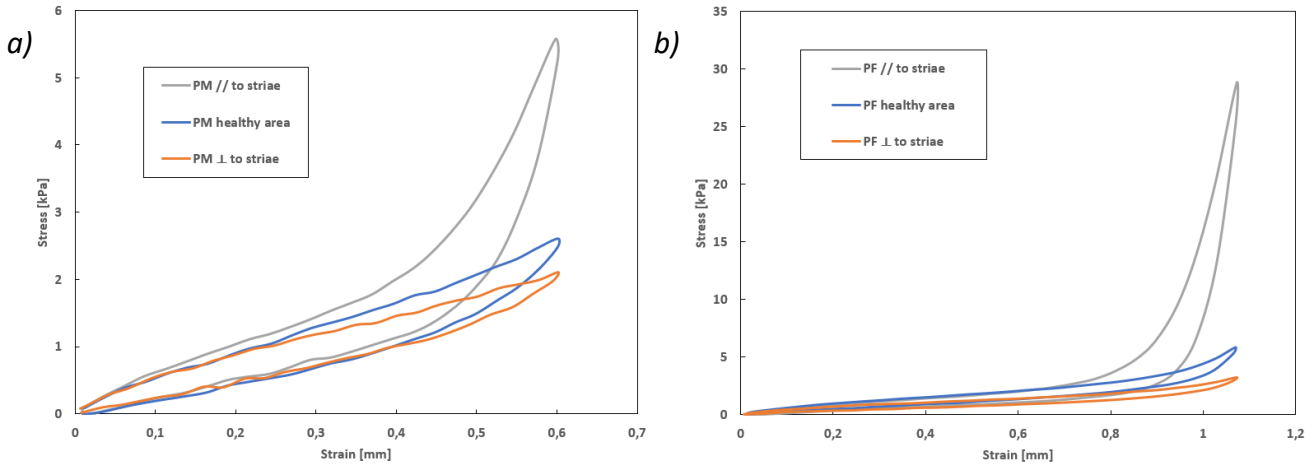

Figure 5.8: Study on stretch marks: 5th cycle of cyclic loading-unloading tests on 2 explants with stretch marks, in 3 load directions (strain = 10% or 22% / speed = 10 mm.min^{-1}). Stress versus strain graphs. Explants PM (a) and PF (b).

Firstly, it can be noted that the mechanical properties, in the three test directions, are stabilised around the 5th cycle, which confirms the results of the preliminary study on the pre-conditioning of skin explants (see Part 3.1).

Figure 5.8 shows that the hysteresis phenomenon, measured when the dissipated energy is stabilised, differs according to the direction in which the explant is loaded. Due to the high stresses reached in the direction parallel to the *striae*, the mechanical energy dissipated during this loading-unloading cycle is greater than that in the healthy zone. Conversely, as shown in Table 5.1, the energy dissipated in the stretch mark is lower than that in the healthy zone, thus demonstrating the poor viscoelastic behaviour of stretch marks.

Finally, Figure 5.9 below shows the results of stress relaxation tests in the three test directions for explants with stretch marks.

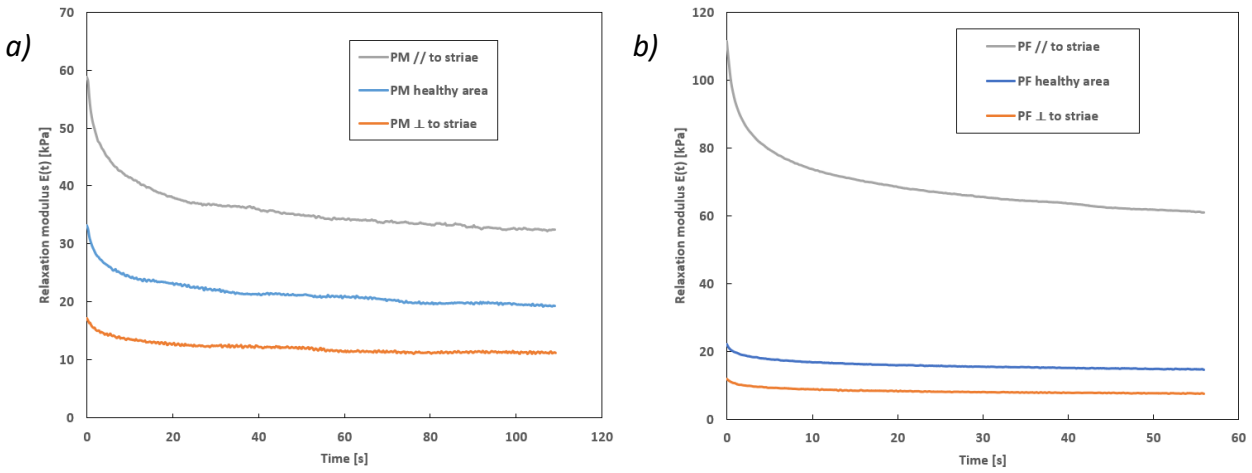

Figure 5.9: Study on stretch marks: stress relaxation tests on 2 explants with stretch marks, in 3 load directions (Parameters: tension = approx. 1 or 2 min / strain = 18%). Graphs of relaxation modulus E(t) as a function of time. Explants PM (a) and PF (b).

These tests show the differences, in the three direction tests, in terms of stress relaxation. Parallel to the *striae*, the recovery of mechanical properties is faster and stronger than in the other

directions. Due to the high stresses reached in this direction, the skin dissipates a lot of energy to gradually return to a more stable state. As shown in Table 5.1, relaxation rates in this direction are the highest. Conversely, recoveries are very slow and relaxation rates are lower for PM skin in the direction perpendicular to the *striae*, also demonstrating the reduced viscoelastic behaviour of stretch marks.

All the biomechanical parameters measured with these five mechanical tests are summarised, for two explants, in Table 5.1 below. These parameters highlight the differences in the viscoelastic properties of the stretch marks. The loss of viscoelasticity and the increase in anisotropy are characteristic of stretch marks.

Table 5.1: Analysis of biomechanical parameters on 2 explants with stretch marks – Measurements in a neutral zone of the explant, in the stretch mark and perpendicular to the stretch mark (with reproducibility standard deviation).

		Traction			Strain scanning			
Explants	Test direction	Young's modulus E0 (kPa)	Modulus at 10% deformation (kPa)	Modulus at 18% deformation (kPa)	Viscoelastic modulus at 1%		Viscoelastic modulus at 18%	
					E' (kPa)	E'' (kPa)	E' (kPa)	E'' (kPa)
PM	Healthy area	25 ± 1	27 ± 1	112 ± 1	34.1 ± 0.5	7 ± 1	37.3 ± 0.5	6 ± 1
	⊥ to striae	22 ± 1	16 ± 1	36 ± 1	30.1 ± 0.5	5 ± 1	21.9 ± 0.5	3 ± 1
	// to striae	25 ± 1	30 ± 1	249 ± 1	38 ± 0.5	6 ± 1	76.2 ± 0.5	12 ± 2
PF	Healthy area	25 ± 1	13 ± 1	33 ± 1	12.2 ± 0.5	3 ± 1	9.3 ± 0.5	1 ± 1
	⊥ to striae	20 ± 1	7 ± 1	16 ±1	9.5 ± 0.5	2 ± 1	5.1 ± 0.5	0.7 ± 0.5
	// to striae	29 ± 1	25 ± 1	581 ± 1	12.4 ± 0.5	3 ± 1	52.6 ± 0.5	6 ± 4

		Frequency scanning				Hysteresis cycles	Stress relaxation
Explants	Test direction	Viscoelastic modulus at 0,01Hz		Viscoelastic modulus at 1 Hz		Dissipated energy (µJ)	Relaxation rate (%)
		E' (kPa)	E'' (kPa)	E' (kPa)	E'' (kPa)		
PM	Healthy area	17.9 ± 0.5	3.7 ± 0.5	23.5 ± 0.5	6 ± 1	1.7 ± 0.8	43 ± 3
	⊥ to striae	13.9 ± 0.5	2.9 ± 0.5	18.3 ± 0.5	5 ± 1	1.3 ± 0.8	34 ± 5
	// to striae	18.6 ± 0.5	2.4 ± 0.5	22.6 ± 0.5	6 ± 1	2.6 ± 0.8	45 ± 1
PF	Healthy area	6.8 ± 0.5	1.6 ± 0.2	8.7 ± 0.5	1.7 ± 0.5	4 ± 2	34 ± 3
	⊥ to striae	4.8 ± 0.5	1.4 ± 0.2	6.2 ± 0.5	1.2 0.5	3 ± 2	35 ± 5
	// to striae	6.5 ± 0.5	1.4 ± 0.2	9.1 ± 0.5	1.7 ± 0.5	11 ± 2	45 ± 1

5.1.3 Conclusion

Stretch marks result from dermal scarring and epidermal atrophy. SD mostly occur by rapid stretching of intrinsic tissues and appear as parallel streaks aligned in a direction perpendicular to the direction of the skin tension. Histologic and biochemical analyses have revealed that SD are characterized by a decrease in extracellular matrix (ECM) components in the dermis, a strong alignment of collagen fibres, and a decrease in elasticity and viscoelasticity [Kim *et al.*, 2019]; [Cho *et al.*, 2018]; [Stamatas *et al.*, 2014].

Measurements of SD are not only important for studying and understanding the pathophysiology of SD, but also for developing and evaluating preventive methods and more effective treatments. There is currently a lack of information about the mechanical properties of such lesions. Some mechanical studies have described that the SD-involved skin has significantly less elasticity and exhibited less deformability than normal skin. Moreover, few studies take into account the mechanical anisotropy of SD.

In this study, we propose a complete characterisation of the viscoelastic properties of SD. The tests carried out highlight the differences in mechanical properties between a healthy area and a stretch mark area of an explant. Our instrumentation is perfectly adapted to study this type of skin lesion differentiating elasticity and dissipation. Because SD are linear scars, the directionality of our tests means that we can analyse the properties of this damaged area precisely and in all directions. Generally speaking, the results show:

- Significantly higher mechanical properties in the direction parallel to the *striae*;

- Weaker viscoelastic properties along the axis of the stretch marks, i.e., perpendicular to the *striae*.

These mechanical results are consistent with histological analyses in the scientific literature. According to this literature, stretch marks can be represented schematically as shown in Figure 5.10.

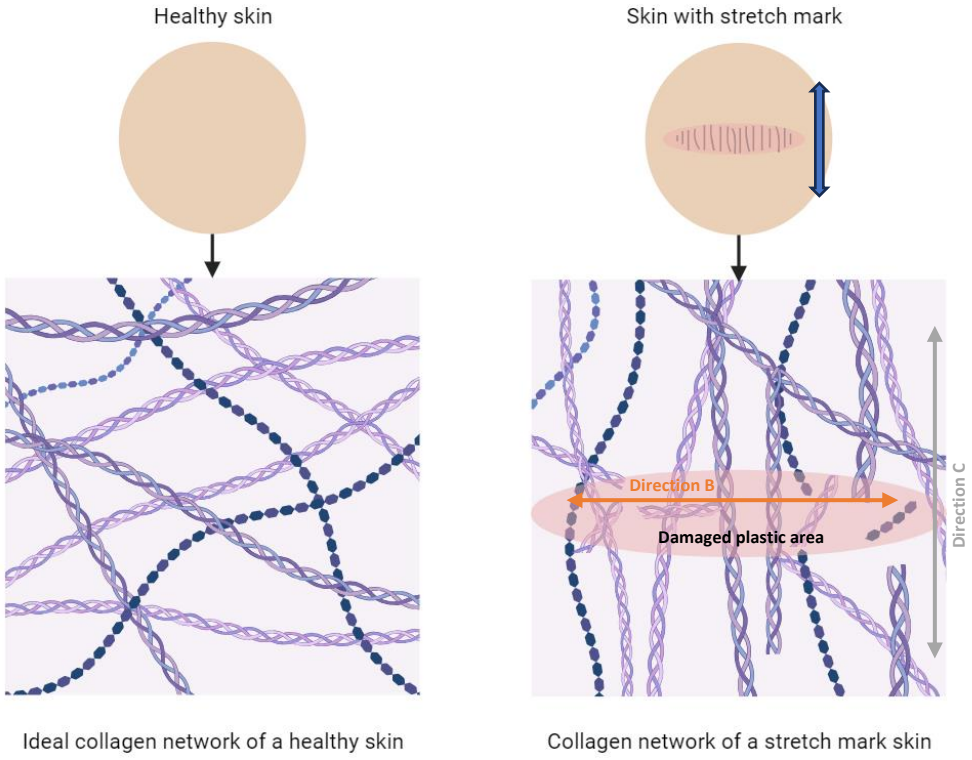

Figure 5.10: Study on stretch marks: Schematic diagrams showing the dermal collagen network of healthy skin and skin with a stretch mark.

The stretch mark area, characterised by the **B test**, is an area where the structure of the connective tissue has been severely altered. There are fewer ECM components and the collagen and elastin fibre network are destroyed and broken. These structural changes therefore lead to a reduction in the viscoelastic properties of stretch mark skin. Elastic and viscous moduli are reduced.

Parallel to the *striae* of the stretch marks, **test direction C**, the mechanical properties are significantly higher. In fact, this is the direction of the mechanical stress that caused the scars. The fibre networks have been greatly stretched and some have certainly become plastic, resulting in stiffer properties. In this direction, the stress required to deform the skin must be higher than in other directions. It is therefore in this direction that the fibres are pre-oriented/aligned and that the new regenerated elastin and collagen fibres are oriented. Elastic and viscoelastic moduli are high because collagen fibres are rapidly stressed.

The biomechanical analyses carried out in this Section are in agreement with the histological results and observations of structural differences between SD and normal skin reported in the scientific literature. The structural differences caused by SD therefore result in differences in mechanical properties, making SD less viscoelastic and significantly more anisotropic than the adjacent normal skin. The altered dermis composition, with the realignment of fibre network in the direction of skin tension explain these mechanical properties.

By highlighting changes in the mechanical behaviour of the skin in the stretch mark zone, this type of lesion can be better understood. Overall, this study is of high interest for medical or cosmetic products designed to treat stretch marks and enhance the well-being of patients. The aim of creams could therefore be to reduce the excess of internal tension created by stretch marks, or to reinforce the viscoelastic properties of the discoloured central zone.

Because of their high prevalence and impact on patients' quality of life, there is great demand for an effective treatment. A vast array of treatment modalities has been investigated, ranging from topicals and acid peel treatment to more invasive methods such as laser therapy. Although complete eradication of SD is not achievable, improving the appearance whilst reducing physical symptoms certainly is.

5.2 Effect of freezing on the mechanical properties of human skin

This Part is dedicated to the experimental characterisation of the effect of an external stress on the skin: freezing. This type of stress was chosen because freezing is a technique commonly used to preserve soft tissues. This method of preservation is employed by Eurofins - BIO-EC.

5.2.1 Introduction and literature review on the effect of freezing

Researchers rely on human skin substitutes and skin preservation techniques, such as freezing, to overcome the lack of human skin availability. The process of freezing is widely employed as a preservation technique for soft tissues. Frozen human skin samples can be stored and used when

no fresh skin plasty is available for studies. In fact, these frozen human skin samples are suitable for carrying out *in vitro* studies, such as skin absorption, for example.
The freezing process preserves the tissue and inactivates the activity of proteolytic enzymes, which means that skin degradation is halted during this preservation process. During our work, we have carried out numerous tests on frozen *ex vivo* skin explants, due to a lack of fresh plasty during our test campaigns. The frozen explants come from a fresh plasty which has been defatted, decontaminated and frozen at -20 °C or -80 °C within 24 hours after the surgery.
Freezing conditions at -80 °C are often used to rapidly freeze skin samples and to minimise the impact of ice-crystal formation in the specimens [Ranamukhaarachchi *et al.*, 2016]. Samples are then thawed (fifteen minutes to one hour at room temperature) before testing to ensure that all ice formed during freezing melts.

However, it is well-known that cold storage can cause several changes in the tissue's mechanical behaviour because it may result in bulk redistribution of water, damage to the collagen network, and breaking of cross-links in the ECM. In fact, freezing causes ice crystals formation that can affect the integrity of the tissue [Meryman, 1957]. Ice crystals formed in the extracellular space can displace, disrupt, and dehydrate the components of the dermis and epidermis.

To the best of our knowledge, there is no consensus on the impact of freezing on the mechanical properties of tissues. Several studies have shown that biomechanical changes occur in certain tissues as a result of freezing. As an example, Quirinia and Viidik found that freezing had an adverse effect on the tensile mechanical properties of rat skin: extension properties were reduced [Quirinia and Viidik, 1991]. Ranamukhaarachchi showed, using a micro-indentation technique, that after freezing the Young's modulus of human skin increased, while that of porcine skin decreased [Ranamukhaarachchi, 2017]. Using a biaxial tensile testing device, Chow and Zhang showed a significant increase in the tensile rigidity of bovine aortic tissue after storage by freezing [Chow and Zhang, 2011].
Other studies have shown that tissues are not affected by freezing. Foutz *et al.* showed that freezing did not affect the strength and response of rat skin to linear tensile loading [Foutz *et al.*, 1992]. By performing rheological measurements, Geerligs showed that freezing does not seem to have any effect on the mechanical properties of porcine adipose tissue [Geerligs, 2010]. At last, Ridge also found no changes in the mechanical properties of human skin [Ridge, 1964].

Although this preservation technique is widely used, this subject is not common because little research has focused on the preservation of the mechanical properties of human skin after a freezing period. We therefore believe that it is important to assess whether or not freezing has an impact on the mechanical properties of human skin explants. The numerous mechanical tests that can be carried out with our developed device will provide new results on this subject.
The aim of our analysis is to assess the possible impact of freezing on the mechanical properties of *ex vivo* human skin explants by using the different modes of solicitations which can be performed with Mécapeau.

5.2.2 Methodology and presentation of the results

Characterisations of the mechanical properties of skin explants before and after a period of freezing have been performed on the same skin explant: fresh at first and after freezing. The *ex vivo* skin explants used came from three different donors: PE (P2613-AB 54), PH (P22620-AB 50), et PT (P2646-AB 33).

First of all, the explants used are considered to be 'fresh': they come from a plasty of skin taken from the body of a donor and preserved and maintained for a few days in physiological-like conditions by the Eurofins BIO-EC laboratory. An initial series of tests is carried out on this 'fresh' explant. At the end of this series of tests, the explant is removed from the device and frozen directly in a freezer at -20°C.
After one or two days in the frozen state, the explant is removed from the freezer. A second series of tests is then carried out on the explant, which has undergone a freeze-thaw cycle. A thawing time of 30 minutes was chosen before carrying out the mechanical tests. This time is long enough for the explant to be completely thawed but also short enough to not degrade over time.

The same explant is therefore characterised completely and identically (same tests and same parameters) in a fresh state and in a thawed state (Figure 5.11). The results can therefore be compared, and are representative of the evolution of the mechanical properties for the same piece of skin before and after a freeze-thaw cycle. Any differences in mechanical properties will be characteristic of the impact of freezing on the skin within the error generated by the measurement.

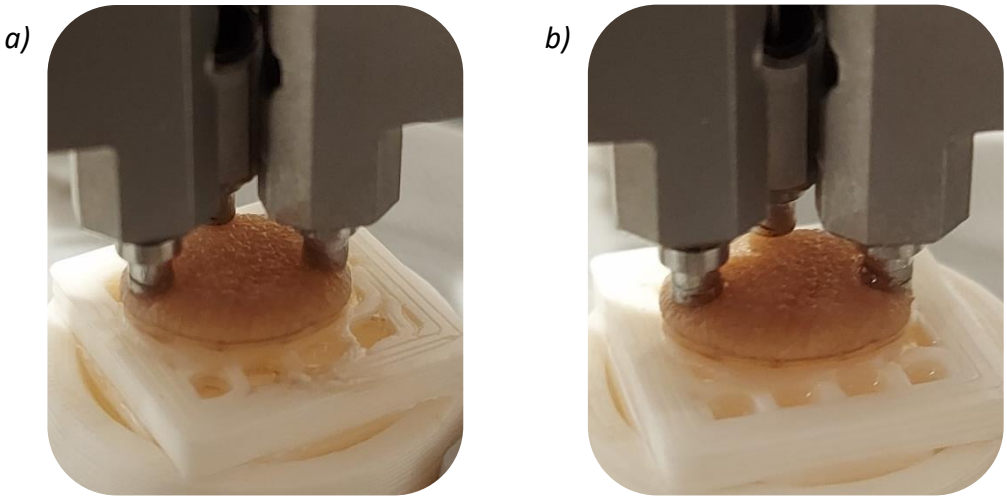

Figure 5.11: Freezing study: photos of the PD explant in the test configuration, fresh (a) and thawed (b). Visual and tactile observation of the explant shows no difference between the 2 states.

Figure 5.12 shows the results of mechanical tensile tests for several skin explants, before and after a period of freezing. This series of tests was carried out during the first experiments on human skin with the first configuration of the equipment (see Part 2.1.1). As the vertical pressure exerted by the instrument's studs on the skin is not controlled, errors induced by this possible variation in pressure may occur (as seen in Part 3.5, this compression force influences the mechanical results).

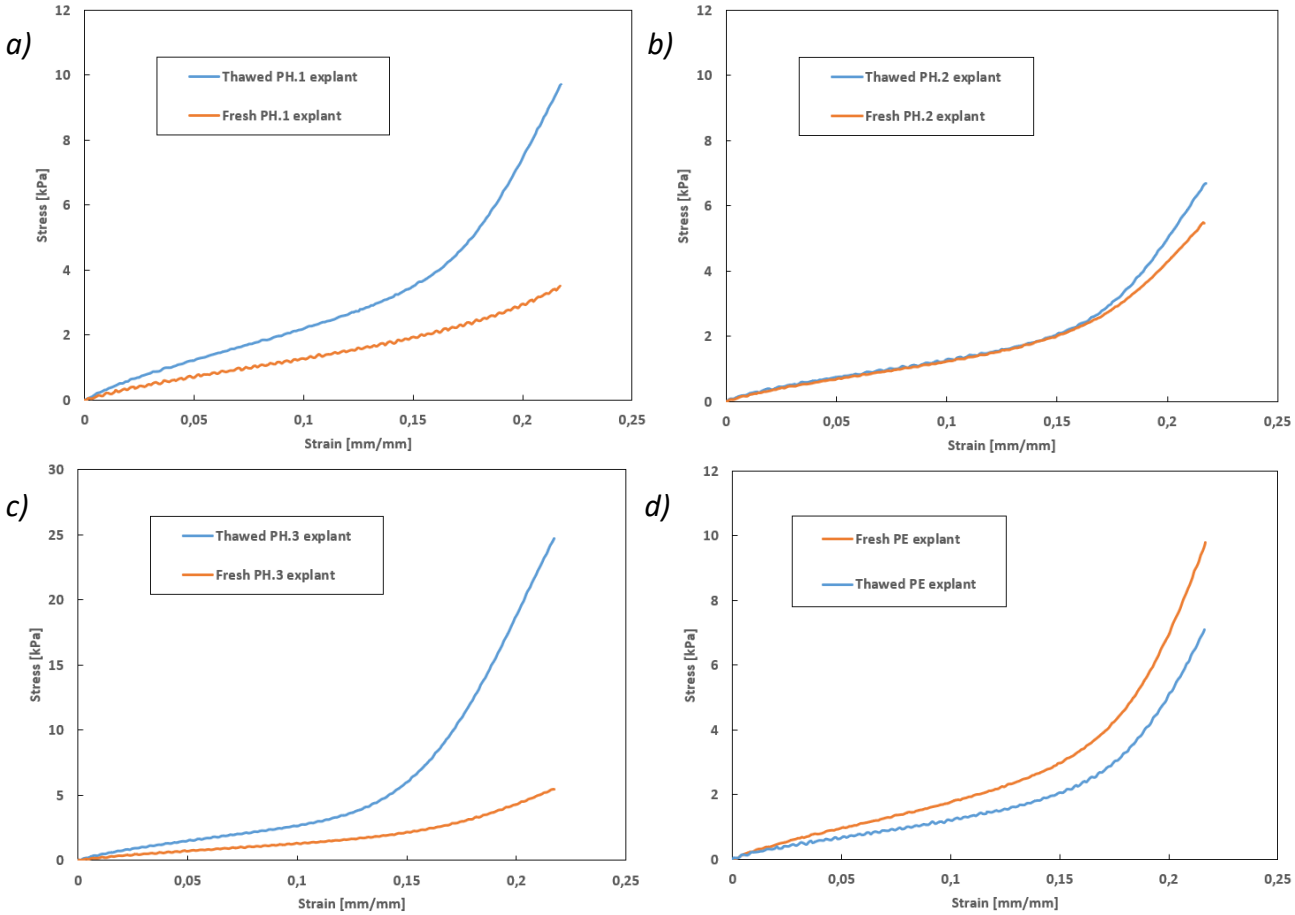

Figure 5.12: Freezing study: traction tests on 4 explants, before and after a period of freezing (speed = 10 mm.min^{-1}). Stress versus strain graphs. 3 explants PH (a,b,c) and 1 explant PE (d).

The results show differences in elasticity between the fresh and thawed explants.
For explants PH.1 and PH.3, the mechanical properties are superior from the first percentages of deformation. The elastic modulus of the first part of the curves, at 10% strain, is multiplied by a factor of 2 for PH.1 and by a factor of 3 for PH.3. The first tensile phase is therefore stiffer and the second tensile phase (J-shaped curves) occurs much earlier for these explants. Freezing therefore caused these two explants to become stiffer and less extensible.
For explant PH.2, the mechanical properties before and after freezing were similar at low deformations, and a slight stiffening occurred during the second phase of stiffening of the explant's mechanical behaviour (J-shaped curve).
Finally, the results for the PE explant are contradictory with the other three explants. In fact, the mechanical behaviour of the thawed PE explant is less rigid than that of the fresh explant over the entire deformation range. However, the bilinear elastic behaviour is identical. For this explant, freezing leads to a reduction in mechanical properties.

These initial results show that freezing can have an impact on the mechanical properties of *ex vivo* explants. The general tendency is for the *ex vivo* explants to stiffen after the freezing process. As shown in Figure 5.13, this initial trend in the results was subsequently supported with measurements with the new configuration of the device (see Part 2.1.3). This Figure shows the complete mechanical characterisation of a skin explant before and after a freezing phase.

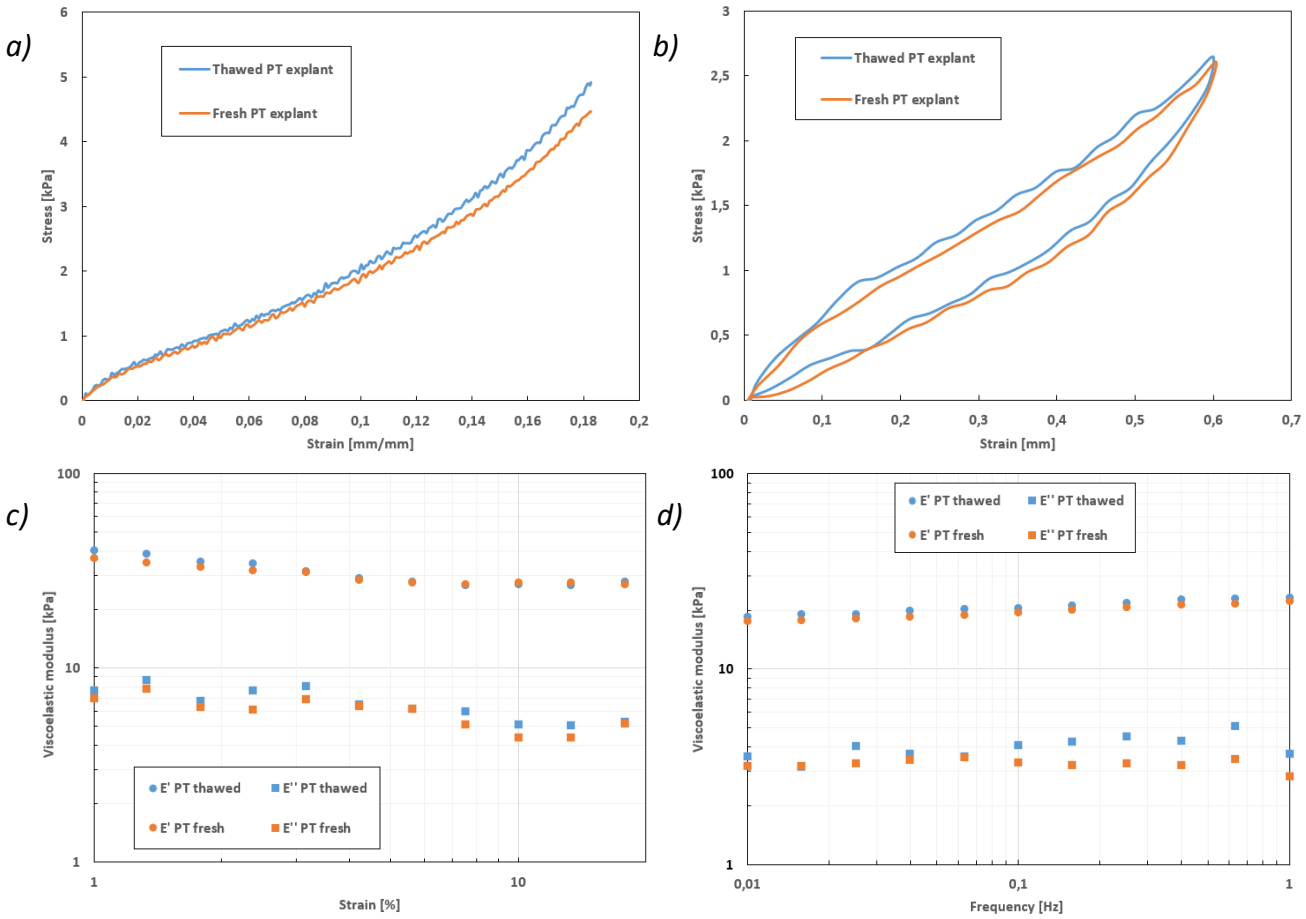

Figure 5.13: Freezing study: complete characterisation of the PT explant before and after a freezing period. a) Traction. b) Cyclic loading-unloading. c) Strain sweep. d) Frequency sweep.

This PT explant is characteristic of the general trend in these experiments: a slight stiffening of the mechanical behaviour of the explant after it has been frozen.
The tensile test showed slightly superior mechanical properties for the thawed explant over the entire deformation range. The mechanical behaviour of the explant in extension remained identical. The cyclic test confirmed the similarity of mechanical behaviour before and after freezing. In addition, the mechanical energies dissipated during the loading-unloading cycles were identical. Finally, the dynamic scanning tests were almost similar before and after the freezing of the explant. As shown in Table 5.2, the tendency for the explant to stiffen is not significant for these dynamic tests.

This slight tendency to stiffen is shown by analysing the biomechanical parameters measured during these mechanical tests. These are summarised for the PT explant in Table 5.2. These parameters highlight the very slight increase in the mechanical properties of the explant after freezing.

Table 5.2: Analysis of biomechanical parameters on the same explant, in a fresh state and in a thawed state (with reproducibility standard deviation).

		Traction			Strain scanning		Frequency scanning		Hysteresis cycles
Explant	Skin condition	Young's modulus E0 (kPa)	Modulus at 10% deformation (kPa)	Modulus at 18% deformation (kPa)	Viscoelastic modulus at 1% (kPa)	Viscoelastic modulus at 18% (kPa)	Viscoelastic modulus at 0,01 Hz (kPa)	Viscoelastic modulus at 1 Hz (kPa)	Dissipated energy (µJ)
PT (P2646-AB 33)	FRESH	34 ± 1	22 ± 1	43 ± 1	E' : 36.8 ± 0.5	E' : 27 ± 0.5	E' : 17.7 ± 0.5	E' : 22.4 ± 0.5	1.5 ± 0.8
					E'' : 7 ± 1	E'' : 5 ± 1	E'' : 3.2 ± 0.5	E'' : 3 ± 1	
	THAWED	36 ± 1	24 ± 1	**51 ± 1**	**E' : 40.2 ± 0.5**	E' : 27.8 ± 0.5	E' : 18.5 ± 0.5	E' : 23.3 ± 0.5	1.5 ± 0.8
					E'' : 8 ± 1	E'' : 5 ± 1	E'' : 3.6 ± 0.5	E'' : 4 ± 1	

5.2.3 Conclusion

For storage, skin is generally frozen to preserve its mechanical properties without inducing biological decomposition or structural changes. Freezing is often necessary to transport tissues for further usage in research, as it helps to preserve tissue structure and integrity. Researchers therefore regularly use skin samples that have been previously stored in refrigerators or freezers, although the impact of storage on the mechanical properties of the skin is not entirely clear.

In this Section, we report the study and evaluation of the impact of this external stress on the mechanical properties of human skin *ex vivo*. The external stress studied here is the process of freezing explants in a freezer at -20 °C.

The overall results of this study show that the freezing process appears to have a slight impact on the mechanical properties of human skin. More specifically, our experiments seem to show a very modest effect of stiffening on skin elasticity and no effect on dissipative properties. For most of the explants analysed, tensile tests after freezing showed stiffer mechanical properties.
However, the latest experiment shows that there does not appear to be any profound change in the mechanical behaviour of the explant before and after freezing. The impact of freezing does not appear to modify the overall mechanical behaviour of the explant, which is essential as most of the tests are carried out on thawed explants.

The impact of freezing seems slight but would demonstrate that the skin undergoes stress by being frozen and then thawed. This stiffening effect could be attributed to possible biochemical and microstructural changes in the skin due to storage by freezing, such as dehydration of the tissue, which would increase its density and therefore its mechanical properties.

Note on the limitations of the study:

- These results are not numerous enough and the overall trend is not clear enough to firmly assert the rigidification of the explant by the freezing preservation process. Further tests are required to confirm this trend.

- This slight stiffening of the explant may be due to insufficient waiting time after removal from the freezer. After ten to fifteen minutes, the explant is no longer as rigid as in its frozen state; it is

malleable and appears visually and tactilely thawed. However, there is nothing to tell us that this is the case. A thawing time of thirty minutes was arbitrarily chosen to ensure that the explant thawed properly, but this time may not be long enough.

5.3 Effect of enzymatic stress on the mechanical properties of human skin

This third Part is dedicated to the experimental characterisation of the effect of an enzymatic stress on the skin. Proteolytic enzymes will be added to the culture medium of *ex vivo* explants. These proteolytic enzymes are **collagenases** and **elastases**. This type of stress, which can be considered as an internal stress, was chosen because it mimics one of the main causes of decreases in mechanical properties over time: an accelerated ageing of the skin. Moreover, these two enzymes are naturally present in the skin.

5.3.1 Introduction and literature review on proteolytic enzymes

Breakdown and disorganisation of extracellular matrix proteins like collagen, fibronectin and elastin are the main characteristics of skin ageing due to the enhanced activation of proteolytic enzymes such as collagenases and elastases. Proteolytic degradation of extracellular matrix (ECM) is thought to play a major role in tissue remodelling. Two major proteolytic systems, namely matrix metalloproteinases (MMPs) and serine proteinases, have been implicated in several pathophysiological processes involving extensive ECM remodelling.

Collagenases are metalloproteinases capable of cleaving other molecules present in cells. Collagenase hydrolyses the triple-helix collagen by cleaving its X-Gly bond, as well as peptides containing the sequence -Pro-X-Gly-Pro, where X can be any amino acid. For example, collagenase-2 (MMP-8) can cleave elastin and fibronectin as well as collagen.
Elastases are serine proteinases that are also involved in ECM degradation. Elastase is mainly responsible for the breakdown of elastin: these enzymes catalyse the hydrolysis of elastin. As well as cleaving elastin, elastases have a wide portfolio of substrates, giving them the ability to cleave collagen, fibronectin, and other ECM proteins [Robert *et al.*, 1984]; [Bieth, 2001].
Elastase and collagenase are enzymes naturally present in the skin. Indeed, fibroblasts enable the synthesis of collagen, elastin, proteoglycans, and other molecules that make up the ECM. In addition, they also participate in the synthesis of proteins capable of degrading this ECM such as collagenases and proteases, thus enabling it to be renewed. In normal tissues, a balance is reached between the formation of the ECM and destruction of the ECM by these enzymes, leading to a state of homeostasis.

These enzymes are naturally expressed with the ageing of the skin and under exposure to UV rays. We might think that all molecule synthesis slows down with age, which is true for most of them, but some molecules are produced in greater quantities, such as type III collagen, fibronectins, elastase, and collagenase. Indeed, in terms of enzymes, with age we observe an increase in the production of metalloproteinases such as collagenases, which destroy collagen and elastin fibres. In addition, the production of tissue inhibitors of metalloproteinase (anti-metalloproteinases) is reduced during the ageing process [Jenkins, 2002].
As with natural ageing of the skin, UV exposure (UVA and UVB irradiation) results in a significant increase in elastase and MMPs activities within the dermal tissue, resulting in the destruction of both the collagen and elastic fibre network [Jenkins, 2002].

The elevation in dermal elastase activity as well as in metalloprotease activity leads to the degradation of the skin collagen and components of the elastic network. As a result of the breakdown of elastin and collagen, which are the main elements of connective tissue, the skin's elastic properties decrease, predisposing the formation of wrinkles [Tsuji *et al.*, 2001].
Gundiah studied the effects of enzyme treatment on the main structural proteins of an arterial tissue [Gundiah *et al.*, 2013]. Histological sections from this study, presented in Figure 5.14, show changes in tissue microstructure after enzymatic treatments. Collagenase treatment shows fragmentation and dissolution of collagen fibres with a lower fibre density (Figure 5.14a). Elastase treatment induces fragmented elastin fibres, with an associated loss in tissue organisation (Figure 5.14b). Elastin fibre thickness and density are also lower in elastase-treated slides than in the corresponding controls.

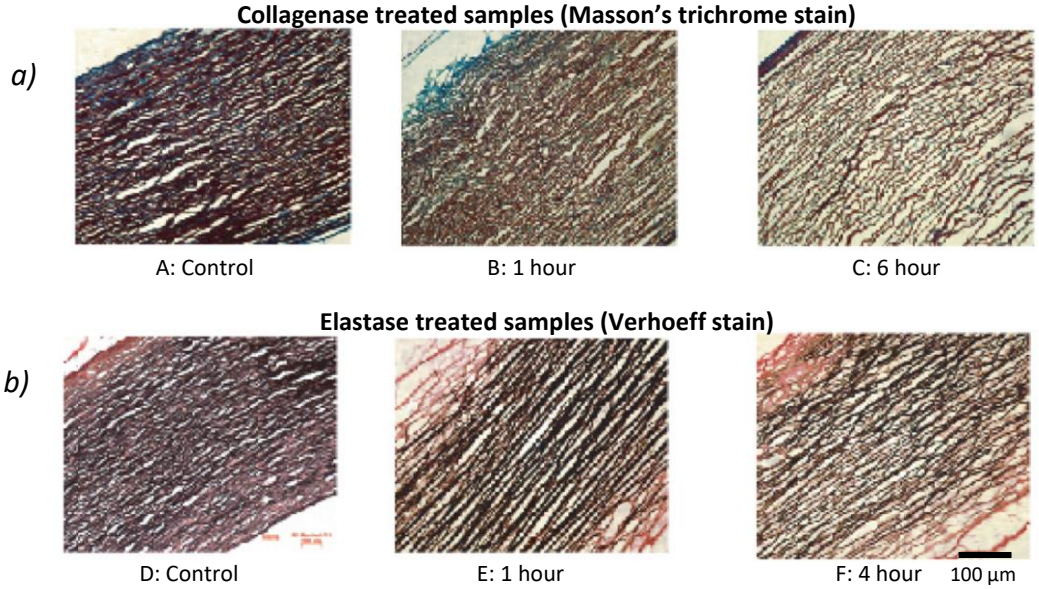

Figure 5.14: Histological section of porcine aorta showing changes in tissue microstructure before and after enzyme treatments [Gundiah et al., 2013]. a) Collagenase treated samples - Masson trichrome staining to identify the presence of collagen (blue staining). b) Elastase treated samples - Verhoeff counterstaining with Picro-ponceau to clearly delineate the presence of elastin (black staining).

Even though the damage caused by these enzymes to ECM components is well known, to our knowledge there have been no studies measuring the impact of enzymatic treatment on the mechanical properties of human skin.

The use of these enzymes in research therefore enables to study skin ageing and photoageing, since these enzymes are expressed naturally in ageing skin or under exposure to UV rays. These enzymes therefore represent a very important subject in the cosmetics area, which is working to create anti-ageing products to counter its effects.

5.3.2 Methodology and presentation of the results

In this Section, we report the characterisation of the mechanical properties of skin explants before and after the introduction of proteolytic enzymes in their culture medium. The introduction of collagenases and elastases into the culture medium of *ex vivo* explants will enable the enzymes to come into direct contact with the dermis. This enzymatic stress, which is known to degrade the skin and in particular the dermal fibres of the ECM, is intended to mimic the accelerated ageing of human skin explants.

The aim is therefore to investigate and evaluate the effect of these enzymes on the mechanical properties of human skin explants *ex vivo* and to propose a model of variation of mechanical properties with the ageing.
In this way, several explants from the same plasty will be allowed to survive with or without enzymes in their culture medium. Two enzymatic studies on two different plasty were carried out: PT (P2746-AB 33) and PD (P2749-AB 42). For this study, several explants from the same plasty were tested over several days. Some explants were not subjected to enzymatic stress and called the Control explants. The other explants were exposed to the enzymes and called the Stressed explants. As both enzymes are introduced into the culture medium of the explant, the dermis of the explant will be directly in contact with these enzymes for the duration of the study.

A first series of tests is carried out on all these explants, before the enzymes are introduced: this is day D0. At the end of these initial tests, on D0, the two enzymes were introduced into the culture medium of the Stressed explants. The culture medium used had a concentration of 50 $U.ml^{-1}$ for collagenase and 6 $U.ml^{-1}$ for elastase (Collagenase from *Clostridium histolyticum* - Sigma ref. C9891 & Elastase from porcine pancreas - Sigma ref. E0127). Enzymatic stress was induced in the Stressed explants throughout the whole study. Then, after 24 to 48 hours (on D+1 and/or D+2), the same series of tests was carried out on all the explants (Control and Stressed).
We observed and quantified the impact of this stress on the mechanical properties of the explants. For all the explants and throughout this campaign, the procedure for placing the explant in the device and the experimental conditions were identical in order to be able to compare the results accurately. The results of the Control skins will be used to validate the viability of the studied explants over time. The results of the Stressed skins will be compared before and after enzymatic stress, in order to measure possible differences in mechanical properties. These differences will therefore be characteristic of the impact of enzymes in the skin.

Visual observation of the explants before and after enzymatic stress already shows some changes of the surface of the explant. The Stressed explant, and in particular its dermis, is clearly degraded.

Furthermore, to the touch, the Stressed explant is looser and flabbier than in its initial state. Figure 5.15 shows this degradation of a skin explant *ex vivo*.

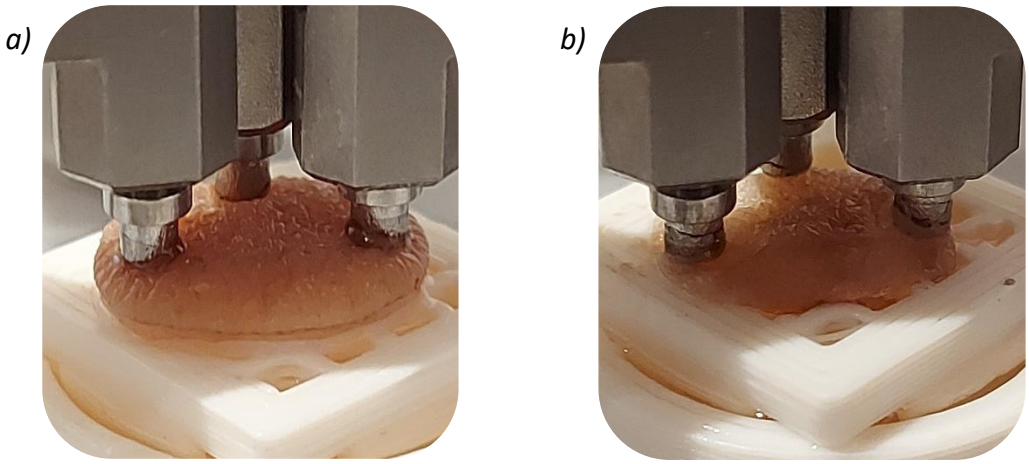

Figure 5.15: Study on enzymatic stress: photos of the PD explant in test configuration, before stress (a) and after 2 days of enzymatic stress (b). Visual observation of the explant clearly shows the degradation of the dermis caused by collagenases and elastases.

5.3.2.A First enzymatic study

This paragraph is dedicated to the results of the first study on the enzymatic stress induced in PT explants. Three Control explants and three Stressed explants were used in this enzymatic study. Figure 5.16 shows the mechanical tensile results, on three Stressed explants, before and after 48 hours of exposure to the enzymes. These graphs highlight the difference in the mechanical tensile behaviour of human skin explants before and after enzyme stress.

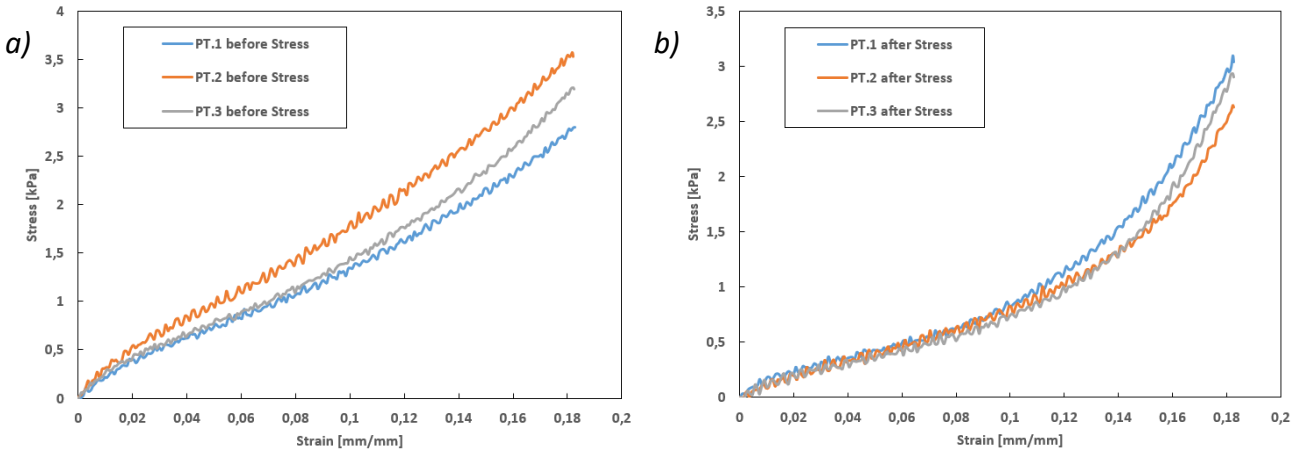

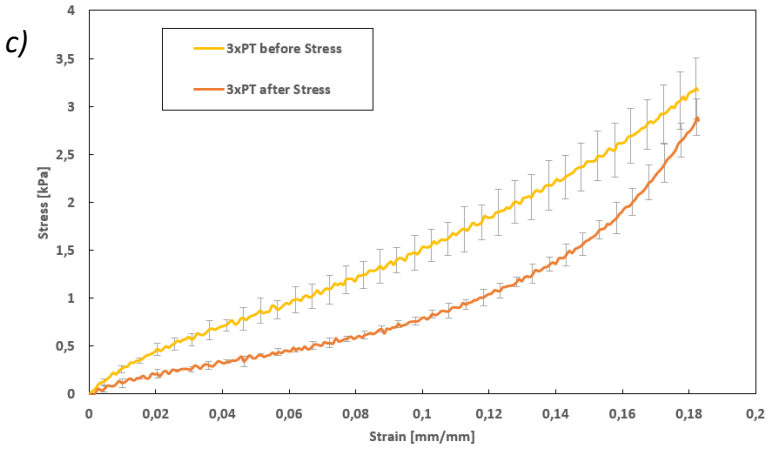

Figure 5.16: Study n°1 on enzymatic stress. Tensile tests on 3 explants, before and after introduction of collagenases and elastases (speed = 10 mm.min^{-1}). Stress versus strain graphs. a) Before stress. b) After stress. c) Comparison of average curves.

First of all, it can be noted that the mechanical behaviour of the three PT explants is relatively similar (approximately 10% of maximum variation before stress over the whole deformation measured). The mechanical behaviour before stress is classic and typical of *ex vivo* human skin explants, as reported in Chapter 4. At this deformation level, the explants exhibit relative linear elastic behaviour.

Two days after the introduction of stress, the mechanical behaviour of the three explants drastically changed. Firstly, the second phase of tissue stretching, well define previously, is visible for these same range of deformations (J-shaped curves). This second phase of stiffening of the mechanical behaviour occurs at strains of around 12%. We also notice that the stress-strain curve is 'hollowed out' at low strains: the elastic behaviour of the skin is greatly reduced. From the very first percentages of deformation, the stresses and moduli measured are much lower than before stress. Before stress, the average Young's modulus of the skins was (27 ± 1) kPa; after stress, the average modulus was (13 ± 1) kPa.
Enzymatic stress has therefore firstly reduced the skin's elasticity and secondly its deformation capacity. The apparent elastic moduli measured and summarised in Table 5.3 confirm this loss of elasticity at low deformations and this stiffening at high deformations.

Figure 5.17 shows the results of dynamic strain sweep tests on the three "Stressed" explants, before and after 48 hours of exposure to the enzymes.

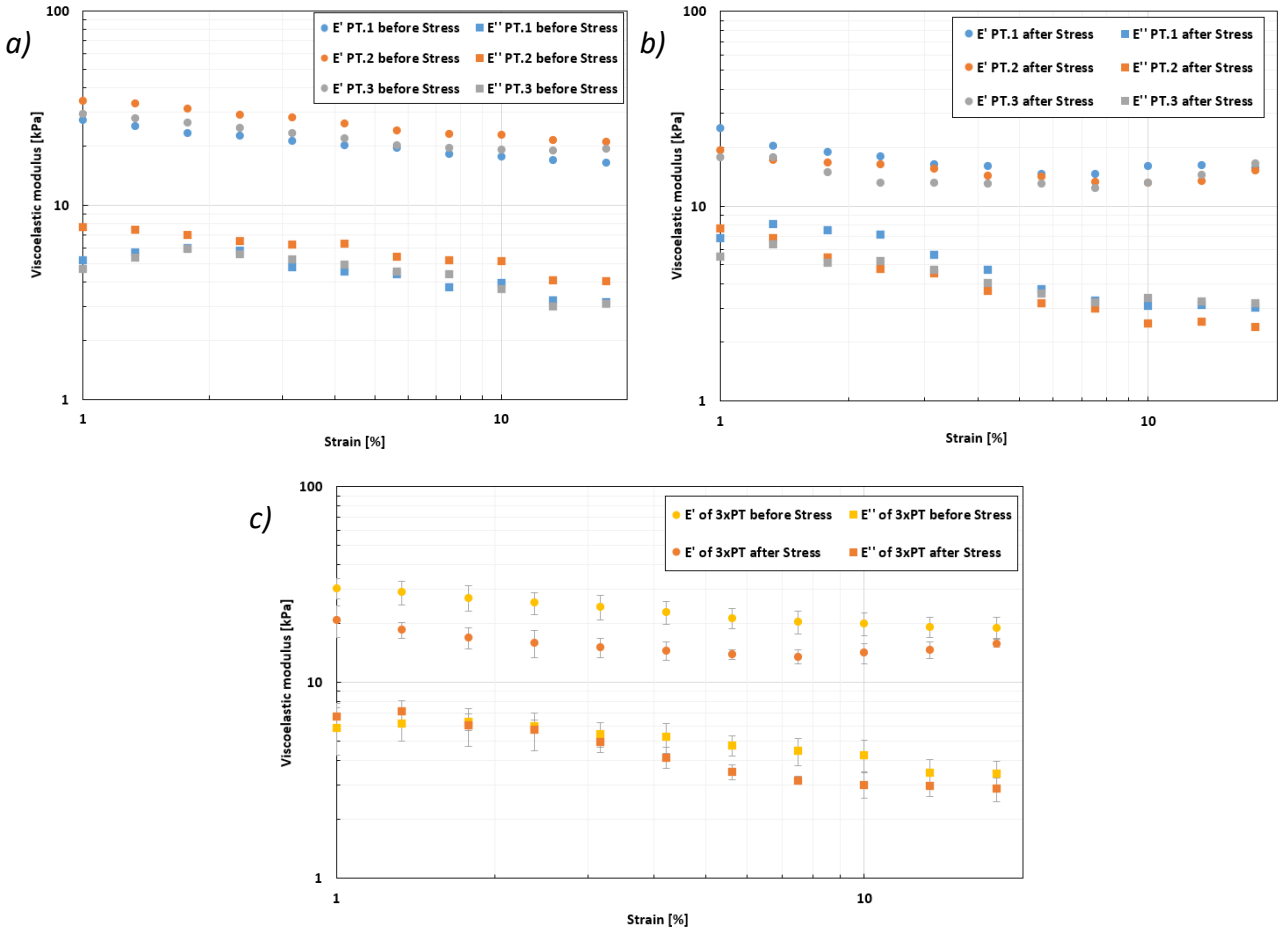

Figure 5.17: Study n°1 on enzymatic stress. Strain sweep tests on 3 explants, before and after introduction of collagenases and elastases (f = 0.5 Hz). Graphs of viscoelastic moduli as a function of strain. a) Before stress. b) After stress. c) Comparison of average curves.

The strain sweep tests show differences in viscoelasticity for the explants before and after stress. The viscoelastic behaviour of the skins before stress is classic and typical of *ex vivo* human skin explants, as reported in Chapter 4.

Two days after the introduction of stress, the viscoelastic properties of all three explants decreased slightly. After stress, the storage modulus is lower over the entire deformation range, confirming the loss of elasticity of the tissue. At low deformations, the modulus of elasticity E' after stress is reduced by around 35%. The loss modulus is less affected and shows an almost similar variation before and after stress, demonstrating a very slight reduction in the viscous part of the mechanical properties of the tissue. As a conclusion, the elastic properties after stress are lower without marked transition with the strain: the linear domain seems about the same. Based on these results, we choose a strain of 10% to perform the spectromechanical analysis which are represented in Figure 5.18.

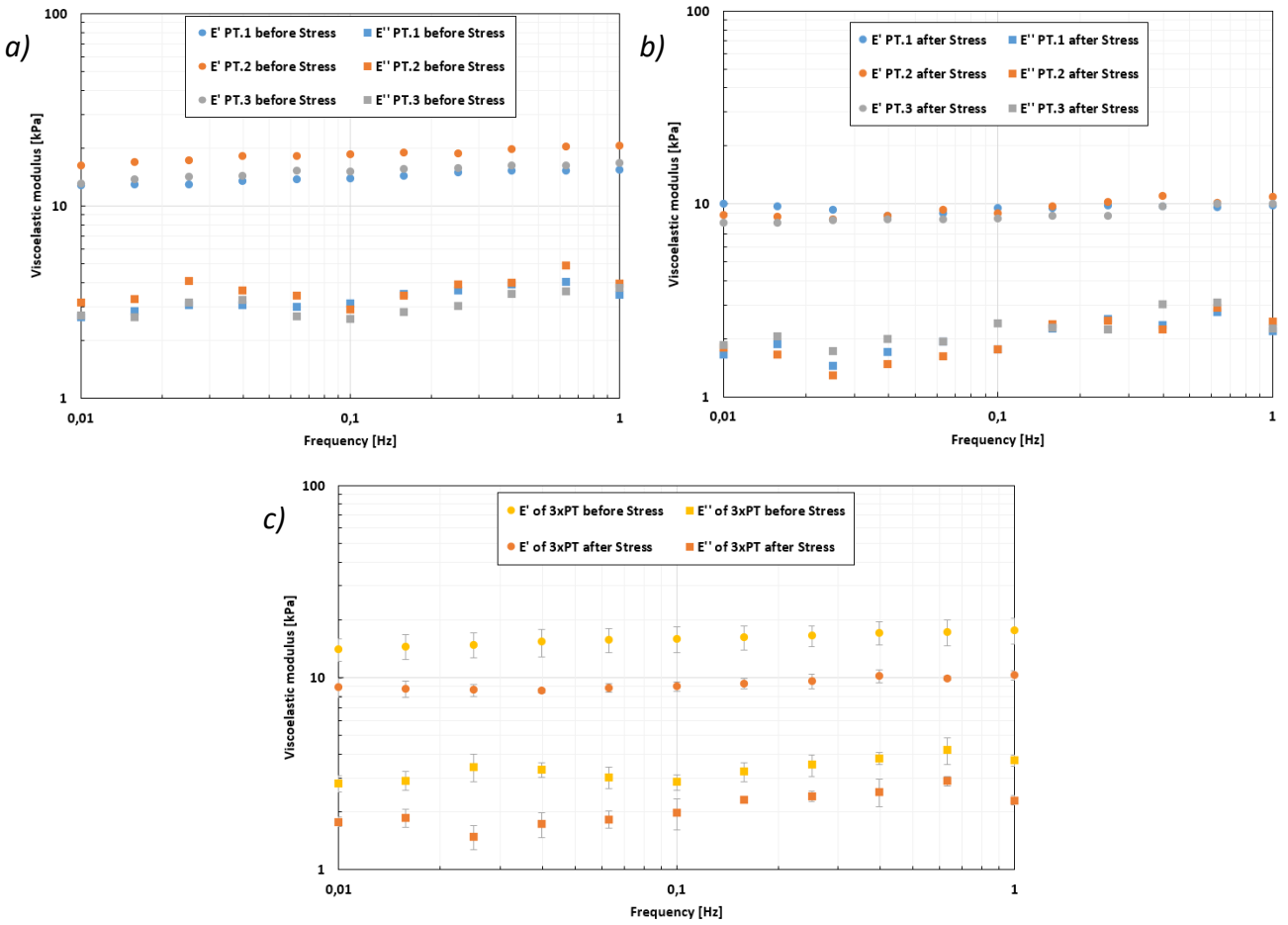

Figure 5.18: Study n°1 on enzymatic stress. Frequency sweep tests on 3 explants, before and after introduction of collagenases and elastases (strain = 10%). Graphs of viscoelastic moduli as a function of frequency. a) Before stress. b) After stress. c) Comparison of average curves.

The frequency sweep tests clearly show differences in terms of elastic and viscous modulus for the explants before and after stress. The viscoelastic behaviour of the skin before stress is classic and typical of *ex vivo* human skin explants, as reported in Chapter 4.

Two days after the introduction of stress, the moduli of all three explants decreased without change for the global variation with the frequency. Over the entire frequency range, the storage and dissipation moduli after stress are significantly lower than before stress: the modulus of elasticity E' is reduced by approximately 45% and the modulus of dissipation E'' is reduced by approximately 30%.

The differences in viscoelastic properties, demonstrated by the spectromechanical analysis, highlight the loss of viscoelasticity due to enzymatic stress. The moduli of elasticity and dissipation, measured and summarised in Table 5.3, confirm this analysis.

Figure 5.19 shows the results of cyclic loading-unloading tests on the three "Stressed" explants, before and after 48 hours of exposure to the enzymes.

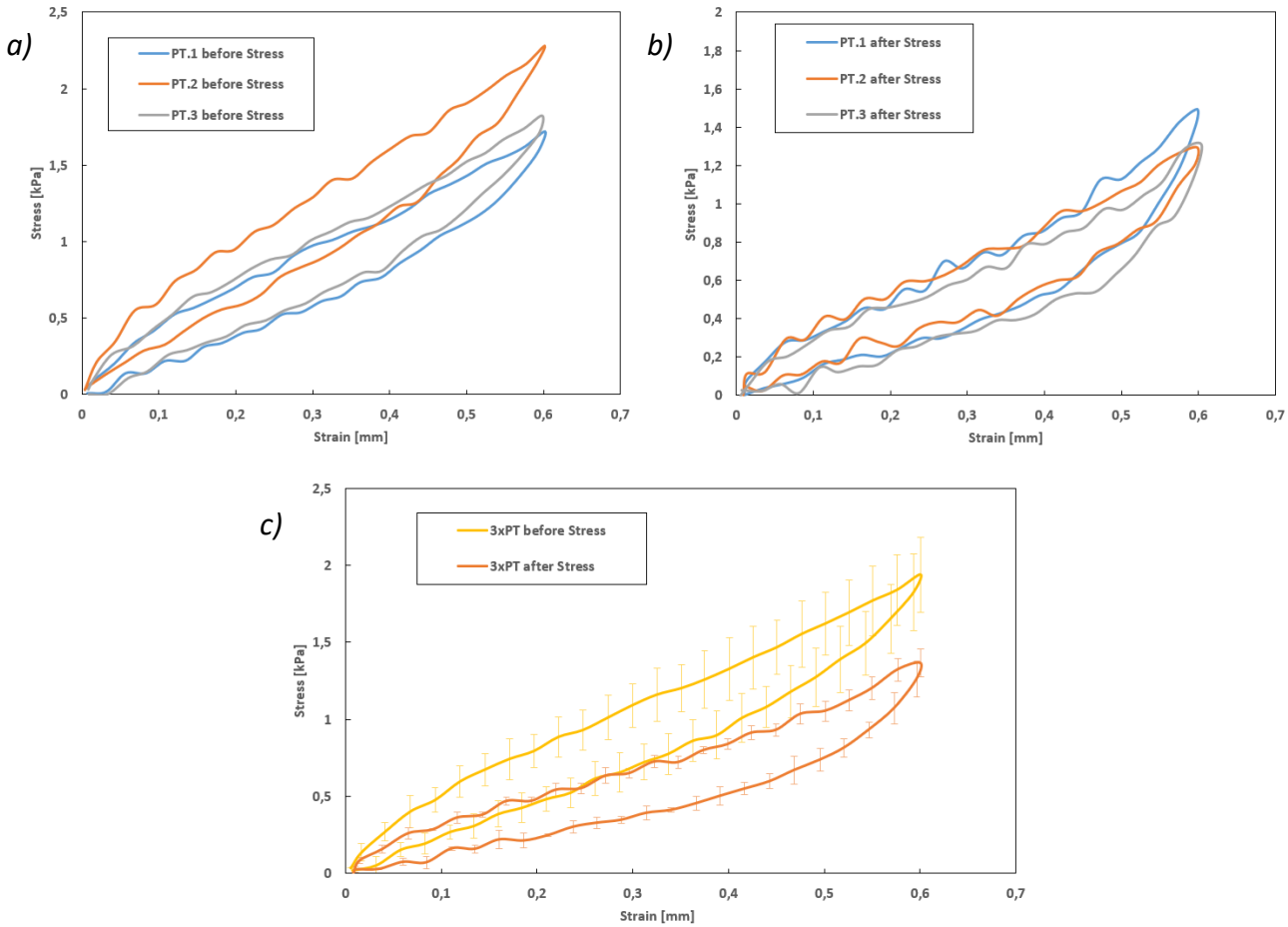

Figure 5.19: Study n°1 on enzymatic stress. 5th cycle of cyclic loading-unloading tests on 3 explants, before and after introduction of collagenases and elastases (strain = 10% / speed = 10 mm.min^{-1}). Stress versus strain graphs. a) Before stress. b) After stress. c) Comparison of average curves.

During these tests, and as presented in the preliminary study on the pre-conditioning of skin explants (see Part 3.1), it can be seen that the mechanical properties stabilise at the 5th cycle.
Figure 5.19 shows that the hysteresis phenomenon is clearly different before and after stress. However, as shown in Table 5.3, the mechanical energy dissipated during a loading-unloading cycle is almost identical before and after stress.

Finally, to demonstrate the reliability of this study, the mechanical results on a "Control" explant tested at D0 and D+2 are presented in Figure 5.20.

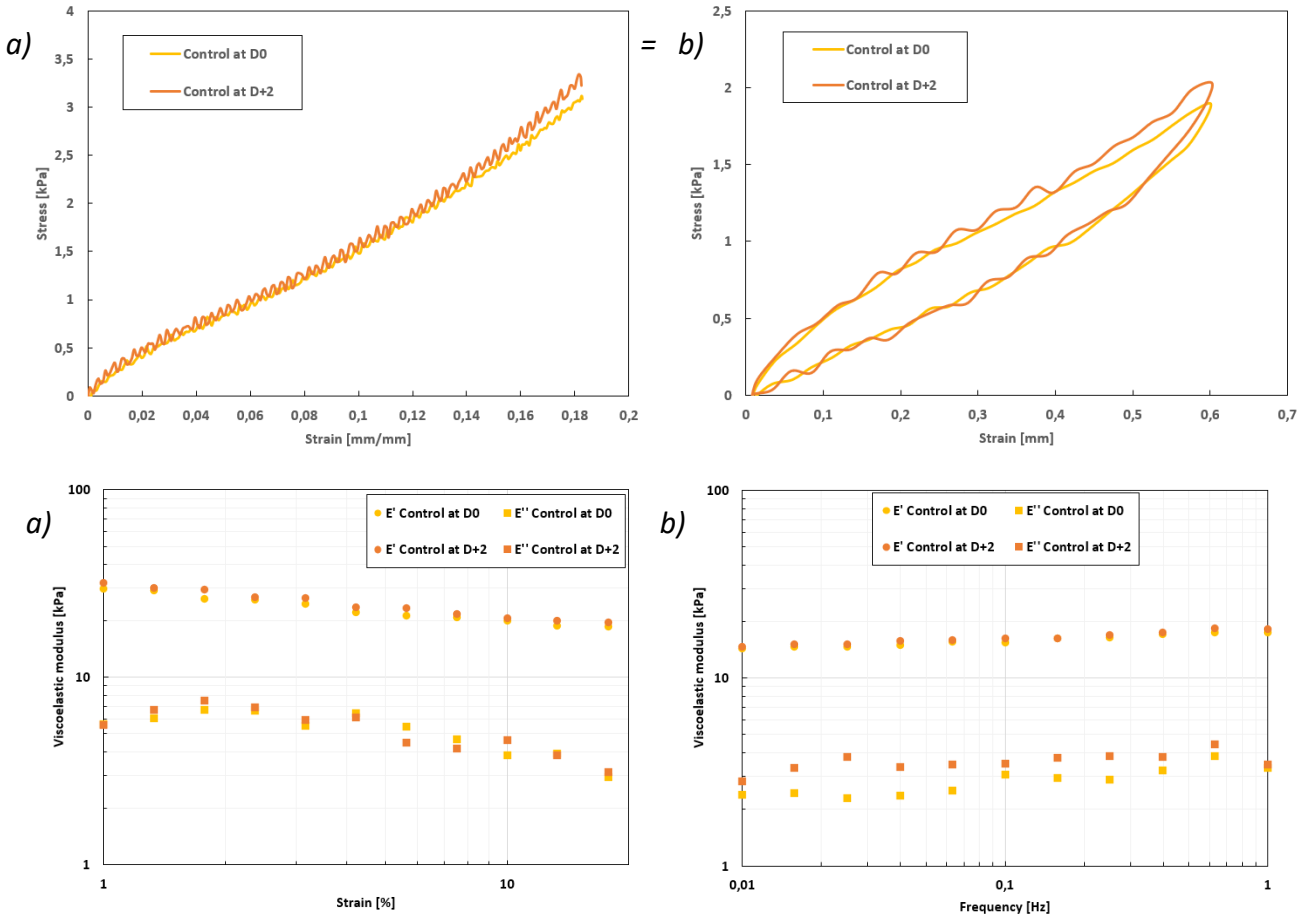

Figure 5.20: Study n°1 on enzymatic stress: complete characterisation of the "Control" explant at D0 and D+2. a) Traction. b) Cyclic loading-unloading. c) Strain sweep. d) Frequency sweep.

As shown in this Figure, the mechanical properties of the "Control" explant were virtually identical over time. The results on this explant confirm the viability of *ex vivo* skin explants during the study period. As demonstrated in Part 4.1.2, the mechanical properties of explants not subjected to external aggression are preserved and considered stable over a period of approximately one week. The conservation of the mechanical properties of the "Control" explant proves the reliability and relevance of the results of this study.

Conclusions: it is clear from all these mechanical tests that the skin is physically damaged after stress. Enzymatic stress therefore has a major adverse impact on the mechanical behaviour of human skin explants *ex vivo*.
The tensile test shows a clear change in the mechanical behaviour of the stressed explant, with a loss of elasticity and deformation capacity (J-shaped and 'hollowed out' stress-strain curve). Dynamic tests also show a reduction of around 30 to 40% in the elastic component of the explants induced by this stress.

All the biomechanical parameters measured during this first study on enzymatic stress are summarised in Table 5.3. These parameters highlight the effect of enzymatic stress on the viscoelastic properties of the explants. As expected, the general loss of viscoelasticity is therefore characteristic of the effect of collagenases and elastases on the skin.

Table 5.3: Study n°1 on enzymatic stress: analysis of biomechanical parameters on PT explants, before and after introduction of collagenases and elastases (with standard deviation of the tests).

		Traction			Strain scanning		Frequency scanning		Hysteresis cycles
Explants	Skin condition	Young's modulus E0 (kPa)	Modulus at 10% deformation (kPa)	Modulus at 18% deformation (kPa)	Viscoelastic modulus at 1% (kPa)	Viscoelastic modulus at 18% (kPa)	Viscoelastic modulus at 0,01 Hz (kPa)	Viscoelastic modulus at 1 Hz (kPa)	Dissipated energy (µJ)
3 × PT (P2646-AB 33)	BEFORE STRESS	**27 ± 1**	**17 ± 1**	26 ± 2	**E' : 30 ± 4**	**E' : 19 ± 3**	**E' : 14 ± 2**	**E' : 18 ± 3**	1 ± 1
					E'' : 6 ± 2	E'' : 3 ± 1	**E'' : 2.8 ± 0.5**	**E'' : 4 ± 1**	
	AFTER STRESS	13 ± 1	12 ± 1	**47 ± 1**	E' : 21 ± 4	E' : 16 ± 1	E' : 9 ± 1	E' : 10.3 ± 0.6	1 ± 1
					E'' : 7 ± 1	E'' : 3 ± 1	E'' : 1.8 ± 0.5	E'' : 2 ± 1	

5.3.2.B Second enzymatic study

This paragraph is dedicated to the results of the second study on the enzymatic stress induced in PD skin explants. A "Control" explant and a single "Stressed" explant were used in this enzymatic study. Figure 5.21 presents the complete characterisation of the viscoelastic properties of the "Stressed" *ex vivo* explant, before stress and at D+1 and D+2 after enzymatic stress. These graphs highlight the difference in the mechanical behaviour of the explant before and after stress, as well as the evolution of the effect of stress over time.

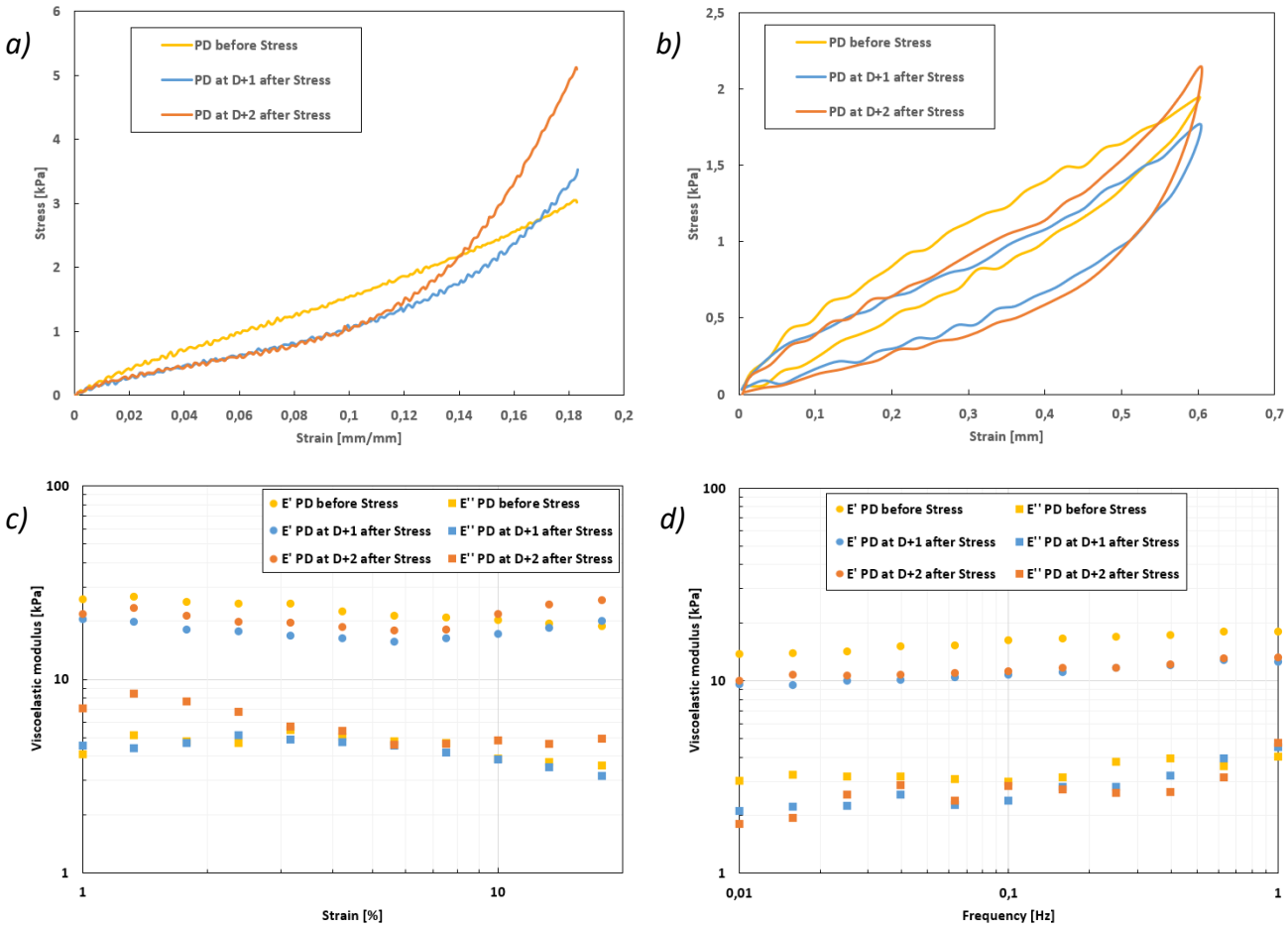

Figure 5.21: Study n°2 on enzymatic stress: complete characterisation of the PD explant before introduction of collagenases and elastases, at D+1 after this stress and at D+2 after this stress. a) Traction. b) Cyclic loading-unloading. c) Strain sweep. d) Frequency sweep.

The tensile and cyclic loading tests show the change in the general mechanical behaviour of the explant with exposure to stress (Figure 5.21a&b). As with the stressed PT explants, the second phase of stiffening in the mechanical behaviour of the explant is visible with stress and becomes increasingly marked with time. In addition, the stress-strain curve is hollowed out at low strains, demonstrating a loss of elasticity in the explant.
The dynamic tests show some changes in the elastic part of the explants with a decrease in their elastic moduli (Figure 5.21c&d). The elastic modulus E' of the explant was reduced by 30% after stress over the entire frequency range. However, there was no visible change in the dissipative behaviour of the explants after stress.
The overall behaviour of the explants does not change, we have the behaviour of a viscoelastic solid with a very slight slope of E' (slope between 0.65 and 1) and E'' (slope between 0.2 and 0.45) as a function of frequency before and after stress.

Finally, to demonstrate the reliability of this study, the mechanical results on a "Control" explant tested from D0 to D+2 are presented in Figure 5.22.

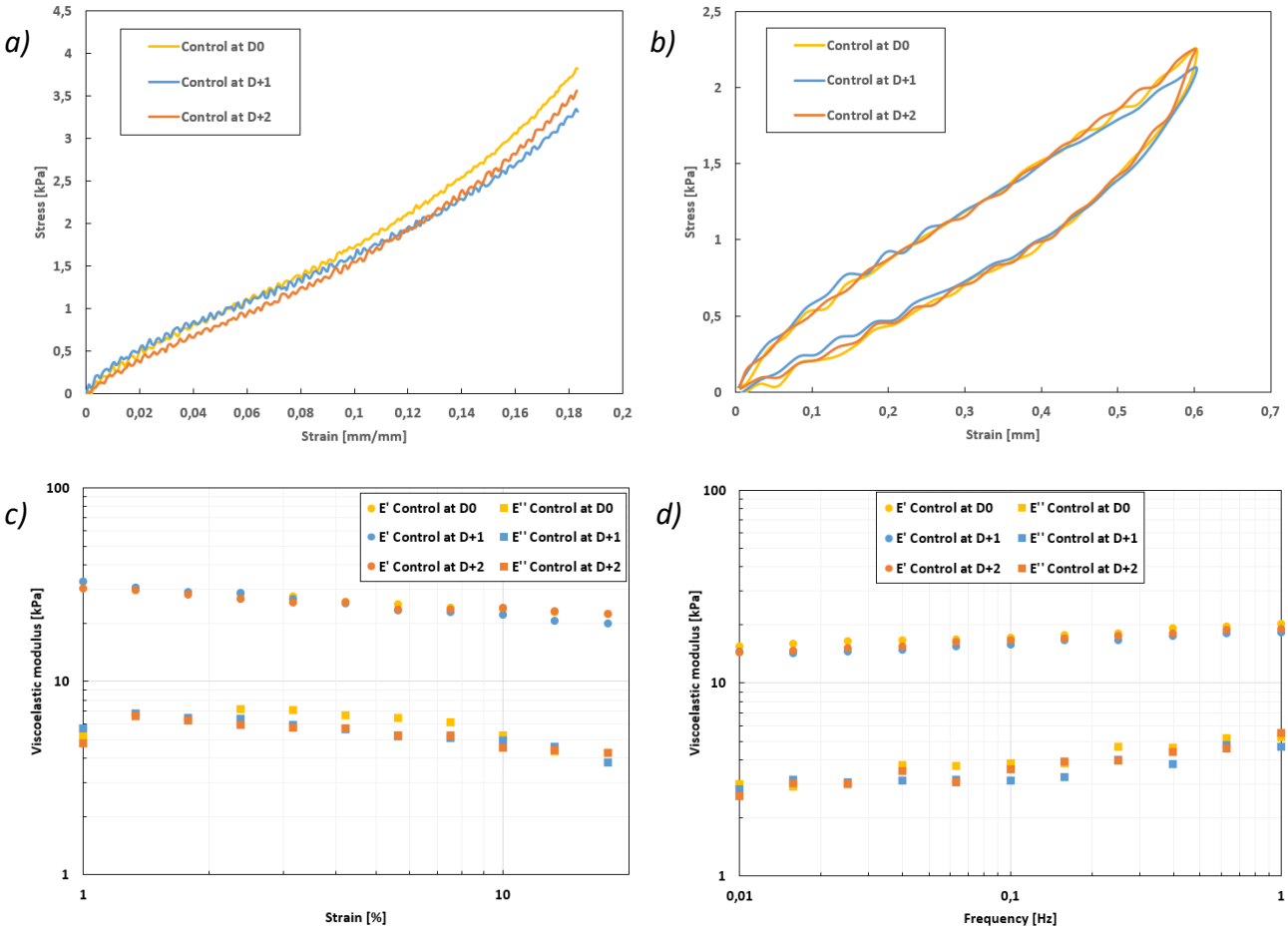

Figure 5.22: Study n°2 on enzymatic stress: complete characterisation of the "Control" explant at D0, D+1 and D+2. a) Traction. b) Cyclic loading-unloading. c) Strain sweep. d) Frequency sweep.

The mechanical properties of the "Control" explant therefore remained unchanged over time, confirming the viability of the explants in the study. The mechanical differences in the "Stressed" skin are therefore attributable to the effect of collagenases and elastases on the skin.

Conclusions: as with the PT-stressed explants, these mechanical tests highlight the harmful impact of this stress on the mechanical properties of *ex vivo* human skin explants. The results show a change in the mechanical behaviour of the stressed explant, with a loss of viscoelasticity and deformation capacity. By monitoring the properties of the explants over time, we were able to observe the evolution of skin degradation. The mechanical changes caused by the enzymes become more pronounced over time. The longer the explant is in contact with these enzymes, the more they will act on the skin, and the more marked these modifications and physical degradations will be.

All the biomechanical parameters measured during this second study on enzymatic stress are summarised in Table 5.4. These parameters highlight the harmful effect of enzymatic stress on the viscoelastic properties of the explants.

Table 5.4: Study n°2 on enzymatic stress: analysis of biomechanical parameters on the same PD explant, before and after introduction of collagenases and elastases (with reproducibility standard deviation).

		Traction			Strain scanning		Frequency scanning		Hysteresis cycles
Explants	Skin condition	Young's modulus E0 (kPa)	Modulus at 10% deformation (kPa)	Modulus at 18% deformation (kPa)	Viscoelastic modulus at 1% (kPa)	Viscoelastic modulus at 18% (kPa)	Viscoelastic modulus at 0,01 Hz (kPa)	Viscoelastic modulus at 1 Hz (kPa)	Dissipated energy (µJ)
Explant PD (P2749-AB 42)	BEFORE STRESS	**23 ± 1**	**17 ± 1**	23 ± 1	**E' : 25.9 ± 0.5**	E' : 18.8 ± 0.5	**E' : 13.7 ± 0.5**	**E' : 18.1 ± 0.5**	1.1 ± 0.8
					E'' : 4 ± 1	E'' : 4 ± 1	E'' : 3 ± 0.5	E'' : 4 ± 1	
	J+1 AFTER STRESS	18 ± 1	14 ± 1	53 ± 1	E' : 20.4 ± 0.5	E' : 20.1 ± 0.5	E' : 9.6 ± 0.5	E' : 12.6 ± 0.5	1.2 ± 0.8
					E'' : 5 ± 1	E'' : 3 ± 1	E'' : 2.1 ± 0.5	E'' : 5 ± 1	
	J+2 AFTER STRESS	18 ± 1	13 ± 1	**81 ± 1**	E' : 21.9 ± 0.5	**E' : 25.8 ± 0.5**	E' : 10 ± 0.5	E' : 13.2 ± 0.5	1.5 ± 0.8
					E'' : 7 ± 1	E'' : 5 ± 1	E'' : 1.8 ± 0.5	E'' : 5 ± 1	

5.3.3 Conclusion

Skin ageing is a complex biological phenomenon influenced by several factors, including genetics, environmental exposure, hormonal changes, and metabolic processes. As the skin is the only organ directly exposed to the environment, the ageing processes resulting from environmental damage are of considerable importance. Studying the effect of proteolytic enzymes that are naturally over-expressed with age or external stress such as UV rays is therefore of crucial importance.

This study therefore focuses on the effect of a stress with a recognised impact on the skin: collagenases and elastases. These are proteolytic enzymes (or peptidases) that break the peptide bonds of proteins. This is known as proteolytic cleavage or proteolysis. In the dermis of skin explants, these enzymes break the bonds of collagen and elastin fibres, thereby affecting the mechanical behaviour of the skin.

The results of this study demonstrate a change in the mechanical behaviour of the explant in extension after exposure to this enzymatic stress.
As the elastic fibrous network, composed of elastin fibres, was altered by the enzymes, the elastic behaviour of the skin was reduced. As reported in tables 5.3 and 5.4, at low deformations, the apparent elastic moduli of the explants are lower after the stress. At higher deformations, the apparent elastic moduli are then higher. We can therefore assume that the network of collagen

fibres, although degraded, is involved more quickly in the skin extension process, making the skin less deformable. To a lesser extent, some dynamic tests seem to show a reduction in the viscous loss properties of the skin.
Stressed skin therefore has weaker elastic and viscoelastic properties, confirming the negative effect of the enzymes. The skin becomes softer at slight deformations and seems to become stiffer at major deformations. This damaged skin can therefore be considered looser and less deformable.
Finally, the analysis on control skin validates the viability of the explants over time and allows to confirm that proteolytic enzymes are the cause of this skin degradation.

These mechanical results are consistent with histological analyses in the scientific literature. Schematically, the phenomenon of degradation of the dermal network by proteolytic enzymes can be represented as in Figure 5.23. The enzymes present in the explants break the peptide bonds of the dermal fibres, which degrade these fibrous networks, and therefore the general mechanical behaviour of the skin.

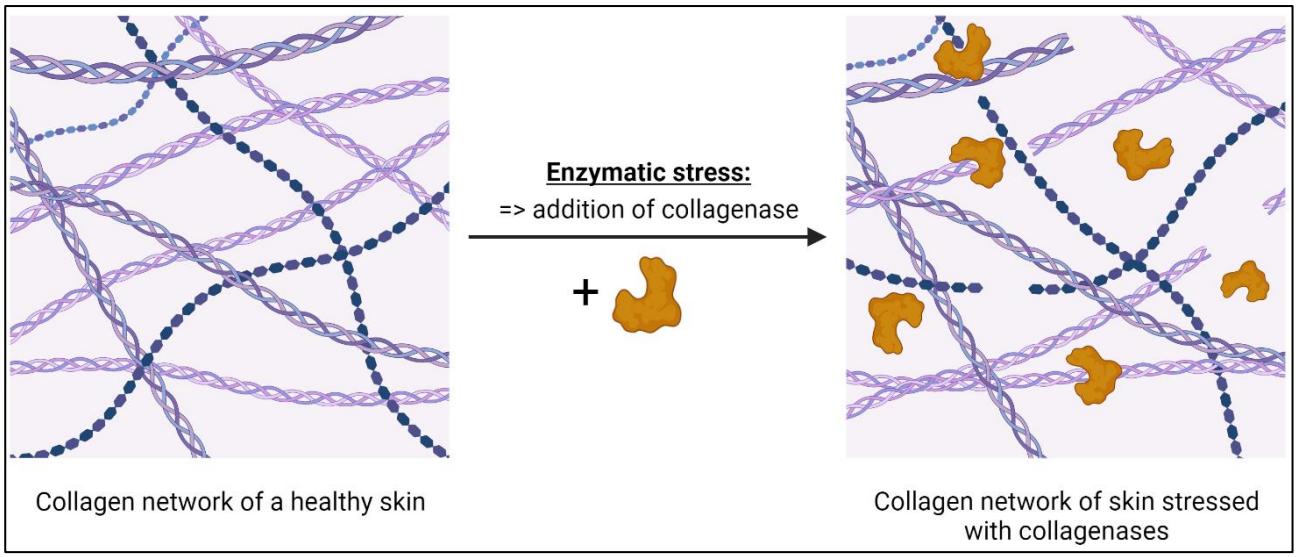

Figure 5.23: Study of enzymatic stress: Schematic diagrams showing the dermal collagen network of healthy skin and of skin exposed to proteolytic enzymes (the same is true for the degradation of the network of dermal elastin fibres).

Enzymatic stress therefore leads to a reduction in the elastic properties of the skin and a stiffening of its mechanical behaviour at large deformations; this is the same mechanical phenomenon as is found during the natural skin ageing process (see Part 4.1.4). Indeed, aged skin will exhibit reduced mechanical properties at low deformations and a rapid increase in the rigidity of the explant, demonstrating reduced extension capacity with ageing.

Since these enzymes are increasingly expressed naturally as the skin ages, we were able to mimic accelerated ageing of the studied explants. The results of our study on this enzymatic stress induced in the skin are rather similar with the results of our study comparing young and aged skin. Figure 5.24 shows the these similarities between the second study on enzymatic stress (Part 5.3.2.B) and the study on the mechanical properties of skins of different ages (Part 4.1.4).

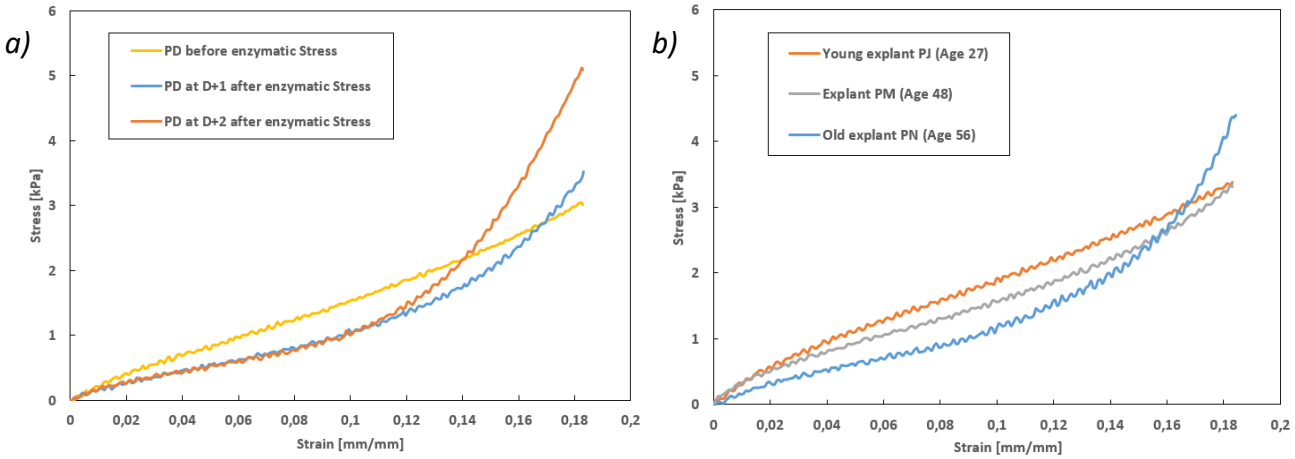

Figure 5.24: Comparison between the study on enzymatic stress (a) and the study on skin ageing (b). Similarities in the mechanical behaviour of these 2 studies.

As shown in this Figure, the mechanical behaviour of young PJ skin (Figure 5.24b) resembles the behaviour of the PD explant before stress (Figure 5.24a). Stressing the skin with collagenase and elastase enzymes seems to have the same effect as skin ageing. Indeed, the mechanical behaviour of the aged PN explant (Figure 5.24b) also resembles the behaviour of the PD explant after enzyme stress (Figure 5.24a).

Generally speaking, the more enzymes are present in the skin (aged skin or intentionally stressed skin as in our study), the more its viscoelastic properties will be damaged. As with aged skin, skin stressed with collagenases and elastases has less viscoelasticity and less capacity for deformation than healthy or young skin.

5.4 Effect of collagenases, elastases, and inhibitors of these proteolytic enzymes on the mechanical properties of human skin

The previous study on proteolytic enzymes is conclusive and of high interest from the point of view of mechanical properties. To go further in terms of understanding degradation phenomena, we have extended experimental work with the analysis of the effect of both enzymes, collagenases and elastases, separately.
Moreover, we have also added a study of the effect of inhibitors of these enzymes on the overall mechanical behaviour of the skin. To complete the understanding of phenomena linked to skin structure, we performed histological experiments.

The first objective of this new study is to investigate the degradation attributable to each of these enzymes, in contrast to Part 5.3 where both enzymes were present in contact with the skin at the same time. In this Part, some skin explants will be exposed only to elastases, while other explants will be exposed only to collagenases. The use of enzymatic degradation treatments specific to fibres (collagenase and elastase separately) would therefore enable to obtain information on the individual and interconnected roles of fibres when the skin undergoes deformation, and to differentiate between skin degradation induced by the two types of enzymes. The second objective is to test the efficacy of inhibitors of these proteolytic enzymes, whose role is to counter the destructive actions of collagenases and elastases.

As seen in Part 5.3.1, although naturally present in the skin, these enzymes are responsible for degrading the tissue's extracellular matrix (Figure 5.14). Collagenases are metalloproteinases that are mainly responsible for breaking down collagen fibres, and elastases are serine proteinases which are mainly involved in the breakdown of elastin. These enzymes are naturally expressed with the ageing of the skin and under exposure to UV rays [Jenkins, 2002].

As well as studying the damage to the skin caused by these enzymes, it is also necessary to find molecules that can counteract and inactivate the effects of this stress. In anti-ageing, finding and proving the efficacy of proteolytic enzyme inhibitors can be useful in preventing the loss of skin elasticity and hence skin slackening. These enzyme inhibitors are molecules that block the activity of proteolytic enzymes, i.e., molecules that prevent them from breaking peptide bonds in proteins. The inhibitors bind to the enzymes, thereby reducing their activity [Rawlings *et al.*, 2004].

In this Section, we report the characterisation of the mechanical properties of skin explants before and after exposure to proteolytic enzymes and inhibitors. As in previous studies, the enzymes and inhibitors will be introduced into the explant culture medium. The experimental methodology used is exactly the same as in Part 5.3.2.

Several *ex vivo* skin explants from the same plasty will therefore be put into survival with or without enzymes, and with and without enzyme-specific inhibitors in their culture medium. Only one skin plasty was used: PI (P2862-AB 59). For this study, an initial characterisation is carried out on all these explants, before any stress: this is day D0. At the end of these initial tests, on D0, each enzyme separately and each inhibitor separately were introduced into the culture medium of the explants. The explants were then all characterised the following day, D+1 after the introduction of the different types of stress.
For this study, we therefore used:

- Control explants, not subjected to stress;
- Explants exposed to collagenases;
- Explants exposed to elastases;
- Explants exposed to collagenases and collagenase inhibitors;
- Explants exposed to elastases and elastase inhibitors.

For all the explants and throughout this campaign, the procedure for placing the explant in the device and the experimental conditions were identical in order to be able to compare the results accurately.

The same enzymes as those in Part 5.3 are used: Collagenase from *Clostridium histolyticum* (*Sigma - ref. C9891)* & Elastase from porcine pancreas (*Sigma - ref. E0127*). Inhibitors specific to each enzyme are also used: Collagenase Inhibitor I (*Merck* - ref. 234140) & Elastase Inhibitor IV (*Merck* - ref. 324759). The same concentrations of enzymes in the culture medium as those used in Part 5.3 are used, i.e., a concentration of 50 $U.ml^{-1}$ for collagenase and 6 $U.ml^{-1}$ for elastase. The amount of collagenase inhibitor is 100 µM, and the amount of elastase inhibitor is 500 µM.

Notes:

- This additional study on these enzymes and their inhibitors has just been completed. Only the initial results of the first mechanical characterisations are presented (histological sections from this study have not been completely analysed).
- However, these initial mechanical results are compared and supported by the results of histological sections taken just before the test campaign at Eurofins BIO-EC Laboratory. In fact, a preliminary histological study, conducted prior to the mechanical testing campaign, was used to validate the choice and quantities of inhibitors beforehand, and to validate the transition to the next stage of the study: ex vivo mechanical characterisation. The histological sections presented below are taken from this preliminary study.

Figure 5.25 shows the mechanical results of tensile tests on an explant exposed to collagenase enzymes and on another explant exposed to elastase enzymes.

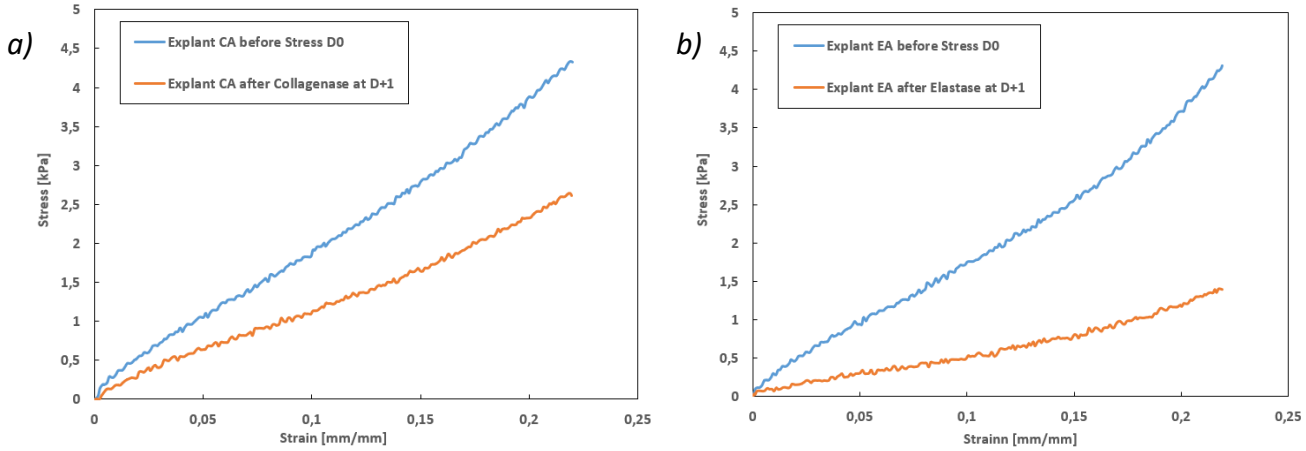

Figure 5.25: Study on collagenases, elastases, and inhibitors. Tensile tests on 2 different explants of the PI plasty: (a) CA explant before and after exposure to collagenases, and (b) EA explant before and after exposure to elastases. Stress versus strain graphs (speed = 10 $mm.min^{-1}$).

This Figure shows that, as reported in Part 5.3 with the enzyme blend, collagenases and elastases have a distinct impact on the mechanical properties of the skin. Indeed, one day after the application of enzymatic stress, the mechanical properties of the explants were significantly reduced. At 10% strain, the apparent modulus of elasticity of the CA explant decreases from (17 ± 1) kPa to (11 ± 1) kPa with the degradation of collagenases (reduction of around 35%). This modulus for the EA explant decreases from (15 ± 1) kPa to (5 ± 1) kPa with the degradation of elastases (reduction of around 65%). These results indicate that the degradation by elastase enzymes (Figure 5.25b) has a much

greater effect on the mechanical properties of the explants than degradation by collagenases (Figure 5.25a).

It should be remembered that the degradation induced by collagenase enzymes is not the same as that induced by elastase enzymes: collagenase enzymes specifically degrade collagen fibres, whereas elastase enzymes degrade mainly elastin fibres. Thus, according to the results reported in Figure 5.25, the elastin fibres are mainly solicited during skin extensions at these levels of deformation.

This reduction in the mechanical properties of the explants following their exposure to proteolytic enzymes is confirmed in Figure 5.26 by the histological sections from the preliminary study.

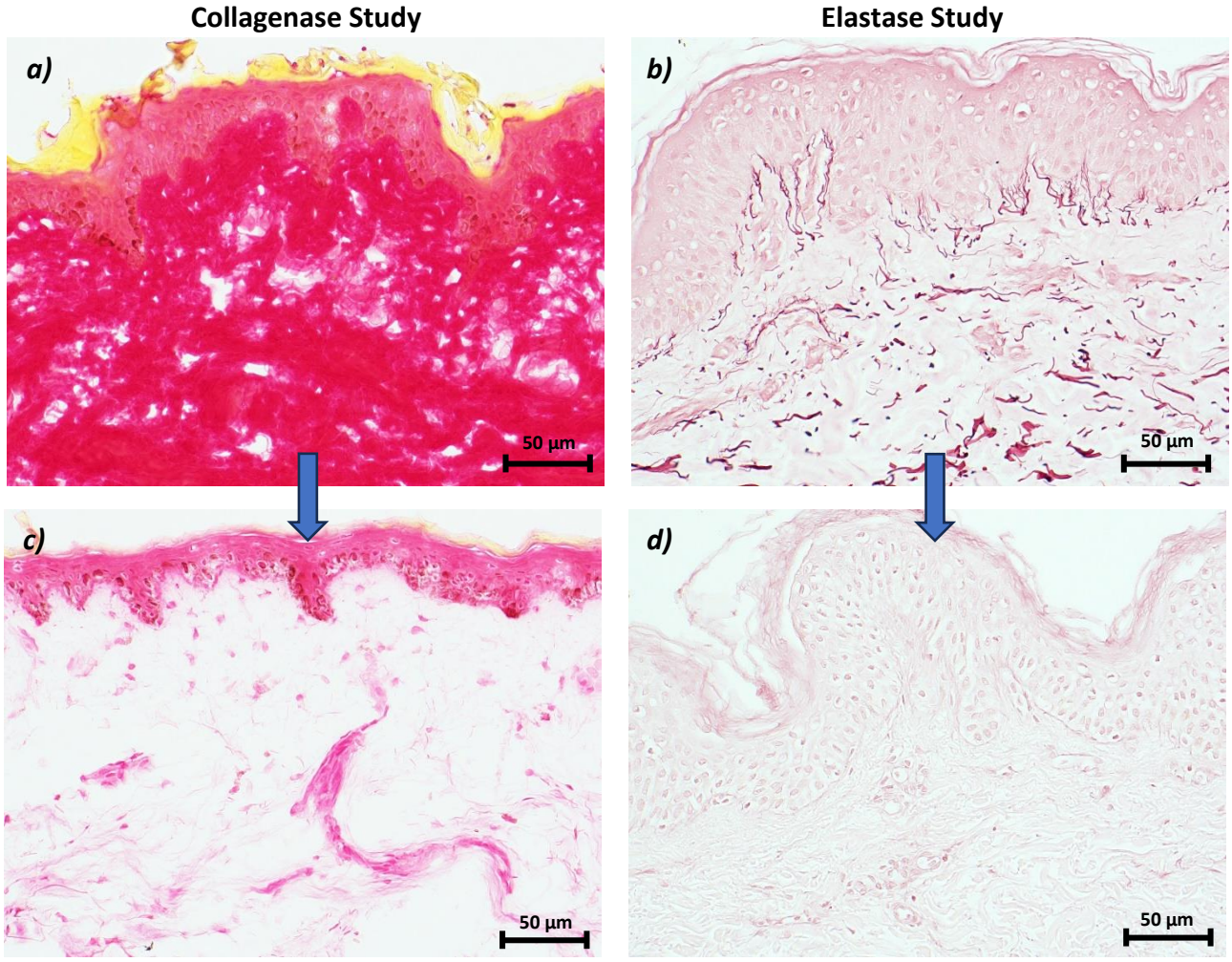

Figure 5.26: Histological sections of ex vivo human skin explants showing changes in tissue microstructure before and after enzyme treatment, without inhibitor. Histological sections produced at Eurofins BIO-EC. Collagenase study (Picro-Sirius red staining to identify collagen): a) Healthy control explant. c) Explant exposed to collagenases (collagenase concentration = 100 U.ml^{-1}). Elastase study (orcein staining to identify elastin (purple colour)): b) Healthy control explant. d) Explant exposed to elastases (elastase concentration = 6 U.ml^{-1}).

These histological sections therefore demonstrate the degradation of dermal fibres caused by proteolytic enzymes. The collagen fibres, stained red in Figure 5.26a for the healthy explant, were almost all degraded in the presence of collagenases: this red coloration is almost no longer present

in Figure 5.26c. Elastin fibres, stained purple in Figure 5.26b for the healthy explant, were also all degraded in the presence of elastases: this purple coloration is no longer present in Figure 5.26d. Histological sections are in agreement with the evolution of the mechanical properties after enzyme applications.

In the same way, we have exposed an explant of the same plasty to "collagenase enzymes + collagenase inhibitors", and another explant to "elastase enzymes + elastase inhibitors". Figure 5.27 shows the mechanical results of tensile tests on each explant.

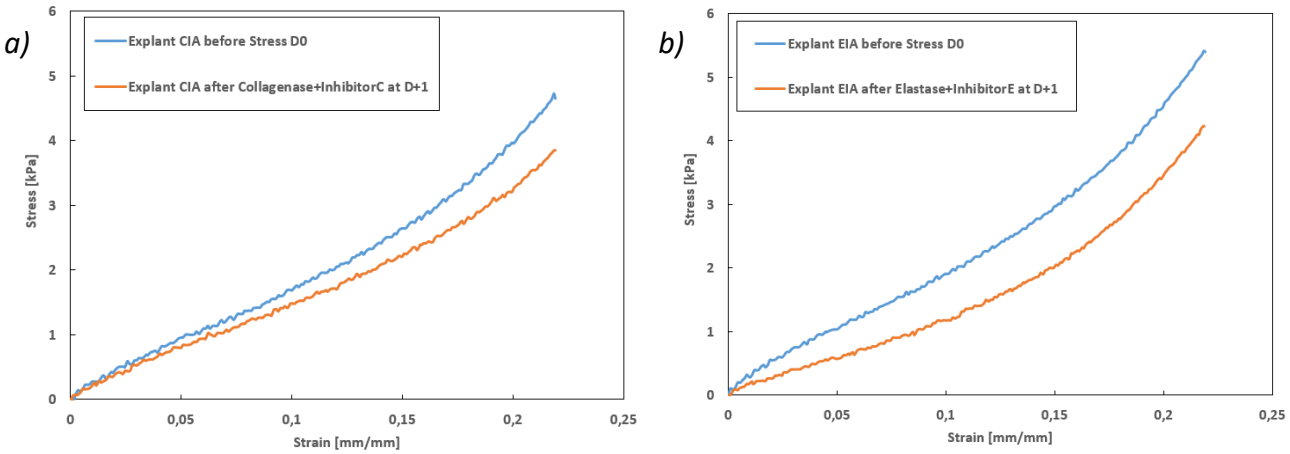

Figure 5.27: Study on collagenases, elastases, and inhibitors. Tensile tests on 2 different explants of the PI plasty: (a) CIA explant before and after exposure to collagenases + collagenase inhibitors, and (b) EIA explant before and after exposure to elastases + elastase inhibitors. Stress versus strain graphs (speed = 10 mm.min^{-1}).

It has been observed that even in the presence of enzyme inhibitors, collagenases and elastases will have an impact on the mechanical properties of the skin. However, there is a significant reduction in enzyme degradation when the inhibitors are present. At 10% strain, the apparent modulus of elasticity of the CIA explant decreases from (18 ± 1) kPa to (14 ± 1) kPa with collagenases and collagenase inhibitors (reduction of around 20%). This modulus for the EIA explant also decreases from (18 ± 1) kPa to (14 ± 1) kPa with elastases and elastase inhibitors (reduction of around 20%).

While we have measured a decrease in modulus of between 65% and 35% with elastase and collagenase respectively, the reduction is lower than 20% when inhibitors are present, confirming the positive effect on the degradation of the mechanical properties of the enzymes in presence of inhibitors.

This protective effect of inhibitors on the different fibres is confirmed in Figure 5.28 by the histological sections from the preliminary study. These histological sections therefore demonstrate that, contrary to Figure 5.26c&d, the degradation of dermal fibres caused by proteolytic enzymes is reduced in the presence of inhibitors. Collagen fibres stained red in Figure 5.28a, as well as elastin fibres stained violet in Figure 5.28b, are present after exposure to stress.

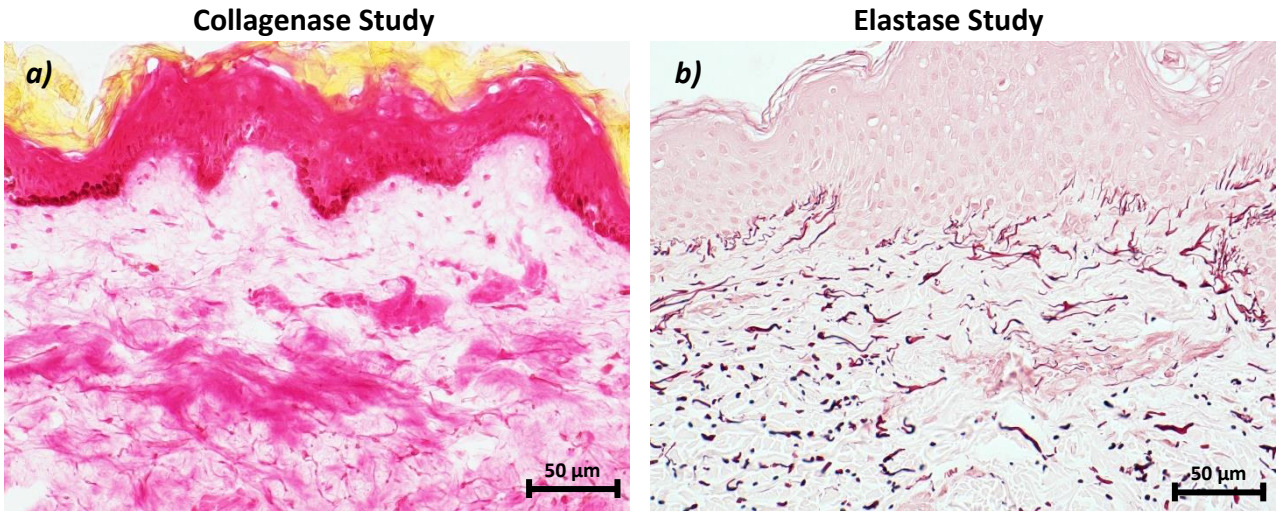

Figure 5.28: Histological sections of ex vivo human skin explants showing the positive impact of enzyme inhibitors on the amount of fibre. Histological sections produced at Eurofins BIO-EC. Collagenase study (Picro-Sirius red staining to identify collagen): a) Explant exposed to collagenase, in the presence of collagenase inhibitor (collagenase concentration = 100 U.ml^{-1} and amount of collagenase inhibitor = 50 µM). Elastase study (orcein staining to identify elastin (violet colour)): b) Explant exposed to elastases, in the presence of elastase inhibitor (elastase concentration = 6 U.ml^{-1} and amount of elastase inhibitor = 500 µM).

Conclusions: the first objective of the study was to examine and compare the degradation of the mechanical properties of the skin induced by each enzyme. The mechanical results presented in Figure 5.25 show a significant deterioration in the mechanical properties of human skin under the effect of the two enzymes. The resulting mechanical properties of the stressed explants are different depending on the enzymes, as they preferentially degrade one type of fibre. These initial results seem to show that the elastin fibre network is mainly solicited during skin extensions at these levels of deformation. These results will have to be confirmed even if, as demonstrated in the scientific literature (see Part 1.3.2) and during our characterisations in Chapter 4, the first phase of skin extension is mainly attributable to elastin fibre networks for low deformations.

The second aim was to prove the possible efficacy of enzyme inhibitors in terms of mechanical properties. The mechanical results presented in Figure 5.27 show a reduction in the deterioration of the mechanical properties of human skin when the inhibitors are present at the same time as the enzymes. The chosen collagenase and elastase inhibitors reduce the activity of collagenases and elastases respectively. We could therefore imagine that these types of inhibitors could, for example, be incorporated into cosmetic product formulations with the aim of achieving an anti-ageing effect.

All these mechanical investigations are supported by the analysis of histological sections (Figures 5.26 & 5.28), confirming:

- The ability of enzymes to degrade dermal fibres. Elastases degrade dermal elastin fibres (Figure 5.26d) and collagenases degrade dermal collagen fibres (Figure 5.26c);
- The ability of enzyme inhibitors to preserve some of the components of the dermal extracellular matrix. Elastase inhibitors protect elastin fibres (Figure 5.28b) and collagenase inhibitors protect collagen fibres (Figure 5.28a).

5.5 General conclusion of the effect of stress

Most studies have focused on the causes and biochemical events leading to the formation of diseased tissues. Fewer researchers have studied the mechanical consequences of such events, which are ultimately important to understand disease progression and designing appropriate treatments.

The device we have developed can be used to characterise, evaluate, and demonstrate the effects of different stresses on the mechanical properties of human skin. In this Chapter, this method has been used to carry out various in-depth mechanical studies on skin *ex vivo*, demonstrating its potential and the diversity of tests it can perform.

Skin lesions such as **stretch marks** have been characterised. Stretch marks (or Striae Distensae) are small purplish-red or whitish cracks that appear when the skin is subjected to excessive stretching. They are often caused by stretching the skin too much, too quickly and too abruptly.
Our study has demonstrated and highlighted the damage and changes of the skin caused by stretch marks. The mechanical properties of stretch marks were compared with those of healthy skin on the same individual. We have physically demonstrated that the mechanical properties are deteriorated in the damaged zone and that they are abnormally high perpendicular to this zone. These analyses are consistent with and complementary to the scientific literature on the physiology of stretch marks.
This study on the characterisation of this damaged area of skin is of high interest as it opens up prospects in the cosmetics and medical fields for researching and testing products that could improve and 'repair' this damaged area.

Ex vivo skin characterisations, which were subjected to various types of stress, were also carried out.
The first stress study investigated the impact of **freezing** skin explants on their mechanical properties. The freezing of living soft tissue is widely used in the medical field to preserve the biological, chemical, and physical properties of samples over time. This technique is very useful for professionals in the field, who can move samples to different locations and use them after a certain period of time. However, due to the formation and disappearance of water crystals during the freeze-thaw cycle, this method of storage could affect the skin.
Our study demonstrated the slight stiffening effect of freezing on the mechanical properties of human skin explants. The mechanical properties of explants before and after a period of freezing were compared. The results show that thawed skin has slightly stiffer mechanical properties than fresh skin.
This study on freezing warns users of this method of preserving soft tissues about its possible impact on the mechanical properties of the tissue.

The second stress study investigated the impact of **enzymatic stress** on the mechanical properties of skin explants. This stress was chosen because proteolytic enzymes are naturally over-expressed with age or an external stress such as UV rays. To mimic accelerated ageing of the skin, we designed a series of experiments aimed at modifying the main mechanical constituents of the skin, collagen and elastin, by enzymatic degradation of tissues *ex vivo*.

Our study demonstrated and highlighted the mechanical consequences of skin degradation induced by collagenases and elastases. The mechanical properties of explants before and after contact with the enzymes were compared. The targeted treatment of these dermal fibres (collagen and elastase) therefore led to alterations in the mechanical behaviour of the explants. Indeed, we have demonstrated that the mechanical properties deteriorate when the explants are brought into contact with these enzymes. The viscoelastic behaviour of the skin is greatly reduced, quantifying the known negative effect of these enzymes on the mechanical properties of the skin.
This study on enzymatic stress further enables to mimic the natural phenomenon of skin ageing in order to study it better. With this mechanical characterisation of human skin treated with elastase and collagenase a basis for the construction of constitutive models to represent various states and progressions of skin ageing is provided.

Finally, the last study on stress inhibitors demonstrated the positive impact of these inhibitors in delaying the degradation of dermal fibres. This study also opens up prospects in the cosmetics and medical fields for researching and testing products that could 'counteract' or delay this ageing of the skin.

These various studies prove that our instrumentation can address medical and cosmetic issues. Specific subjects in dermatology and cosmetics have therefore been studied so that this research can help in the prevention, diagnosis, and treatment of skin diseases.
This Chapter therefore demonstrates the scientific contribution made by our instrumentation to innovative subjects in these fields. The purpose of our method, which is to evaluate the negative effect of various stresses and the effectiveness of therapeutic treatments, is therefore demonstrated as described in this final Chapter.

Note on the use of ex vivo human skin explants:
One of the main advantages of our instrumentation, and not the least, is the use of small ex vivo human skin explants to perform the studies (explants less than 2 cm in diameter). As human skin explants are rare and expensive 'materials', using little pieces of skin is an advantage for the user. Indeed, to carry out complete studies on the impact of a stress or cosmetic product on the mechanical properties of the skin, only a few small-sized explants are needed.

Conclusions and Prospects

Global mechanical properties measurements are of great interest for measuring the 'health' status of the skin and determining any correlation with the development of a disease. Measurements of mechanical properties skin are not only essential in dermatology, but also for testing the efficacy of cosmetic and pharmaceutical products as well as the effect of environmental stresses.
These measurements enable to determine several biomechanical parameters used to characterise the skin. Alongside biochemical characterisation of the skin, these properties now have their place in dermatological diagnosis, therapy, research, and development.

The instrumentation development work was crucial during the first two years of the thesis, as the relevance of this research is based on the performance and reliability of the instrumentation.
If we compare the initial version of the equipment with its final version, we can see that numerous modifications have greatly improved its ability to accurately characterise the overall mechanical behaviour of human skin. The first modifications made possible to carry out dynamic tests and adapt the device to measurements with *ex vivo* human skin samples. Other modifications have enhanced the accuracy of the measurements, such as replacing the force and distance sensors. Finally, the addition of sensors measuring the compression force (in the normal direction to the surface of the sample) of the studs on the skin has made the device more reproducible and less operator-dependent.

Developing a device can be a never-ending process. Indeed, each improvement that is made generates new ideas and possibilities that could lead to further adjustments to the equipment. However, during the second year of this present work, we took the decision to put the development of the device on hold in order to devote our time to carrying out as many experimental studies on human skin as possible.

The final version of the equipment, described in Part 2.1.3, enabled us to accurately characterise the overall mechanical properties of the skin. One measurement axis is used to obtain information on the deformation and tensile strength of the skin sample, while the other axis is dedicated to controlling the positioning of the samples. The final configuration, measurement methods and protocols used can be considered reliable and robust for measuring the mechanical properties of human skin. The results obtained are considered as repeatable and reproducible, and the values measured by the various sensors were initially validated and certified by tests on tension springs.
In addition, the variety of tests that can be performed gives the opportunity to carry out an in-depth analysis of the viscoelastic properties of the skin. These properties can be fully characterised either statically or quasi-statically using tensile and stress relaxation tests, or dynamically using spectromechanical analysis.

With this thesis, we have therefore developed an innovative device for assessing the viscoelastic properties of different types of materials in a precise and thorough manner.

Thanks to the collaboration established during the thesis with the company Eurofins BIO-EC, we were able to carry out some extremely valuable tests on *ex vivo* human skin samples. These tests

represented a significant advance in the development of our equipment and in the overall achievements of our project.

This thesis work firstly demonstrated the reliability of our device for characterising the viscoelastic properties of healthy, stress-free *ex vivo* human skin explants. These tests on different explants have made possible the exploration of the overall rheological properties of the skin and to obtain a broad spectrum of mechanical properties.
The same mechanical characterisations were then carried out on explants that had been subjected to various stresses, with the aim of analysing their impact on the mechanical properties of human skin. This work has led to innovative research into topics that have received little attention in the scientific literature. Thanks to in-depth bibliographic research on these different stresses, we were able to establish a phenomenological link between the physiology of the skin and its mechanical properties, which enabled us to corroborate the initial mechanical results obtained with our instrumentation.
Skin lesions such as stretch marks were studied on the explants. The results showed a degradation of mechanical properties in the damaged skin zone and abnormally high mechanical properties perpendicular to this zone. The freezing process of the explants was also analysed, showing a weak stiffening effect on their mechanical properties induced by this method of sample preservation. Exposing the explants to proteolytic enzymes induced stress similar to accelerated skin ageing. Collagenases and elastases, degrading the dermal fibres of the explants, led to a significant reduction in their viscoelastic properties.
Finally, mechanical analysis coupled with histological analysis confirmed the degradation of dermal fibre networks induced by these proteolytic enzymes. This last study also enabled to validate the positive effect of inhibitors of these enzymes, allowing to reduce their activities and thus to reduce the degradation of the mechanical properties of the skin.

During this thesis work, these latest mechanical studies on the analysis of damaged skin or on the effect of stresses that have a recognised impact on the skin have shown that this new instrumentation could be used to deal with concrete and topical subjects in the fields of dermatology, cosmetics, and medicine.

Due to the time required to develop the instrumentation, the collaboration established with Eurofins BIO-EC during the thesis, and the limited availability of human skin plasty, a limited number of explants were analysed during the various studies. The main limitation of this research work lies in the fact that the limited number of skin samples analysed does not allow statistical analyses to be carried out to reinforce the initial results obtained.

The biomechanical properties of the skin have always been considered very important by dermatologists and biophysicists. The elasticity is considered as the most important parameter because it is the most frequently measured parameter and is characteristic of this organ of the human body. However, and as describe in this work, we consider that the global viscoelastic properties must be taken into account. These properties vary during the skin's ageing process or when it is subjected to certain stresses or diseases.

Measuring elasticity is a standard parameter for all cosmetic applications. This measurement is essential for product development in order to prove efficacy and justify advertising claims. Typical claims such as 'firming', 'anti-ageing', 'promotes skin elasticity', 'against skin slackening', etc., can be validated using our instrumentation. This measurement is also important in fundamental dermatological research on humans and animals. The device developed in this work therefore has applications in the fields of cosmetics, medicine and any other field related to human skin.

Compared with the instruments already on the cosmetics market, such as the Cutometer® presented in Appendix 4, we have identified several advantages of the equipment designed:

- A complete assessment of the viscoelastic properties of human skin. The ability to carry out dynamic mechanical tests provides precise information on the elastic and dissipative behaviour of the skin at different load frequencies;

- The ability to study the effect of different stresses, positive or negative, on the mechanical properties of the skin by combining instrumentation with the use of *ex vivo* human skin explants maintained under physiological conditions for several days. The effect of these stresses can therefore be assessed and monitored over time;

- The use of small *ex vivo* explants (12 to 20 mm in diameter) to carry out the tests, enabling analyses to be carried out even when there are limited quantities of skin samples available. As human skin explants are precious and expensive 'materials', using little skin is a fundamental advantage for the user. Indeed, to carry out complete studies on the impact of a stress or a cosmetic product on the mechanical properties of the skin, only few small-sized explants are needed;

- An easily transportable device, with limited dimensions and weight, that can be set up quickly. It can be moved to any laboratory, offering great flexibility, and facilitating its use in different contexts and working environments.

Prospects

The first prospect of this research work is to continue the initial studies carried out, increasing the number of tests performed on skin explants to reinforce the initial conclusions. These future tests will offer the possibility of conducting quantitative and statistical evaluations with a larger sample size.

As demonstrated in Chapter 5, the instrumentation developed enables the study of the impact of different types of stress on the mechanical properties of human skin. A wide range of stresses can therefore be considered and studied. These include external stresses that damage the skin, such as UV rays, but also medical or cosmetic products that protect or are beneficial to the tissue.

In view of the initial conclusive results of the study on the effect of enzymatic stress on the mechanical properties of human skin, it would be interesting to continue the analysis of the effect of inhibitors of these enzymes. The research work would enable to identify collagenase and elastase inhibitors that could delay the accelerated skin ageing imposed on the explants. This *ex vivo* study on the effectiveness of an anti-ageing treatment would have a direct application in the field of cosmetics and would show that this new instrumentation could help in the development of products intended for treatments.

Another important prospect for our device is the study of skin healing. By making incisions on skin explants *ex vivo*, we will be able to observe the skin healing process. As presented in Appendix 5, skin has an excellent regenerative capacity, which allows rapid healing in the event of skin injury. However, if wounds do not heal in an orderly and rapid fashion, this can lead to chronic ulcers. Effective treatment of chronic wounds remains a global challenge. Our equipment can therefore be used to address this issue, to study the healing process without treatment and to evaluate the effectiveness of treatments that promote healing. The potential of innovative dressings to promote wound repair and healing can also be analysed. In the medical field, measurements of mechanical properties will enable to monitor the effect of products applied to promote healing or treat an injured area.

The innovative instrumentation presented in this research work was initially developed with the aim of measuring the mechanical properties of *ex vivo* skin samples. Performing tests in this configuration enables to induce and monitor skin degradation on *ex vivo* skin explants. However, our system also allows *in vivo* tests to be carried out using the central space under the four mechanical loading arms. Indeed, as Figure 5.29 shows, it is possible to position a person's forearm in the device. In addition to *ex vivo* tests, the equipment therefore has a test configuration designed to study the mechanical properties of human skin *in vivo*.
Being able to work *in vivo* with our instrumentation is an advantage because it allows preliminary *ex vivo* research to be extended or complemented, which can contribute to improving the prevention and treatment of various skin conditions, as well as developing cosmetic products that are better adapted to individual skin care needs.

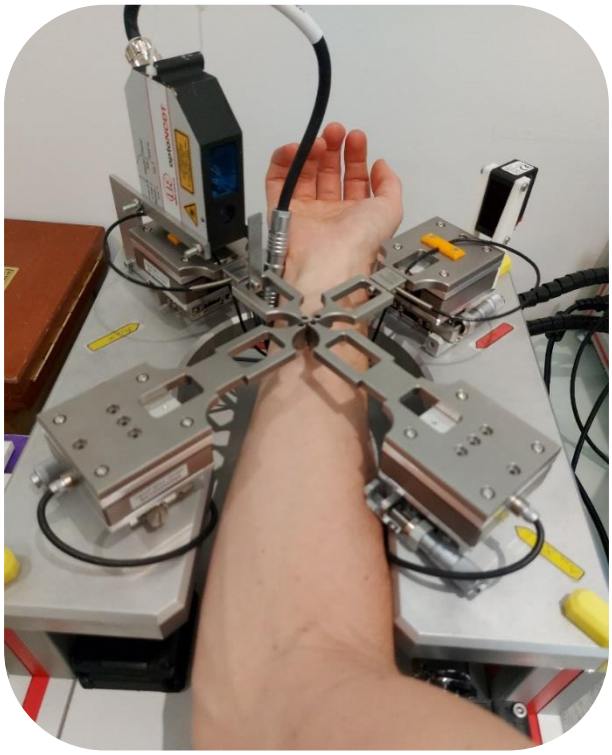

Figure C.1: Photo of the configuration of the device in "in vivo" mode with the forearm of a volunteer patient.

Another potential use for our instrumentation is to characterise the mechanical properties of burnt skin (the skin of 'burn victims') or injured skin, such as skin confined under dressings, pressure sores caused by friction, or scars following surgery. These analyses will enable to understand the behaviour of these types of skin so that medical treatments can be better adapted, and to propose possible grafts with mechanical properties similar to those of the skin of the burned or injured patient. Our equipment could therefore also be used in surgery.

Although our device is initially designed to characterise the mechanical properties of human skin, it can also be used to measure the mechanical properties of any soft tissue or material with similar mechanical properties. For example, it is possible to carry out tests on collagen matrices that mimic the mechanical behaviour of skin. These tests would enable, for example, to avoid the use of human skin explants to analyse the effect of different types of stress on collagen fibres beforehand.
Characterisation and analysis of the mechanical properties of artificial skins would also be invaluable in the medical field, as a better understanding of these materials would enable possible grafts to be better adapted for patients.

Finally, phenomenological modelling of these changes in mechanical properties and their evolution over time could be proposed with the aim of monitoring and anticipating the impact of various stresses on the elasticity of human skin.

During this research work, the preparation process of human skin explants, carried out by the Eurofins BIO-EC laboratory, does not take into account the anisotropy and tension lines of the skin.

It would be beneficial to initiate biopsy monitoring as soon as the skin plasty is cut, enabling the initial contraction of the explants to be observed and followed to determine skin tension lines.
In addition, preliminary tests in different directions of the explant prior to full mechanical characterisation could be carried out, similar to those presented in Part 3.7, with the aim of determining the specific tension lines of the examined skin.
These preliminary observations and tests, carried out before each full characterisation, would facilitate the comparison of the mechanical properties of several skins, by ensuring that they were all measured in the same direction relative to the skin tension lines (for example, either parallel to the Langer lines or perpendicular to them).

The equipment we have developed can still benefit from various improvements and can also be used to carry out other types of complementary mechanical tests on the skin, in particular tests under multiaxial loads using the second measurement axis. This type of load would enable to reach the anisotropic equilibrium of the skin and directly study its anisotropic behaviour.

It would also be interesting to be able to measure the mechanical properties of the skin over larger deformations. Our current piezoelectric actuators only allow a maximum displacement of 600 µm. These tests would enable us to observe the behaviour of the skin at higher deformations and to study its behaviour at break. This information would be complementary to that we already have for low deformations. In fact, taking measurements on an *ex vivo* sample provides an advantageous way of studying mechanical properties beyond the elastic region by subjecting the skin sample to large deformations.
Furthermore, the results obtained on the notion of skin pre-tension, in Part 3.6, encourage us to think about new types of attachment of the sample to the device with the aim of proposing characterisations with different types of pre-tension and getting closer to *in vivo* test conditions.

In addition, the programming of the software and the processing of the results can still be improved. One improvement would be to create a command in the software interface to run a series of successive tests without operator intervention. For example, a sequence of rapid tensile and frequency sweep tests for a quick 5 min analysis, or a more complete sequence including all the mechanical tests for an overall analysis of the skin's mechanical properties. This would simplify procedures and reduce operator handling time.
Another important point would be to automate the data processing to obtain the final results directly, such as the apparent moduli in simple traction, as well as the viscoelastic moduli in dynamic mechanical analysis.

Finally, to improve patient comfort during *in vivo* tests, modifications to the device could be considered, such as installing a removable 'splint' to place the forearm in place of the 3D-printed sample holder, or adding metal shims to the device's translation arms to raise them so as to have more space to accommodate the forearm at the centre of the instrumentation. These *in vivo* improvements could possibly be followed by an embellishment of the instrumentation to make it more aesthetically pleasing from a visual point of view.

Conclusions et Perspectives

Les mesures des propriétés mécaniques globales sont d'un grand intérêt pour évaluer la "santé" de la peau et déterminer toute corrélation avec le développement d'une maladie. Les mesures des propriétés mécaniques de la peau sont non seulement essentielles en dermatologie, mais aussi pour tester l'efficacité des produits cosmétiques et pharmaceutiques ainsi que pour mesurer l'effet des contraintes environnementales.
Ces mesures permettent de déterminer plusieurs paramètres biomécaniques servant à caractériser la peau. À côté des caractérisations biochimiques de la peau, ces propriétés ont maintenant leur place dans le diagnostic, la thérapie, la recherche et le développement dermatologique.

Le travail d'instrumentation et de développement technologique fut très important lors des deux premières années de thèse car la pertinence de ces recherches repose sur la performance et la fiabilité de l'instrumentation.
En comparant la version initiale de l'appareil à sa version finale, on peut noter de nombreuses modifications qui ont grandement amélioré sa capacité à caractériser avec précision le comportement mécanique global de la peau humaine. Les premières modifications ont permis d'effectuer des tests dynamiques et d'adapter l'instrument à des échantillons de peau humaine *ex vivo*. D'autres modifications ont augmenté la précision des mesures, tels que le remplacement des capteurs de force et de distance. Enfin, l'ajout de capteurs mesurant la force de compression (dans la direction normale à la surface de l'échantillon) des plots sur la peau a rendu cet appareillage reproductible et moins dépendante de l'opérateur.

Le développement d'une nouvelle instrumentation peut être un processus sans fin. En effet, chaque amélioration apportée génère de nouvelles idées et possibilités qui pourraient conduire à d'autres ajustements de l'instrument. Néanmoins, au cours de la deuxième année de ce travail, nous avons pris la décision de suspendre le développement du dispositif afin de consacrer notre temps à la réalisation d'un plus grand nombre possible d'études expérimentales sur la peau humaine.

La version finale de l'appareil, décrite dans la Partie 2.1.3, nous a permis de caractériser de façon précise les propriétés mécaniques globales de la peau. Un axe de mesure est utilisé pour obtenir des informations sur la déformation et la force de traction de l'échantillon de peau, tandis que l'autre axe est dédié au contrôle du positionnement des échantillons. La configuration finale, les méthodes de mesures et les protocoles employés, peuvent être considérés comme fiables et robustes pour mesurer les propriétés mécaniques de la peau humaine. En effet, les résultats obtenus sont considérés comme répétables et reproductibles, et les valeurs mesurées par les différents capteurs ont initialement été validées et certifiées par des tests sur des ressorts de traction.
De plus, la variété de tests réalisables offre la possibilité d'effectuer une analyse approfondie des propriétés viscoélastiques de la peau. La caractérisation complète de ces propriétés peut se faire soit de manière statique ou quasi-statique grâce aux essais de traction et de relaxation des contraintes, soit de manière dynamique à l'aide d'une analyse spectromécanique.

Au cours de cette thèse, nous avons donc développé une instrumentation innovante qui permet d'évaluer les propriétés viscoélastiques de différents types de matériaux de manière précise et approfondie.

Grâce à la collaboration établie lors de la thèse avec l'entreprise Eurofins BIO-EC, nous avons pu effectuer des premiers tests extrêmement précieux sur des échantillons de peau humaine *ex vivo*. Ces tests ont constitué une avancée significative dans le développement de notre dispositif et dans la réalisation globale de notre projet.

Ce travail de thèse a tout d'abord démontré la fiabilité de notre appareil pour caractériser les propriétés viscoélastiques d'explants de peau humaine *ex vivo* sains *et* sans *stress*. Ces tests sur différents explants ont permis d'explorer les propriétés rhéologiques globales de la peau et d'obtenir un large spectre de propriétés mécaniques.
Ensuite, ces mêmes caractérisations mécaniques ont été effectuées sur des explants ayant subi divers *stress* dans le but d'analyser leurs impacts sur les propriétés mécaniques de la peau humaine. Ce travail a conduit à des recherches novatrices portant sur des sujets peu rapportés dans la littérature scientifique. Grâce à une recherche bibliographique approfondie sur ces différentes contraintes, nous avons pu établir un lien phénoménologique entre la physiologie de la peau et ses propriétés mécaniques, ce qui a permis de corroborer les premiers résultats mécaniques obtenus avec notre instrumentation.
Des lésions cutanées telles que les vergetures ont été étudiées sur les explants. Les résultats ont montré une dégradation des propriétés mécaniques dans la zone de peau endommagée et des propriétés mécaniques anormalement élevées perpendiculairement à cette zone. Le processus de congélation des explants a également été analysé, montrant un faible effet de rigidification de leurs propriétés mécaniques induit par cette méthode de conservation des échantillons.
L'exposition des explants à des enzymes protéolytiques a permis d'induire un *stress* similaire à une accélération du vieillissement cutané. Les collagénases et élastases, dégradant les fibres dermiques des explants, ont conduit à une diminution significative de leurs propriétés viscoélastiques.
Enfin, une analyse mécanique, couplée à une analyse histologique, a permis de confirmer la dégradation des réseaux fibreux dermiques induite par ces enzymes protéolytiques. Cette dernière étude nous a également permis de valider l'effet positif d'inhibiteurs de ces enzymes, permettant de réduire leurs activités et donc de diminuer la dégradation des propriétés mécaniques de la peau.

Lors de ce travail de thèse, ces dernières études mécaniques sur les analyses de peaux endommagées ou sur l'effet de *stress* ayant un impact reconnu sur la peau ont permis de montrer que cette nouvelle instrumentation pourrait être utilisée pour traiter de sujets concrets et d'actualité dans les domaines de la dermatologie, de la cosmétique et de la médecine.

En raison du temps nécessaire au développement de l'instrumentation, de la collaboration établie avec l'entreprise Eurofins BIO-EC au cours de la thèse, ainsi que de la disponibilité limitée des plasties de peau humaine, un nombre restreint d'explants a été analysé au cours des différentes études. La limitation principale de ces travaux de recherche réside dans le fait que le nombre restreint d'échantillons de peau analysés ne permet pas la réalisation d'analyses statistiques pour renforcer les premiers résultats obtenus.

Les propriétés biomécaniques de la peau ont toujours été considérées comme très importantes par les dermatologues et les biophysiciens. L'élasticité est considérée comme le paramètre le plus important car c'est le paramètre le plus fréquemment mesuré et il est caractéristique de cet organe du corps humain. Cependant, et comme décrit dans ce travail, nous considérons que les propriétés viscoélastiques globales doivent être prises en compte. Ces propriétés varient au cours du processus de vieillissement de la peau ou lorsqu'elle est soumise à certaines contraintes ou maladies.

La mesure de l'élasticité est un paramètre standard pour toutes les applications cosmétiques. Cette mesure est indispensable pour le développement de produits afin de prouver leur efficacité et de justifier les allégations publicitaires. Des revendications typiques comme « raffermissant », « anti-âge », « favorise l'élasticité de la peau », « contre le relâchement cutané », etc., pourront par exemple être validées grâce à notre instrumentation. Cette mesure est également importante en recherche dermatologique fondamentale sur les humains et les animaux. L'instrumentation développée dans ce travail trouve donc des applications dans les domaines de la cosmétique, de la médecine et de tout autre domaine lié à la peau humaine.

En comparaison des instruments déjà présents sur le marché de la cosmétique, comme par exemple le Cutomètre® qui est présenté en Annexe 4, nous avons identifié quelques avantages de l'appareillage conçu :

- Une évaluation complète des propriétés viscoélastiques de la peau humaine. La possibilité de réaliser des essais mécaniques dynamiques permet d'obtenir des informations précises sur le comportement élastique et dissipatif de la peau à différentes fréquences de sollicitation ;

- La possibilité d'étudier l'effet de différentes contraintes, positives ou négatives, sur les propriétés mécaniques de la peau grâce à la combinaison de l'instrumentation avec l'utilisation d'explants de peau humaine *ex vivo* maintenus dans des conditions physiologiques durant plusieurs jours. L'évaluation et le suivi dans le temps de l'effet de ces contraintes sont donc réalisables ;

- Une utilisation d'explants *ex vivo* de petites tailles (diamètre de 12 à 20 mm) pour réaliser les tests, ce qui permet d'effectuer des analyses même lorsque les échantillons de peau disponibles sont en quantité limitée. Les explants de peau humaine étant des « matériaux » précieux et couteux, le fait d'utiliser peu de peau est un avantage fondamental pour l'utilisateur. En effet, pour réaliser des études complètes sur l'impact d'une contrainte ou d'un produit cosmétique sur les propriétés mécaniques de la peau, seulement quelques explants de petites tailles sont nécessaires ;

- Un dispositif facilement transportable, avec des dimensions et un poids limité, qui peut être installé rapidement. Il peut être déplacé dans n'importe quel laboratoire, offrant une grande flexibilité et facilitant son utilisation dans différents contextes et environnements de travail.

Perspectives

La première perspective de ce travail de recherche consiste à poursuivre les premières études menées, augmentant ainsi le nombre de tests effectués sur les explants cutanés pour renforcer les conclusions initiales. Ces futurs essais offriront la possibilité de réaliser des évaluations quantitatives et statistiques avec un échantillonnage plus important.

Comme démontré dans le Chapitre 5, l'instrumentation développée permet d'étudier l'impact de différents types de *stress* sur les propriétés mécaniques de la peau humaine. De nombreux *stress* peuvent donc être envisagés et étudiés. Il peut s'agir d'agressions externes qui endommagent la peau, comme les rayons UV par exemple, mais également de produits médicaux ou cosmétiques qui protègeraient ou seraient bénéfiques au tissu.

Étant donné les premiers résultats concluants de l'étude sur l'effet du *stress* enzymatique sur les propriétés mécaniques de la peau humaine, il serait intéressant de poursuivre les analyses sur l'effet des inhibiteurs de ces enzymes. Le travail de recherche permettrait d'identifier des inhibiteurs de collagénases et d'élastases qui pourraient donc retarder le vieillissement cutané accéléré imposé aux explants. Ce travail *ex vivo* sur l'efficacité d'un traitement anti-âge aurait une application directe dans le domaine de la cosmétique et permettrait de montrer que cette nouvelle instrumentation pourrait aider au développement de produits destinés aux traitements.

Une autre perspective importante pour notre dispositif est l'étude de la cicatrisation de la peau. En réalisant des incisions sur les explants de peau *ex vivo*, nous pourrons observer le processus de cicatrisation de la peau. Comme présenté dans l'Annexe 5, la peau possède une excellente capacité de régénération, ce qui lui permet de cicatriser rapidement en cas de lésion cutanée. Cependant, si les blessures ne cicatrisent pas de manière ordonnée et rapide, cela peut entraîner des ulcères chroniques. Le traitement efficace des plaies chroniques reste un défi universel. Notre appareil peut donc être utilisée pour traiter ce sujet afin d'étudier le processus de cicatrisation sans traitement et d'évaluer l'efficacité de traitements favorisant la cicatrisation. Le potentiel de pansements innovants qui favoriseraient la réparation et la cicatrisation des plaies pourra également être analysé. Dans le domaine médical, les mesures des propriétés mécaniques permettront donc de suivre l'effet des produits appliqués pour favoriser la cicatrisation ou soigner une zone lésée.

L'instrumentation innovante présentée dans ce travail de recherche a été initialement développée dans le but de mesurer les propriétés mécaniques d'échantillons de peau *ex vivo*. La réalisation d'essais dans cette configuration permet d'induire et de surveiller la dégradation de la peau sur ce type d'explants. Cependant, notre système permet également d'effectuer des tests *in vivo* en utilisant l'espace central sous les quatre bras de chargement mécanique. En effet, comme le montre la Figure 5.29, il est possible de positionner l'avant-bras d'une personne dans le dispositif. En plus des essais *ex vivo*, notre instrumentation dispose donc d'une configuration d'essai conçue pour étudier les propriétés mécaniques de la peau humaine *in vivo*.
Pouvoir travailler *in vivo* avec notre instrumentation est un avantage car cela permet d'étendre ou de compléter les recherches préliminaires *ex vivo*, ce qui peut contribuer à améliorer la prévention et le traitement de diverses affections cutanées, ainsi qu'à développer des produits cosmétiques mieux adaptés aux besoins individuels en matière de soins de la peau.

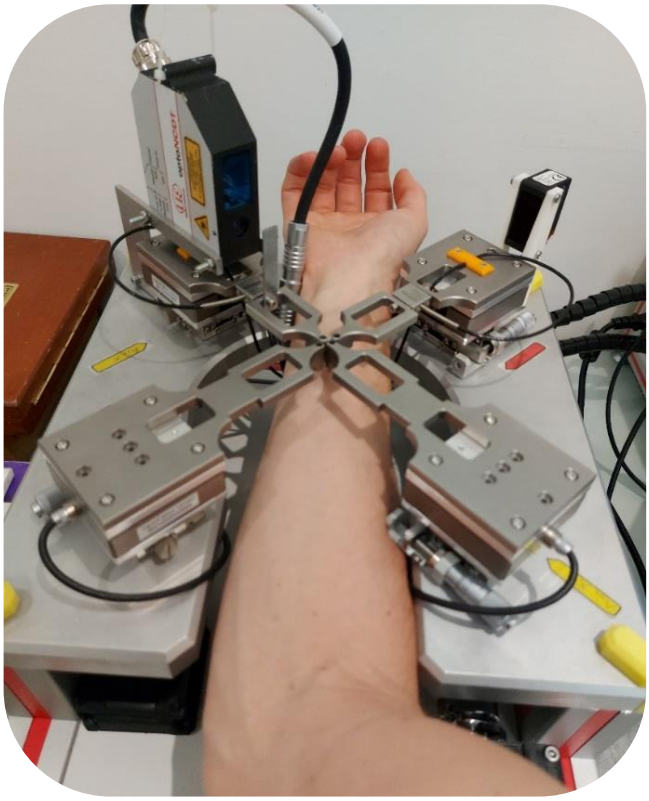

Figure C.1: Photo de la configuration de l'instrumentation en mode "in vivo" avec l'avant-bras d'un patient volontaire.

Une autre perspective d'utilisation de notre instrumentation est la caractérisation des propriétés mécaniques de peaux brûlées (la peau des « grands brulés ») ou de peaux lésées, comme les peaux confinées sous pansements, les escarres sous l'effet de frictions, ou les cicatrices suite à des opérations chirurgicales. Ces analyses permettraient de comprendre le comportement de ces types de peau afin d'adapter au mieux les traitements médicaux et de proposer de possibles greffons ayant des propriétés mécaniques similaires à celles de la peau du patient brûlé ou blessé. Notre instrumentation peut donc également concerner des travaux de chirurgie.

Bien que notre dispositif ait été initialement conçue pour caractériser les propriétés mécaniques de la peau humaine, elle peut également permettre de mesurer les propriétés mécaniques de tout tissu mou ou matériau présentant des propriétés mécaniques similaires. Par exemple, il est possible de réaliser des tests sur des matrices de collagène imitant le comportement mécanique de la peau. Ces tests permettraient par exemple d'éviter l'utilisation d'explants de peau humaine pour analyser préalablement l'effet de différents types de *stress* sur les fibres de collagène.
Une caractérisation et une analyse des propriétés mécaniques de peaux artificielles serait également précieuse dans le domaine médical, car une meilleure connaissance de ces peaux permettrait d'adapter au mieux de possibles greffons pour les patients.

Enfin, des modélisations phénoménologiques de ces évolutions de propriétés mécaniques et de leurs évolutions dans le temps pourront être proposées dans le but de suivre et d'anticiper les impacts de divers *stress* sur l'élasticité de la peau humaine.

Au cours de ce travail de recherche, le processus de préparation des explants de peau humaine, effectué par le laboratoire Eurofins BIO-EC, ne prend pas en considération l'anisotropie et les lignes de tension de la peau. Il serait bénéfique d'initier un suivi de la biopsie dès la découpe des plasties de peau, permettant ainsi d'observer et de suivre la contraction initiale des explants pour déterminer les lignes de tension cutanées.
De plus, des essais préliminaires dans différentes directions de l'explant avant les caractérisations mécaniques complètes pourraient être effectués, similaires à ceux présentés dans la Partie 3.7, dans le but de déterminer les lignes de tension spécifiques de la peau examinée.
Ces observations et ces tests préliminaires, réalisés avant chaque caractérisation complète, faciliteraient la comparaison des propriétés mécaniques de plusieurs peaux, en garantissant qu'elles ont toutes été mesurées dans une même direction par rapport aux lignes de tension cutanées (par exemple, soit parallèlement aux lignes de Langer, soit perpendiculairement à ces lignes).

L'instrumentation que nous avons développée peut encore bénéficier de diverses améliorations et peut également être utilisée pour réaliser d'autres types d'essais mécaniques complémentaires sur la peau et plus particulièrement des essais sous sollicitations multiaxiales en se servant du deuxième axe de mesure. Ce type de sollicitation permettrait d'atteindre les équilibres anisotropes de la peau et d'étudier directement son comportement anisotrope.

Il serait également intéressant de pouvoir mesurer les propriétés mécaniques de la peau sur de plus grandes déformations. Nos actionneurs piézo-électriques actuels ne permettent qu'un déplacement maximal de 600 µm. Ces tests nous permettraient d'observer le comportement de la peau aux plus grandes déformations et d'étudier son comportement en cas de rupture. Ces informations seraient complémentaires à celles que nous possédons déjà pour de faibles déformations. En effet, effectuer des mesures sur un échantillon *ex vivo* permet d'étudier avantageusement les propriétés mécaniques au-delà de la région élastique en soumettant l'échantillon de peau à des déformations importantes.
Par ailleurs, les résultats obtenus sur la notion de pré-tension cutanée, dans la partie 3.F, nous incitent à réfléchir à de nouveaux types de fixation de l'échantillon sur l'appareil dans le but de proposer des caractérisations avec différents types de pré-tension et de se rapprocher des conditions d'essais *in vivo*.

De plus, la programmation du logiciel ainsi que le traitement des résultats peuvent encore être perfectionnés. Une amélioration consisterait à créer une commande dans l'interface logicielle permettant d'effectuer une série de tests successifs sans intervention de l'opérateur. Par exemple une séquence de tests rapides de traction et de balayage en fréquence pour une analyse rapide de 5 min, ou une séquence plus complète comprenant l'ensemble des essais mécaniques pour une analyse globale des propriétés mécaniques de la peau. Cela simplifierait les procédures et réduirait le temps de manipulation pour l'opérateur.
Un autre point important serait d'automatiser le traitement des données pour obtenir directement les résultats finaux, tels que les modules apparents en traction simple, ainsi que les modules viscoélastiques en analyse mécanique dynamique.

Enfin, afin d'améliorer le confort du patient lors de tests en conditions *in vivo*, des modifications du dispositif pourraient être envisagées, comme l'installation d'une « attelle/gouttière » amovible pour placer l'avant-bras à la place du porte-échantillon imprimé en 3D, ou l'ajout de cales métalliques aux bras de translation de l'appareil pour les surélever afin d'avoir plus d'espace pour accueillir l'avant-bras au centre de l'instrumentation. Ces améliorations *in vivo* pourront possiblement être suivies d'un embellissement de l'instrumentation afin qu'elle soit plus esthétique d'un point de vue visuel.

References

[Abellan *et al.,* 2013]: M. Abellan, H. Zahouani, and J. Bergheau. Contribution to the determination of in vivo mechanical characteristics of human skin by indentation test. *Computational and Mathematical Methods in Medicine*, Article ID 814025, 2013.

[Agache *et al.,* 1980]: P. Agache, C. Monneur, J. Levêque, and J. De Rigal. Mechanical properties and young's modulus of human skin in vivo. *Archives of Dermatologgical Research*, 269 :221-232, 1980.

[Agache, 2000]: P. Agache. *Physiologie de la peau et explorations fonctionnelles cutanées.* Edition Médicale Internationale, 2000.

[Alexander *et al.,* 1977]: H. Alexander and T. Cook. Accounting for natural tension in the mechanical testing of human skin. *The Journal of Investigative Dermatology*, 69 :310-314, 1977.

[Alexander *et al.,* 1979]: H. Alexander and D. Miller. Determining skin thickness with pulsed ultra sound. *The Journal of Investigative Dermatology*, 72 :17-19, 1979.

[Alexander *et al.,* 2006]: H. Alexander and T. Cook. Variations with age in the mechanical properties of human skin in vivo. *Journal of tissue viability*, 16: 6-11, 2006.

[Amaied *et al.,* 2015]: E. Amaied, R. Vargiolu, J. Bergheau, and H. Zahouani. Aging effect on tactile perception: Experimental and modelling studies. *Wear*, 332-333 :715-724, 2015.

[Ankersen *et al.,* 1999]: J. Ankersen, A. Birkbeck, R. Thomson, and P. Vanezis. Puncture resistance and tensile strength of skin simulants. *Proceedings of the Institution of Mechanical Engineers,* 213 :493-501, 1999.

[ANSM, 2013]: Agence Nationale de Sécurité du Médicament et des produits de santé. Recommandations relatives aux recherches biomédicales portant sur des produits cosmétiques entrant dans le champ d'application de la loi relative à la politique de santé publique du 9 aout 2004, 2013.

[Arem *et al.*, 1980]: A. J. Arem and C. W. Kischer. Analysis of Striae. *Palst Reconstr Surg*, 65: 22-29, 1980.

[Arnold *et al.,* 2023]: N. Arnold, J. Scott, and T. R. Bush. A review of the characterizations of soft tissues used in human body modeling: Scope, limitations, and the path forward. *J Tissue Viability*, 32(2): 286-304, 2023.

[Arumugam *et al.,* 1994]: V. Arumugam, M. Naresh, and R. Sanjeevi. Effect of strain rate on the fracture behaviour of skin. *J. Biosci*. 19(3), 307–313, 1994.

[Asserin, 1996]: J. Asserin. *Etude par test d'extension des propriétés mécaniques de la peau humaine in vivo et d'un derme équivalent in vitro*. PhD thesis. Université de Franche Comté, 1996.

[Auber *et al.,* 1985]: L. Aubert, P. Anthoine, J. De Rigal, and J. Leveque. An in vivo assessment of the biomechanical properties of human skin modifications under the influence of cosmetic products. *International Journal of Cosmetic Science*, 7 :51-59, 1985.

[Ayadh *et al.,* 2023]: M. Ayadh, A. Guillermin, M.-A. Abellan, A. Bigouret, and H. Zahouani. The assessment of natural human skin tension orientation and its variation according to age for two body areas: Forearm and thigh. *Journal of the mechanical behavior of biomedical materials*. 141: 105798, 2023.

[Azzez, 2019]: K. Azzez. *Caractérisation et modélisation du comportement mécanique in vivo de la peau*. PhD thesis. Ecole centrale de Lyon, 2019.

[Bader *et al.,* 1983]: D. Bader and P. Boker. Mechanical characteristics of skin and underlying tissues in vivo. *Biometerials*, 4 :305-308, 1983.

[Bancelin, 2013]: S. Bancelin. *Imagerie quantitative du collagène par génération de seconde harmonique*. PhD thesis. Ecole Polytechnique, 2013.

[Barbenel *et al.,* 1977]: J. Barbenel and J. Evans. The time-dependent mechanical properties of skin. *The Journal of Investigative Dermatology*, 69 :318-320, 1977.

[Barel *et al.,* 1998]: A. Barel, R. Lambrecht, and P. Clarys. Mechanical function of the skin: state of the art. *Current Problems in Dermatology*, 26 :69-83, 1998.

[Barel *et al.,* 2006]: A. Barel, W. Courage, and P. Clarys. Suction chamber method for measurement of skin mechanics: the new digital version of the cutometer. In *Handbook of Non-Invasive Methods and The Skin*, p 583-589. CRC Press, 2nd edition, 2006.

[Barnhill *et al.,* 1984]: R. Barnhill, D. Bader, and T. Ryan. A study of uniaxial tension on the superficial dermal microvasculature. *The Journal of Investigative Dermatology*, 82: 511-514, 1984.

[Belkoff *et al.,* 1991]: S. Belkoff and R. Haut. A structural model used to evaluate the changing microstructure of maturing rat skin. *Journal of Biomechanics*, 24 :711-720, 1991.

[Bercoff *et al.,* 2003]: J. Bercoff, S. Chaffai, M. Tanter, L. Sandrin, S. Catheline, M. Fink, J. Gennisson, and M. Meunier. In vivo breast tumor detection using transient elastography. *Ultrasound in Medicine and Biology*, 29: 1387-1396, 2003.

[Bernhard *et al.,* 2007]: D. Bernhard, C. Moser, A. Backovic, and G. Wick. Cigarette smoke – an aging accelerator? *Experimental Gerontology*, 42 :160-165, 2007.

[Bertin *et al.*, 2014]: C. Bertin, A. Lopes-DaCunha, A. Nkengne, R. Roure and G. N. Stamatas. Striae distensae are characterized by distinct microstructural features as measured by non-invasive methods in vivo. *Skin Res Technol*, 20: 81–86, 2014.

[Bieth, 2001]: J. G. Bieth. Les élastases. *J. Soc. Biol.* 195(2):173-179, 2001.

[Billiar *et al.,* 2000]: K. Billiar and M. Sacks. Biaxial mechanical properties of the natural and glutaraldehyde treated aortic valve cusp - Part II: A structural constitutive model. *Journal of Biomechanical Engineering*, 122 :327-335, 2000.

[Bischoff *et al.,* 2000]: J. Bischoff, E. Arruda, and K. Grosh. Finite element modeling of human skin using an isotropic, nonlinear elastic constitutive model. *Journal of Biomechanics*, 33 :645-652, 2000.

[Bischoff *et al.,* 2002]: J. Bischoff, E. Arruda, and K. Grosh. A microstructurally based orthotropic hyperelastic constitutive law. *Journal of Applied Mechanics*, 69 :570-579, 2002.

[Black *et al.,* 2005]: L. Black, K. Brewer, S. Morris, B. Schreiber, P. Toselli, M. Nugent, B. Suki and P. Stone. Effects of elastase on the mechanical and failure properties of engineered elastin-rich matrices. *Journal of Applied Physiology*, 98: 1434-1441, 2005.

[Boismal *et al.,* 2020]: F. Boismal, K. Serror, G. Dobos, E. Zuelgaray, A. Bensussan and L. Michel. Vieillissement cutané - Physiopathologie et thérapies innovantes. *Med Sci (Paris),* 36 : 1163-1172, 2020.

[Boisnic *et al.,* 2005]: S. Boisnic and M. Branchet. Vieillissement cutanée chronologique. *EMC-Cosmétologie et Dermatologie esthétique*, 1 :1-7, 2005.

[Bordenave *et al.,* 2002]: E. Bordenave, E. Abraham, G. Jonusauskas, J. Oberlé, and C. Rullière. Longitudinal imaging in biological tissues with a single laser shot correlation system. *Optics Express*, 10 :35-40, 2002.

[Borges *et al.,* 1962]: A. Borges and J. Alexander. Relaxed skin tension lines, z-plasties on scars, and fusiform excision of lesions. *British Journal of Plastic Surgery*, 15 :242-254, 1962.

[Bousquet *et al.,* 2002]: O. Bousquet and P. Coulombe. Les kératines : un autre regard sur la biologie de la peau. *Médecines/Sciences*, 18 :45-54, 2002.

[Boyer *et al.,* 2007]: G. Boyer, H. Zahouani, A. Le Bot, and L. Laquieze. In vivo characterization of viscoelastic properties of human skin using dynamic micro-indentation. *Conference of the IEEE EMBS*, Lyon, p 4584-4587, 2007.

[Boyer *et al.,* 2009]: G. Boyer, L. Laquieze, A. Le Bot, S. Laquieze, and H. Zahouani. Dynamic indentation on human skin in vivo: ageing effects. *Skin Research and Technology*, 15 :55-67, 2009.

[Boyer, 2010]: G. Boyer. *Modélisation du comportement mécanique de la peau humaine in vivo : application au vieillissement et aux gestes du clinicien*. PhD thesis. Ecole Nationale Supérieure des Mines de Saint-Etienne, 2010.

[Boyer *et al.,* 2012]: G. Boyer, C. Pailler-Mattei, J. Molimard, M. Pericoi, S. Laquieze, and H. Zahouani. Non contact method for in vivo assessment of skin mechanical properties for assessing effect of ageing. *Medical Engineering and Physics*, 34 :172-178, 2012.

[Boyer *et al.,* 2013]: G. Boyer, J. Molimard, M. Ben Tkaya, H. Zahouani, M. Pericoi, and S. Avril. Assessment of the in-plane biomechanical properties of human skin using a finite element model updating approach combined with an optical full-field measurement on a new tensile device. *Journal of the Mechanical Behavior of Biomedical Materials*, 27 :273-282, 2013.

[Brakenhoff, 1979]: G. Brakenhoff. Imaging modes in confocal scanning light microscopy (CSLM). *Journal of Microscopy*, 117 :233-242, 1979.

[Brancaleon *et al.,* 2001]: L. Brancaleon, M. Bamberg, T. Sakamaki, and N. Kollias. Attenuated total Reflection-Fourier transform infrared spectroscopy as a possible method to investigate biophysical parameters of stratum corneum in vivo. *Journal of Investigative Dermatology*, 116 :380-386, 2001.

[Brèque, 2002] : C. Brèque. *Développement et mise en œuvre de méthodes optiques pour la mesure de relief et de champ de déformations en vue de la modélisation d'organes biologiques*. PhD thesis. Université de Poitiers, 2002.

[Brown, 1973]: I. Brown. A scanning electron-microscope study of effects of uniaxial tension on human skin. *British Journal of Dermatology*, 89 :383-393, 1973.

[Capek *et al.,* 2010]: L. Capek, Z. Lochman, L. Dzan, and E. Jacquet. Biaxial extensometer for measuring of the human skin anisotropy in vivo. In *5th Cairo International Biomedical Engineering Conference (CIBEC),* Egypt, p 83-85, 2010.

[Catheline, 1998]: S. Catheline. *Interferomètrie-speckle ultrasonore : Application à la mesure d'élasticité*. PhD thesis, Université Paris VII, 1998.

[Cavalcante *et al.,* 2005]: F. Cavalcante, S. Ito, K. Brewer, H. Sakai, A. Alencar, M. Almeida, J. Andrade, A. Majumbar, E. Ingenito, and B. Suki. Mechanical interactions between collagen and proteoglycans: implications for the stability of lung tissue. *Journal of Applied Physiology*, 98 :672-679, 2005.

[Chartier, 2017]: C. Chartier. *Caractérisation des propriétés mécaniques du tissu cutané par élastographie impulsionnelle haute fréquence ; Applications en dermatologie et en cosmétique*. PhD thesis. Université François Rabelais de Tours, 2017.

[Cho *et al.*, 2018]: C. Cho, E. Cho, N. Kim, J. Shin, S. Woo, J. Lee, J. Lee, E. Lee and J. Ha. Biophysical properties of striae rubra and striae alba in human skin: Comparison with normal skin. *Skin Res Technol*, 1–6, 2018.

[Chow and Zhang, 2011]: M. J. Chow MJ, and Y. Zhang. Changes in the mechanical and biochemical properties of aortic tissue due to cold storage. *J Surg Res*. 171(2):434–442, 2011.

[Chowdhury *et al.,* 2023]: S. C. Chowdhury, T. Longoria, and J. W. Gillespie Jr. Effects of transverse compression on the structure and axial tensile properties of polyethylene: A molecular simulation study. *Polymer.* 267: 125660, 2023.

[Clark *et al.,* 1996]: J. Clark, C. Cheng, and K. Leung. Mechanical properties of normal skin and hypertrophic scars. *Burns*, 22 :443-446, 1996.

[CNRS Peau]: La peau, un tissu précieux - Dossier SagaScience - Chimie et Beauté. *https://sagascience.cnrs.fr › doschim › decouv › peau.*

[Cox, 1941]: H. T. Cox. The cleavage lines of the skin. *The British Journal of Surgery*. Vol 29, Issue 114, p 234–240, 1941.

[Convelbo, 2017]: C. Convelbo. *Mise au point de nouvelles méthodes d'analyse du traumatisme valvulaire des bioprothèses percutanées*. PhD thesis. Université Paris-Est, 2017.

[Cook *et al.,* 1977]: T. Cook, H. Alexander, and M. Cohen. Experimental method for determining the 2-dimensional mechanical properties of living human skin. *Medical and Biological Engineering and Computing*, 15 :381-390, 1977.

[Cowper, 1698]: W. Cowper. *The anatomy of human bodies*. Oxford, 1698.

[Cribb *et al.,* 1995]: A. Cribb and J. Scott. Tendon response to tensile-stress - an ultrastructural investigation of collagen - proteoglycans interactions in stressed tendon. *Journal of Anatomy*, 187 :423-428, 1995.

[Crichton *et al.,* 2011]: M. Crichton, B. Donose, X. Chen, A. Raphael, H. Huang, and M. Kendall. The viscoelastic, hyperelastic and scale dependent behaviour of freshly excised individual skin layers. *Biomaterials*, 32 :4670-4681, 2011.

[Daly, 1966]: C. Daly. *The biomechanical characteristics of human skin*. PhD thesis. University of Strathclyde, Scotland, 1966.

[Daly *et al.,* 1979]: C. Daly and G. Odland. Age-related changes in the mechanical properties of human skin. *The Journal of Investigative Dermatology*, 73 :84-87, 1979.

[Daly, 1982]: C. Daly. Biomechanical properties of dermis, The Journal of Investigative Dermatology, 79: 17-20, 1982.

[Danielson, 1973]: D. Danielson. Human skin as an elastic membrane. *Journal of Biomechanics*, 6 :539-546, 1973.

[Decreamer *et al.,* 1980]: W. Decraemer, M. Maes, V. Vanhuyse, and P. Vanpeperstraete. A non-linear viscoelastic constitutive equation for soft biological tissues, based upon a structural model. *Journal of Biomechanics*, 13 :559-564, 1980.

[De Jong, 1995]: L. De Jong. *Pre-tension and anisotropy in skin. Modelling and Experiments*. Master of Science Thesis. Eindhoven University of Technology, 1995.

[Delalleau *et al.,* 2006]: A. Delalleau, G. Josse, J. Legarde, H. Zahouani, and J. Bergheau. Characterization of the mechanical properties of skin by inverse analysis combined with indentation test. *Journal of Biomechanics*, 39 :1603-1610, 2006.

[Dellaleau, 2007]: A. Delalleau. *Analyse du comportement mécanique de la peau in vivo.* PhD thesis, Université de Saint-Etienne, 2007.

[Delalleau *et al.,* 2008a]: A. Delalleau, G. Josse, J. Lagarde, H. Zahouani, and J. Bergheau. Characterization of the mechanical properties of skin by inverse analysis combined with an extensometry test. *Wear*, 264 :405-410, 2008.

[Delalleau *et al.,* 2008b]: A. Delalleau, G. Josse, J. Legarde, H. Zahouani, and J. Bergheau. A nonlinear elastic behavior to identify the mechanical parameters of human skin in vivo. *Skin Research and Technology*, 14 :152-164, 2008.

[Della Volpe *et al.,* 2012]: C. Della Volpe, L. Andrac, D. Casanova, R. Legré, and G. Magalon. La diversité de la peau : étude histologique de 140 résidus cutanés, adaptée à la chirurgie plastique. *Annales de chirurgie plastique et esthétique*, 57 :423-449, 2012.

[Del Prete *et al.,* 2004]: Z. Del Prete, S. Antoniucci, A.H. Hoffman, and P. Grigg. Viscoelastic properties of skin in Mov-13 and Tsk mice. *Journal of Biomechanics*, 37 :1491-1497, 2004.

[De Pascalis, 2010]: R. De Pascalis. *The Semi-Inverse Method in solid mechanics: Theoretical underpinnings and novel applications.* PhD thesis. Université Pierre et Marie Curie, 2010.

[Derail *et al.,* 2022]: C. Derail, F. Ehrenfeld, A. Laffore, C. Nardin, and B. Blanchard. *Système de mesure des propriétés mécaniques d'un échantillon de peau*. Patent WO 2022/129813 A1. OMPI, 2022.

[De Rigal *et al.,* 1985]: J. De Rigal and J. Leveque. In vivo measurement of the stratum corneum elasticity. *Bioengineering and the Skin* 1 :13-23, 1985.

[Devillers *et al.,* 2010]: C. Devillers, C. Piérard-Franchimont, A. Schreder, V. Docquier and G. E. Piérard. High resolution skin colorimetry, strain mapping and mechanobiology. *International Journal of Cosmetic Science*, 32, 241–245, 2010.

[Diani *et al.,* 2009]: J. Diani, B. Fayolle, and P. Gilormini. A review on the Mullins effect. *European Polymer Journal*, 45 :601-612, 2009.

[Dikstein *et al.,* 1979]: S. Dikstein and A. Hartzshtark. In-vivo measurement of some elastic properties of human skin. *Bioengineering and the Skin*. MTA Press, 1979.

[Dikstein *et al.,* 1983]: S. Dikstein and A. Hartzshtark. What does low pressure indentometry measure? *Arztliche Kosmetologie*, 13 :327-328, 1983.

[Dikstein *et al.,* 2006]: S. Dikstein and J. Fluhr. Indentometry. In *Handbook of Non-Invasive Methods and the Skin*, p 617-620. CRC Press, 2nd edition, 2006.

[Diridollou, 1994]: S. Diridollou. *Etude du comportement mécanique cutané par technique ultrason haute résolution*. PhD thesis. Université François Rabelais, 1994.

[Diridollou *et al.,* 1998]: S. Diridollou, M. Berson, V. Vabre, D. Black, B. Karlsson, F. Auriol, J. Gregoire, C. Yvon, L. Vaillant, Y. Gall, and F. Patat. An in vivo method for measuring the mechanical properties of the skin using ultrasound. *Ultrasounds in Medicine & Biology*, 24 :215-224, 1998.

[Diridollou *et al.,* 2000]: S. Diridollou, F. Patat, F. Gens, L. Vaillant, D. Black, J. Lagarde, Y. Gall, and M. Berson. In vivo model of the mechanical properties of the human skin under suction. *Skin Research and Technology*, 6 :214-221, 2000.

[Diridollou, 2001]: S. Diridollou, V. Vabre, M. Berson, L. Vaillant, D. Black, J. Lagarde, J. Grégoiret, Y. Gall, and F. Patat. Skin ageing: changes of physical properties of human skin in vivo. *International Journal of Cosmetic Science*, 23 :353-362, 2001.

[Dobrev, 2000]: H. Dobrev. Use of cutometer to assess epidermal hydration. *Skin Research and Technology*, 6 :239-244, 2000.

[Dobrev, 2005]: H. Dobrev. Application of cutometer area parameters for the study of human skin fatigue. *Skin Research and Technology*, 11 :120-122, 2005.

[Dombi *et al.,* 1993]: G. Dombi, R. Haut, and S. Sullivan. Correlation of high-speed tensile strength with collagen content in control and lathyritic rat skin. *Journal of Surgical Research*. 54, 21–28, 1993.

[Drobez *et al.,* 2013]: H. Drobez, H. Reynaud, L. Picot, H. Jaffal, V. Corre, R. Klausz, and S. Muller. Une approche mécanique pour la simulation d'un examen de mammographie. In *Congrès Français de Mécanique*, 2013.

[Dubertret, encyclopédie] : L. Dubertret. PEAU. Encyclopædia Universalis France.

[Dunn *et al.,* 1983] : M. Dunn and F. Silver. Viscoelastic behavior of human connective tissues: relative contribution of viscous and elastic components. *Connective Tissue Research*, 12 :59-70, 1983.

[Du Pont De Romemont, 2014]: B. Du Pont De Romemont. *Effet des contraintes mécaniques appliquées aux fibroblastes humains lors de la reconstruction d'un modèle de peau in vitro : Etude de faisabilité*. PhD thesis. Université de Lyon, 2014.

[Dupuytren, 1834]: G. Dupuytren. *Traité théorique et pratique des blessures par armes de guerre*. Berlin, 1834.

[Ebling, 1982]: F. Ebling. Physiological background to skin ageing. *International Journal of Cosmetic Science*, 4 :103-110, 1982.

[Edwards *et al.,* 1995]: C. Edwards and R. Marks. Evaluation of biomechanical properties of human skin. *Clinics In Dermatology*, 13 :375-380, 1995.

[El Gammal *et al.,* 1996]: S. El Gammal, R. Hartwig, S. Aygen, T. Mauermann, C. El Gammal, P. Altermeyer. Improved resolution of magnetic resonance microscopy in examination of skin tumors. *Journal of Investigative Dermatology*, 106 :1287-1292, 1996.

[Elias, 2005]: P. Elias. Stratum corneum defensive functions: An integrated view. *Journal of Investigative Dermatology*, 125 :183-200, 2005.

[Elouneg *et al.,* 2023]: A. Elouneg, J. Chambert, A. Lejeune, Q. Lucot, E. Jacquet, and S.P.A. Bordas. Anisotropic mechanical characterization of human skin by in vivo multi-axial ring suction test. *Journal of the mechanical behavior of biomedical materials*. 141: 105779, 2023.

[Elsedfy, 2020]: H. Elsedfy. Striae distensae in adolescents: a mini review. *Acta Biomed* 2020; 91(1): 176-181, 2010.

[Escoffier *et al.,* 1989]: C. Escoffier, M. Pharm, J. De Rigal, A. Rochefort, R. Vasselet, J. Lévêque, and P. Agache. Age-related mechanical properties of human skin: An in vivo study. *Journal of Investigative Dermatology*, 93 :353-357, 1989.

[Eshel *et al.,* 2001]: H. Eshel and Y. Lanir. Effects of strain level and proteoglycan depletion on preconditioning and viscoelastic responses of rat dorsal skin. *Annals of Biomedical Engineering*, 29 :164-172, 2001.

[Evans *et al.,* 1967]: J. Evans and W. Siesennop. Controlled quasi-testing of human skin in vivo. *Digest of the 7th International Conference on Medical and Biological Engineering*, Stockholm, p371, 1967.

[Finlay, 1970]: B Finlay. Dynamic mechanical testing of human skin in vivo. *Journal of Biomechanics*, 3 :557-568, 1970.

[Flagothier *et al.,* 2005]: C. Flagothier, C. Piérard-Franchimont, and G. Piérard. La peau et ses nuances ethniques. *Revue médicale de Liège*, 60 :53-56, 2005.

[Flynn *et al.,* 1998]: D. Flynn, G. Peura, P. Grigg, and A. Hoffman. A finite element based method to determine the properties of planar soft tissue. *Journal of Biomechanical Engineering*, 120 :202-210, 1998.

[Flynn *et al.,* 2011]: C. Flynn, A. Taberner, and P. Nielsen. Mechanical characterisation of in vivo human skin using a 3D force-sensitive micro-robot and finite element analysis. *Biomechanical Model Mechanobiology*, 10 :27-38, 2011.

[Foutz *et al.*, 1992]: T. L. Foutz, E. A. Stone, and C. F. Abrams Jr. Effects of freezing on mechanical properties of rat skin. *American Journal of Veterinary Research*. 53(5): 788–792, 1992.

[Frances *et al.,* 1990]: C. Frances, M. Branchet, S. Boisnic, C. Lesty, and L. Robert. Elastic fibers in normal human skin. Variations with age: A morphometric analysis. *Archives of Gerontology and Geriatrics*, 10 :57-67, 1990.

[Fthenakis *et al.,* 1991]: C. Fthenakis, D. Maes, and W. Smith. In vivo assessment of skin elasticity using ballistometry. *Journal of the Society of Cosmetic Chemists*, 42 :211-222, 1991.

[Fujimoto *et al.,* 1995]: J. Fujimoto, M. Brezinski, G. Tearney, S. Boppart, B. Bouma, M. Hee, J. Southern, and E. Swanson. Optical biopsy and imaging using optical coherence tomography. *Nature Medicine*, 1 :970-972, 1995.

[Fujimoto, 2003]: J. Fujimoto. Optical coherence tomography for ultrahigh resolution in vivo imaging. *Nature Biotechnology*, 21 :1361-1367, 2003.

[Fung, 1993]: Y. Fung. *Biomechanics: Mechanical properties of living tissues*. Springer, 2nd edition, 1993.

[Gahagnon, 2009]: S. Gahagnon. *Étude in vivo du comportement mécanique du derme par une méthode élastographique haute résolution : applications à l'exploration d'anomalies du tissu élastique (syndrome de Marfan).* PhD thesis. Université François Rabelais de Tours, 2009.

[Gallagher *et al.,* 2012]: A. Gallagher, A. Anniadh, K. Bruyere, M. Otténio, and H. Xie. Dynamic tensile properties of human skin. In *International Research Council on the Biomechanics of Injury Conference*, 2012.

[Gambichler *et al.,* 2007]: T. Gamblicher, P. Regeniter, F. Bechara, A. Orlikov, R. Vasa, G. Moussa, M. Stüker, P. Altmeyer, and K. Hoffman. Characterization of benign and malignant melanocytic skin lesions using optical coherence tomography in vivo. *American Academy of Dermatology*, 57 :629-637, 2007.

[Garrone *et al.,* 1997]: R. Garrone, C. Lethias, and D. Le Guellec. Distribution of minor collagens during skin development. *Microscopy Research and Technique*, 38 :407-412, 1997.

[Gaspari *et al.,* 2009]: R. Gaspari, D. Blehar, M. Mendoza, A. Montoya, C. Moon, and D. Polan. Use of ultrasound elastography for skin and subcutaneous abscesses. *Journal of Ultrasound Medicine*, 28 :855-860, 2009.

[Gasser *et al.,* 2006]: T. Gasser, R. Ogden, and G. Holzapfel. Hyperelastic modelling of arterial layers with distributed collagen fibre orientations. *Journal of the Royal Society Interface*, 3 :15-35, 2006.

[Gautieri *et al.,* 2011]: A. Gautieri, S. Vesentini, A. Redaelli, and M. Buehler. Hierarchical structure and nanomechanics of collagen microfibrils from the atomistic scale up. *Nano Letters*, 11 :757-766, 2011.

[Gennisson, 2003]: J. Gennisson. *Le palpeur acoustique : un nouvel outil d'investigation des tissus biologiques*. PhD thesis. Université de Paris 6, 2003.

[Gennisson *et al.,* 2004]: J. Gennisson, T. Baldeweck, M. Tanter, S. Catheline, M. Fink, L. Sandrin, C. Cornillon, and B. Querleux. Assessment of elastic parameters of human skin using dynamic elastography. *IEEE Transactions on Ultrasonics, Ferroelectrics and Frequency Control*, 51 :980-989, 2004.

[Gerin, 2012]: C. Gerin. *Validation de l'utilisation d'un extensomètre uni-axial pour l'étude des propriétés mécaniques de la peau du chien*. PhD thesis. Université Claude Bernard de Lyon, 2012.

[Geerligs, 2010]: Geerligs M. *Skin layer mechanics* (Thesis). Eindhoven: Technische Universiteit Eindhoven, 2010.

[Giacomoni *et al.,* 2004]: P. Giacomoni and G. Rein. A mechanistic model for the aging of human skin. *Micron*, 35 :179-184, 2004.

[Gibson *et al.,* 1969]: T. Gibson, H. Stark, and J. Evans. Directional variation in extensibility of human skin in vivo. *Journal of Biomechanics*, 2 :201-204, 1969.

[Giles *et al.,* 2007]: J. M. Giles, A. E. Black, and J. E. Bischoff. Anomalous rate dependence of the preconditioned response of soft tissue during load controlled deformation. *Journal of Biomechanics*. 40 :777–785, 2007.

[Ginefri *et al.,* 2001]: J. Ginefri, L. Darrasse, and P. Crozat. High-temperature superconducting surface coil for in vivo microimaging of the human skin. *Magnetic Resonance in Medicine*, 45 :376-382, 2001.

[Gniadecka *et al.,* 1994]: M. Gniadecka, R. Gniadecki, J. Serup, and J. Sondergaard. Skin mechanical properties present adaptation to man's upright position. in vivo studies in young and aged individuals. *Acta Dermatol Venereol*, 74 :188-190, 1994.

[Gniadecka *et al.,* 2006]: M. Gniadecka and J. Serup. Suction chamber method for measurement of skin mechanical properties: The Dermaflex. In *Handbook of Non-Invasive Methods and the Skin*, p 571-577. CRC Press, 2nd edition, 2006.

[Grahame *et al.,* 1969]: R. Grahame and P. Holt. The influence of ageing on the in vivo elasticity of human skin. *Gerontologia*, 15 :121-139, 1969.

[Greaves *et al.,* 2013]: N. Greaves, B. Benatar, S. Whiteside, M. Baguneid et A. Bayat. Optical coherence tomography: a reliable alternative to invasive histological assessment of acute wound healing in human skin? *British Journal of Dermatology*, 170 :840-850, 2013.

[Griffin *et al.,* 2017]: M. F. Griffin, C. Leung, Y. Premakumar, M. Szarko, and P. E. Butler. Comparison of the mechanical properties of different skin sites for auricular and nasal reconstruction. *J Otolaryngol Head Neck Surg*. 46: 33, 2017.

[Groves, 2011]: R. Groves. *Quantifying the mechanical properties of skin in vivo and ex vivo to optimise microneedle device design.* PhD thesis. Cardiff University, 2011.

[Groves *et al.,* 2013]: R. Groves, S. Coulman, J. Birchall, and S. Evans. An anisotropic, hyperelastic model for skin: Experimental measurements, finite element modelling and identification of parameters for human and murine skin. *Journal of the Mechanical Behavior of Biomedical Materials*, 18 :167-180, 2013.

[Guimberteau *et al.,* 2005]: J. Guimberteau, J. Sentucq-Rigall, B. Panconi, R. Boileau, P. Mouton, and J. Bakhach. Introduction à la connaissance du glissement des structures sous-cutanées humaines. *Annales de Chirurgie Plastique Esthétique*, 50 :19-34, 2005.

[Guinot *et al.,* 2006]: C. Guinot, J. Latreille, E. Mauger, L. Ambroisine, S. Gardinier, H. Zahouani, S. Guehenneux, and E. Tschachler. Reference ranges of skin Micro-Relief according to age in french caucasian and japanese women. *Skin Research and Technology*, 12 :268-278, 2006.

[Gundiah *et al.*, 2013]: N. Gundiah, A. R. Babu, and L. A. Pruitt. Effects of elastase and collagenase on the nonlinearity and anisotropy of porcine aorta. *Physiol. Meas*. 34:1657–1673, 2013.

[Gunner *et al.,* 1979]: C. Gunner, W. Hutton, and T. Burlin. The mechanical properties of skin in vivo – a portable hand-held extensometer. *British Journal of Dermatology*, 100 :161-163, 1979.

[Hara *et al.,* 2013]: Y. Hara,Y. Masuda, T. Hirao, and N. Yoshikawa. The relationship between the young's modulus of the stratum corneum and age: a pilot study. *Skin Research and Technology*, 19 :339-345, 2013.

[Hargens, 2006]: C. Hargens. Ballistometry. In *Handbook of Non-Invasive and the Skin*, p 627-632. CRC Press, 2nd edition, 2006.

[Hartmann, 1979]: H. Hartmaan. Daily bath and its effect on the normal human skin flora quantitative and qualitative investigations of the aerobic skin flora. *Archives of Dermathological Research*, 265 :153-164, 1979.

[Hendriks, 2001]: F. Hendriks. Mechanical behavior of human skin in vivo - a literature review. *Nat.Lab. Unclassified report 820. Philips Research Laboratories*, 2001.

[Hendriks *et al.,* 2003]: F. Hendriks, D. Brokken, J. Van Eemeren, C. Oomens, F. Baaijens, and J. Horsten. A numerical-experimental method to characterize the non-linear mechanical behaviour of human skin. *Skin Research and Technology*, 9 :274-283, 2003.

[Hendriks, 2005]: F. Hendriks. *Mechanical behaviour of human epidermal and dermal layers in vivo*. PhD thesis. Université Technique d'Eindhoven, 2005.

[Hendriks *et al.,* 2006]: F. Hendriks, D. Brokken, C. Oomens, D. Bader, and F. Baaijens. The relative contributions of different skin layers to the mechanical behavior of human skin in vivo using suction experiments. *Medical Engineering & Physics*, 28 :259-266, 2006.

[Hiatt *et al.,* 2009]: K. Hiatt and B. Smoller. *Dermatopathology: The Basics.* Springer US, 2009.

[Holzapfel, 2000]: G. Holzapfel. Biomechanics of soft tissue. *Computational Biomechanics*, Paper No. 7, 2000.

[Holzapfel *et al.,* 2000]: G. Holzapfel, T. Gasser, and R. Ogden. A new constitutive framework for arterial wall mechanics and a comparative study of material models. *Journal of Elasticity*, 61 :1-48, 2000.

[Huang *et al.,* 1991]: D. Huang, E. Swanson, C. Lin, J. Schuman, W. Stinson, W. Chang, M. Hee, T. Flotte, K. Gregory, and C. Puliafito. Optical coherence tomography. *Science*, 254 :1178-1181, 1991.

[Hulmes, 2002]: D. Hulmes. Building collagen molecules, fibrils, and suprafibrillar structures. *Journal of Structural Biology*, 137 :2-10, 2002.

[Hutton *et al.,* 1975]: W. Hutton, T. Burlin, and H. Ranu. An apparatus for measuring the effects of radiotherapy on the elastic properties of human skin in vivo. *Medical and Biological Engineering and Computing*, 13 :584-585, 1975.

[Iivarinen *et al.,* 2013]: J. Iivarinen, R. Korhonen, P. Julkunen, and J. Jurvelin. Experimental and computational analysis of soft tissue mechanical response under negative pressure in forearm. *Skin Research and Technology*, 19 :356-365, 2013.

[Jachowicz *et al.,* 2007]: J. Jachowicz, R. McMullen, and D. Prettypaul. Indentometric analysis of in vivo skin and comparison with artificial skin models. *Skin Research and Technology*, 13 :299-309, 2007.

[Jacquemoud, 2007]: C. Jacquemoud. *Caractérisation mécanique et modélisation du comportement jusqu'à rupture de membranes biologiques fibreuses : application à la peau humaine*. PhD thesis. Institut National des Sciences Appliquées, Lyon, 2007.

[Jacquemoud *et al.,* 2007]: C. Jacquemoud, K. Bruyere-Garnier, and M. Coret. Methodology to determine failure characteristics of planar soft tissues using a dynamic tensile test. *Journal of Biomechanics*, 40 :468-475, 2007.

[Jacquet *et al.,* 2008]: E. Jacquet, G. Josse, F. Khatyr, and C. Garcin. A new experimental method for measuring skin's natural tension. *Skin Research and Technology*, 14 :1-7, 2008.

[Jansen *et al.,* 1958]: L. Jansen and P. Rottier. Some mechanical properties of human abdominal skin measured on excised strips*. Dermatology,* 117 :65-83, 1958.

[Jemec *et al.,* 2001]: G. Jemec, E. Selvaag, M. Agren, and H. Wulf. Measurement of the mechanical properties of skin with ballistometer and suction cup. *Skin Research and Technology*, 7 :122-126, 2001.

[Jenkins, 2002]: G. Jenkins. Molecular mechanisms of skin ageing. *Mech Ageing Dev*. 123(7):801-810, 2002.

[Jesudason *et al.,* 2007]: R. Jesudason, L. Black, A. Majumbar, P. Stone, and B. Suki. Differential effects of static and cyclic stretching during elastase digestion on the mechanical properties of extracellular matrices. *Journal of Applied Physiology*, 103 :803-811, 2007.

[Kadler *et al.,* 2007]: K. Kadler, C. Baldock, J. Bella, and R. Boot-Handford. Collagens at a glance. *Journal of Cell Science*, 120 :1955-1958, 2007.

[Kearney *et al.,* 2016]: E. Kearney, C. Messaraa, G. Grennan, G. Koeller, A. Mavon et E. Merinville. Evaluation of skin firmness by the DynaSKIN, a novel non-contact compression device, and its use in revealing the efficacy of a skincare regimen featuring a novel anti-ageing ingredient, acetyl aspartic acid. *Skin Research and Technology*, 0 :1-14, 2016.

[Khatyr *et al.,* 2004]: F. Khatyr, C. Imberdis, P. Vescovo, D. Varchon, and J. Lagarde. Model of the viscoelastic behaviour of skin in vivo and study of anisotropy. *Skin Research and Technology*, 10 :96-103, 2004.

[Khatyr *et al.,* 2006]: F. Khatyr, C. Imberdis, D. Varchon, J. Lagarde, and G. Josse. Measurement of the mechanical properties of the skin using the suction test. *Skin Research and Technology*, 12 :24-31, 2006.

[Kim *et al.*, 2019]: M. A. Kim, Y.C. Jung, E.J. Kim. Evaluation of anisotropic properties of striae distensae with regard to skin surface texture and viscoelasticity. *Skin Res Technol,* 00: 1-6, 2019.

[Kirk *et al.,* 1949]: J. Kirk and S. Kvorning. Quantitative measurements of the elastic properties of the skin and subcutaneous tissue in young and old individuals. *Journal of Gerontology*, 4: 273-284, 1949.

[Kirk *et al.,* 1962]: J. Kirk and M. Chieffi. Variation with age in elasticity of skin and subcutaneous tissue in human individuals. *Journal of Gerontology*, 17 :373-380, 1962.

[Krutmann *et al.,* 2017]: J. Krutmann, A. Bouloc, G. Sore, B. Bernard, and T. Passeron. The skin aging exposome. *Journal of Dermatological Science,* 85 :152-161, 2017.

[Lambert, 2018]: B. Lambert. *Prise en charge du vieillissement cutané : comment les cosmétiques s'inspirent des solutions esthétiques.* PhD thesis. Sciences pharmaceutiques. 2018.

[Lamers *et al.,* 2013]: E. Lamers, T. H. S. van Kempen, F. P. T. Baaijens, G. W. M. Peters, and C. W. J. Oomens. Large amplitude oscillatory shear properties of human skin. *Journal of the Mechanical Behavior of Biomedical Materials,* 28: 462-470, 2013.

[Langer, 1978a]: K. Langer. On the anatomy and physiology of the skin. I. The cleavability of the cutis. (Translated from Langer. sitzungsbericht der mathematisch-naturwissenschaftlichen classe der kaiserlichen academie der wissenschaften, 44, 19, 1861). *British Journal of Plastic Surgery*, 31 :3-8, 1978.

[Langer, 1978b]: K. Langer. On the anatomy and physiology of the skin. II. Skin tension by professor Langer, presented at the meeting of 27th November 1861. *British Journal of Plastic Surgery*, 31 :93-106, 1978.

[Langer, 1978c]: K. Langer. On the anatomy and physiology of the skin. III. The elasticity of the cutis by professor Langer, presented at the meeting of 27th November 1861. *British Journal of Plastic Surgery*, 31 :185-199, 1978.

[Langer, 1978d]: K. Langer. On the anatomy and physiology of the skin. IV. The swelling capabilities of skin by professor Langer, presented at the meeting of 27th November 1861. *British Journal of Plastic Surgery*, 31 :273-286, 1978.

[Lanir *et al.,* 1974]: Y. Lanir and Y. Fung. Two-dimensional mechanical properties of rabbit skin. II. Experimental results. *Journal of Biomechanics*, 7 :171-182, 1974.

[Lanir, 1983]: Y. Lanir. Constitutive equations for fibrous connective tissues. *Journal of Biomechanics*, 16 :1-12, 1983.

[Lanir *et al.,* 1990]: Y. Lanir, S. Dikstein, A. Hartzshtark, and V. Manny. In-vivo indentation of human skin. *Journal of Biomechanical Engineering*, 112 :63-69, 1990.

[Lanir *et al.,* 1993]: Y. Lanir, V. Manny, A. Zlotogorski, A. Shafran, and S. Dikstein. Influence of ageing on the in vivo mechanics of the skin. *Skin Pharmacology and Physiology*, 6 :223-230, 1993.

[Lapière *et al.,* 1988]: C. Lapière, B. Nusgens, G. Pierard. The architectural organization and function of the macromolecules in the dermis. In *The Physical Nature of the Skin*, MTP Press Limited. p 163-176, 1988.

[Larrabee, 1986a] : W. Larrabee. A finite element model of skin deformation. i. Biomechanics of skin and soft tissue: a review. *Laryngoscope*, 96 :399-405, 1986.

[Larrabee *et al.,* 1986b]: W. Larrabee and D. Sutton. A finite element model of skin deformation. ii. An experimental model of skin deformation. *Laryngoscope*, 96 :406-412, 1986.

[Larrabee *et al.,* 1986c]: W. Larrabee and J. Galt. A finite element model of skin deformation. iii. The finite element model. *Laryngoscope*, 96 :413-419, 1986.

[Lebertre, 2001]: M. Lebertre. *Echographie quantitative haute fréquence : propriétés du derme humain et potentiel diagnostique*. PhD thesis. Université de Tours, 2001.

[Lebonvallet *et al.,* 2010]: N. Lebonvallet, C. Jeanmaire, L. Danoux, P. Sibille, G. Pauly, and L. Misery. The evolution and use of skin explants: potential and limitations for dermatological research. *Eur J Dermatol* , 20 (6): 671-684, 2010.

[Le Bras, 2012]: S. Le Bras. *Caractérisation d'un modèle porcin de rupture aigue de la barrière cutanée et étude de sa restauration par examens histopathologiques et mesure de la perte insensible en eau*. PhD thesis. Université Claude-Bernard Lyon 1, 2012.

[Lerner *et al.,* 1987]: R. Lerner, K. Parker, J. Holen, R. Gramiak et R. Waag. Sono-elasticity: medical elasticity images derived from ultrasound signals in mechanically vibrated targets. *Acoustical Imaging*, 16 :317-327, 1987.

[Leung *et al.,* 2002]: W. Leung and I. Harvey. Is skin ageing in the elderly caused by sun exposure or smoking? *British Journal of Dermatology*, 147 :1187-1191, 2002.

[Leveque *et al.,* 1980]: J. Leveque, J. De Rigal, P. Agache, and C. Monneur. Influence of ageing on the in vivo extensibility of human skin at a low stress. *Archives of Dermatological Research*, 269: 127-135, 1980.

[Liang *et al.,* 2010]: X. Liang and S. A. Boppart. Biomechanical properties of in vivo human skin from dynamic optical coherence elastography. *IEEE Trans Biomed Eng.* 57(4): 953-959, 2010.

[Lim *et al.,* 2008]: K. Lim, C. Chew, P. Chen, S. Jeyapalina, H. Ho, J. Rappel, and B. Lim. New extensometer to measure in vivo uniaxial mechanical properties of human skin. *Journal of Biomechanics*, 41 :931-936, 2008.

[Liu *et al.,* 2008]: Z. Liu and K. Yeung. The preconditioning and stress relaxation of skin tissue. *Journal of Biomedical and Pharmaceutical Engineering*, 2 :22-28, 2008.

[Liu *et al.,* 2010]: J. Liu and H. Qi. Dissipated energy function, hysteresis and precondition of a viscoelastic solid model. *Nonlinear Analysis - Real World Applications*, 11 :907-912, 2010.

[Lynch, 2015]: B. Lynch. *Multiscale biomechanics of skin: experimental investigation of the role of the collagen microstructure*. PhD thesis. Ecole Polytechnique, 2015.

[Manschot *et al.,* 1986]: J. Manschot and A. Brakkee. The measurement and modelling of the mechanical properties of human skin in vivo. i. The measurement. *Journal of Biomechanics*, 19 :511-515, 1986.

[Mansour *et al.,* 1993]: J. Mansour, B. Davis, M. Srour, R. Theberge. A method for obtaining repeatable measurements of the tensile properties of skin at low strain. *Journal of Biomechanics*, 26 :211-216, 1993.

[Marcellier *et al.,* 2001]: H. Marcellier, P. Vescovo, D. Varchon, P. Vacher, and P. Humbert. Optical analysis of displacement and strain fields on human skin. *Skin Research and Technology*, 7 :264-253, 2001.

[Marino, 2001]: C. Marino. *Skin physiology, irritants, dry skin and moisturizers*. Report 56-2-2001, Washington State Department of Labor and Industries, 2001.

[Matsumoto, 1993]: B. Matsumoto. *Cell biological applications of confocal microscopy.* Academic Press, 1993.

[McGrath *et al.,* 2010]: J. McGrath, and J. Uitto. Anatomy and Organization of Human Skin. In Rook's Textbook of Dermatology, Oxford, UK, 2010.

[Mears *et al.,* 1969]: D. R. Mears, K. D. Pae, and J. A. Sauer. Effects of Hydrostatic Pressure on the Mechanical Behavior of Polyethylene and Polypropylene. *Journal of Applied Physics*, 40 (11), 4229, 1969.

[Meijer *et al.,* 1999]: R. Meijer, L. Douven, and C. Oomens. Characterization of anisotropic and nonlinear behaviour of human skin in vivo. *Computer Methods in Biomechanics and Biomedical Engineering*, 1 :13-27, 1999.

[Meryman, 1957]: H. T. Meryman. Tissue freezing and local cold injury. *Physiol Rev*, 37(2):233–251, 1957.

[Minns *et al.,* 1973]: R. Minns, P. Soden, and D. Jackson. The role of the fibrous components and ground substance in the mechanical properties of biological tissues: a preliminary investigation. *Journal of Biomechanics*, 6 :153-165, 1973.

[Mitts *et al.*, 2005]: T. F. Mitts, F. Jimenez and A. Hinek. Skin Biopsy Analysis Reveals Predisposition to Stretch Mark Formation. *Aesthetic Surg J,* 25: 593-600, 2005.

[Mofid *et al.,* 2006]: Y. Mofid, S. Gahagnon, F. Patat, and F. Ossant. In vivo high frequency elastography for mechanical behavior of human skin under suction stress: elastograms and kinetics of shear, axial and lateral strain fields. *IEEE Ultrasonics Symposium*, p 1041-1044, 2006.

[Moon *et al.,* 2006]: D. Moon, S. Woo, Y. Takakura, M. Gabriel, and S. bramowitch. The effects of refreezing on the viscoelastic and tensile properties of ligaments. *Journal of Biomechanics*, 39 :1153-1157, 2006.

[Munoz *et al.,* 2008]: M. Munoz, J. Bea, J. Rodriguez, I. Ochoa, J. Grasa, A. Perez del Palomar, P. Zaragoza, R. Osta, and M. Doblare. An experimental study of the mouse skin behaviour: Damage and inelastic aspects. *Journal of Biomechanics*, 41 :93-99, 2008.

[Nehal *et al.,* 2008]: K. Nehal, D. Gareau, M. Rajadhyaksha. Skin imaging with reflectance confocal microscopy. *Seminars in Cutaneous Medicine and Surgery*, 27 :37-43, 2008.

[New *et al.,* 1991]: K. New, W. Petroll, A. Boyde, L. Martin, P. Corcuff, J. Leveque, M. Lemp, H. Cavanagh, and J. Jester. In vivo imaging of human teeth and skin using real-time confocal microscopy. *Scanning,* 13 :369-372, 1991.

[Nguyen, 2012]: T. Nguyen. *Elastographie haute-résolution pour l'évaluation des propriétés élastiques de la cornée et de la peau.* PhD thesis. Université Paris-Diderot, 2012.

[Ni Annaidh *et al.,* 2012]: A. Ní Annaidh, K. Bruyère, M. Destrade, M. D. Gilchrist, and M. Otténio. Characterization of the anisotropic mechanical properties of excised human skin. *Journal of Mechanical Behavior of Biomedical Materials,* 5(1): 139-48, 2012.

[Ni Annaidh *et al.,* 2019]: A. Ní Annaidh and M. Destrade. Tension Lines of the Skin. G. Limbert (ed.), *Skin Biophysics.* Studies in Mechanobiology, Tissue Engineering and Biomaterials, 22: 265–280, 2019.

[Nicolle *et al.,* 2023]: S. Nicolle, J. F. Palierne, D. Mitton, H. Follet, and C.B. Confavreux. Multi-frequency shear modulus measurements discriminate tumorous from healthy tissues. *J Mech Behav Biomed Mater,* 140: 105721, 2023.

[Noorlander *et al.,* 2002]: M. Noorlander, P. Melis, A. Jonker, and C. Van Noorden. A quantitative method to determine the orientation of collagen fibers in the dermis. *The Journal of Histochemistry and Cytochemistry*, 50 :1469-1474, 2002.

[Ogden, 1972]: R. Ogden. Large deformation isotropic elasticity-on the correlation of theory and experiment for incompressible rubberlike solids. *Proceedings of the Royal Society of London. A. Mathematical, Physical & Engineering Sciences,* 326 :565-584, 1972.

[Ophir *et al.,* 1991]: J. Ophir, I. Cespedes, H. Ponnekanti, Y. Yazdi, and X. Li. Elastography: a quantitative method for imaging the elasticity of biological tissues, *Ultrasonic Imaging*, 13 :111-134, 1991.

[Ossant *et al.,* 2001]: F. Ossant, M. Leberte, J. M. Gregoire, J. P. Chemla, and C. Guittet. *Exploration de la peau*. Université de TOURS, 2001.

[Ottenio *et al.,* 2015]: M. Ottenio, D. Tran, A. Annaidh, M. Gilchrist, and K. Bruyère. Strain rate and anisotropy effects on the tensile failure characteristics of human skin. *Journal of the Mechanical Behavior of Biomedical Materials,* 41: 241-250, 2015.

[Oxlund *et al.,* 1988]: H. Oxlund, J. Manschot, and A. Viidik. The role of elastin in the mechanical properties of skin. *Journal of Biomechanics*, 21 :213-218, 1988.

[Pailler-Mattei *et al.,* 2006]: C. Pailler-Mattei and H. Zahouani. Analysis of adhesive behaviour of human skin in vivo by an indentation test. *Tribology International*, 39:12-21, 2006.

[Pailler-Mattei *et al.,* 2008]: C. Pailler-Mattei, S. Bec, and H. Zahouani. In vivo measurements of the elastic mechanical properties of human skin by indentation tests. *Medical Engineering and Physics*, 30 :599-606, 2008.

[Pailler-Mattéi *et al.,* 2012]: C. Pailler-Mattéi and H. Zahouani. Study of adhesion forces and mechanical properties of human skin in vivo. *Journal of Adhesion Science and Technology*, 18:15-16, 1739-1758, 2012.

[Pan *et al.,* 1998]: L. Pan, L. Zan, and F. Foster. Ultrasonic and viscoelastic properties of skin under transverse mechanical stress in vitro. *Ultrasound in Medecine and Biology*, 24 :995-1007, 1998.

[Park *et al.,* 1972]: A. Park and C. Baddiel. Rheology of stratum corneum. I. A molecular interpretation of the stress-strain curve. *Journal of Society of Cosmetics Chem*ists of Great Britain, 23 :3-12, 1972.

[Payne, 1991]: P. Payne. Measurement of properties and function of skin. *Clinical Physics and Physiological Measurement*, 12 :105-129, 1991.

[Pawley, 1990]: J. Pawley. *Handbook of Biological Confocal Microscopy*. Plenum Press, 1990.

[Pearce *et al.,* 2011]: S. Pearce, J. King, and M. Holdsworth. Axisymmetric indentation of curved elastic membranes by a convex rigid indenter. *International Journal of Non-Linear Mechanics*, 46 :1128-1138, 2011.

[Pierard, 1999]: G. Pierard. EEMCO guidance to the in vivo assessment of tensile functional properties of the skin. Part 1: Relevance to the structures and ageing of the skin and subcutaneous tissues. *Skin Pharmacology and Applied Skin Physiology*, 12 :352-362, 1999.

[Pierard *et al.*, 1999]: G. E. Pierard, J. L. Nizet, J. P. Adant, M. Avila Camacho, A. Pans and J. Fissette. Tensile properties of relaxed excised skin exhibiting striae distensae. *Journal of Medical Engineering & Technology*, 23(2): 69-72, 1999.

[Pieraggi *et al.*, 1982]: M. Th. Pieraggi, M. Julian, M. Delmas, and H. Bouissou. Striae: Morphological Aspects of Connective Tissue. *Pathol Anat,* 396: 279-289, 1982.

[Pissarenko *et al.,* 2020]: A. Pissarenkoa, and M. A. Meyersa. The materials science of skin: Analysis, characterization, and modeling. *Progress in Materials Science.* 110: 100634, 2020.

[Potts *et al.,* 1983]: R. Potts and M. Breuer. The low-strain, viscoelastic properties of skin. *Bioengineering of Skin*, 4 :105-114, 1983.

[Prevorovsky *et al.,* 2007]: Z. Prevorovsky, E. Jacquet, V. Placet, and G. Josse. Ultrasonic wave propagation and mechanical properties of human skin stretched in vivo. In *2nd International Conference on Mechanics of Biomaterials & Tissues*, 2007.

[Quatresooz *et al.,* 2005]: P. Quatresooz, Uhoda, C. Piérard-Franchimont, and G. Piérard. Héliodermie, héliophiles et héliophobes. *Revue médicale de Liège*, 60 :57-59, 2005.

[Quatresooz *et al.,* 2006] : P. Quatresooz, L. Thirion, C. Piérard-Franchimont, and G. Piérard. The riddle of genuine skin microrelief and wrinkles. *International Journal of Cosmetic Science*, 28 :389-395, 2006.

[Quirinia and Viidik, 1991]: A. Quirinia, and A. Viidik. Freezing for postmortal storage influences the biomechanical properties of linear skin wounds. *J Biomech* 24(9):819-823, 1991.

[Ranamukhaarachchi *et al.*, 2016]: S. A. Ranamukhaarachchi, S. Lehnert, S. L. Ranamukhaarachchi, *et al.* A micromechanical comparison of human and porcine skin before and after preservation by freezing for medical device development. *Sci Rep* 6, 32074, 2016.

[Ranamukhaarachchi, 2017]: S. Ranamukhaarachchi. *Skin mechanics, intradermal delivery and biosensing with hollow metallic microneedles* (Thesis). University of British Columbia, 2017.

[Rawlings *et al.*, 2004]: N. D. Rawlings, D. P. Tolle, and A. J. Barrett. Evolutionary families of peptidase inhibitors. *Biochem. J.* 378, 705–716, 2004.

[Regulations CE n°1223/2009]: Règlement (CE) n° 1223/2009 du Parlement Européen et du Conseil du 30 novembre 2009 relatif aux produits cosmétiques.

[Reihsner *et al.,* 1995]: R. Reihsner, B. Balog, and E. Menzel. Two-dimensional elastic properties of human skin in terms of an incremental model at the in vivo configuration. *Medical Engineering and Physics*, 17 :304-313, 1995.

[Richard *et al.,* 1993]: S. Richard, B. Querleux, J. Bittoun, O. Jolivet, I. Idy-Peretti, O. De Lacharrière, and J. Lévêque. Characterization of the skin in vivo by high resolution magnetic resonance imaging: Water behavior and age-related effects. *The Journal of Investigative Dermatology*, 100 :705-709, 1993.

[Ridge, 1964]: M. D. Ridge. *The rheology of skin. A bio-engineering study of the mechanical properties of human skin in relation to its structure* (Thesis). University of Leeds, 1964.

[Ridge *et al.,* 1966]: M. Ridge and V. Wright. Rheological analysis of connective tissue. A bioengineering analysis of the skin. *Annals of the Rheumatic Diseases,* 25: 509-515, 1966.

[Ridge and Wright*.,* 1966]: M. D. Ridge and V. Wright. The directional effects of skin. A bio-engineering study of skin with particular reference to Langer's lines. *J Invest Dermatol.* 46(4): 341–346, 1966.

[Robert *et al.*, 1984]: L. Robert, M. P. Jacob, C. Frances, G. Godeau, and W. Hornebeck. Interaction between elastin and elastases and its role in the aging of the arterial wall, skin and other connective tissues. A review. *Mech Ageing Dev*. 28(2-3):155-66, 1984.

[Robert *et al.,* 2009]: L. Robert, J. Labat-Robert, A. Robert. Physiology of skin aging. *Pathologie Biologie*, 57 :336-341, 2009.

[Roche, 1997]: I. Roche. *Relation entre le comportement mécanique et la structuration des lattices de collagène autotendus*. PhD thesis. Université de Franche-Comté, 1997.

[Roeder *et al.,* 2002]: B. Roeder, K. Kokini, J. Sturgis, J. Robinson, and S. Voytik-Harbin. Tensile mechanical properties of three-dimensional type I collagen extracellular matrices with varied microstructure. *Journal of Biomechanical Engineering*, 124 :214-222, 2002.

[Rolhaüser, 1950]: H. Rollhaüser. The tensile strength of human skin. *Gegenbauer morph*. Jb., 90 :249-261, 1950.

[Rorteau *et al.,* 2020]: J. Rorteau, F. P. Chevalier, B. Fromy and J. Lamartine. Vieillissement et intégrité de la peau - De la biologie cutanée aux stratégies anti-âge. *Med Sci (Paris)*, 36 : 1155–1162, 2020.

[Rosado *et al.,* 2015]: C. Rosado, F. Antunes, R. Barbosa, R. Fernando, and L. Rodrigues. Cutiscan® - A new system of biomechanical evaluation of the skin in vivo – comparative study of use depending on the anatomical site. *Biomedical and Biopharmaceutical Research*, 12 :49-57, 2015.

[Sacks, 2000]: M. Sacks. Biaxial mechanical evaluation of planar biological materials. *Journal of Elasticity*, 61 :199-246, 2000.

[Sanders, 1973]: R. Sanders. Torsional elasticity of human skin in vivo. *Pflugers Archiv: European Journal of Physiology*, 342 :255-260, 1973.

[Sangroniz *et al.*, 2023]: L. Sangroniz, M. Fernandez, and A. Santamaria. Polymers and rheology: A tale of give and take*. Polymer*. 271: 125811, 2023.

[Sanjeevi, 1982]: R. Sanjeevi. A viscoelastic model for the mechanical properties of biological materials. *Journal of Biomechanics*, 15 :107-109, 1982.

[Schmid *et al.,* 2005]: F. Schmid, G. Sommer, M. Rappolt, C. Schulze-Bauer, P. Regitnig, G. Holzapfel, P. Laggner, and H. Amenitsch. In situ tensile testing of human aortas by time-resolved small-angle X-ray scattering. *Journal of Synchrotron Radiation*, 12 :727-733, 2005.

[Scott, 1989]: D. Scott. Structure and function of the skin. In Muller & Kirk's Small animal dermatology, 4th edition, Saunders Company, 1989.

[Scott, 1991]: J. Scott. Proteoglycan: collagen interactions in connective tissues. Ultrastructural, biochemical, functional and evolutionary aspects. *International Journal of Biological Macromolecules*, 13 :157-161, 1991.

[Scott, 2003]: J. Scott. Elasticity in extracellular matrix 'shape modules' of tendon, cartilage, etc. A sliding proteoglycan-filament model. *Journal of Physiology*, 553 :335-343, 2003.

[Serup *et al.,* 2006]: J. Serup, J. Keiding, A. Fullerton, M. Gniadecka, and R. Gniadecki. High-Frequency Ultrasound Examination of the skin: Introduction and Guide. In *Handbook of Non-Invasive Methods and the Skin*, p 473-487. CRC Press, 2nd edition, 2006.

[Shade, 1912]: H. Shade. Untersuchungen zur organfunction des bindesgewebes. *Ztschr. Exepr. Pathol. Therap.,* 11 :369-399, 1912.

[Shen *et al.,* 2008]: Z. Shen, M. Reza Dodge, H. Kahn, R. Ballarini, and S. Eppell. Stress-strain experiments on individual collagen fibrils. *Biophysical Journal*, 95 :3956-3963, 2008.

[Shergold *et al.,* 2006]: O. Shergold, N. Fleck, and D. Radford. The uniaxial stress versus strain response of pig skin and silicone rubber at low and high strain rates. *International Journal of Impact Engineering*, 32 :1384-1402, 2006.

[Sheu *et al.*, 1991]: H-M. Sheu, H-S Yu and C-H Chang. Mast cell degranulation and elastolysis in the early stage of striae distensae. *J Cutan Pathol*, 18: 410–416, 1991.

[Shoulders *et al.,* 2009]: M. Shoulders and R. Raines. Collagen structure and stability. *Annual Review of Biochemistry* 78 :929-958, 2009.

[Silver, 1987]: F. Silver. *Biological materials: Structure, mechanical properties and modelling of soft tissues*. NYU Press, 1987.

[Silver *et al.,* 1992]: F. Silver, Y. Kato, M. Ohno, and A. Wasserman. Analysis of mammalian connective tissue: relationship between hierarchical structures and mechanical properties. *Journal of Long-Term Effect of Medical Implants*, 2 :165-198, 1992.

[Silver *et al.,* 2001]: F. Silver, J. Freeman, and D. De Vore. Viscoelastic properties of human skin and processed dermis. *Skin Research and Technology*, 7 :18-23, 2001.

[Silver *et al.,* 2002]: F. Silver, G. Seehra, J. Freeman, and D. Devore. Viscoelastic properties of young and old human dermis: a proposed molecular mechanism for elastic energy storage in collagen and elastin. *Journal of Applied Polymer Science*, 86 :1978-1985, 2002.

[Silver *et al.,* 2003]: F. Silver, L. Siperko, and G. Seehra. Mechanobiology of force transduction in dermal tissue. *Skin Research and Technology*, 9 :3-23, 2003.

[Sinclair, 2006]: C. Sinclair. Risks and benefits of sun exposure: Implications for public health practice based on the Australian experience. *Progress in Biophysics and Molecular Biology*, 92 :173-178, 2006.

[Snedeker *et al.,* 2005]: J. Snedeker, P. Niederer, F. Schmidlin, M. Farshad, C. Demetropoulos, J. Lee, and K. Yang. Strain-rate dependant material properties of the porcine and human kidney capsule. *Journal of Biomechanics*, 38 :1011-1021, 2005.

[Stamatas *et al.*, 2014]: G. N. Stamatas, A. Lopes-DaCunha, A. Nkengne and C. Bertin. Biophysical properties of striae distensae evaluated in vivo using non-invasive assays. *Skin Res Technol,* 0: 1-5, 2014.

[Standard ISO 6721-1]: Plastiques - Détermination des propriétés mécaniques dynamiques - Partie 1 : Principes généraux.

[Stark, 1977]: H. Stark. Directional variations in the extensibility of human skin. *British Journal of Plastic Surgery*, 30 :105-114, 1977.

[Stevens *et al.,* 1994]: J. Stevens, L. Mills, and J. Trogadis. *3D confocal microscopy: volume investigation of biological systems*. Academic Press, 1994.

[Stroumza *et al.,* 2015]: N. Stroumza, R. Bosc, B. Hersant, O. Hermeziu, and J. P. Meningaud. Intérêt du cutomètre pour l'évaluation de l'efficacité des traitements cutanés en chirurgie plastique et maxillo-faciale. *Revue de Stomatologie, de Chirurgie Maxillo-faciale et de Chirurgie Orale*, 116 :77-81, 2015.

[Sugimoto, 1990]: T. Sugimoto, S. Ueha, K. Itoh. Tissue hardness measurement using the radiation force of focused ultrasound. *IEEE Ultrasonics Symposium*, 1990.

[Sun *et al.,* 1996]: Y. Sun, Z. Luo, A. Fertala, and K. An. Direct quantification of the flexibility of type I collagen monomer. *Biochemical and Biophysical Research Communications*, 295 :382-386, 1996.

[Svoboda, 2018]: E. Svoboda. When the first defence fails. Nature, 563 :89-90, 2018.

[Tong *et al.,* 1976]: P. Tong and Y. Fung. The Stress-strain relationship for the skin. *Journal of Biomechanics*, 9 :649-657, 1976.

[Tortora *et al.,* 2007]: G. Tortora and B. Derrickson. *Principes d'anatomie et de physiologie*. Editeur De Boeck*,* 2007.

[Tosti *et al.,* 1977]: A. Tosti, C. Giovanni, M. Fazzini, and S. Villardita. A ballistometer for the study of the plasto-elastic properties of skin. *Journal of Investigative Dermatology*, 69 :315-317, 1977.

[Tran, 2007]: H. V. Tran. *Caractérisation des propriétés mécaniques de la peau humaine in vivo via l'IRM*. PhD thesis. Université de Technologie de Compiègne, 2007.

[Tsuji *et al.*, 2001]: N. Tsuji, S. Moriwaki, Y. Suzuki, Y. Takema, and G. Imokawa. The role of elastases secreted by fibroblasts in wrinkle formation: implication through selective inhibition of elastase activity. *Photochem Photobiol.* 74(2):283-90, 2001.

[Turnbull *et al.,* 1995]: D. Turnbull, B. Starkoski, K. Harasiewicz, J. Semple, L. From, A. Gupta, D. Sauder, and F. Foster. A 40-100 MHz B-Scan ultrasound backscatter microscope for skin imaging. *Ultrasound in Medicine & Biology*, 21 :79-88, 1995.

[Ushiki, 2002]: T. Ushiki. Collagen fibers, reticular fibers and elastic fibers. a comprehensive understanding from a morphological viewpoint. *Archives of histology and cytology*, 65 :109-126, 2002.

[Van der Rijt, 2004]: J. Van der Rijt. *Micromechanical testing of single collagen type I fibrils*. PhD thesis. University of Twente, The Netherlands, 2004.

[Ventre *et al.,* 2009]: M. Ventre, F. Mollica, and P. Netti. The effect of composition and microstructure on the viscoelastic properties of dermis. *Journal of Biomechanics*, 42 :430-435, 2009.

[Veronda *et al.* 1970]: D. Veronda and R. Westmann. Mechanical characterization of skin-finite deformations. *Journal of Biomechanics*, 3 :111-124, 1970.

[Vescovo *et al.,* 2002]: P. Vescovo, D. Varchon, and H. Humbert. In vivo tensile tests on human skin: the extensometers. *Bioengineering of the skin: skin biomechanics*. CRC Press, USA: New York, p77-90, 2002.

[Vitellaro *et al.,* 1994]: L. Vitellaro-Zuccarello, S. Cappelletti, V. Dal Pozzo Rossi, and M. Sari-Gorla. Stereological analysis of collagen and elastic fibers in the normal human dermis: variability with age, sex, and body region. *The Anatomical Record*, 238 :153-162, 1994.

[Vogt *et al.,* 2003]: M. Vogt, S. Scharenberg, R. Scharenberg, K. Hoffmann, P. Altmeyer, and H. Ermert. A high frequency ultrasound elastography system for in vivo skin elasticity imaging. *WCU 2003*, Paris, 2003.

[Waldorf *et al.,* 2002]: J. Waldorf, G. Perdikis, and S. Terkonda. Planning incisions. *Operative Techniques in General Surgery*, 4 :199-206, 2002.

[Waller *et al.,* 2006]: J. Waller and H. Maibach. Age and skin structure and function, a quatitative approach (ii): Protein, glycosaminoglycan, water, and lipid content and structure. *Skin Research and Technology*, 12 :145-154, 2006.

[Watson *et al.*, 1998]: R. E. Watson, E. J. Parry, J. D. Humphries, C. J. Jones, D. W. Polson, C. M. Kielty, C. E. Griffiths. Fibrillin microfibrils are reduced in skin exhibiting striae distensae. *Br J Dermatol*, 138(6): 931-7, 1998.

[Wenger *et al.,* 2007]: M. Wenger, L. Bozec, M. Horton, and P. Mesquida. Mechanical properties of collagen fibrils. *Biophysical Journal,* 93 :1255-1263, 2007.

[Wheater *et al.,* 2004]: P. Wheather, B. Young, and J. Heath. *Histologie fonctionnelle*. De Boeck Université, 2004.

[Wildnauer *et al.,* 1971]: R. Wildnauer, J. Bothwell, and A. Douglas. Stratum corneum biomechanical properties. I. Influence of relative humidity on normal and extracted human stratum corneum. *The Journal of Investigative Dermatology*, 56 :72-78, 1971.

[Wilkes *et al.,* 1973]: G. Wilkes, I. Brown, and R. Wildnauer. The biomechanical properties of skin. *CRC Critical Reviews in Bioengineering*, 1 :453-495, 1973.

[Wijn, 1980]: P. Wijn. *The alinear viscoelastic properties of the human skin in vivo for small deformations*. PhD thesis. Radboud University Nijmegen, 1980.

[Wilson, 1992]: P. Wilson. William cowper's anatomy for human skin. *International Journal of Dermatology*, 31 :361-364, 1992.

[Xing *et al.,* 2006]: M. Xing, Z. Sun, N. Pan, W. Zhong, and H. Maibach. An EFE model on skin-sleeve interactions during arm rotation. *Journal of Biomechanical Engineering*, 128 :872-878, 2006.

[Xu *et al.,* 2008]: F. Xu, T. Lu, and K. Seffen. Biothermomechanical behavior of skin tissue. *Acta Mechanica Sinica*, 24 :1-23, 2008.

[Yamada, 1970]: H. Yamada. Strength of biological materials. *F. Gaynor Evans*, 1970.

[Yazdi *et al.,* 2022]: S. J. M. Yazdi, and J. Baqersad. Mechanical modeling and characterization of human skin: A review. *Journal of biomechanics* 130, 110864, 2022.

[Yuan *et al.,* 2000]: H. Yuan, S. Kononov, F. Cavalcante, K. Lutchen, E. Ingenito, and B. Suki. Effects of collagenase and elastase on the mechanical properties of lung tissue strips. *Journal of Applied Physiology*, 89 :3-14, 2000.

[Zahouani *et al.,* 2006]: H. Zahouani and P. Humbert. The morphological tree of the cutaneous network of lines. In *Handbook of Non-Invasive Methods and the Skin*, p 195-203. CRC Press, 2nd edition, 2006.

[Zahouani *et al.,* 2009]: H. Zahouani, R. Vargiolu, G. Boyer, C. Pailler-Mattei, L. Laquièze, and A. Mavon. Friction noise of human skin in vivo. *Wear*, 267 :1274-1280, 2009.

[Zahouani *et al.,* 2011]: H. Zahouani, G. Boyer, C. Pailler-Mattei, M. BenTkaya, and R. Vargiolu. Effect of human ageing on skin rheology and tribology. *Wear*, 271 :2364–2369, 2011.

[Zeng *et al.,* 2001]: Y. Zeng, J. Yang, K. Huang, Z. Lee, and X. Lee. A comparison of biomechanical properties between human and porcine cornea. *Journal of Biomechanics*, 34 :533-537, 2001.

[Zhang *et al.,* 2011]: X. Zhang, T. Osborn, M. Pittelkow, B. Qiang, R. Kinnick et J. Greenleaf. Quantitative assessment of scleroderma by surface wave technique. *Medical Engineering and Physics*, 33 :31-37, 2011.

[Zheng *et al.,* 1985]: P. Zheng, R. M. Lavker and A. M. Kligman. Anatomy of striae. *British Journal of Dermatology*, 112, 185-193, 1995.

[Zheng *et al.,* 1996]: Y. Zheng and F. Mak. An ultrasound indentation system for biomechanical properties assessment of soft tissues in-vivo. *IEEE Transactions on Biomedical Engineering*, 43 :912-918, 1996.

[Zheng *et al.,* 1999]: Y. Zheng, F. Mak, and B. Lue. Objective assessment of limb tissue elasticity: Development of a manual indentation procedure. *Journal of Rehabilitation Research and Development*, 36, 1999.

[Zhou *et al.,* 2010]: B. Zhou, F. Xu, C. Chen, and T. Lu. Strain rate sensitivity of skin tissue under thermomechanical loading. *Philos. Trans. R. Soc*. A 368, 679–690, 2010.

APPENDIX

Appendix 1: Minor modifications to the device

In order to carry out complete mechanical tests on human skin explants, many modifications to the device have been made. The minor modifications are presented briefly in this Appendix.

- Purchase of stainless-steel studs to replace the original plastic studs which flexed during mechanical testing.

- Configuration of the force sensor power conditioners and calibration of the force sensors. Calibration is the process of checking the sensors to maintain the prescribed measurement values. For each force sensor, the power conditioner was electrically calibrated and the calibration was verified using calibration weights. Finally, tests with tension springs were successfully carried out to validate the calibration.

- Firmware update and calibration of the piezoelectric actuator

- Purchase and cutting of a new, taller camera box to accommodate the new, larger position sensor, visible in Figure A1b.

- The equipment was improved to allow *in vivo* tests to be carried out with the forearm at the centre of the device, and to accompany the purchase of the new, bigger motorised sample holder. This modification can be seen in Figure A1.

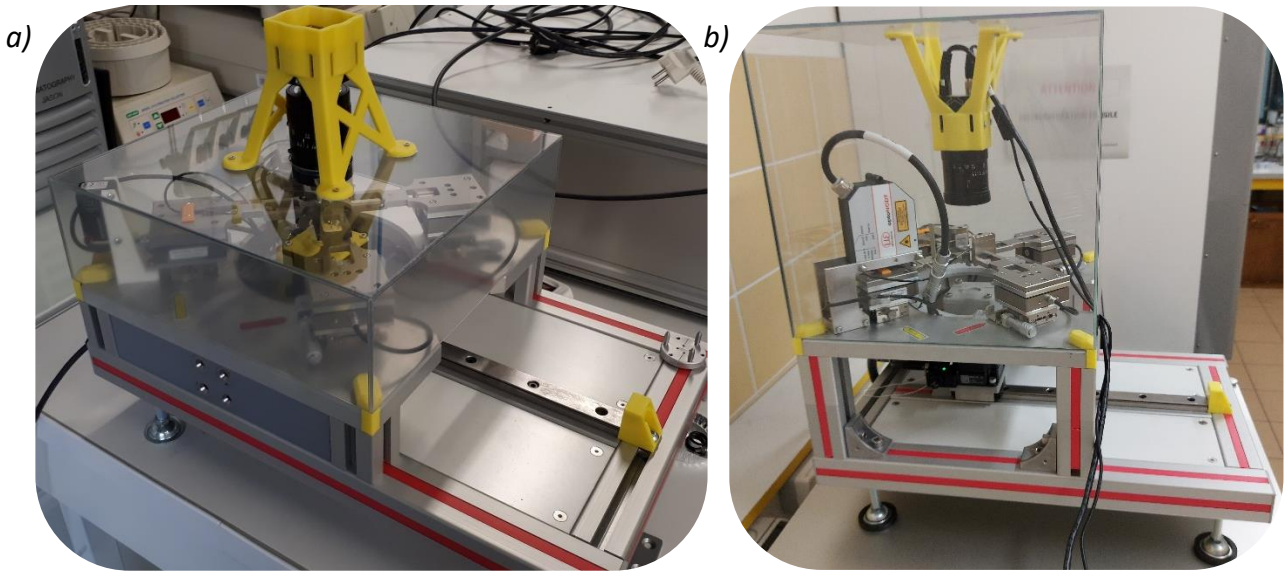

Figure A1: Comparison of the equipment in its initial state (a) and final state (b). Visible change in the camera box and elevation of the device.

- Prototyping of the part holding the new position sensor and machining of this part in aluminium.

- Design and machining of the metal part, in the shape of a strip, which serves as a reference point for the laser of the new position sensor.

- Organisation of the "instrumentation box", shown in Figure A2, which is linked to the device and groups together all the power conditioners and controllers, the acquisition system, the power supplies, and the electrical wiring.

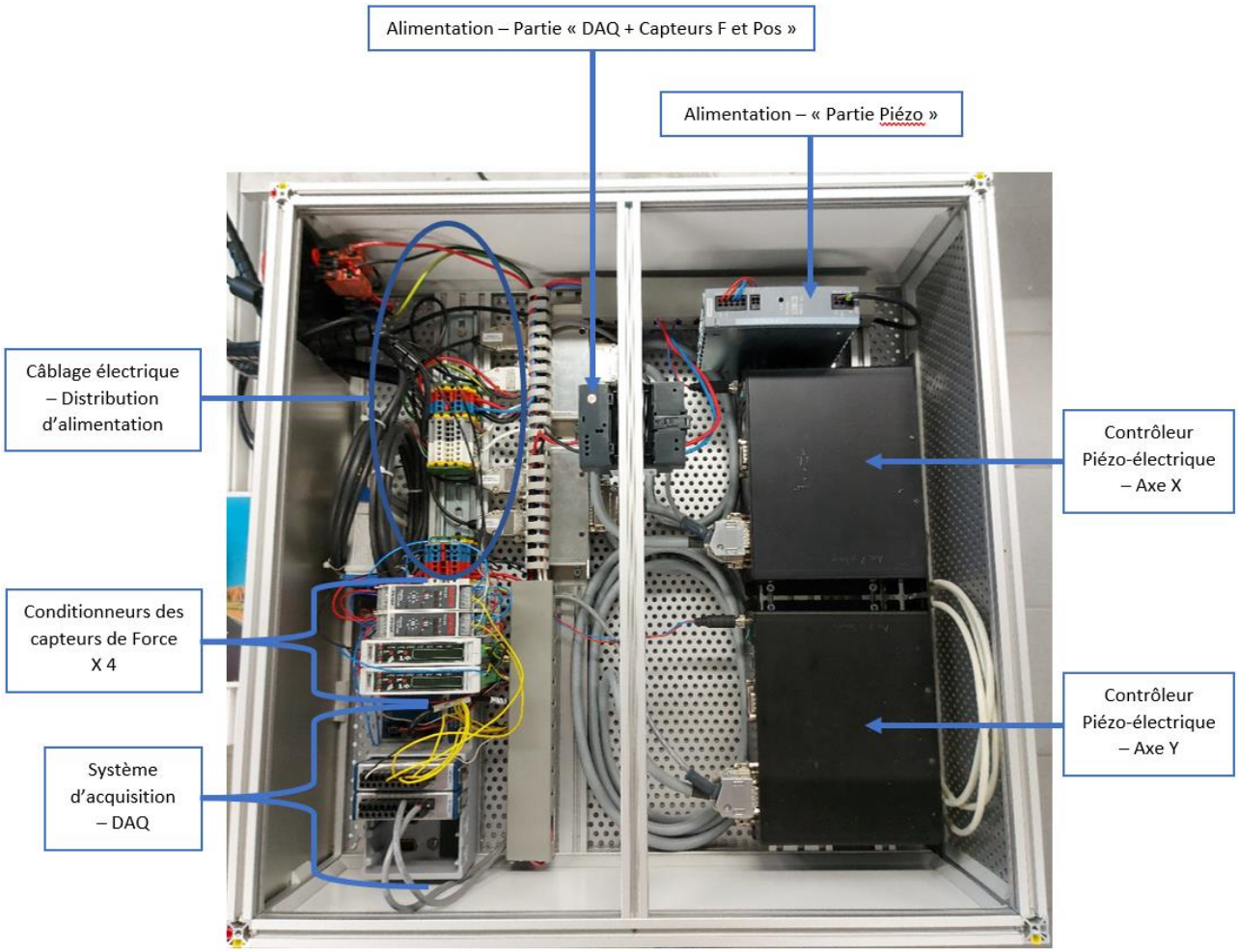

Figure A2: Photo of the "instrumentation box"

- Work on a solution to counter the bending of the arms with the new vertical force sensors: prototyping of a 3D printed plastic part to be used as a 'mould' for the ends of the arms containing the vertical force sensor. This part has to mould to the shape of the arms in order to stiffen them. This solution reduced the bending of the arms but did not completely eliminate the bending. The printed part can be seen in Figure A3. The same type of part in a more rigid material could be a good solution to this problem.

a) *b)*

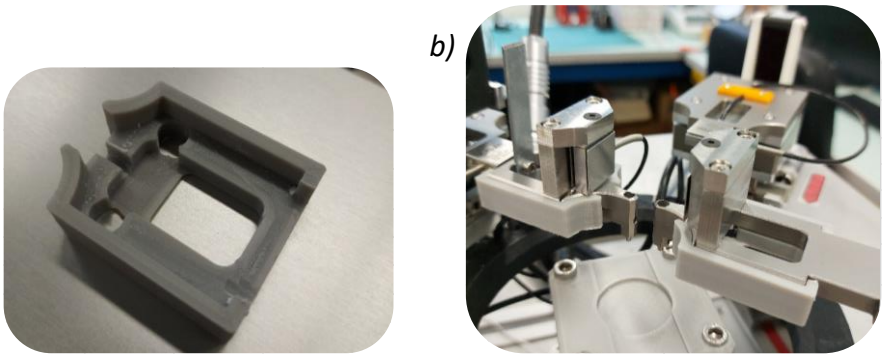

Figure A3: a) Photos of the 3D printed "arm mould" part. b) Photo of this part attached to the arms of the device.

Appendix 2: Latest version of the LabVIEW® interface that enables the operator to carry out mechanical tests with the device

The software interface for this latest version of the program is presented in this Appendix. This Appendix describes all the operations to be carried out in the software in order to perform a mechanical test on a skin sample.

A) The first page of the software interface, shown in Figure A4, is dedicated to the connection and initial verification of the various components of the device. First, the operator selects the various peripherals to be connected: position and force sensors, piezoelectric actuators, sample holder and camera. Next, the operator provides information on the initial air gap, i.e. the starting distance between the two studs on the aligned and opposite arms, as well as the diameter of the studs. These values will later be used to calculate the deformation of the sample and the stresses measured.

An initial software verification stage is then necessary to continue the test protocol. Before each experimental session, a procedure has been set up in the software to check that the device's sensors and actuators are working properly. This step is mandatory before starting any experimental session.
This is an automatic test that will check that the arms and motorised lift support are moving and working correctly without the sample. A margin of error of 1% has been set as the threshold value for the validity of the various measurements. Once the check has been carried out, the operator can then progress through the interface by clicking on “Préparer un nouvel essai”.

The operator can also prepare the *ex vivo* explants so that they are ready for testing.

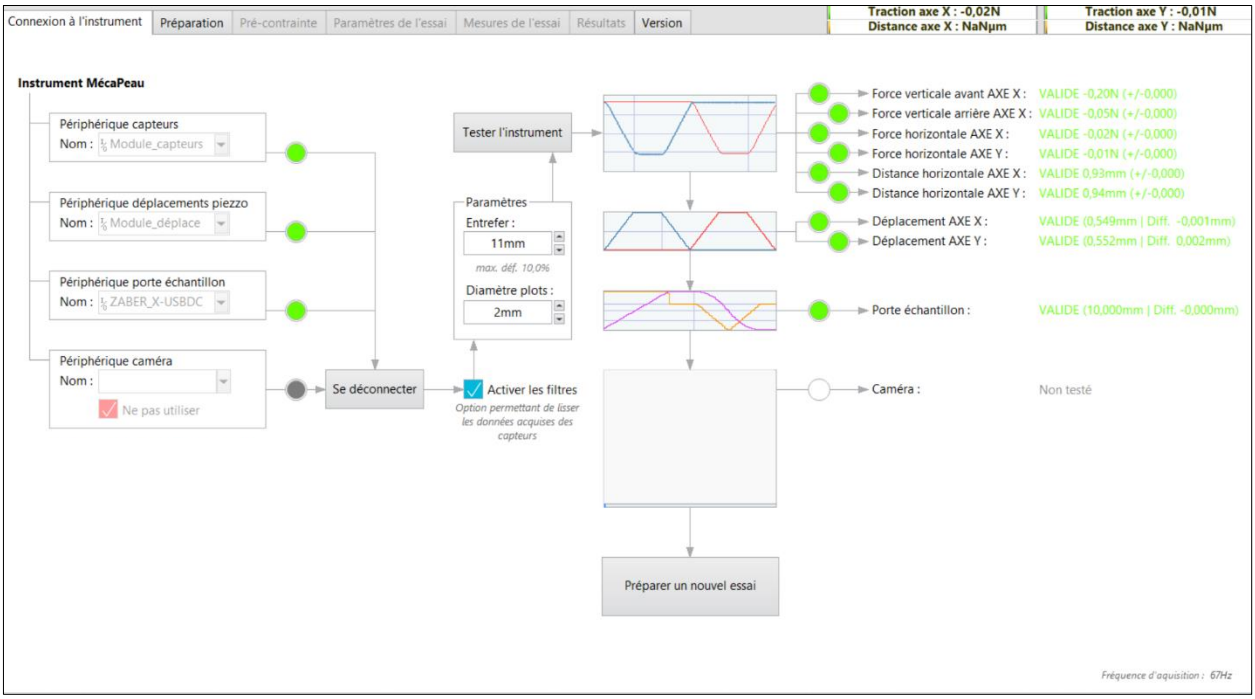

Figure A4: First "Connection à instrument" page of the software interface.

B) The second page of the software interface, shown in Figure A5, is dedicated to the preparation and placement of the skin sample. First of all, the sensors are zeroed. Next, an initial vertical position is defined. An empty cell, which normally contains the skin sample (the metal grids in the case of Eurofins BIO-EC skins), is placed on the motorised sample support. This support is raised until it reaches the instrument studs which are attached to the arms: the initial vertical position is defined.

As a reminder, the mechanical tensile tests are carried out on the X measurement axis, which means that only the two studs on this axis will be bonded. The studs on the Y measurement axis are used to measure the thickness of the skin and the vertical compression force exerted on it when the sample is placed.

The skin sample is then positioned on its cell. Before gluing the studs, the operator must indicate the compression force value that the vertical force sensor above the Y-studs should reach when the studs will come into contact with the skin. The sample support is raised again so that the skin reaches the instrument's studs. As soon as the first value of compression force is reached, meaning that the surface of the skin comes into contact with the studs on the Y axis, the vertical position of the lifting support is measured in order to calculate the total thickness of the skin. Then, once the compression force has been reached, the sample holder stops. The operator then lowers the support until the skin no longer touches any studs. The studs are slightly adjusted on the skin to take into account any surface irregularities on certain skins. Next, the sample support is lowered again and the gluing step can be carried out.

For gluing, the end of the X-studs facing the skin is glued with cyanoacrylate adhesive. It is a liquid cyanoacrylate adhesive from *Loctite* (Reference: Super Glue-3). This cyanoacrylate glue adheres strongly to the skin, making fast and solid bonding (in just a few minutes).
The motorised lifting support finally rises again to bring the skin into contact with the glued studs and to permanently fix the studs to the skin surface with the compression force specified previously. The lifting support stops when the specified compression force is reached.

A period of around ten minutes is required to ensure complete drying and solidification of the adhesive. Before carrying out the mechanical tests on the X-axis, the studs on the Y-axis can be lifted to avoid influencing the tensile measurements. Once the studs have been glued, the mechanical tests can be programmed and started.

The operator can then progress through the interface by clicking on "Paramétrer pré-contrainte".

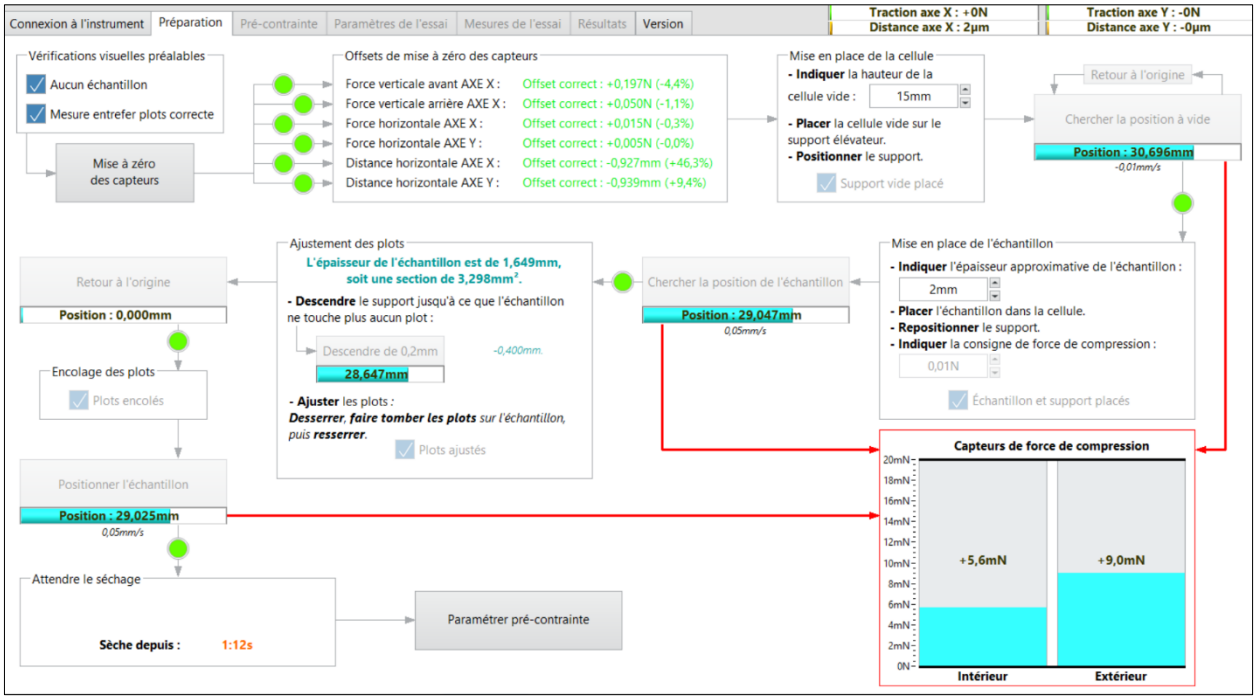

Figure A5: Second "Préparation" page of the software interface.

C) The third page of the software interface, shown in Figure A6, is dedicated to the possibility of performing an initial pre-stress on the skin before the mechanical tests. This pre-stress can be applied in terms of deformation or force. The operator indicates whether or not he wants a pre-stress and progresses through the interface by clicking on "Paramétrer un essai".

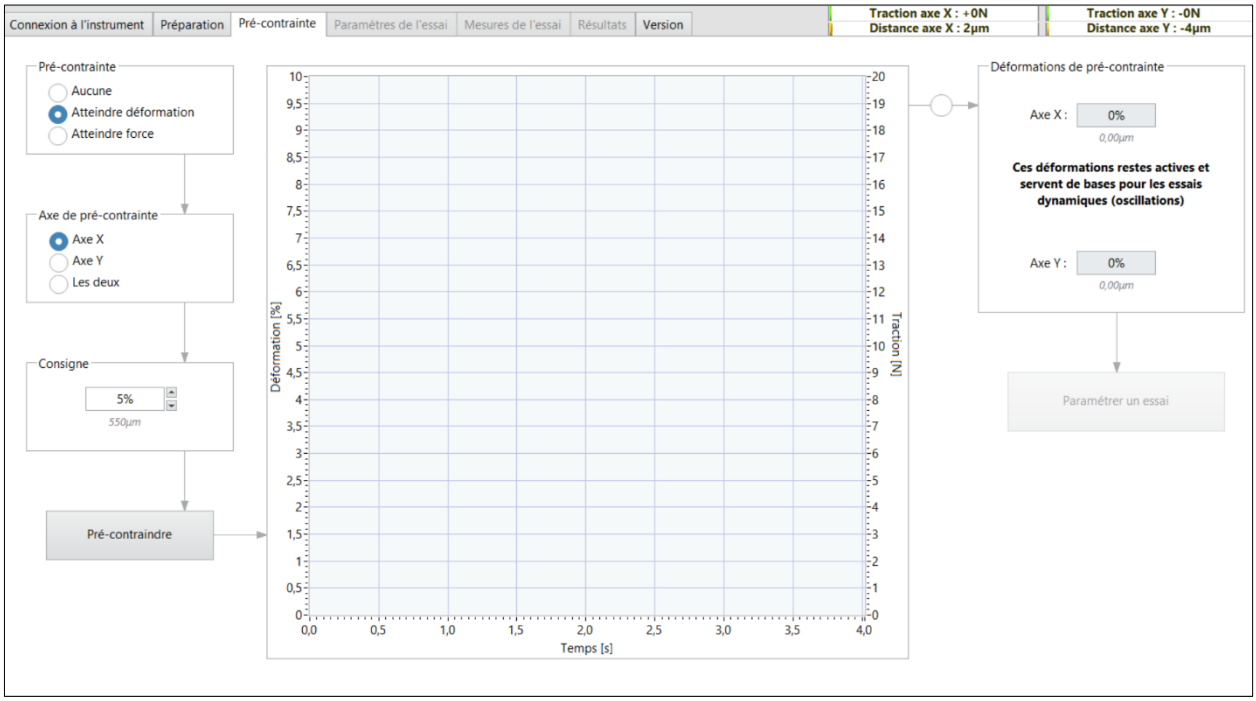

Figure A6: Third "Pré-contrainte" page of the software interface.

D) The fourth page of the software interface, shown in Figure A7, is dedicated to setting the mechanical test parameters. The operator chooses in order:

- the type of oscillatory measurement: single, strain sweep or frequency sweep.
- the percentage of deformation
- test frequency
- signal shape: sinusoidal, triangular, or rectangular.
- test axis: X-axis, Y-axis or synchronous axes.
- the number of cycles per measurement.

The operator then validates these variables, checks the instructions on the dedicated central graph before naming the file to record all the data. The mechanical test can then be started by clicking on "Lancer les mesures".

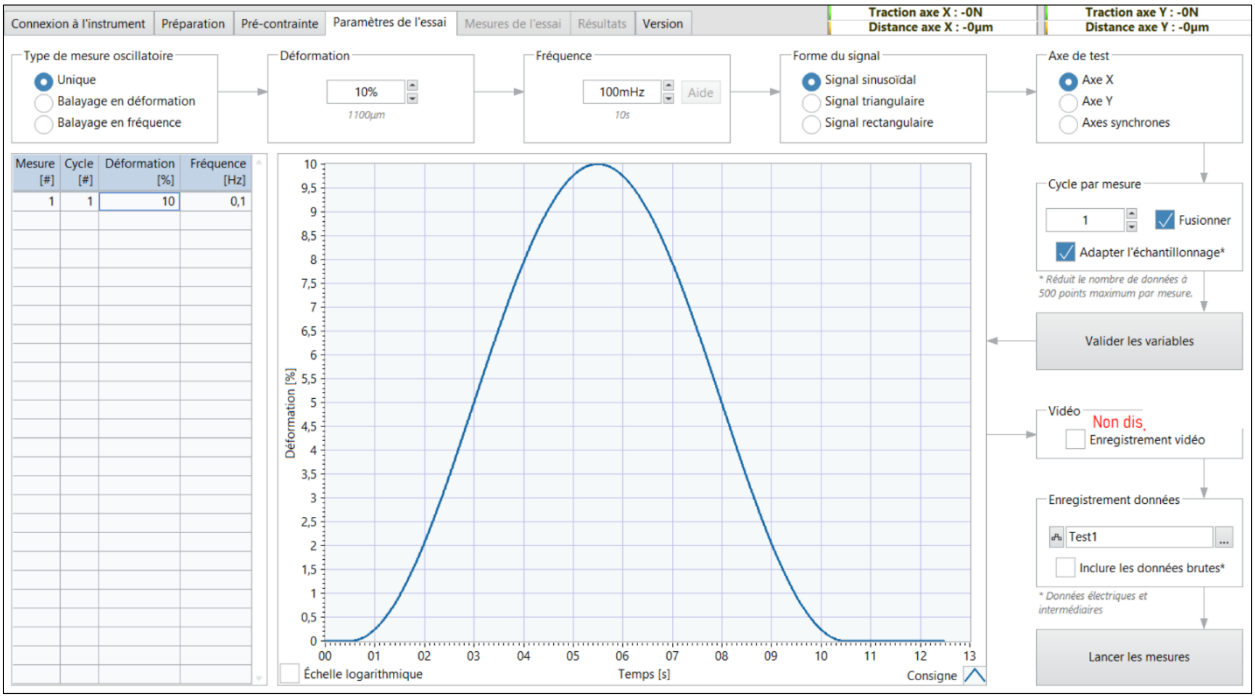

Figure A7: Fourth "Paramètres de l'essai" page of the software interface.

E) Finally, the fifth and sixth pages of the software interface, shown in Figure A8 and A9, are devoted respectively to the mechanical test measurements and the results obtained. The operator can view the results as well as the live camera image of the tests. These sections are currently being developed to analyse the results directly with the interface.

The last page of the software interface summarises the latest programming changes.

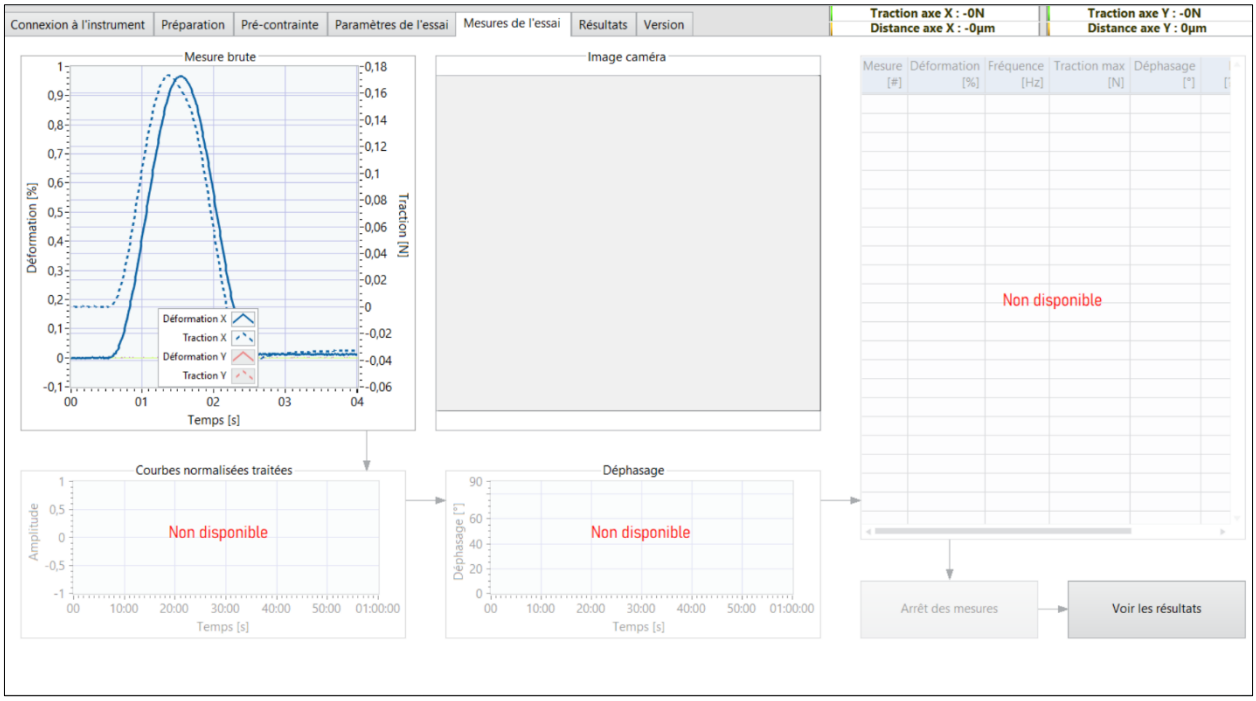

Figure A8: Fifth "Mesures de l'essai" page of the software interface.

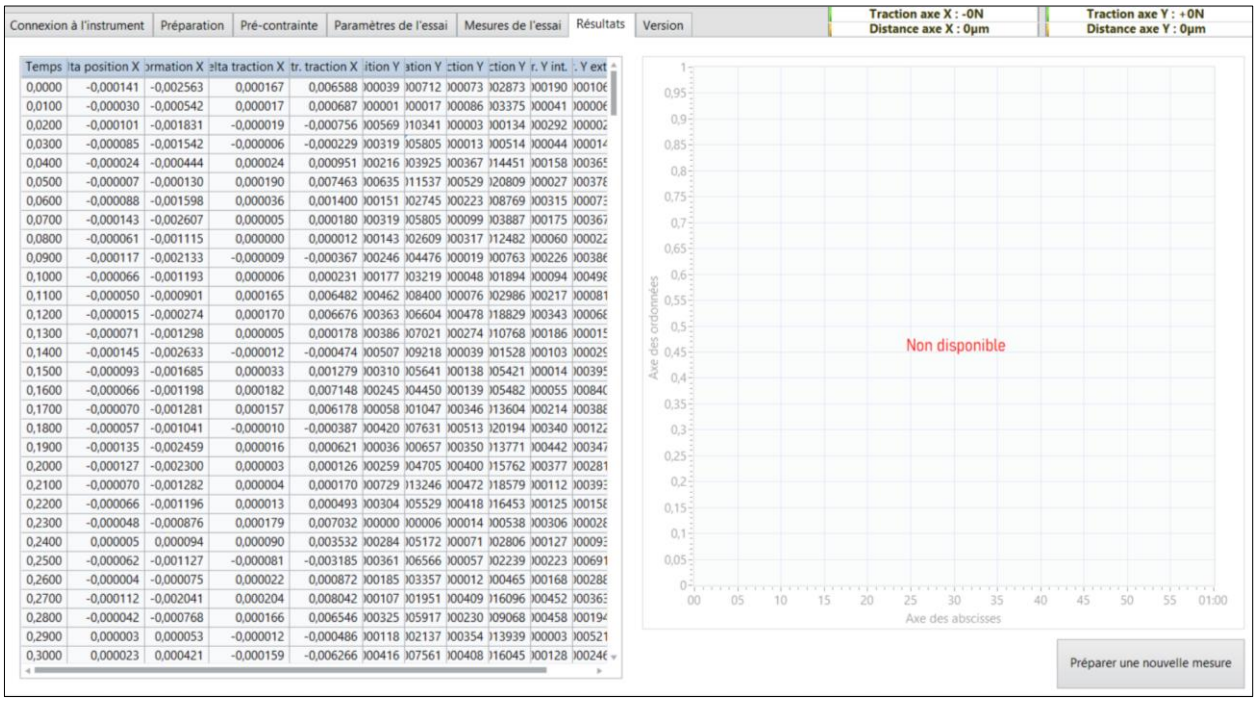

Figure A9: Sixth "Résultats" page of the software interface.

Appendix 3: Power supply principle and communication principle of the device

The connectivity of all the components of the device, in terms of power and data, is presented in this Appendix.

A) The power supply principle for the various components of the equipment is described in Figure A10 in the form of a single-line diagram. Power will be supplied to the various components of our equipment. The EDF power supply has a voltage of 230 V. We use converters to transform the 230 V alternating current into 24 V or 48 V direct current. The various converters supply:

- The acquisition system (DAQ), the 2 position sensors and the 4 force sensor conditioners that power these 4 sensors.
- The 2 piezoelectric controllers, each powering 2 piezoelectric actuators.
- The motorised support lift controller.
- The camera.

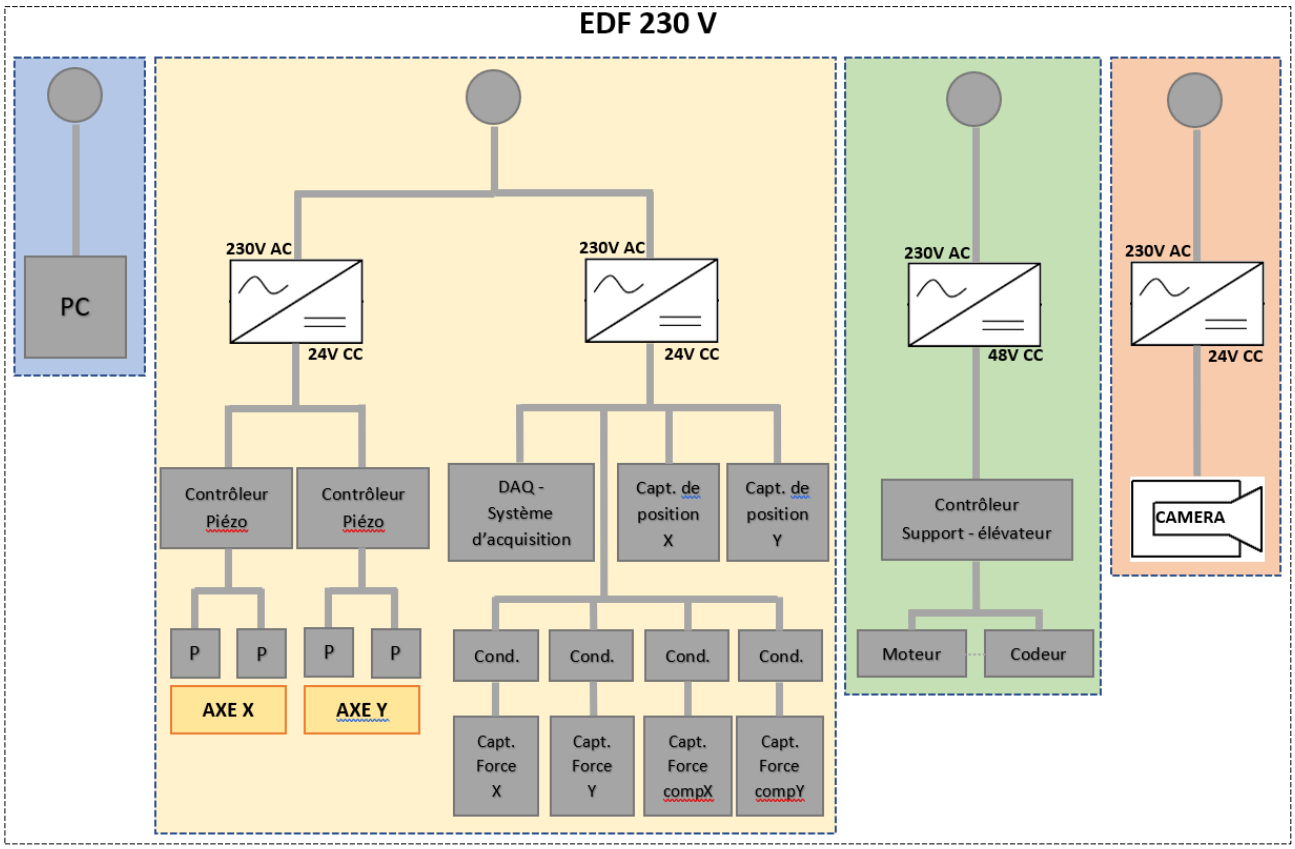

Figure A10: Single-line diagram of the power supply principle for our device.

B) The principle of communication between the various components of the equipment is described in Figure A11 in the form of a connectivity diagram. Everything that involves the transfer of information (information going back and forth between the different components) is represented here.

The exchange of information is represented by the lines in the diagram. The PC retrieves all the information and controls the various components; it is central.
This PC is connected:

- To the acquisition system (DAQ) via a USB connection
- To the camera via an Ethernet connection
- To the motor unit of the lift support (the movement plate) via a USB connection.

The DAQ has a control card and an acquisition card. The control card sends information to the 2 piezoelectric controllers via a 0 - 10 V voltage (voltage = information exchanged). The acquisition card receives information from the 2 position sensors and the 4 force sensor conditioners (which themselves receive voltage information from the force sensors) using a current of 4 - 20 mA (current = information exchanged).

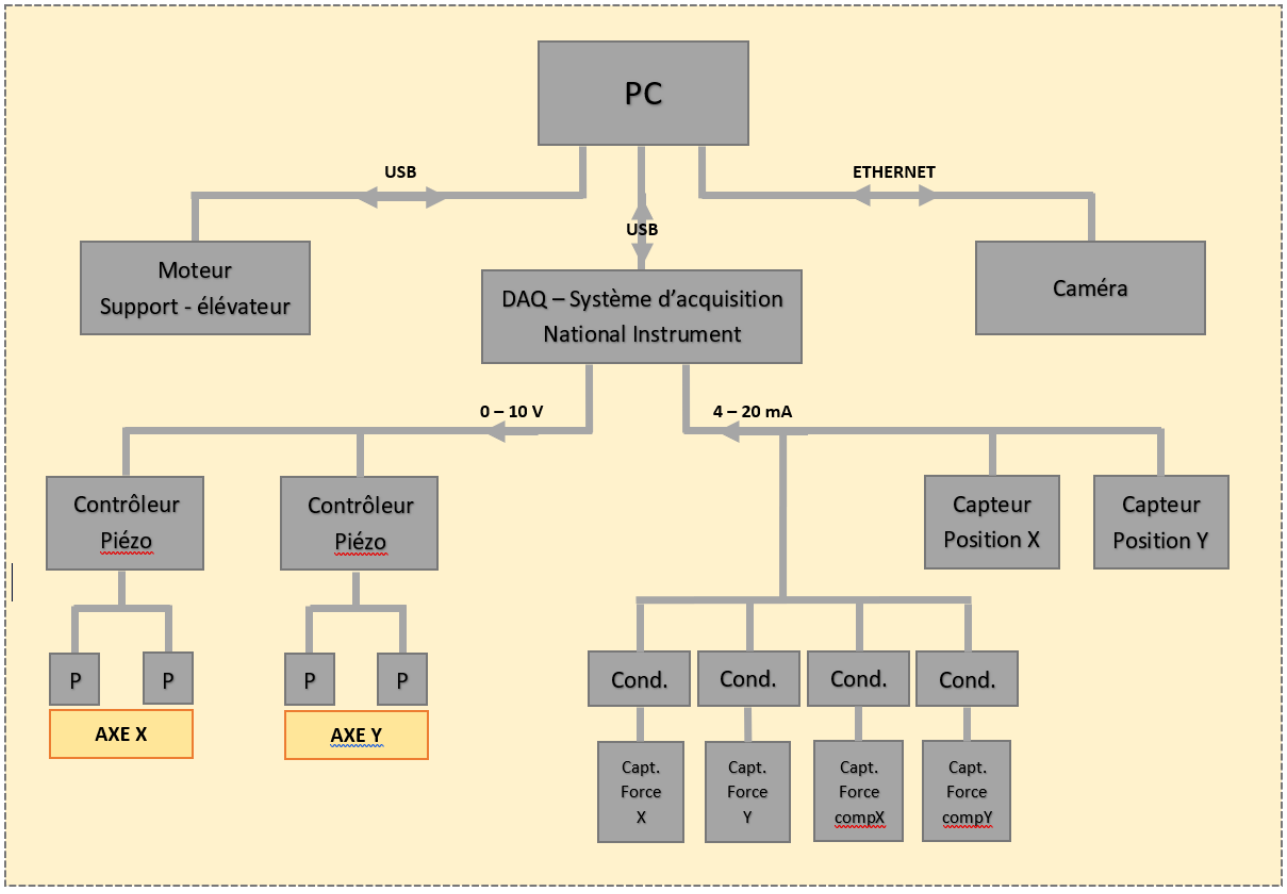

Figure A11: Diagram of the communication principle for our device.

Appendix 4: The Cutometer®

In general, the visual and tactile evaluation and assessment carried out by clinicians and dermatologists in pathological or aesthetic situations (wounds and skin anomalies) is often too subjective. The validity of these assessments remains inferior to that obtained by measurement using a neutral device. The development of tools enabling objective and reproducible analyses of skin properties is becoming increasingly necessary to measure physical quantities and progressively improve the surgical methods used in pathology or aesthetics. Our device and the Cutometer® are tools that enable objective measurements to be taken on the skin.

A) Description of the Cutometer®

The Cutometer (Cutometer® Dual MPA 580 from *Courage+Khazaba electronic GmbH*) is a medical device for measuring the mechanical properties of the skin (Figure A.12.a). This device has been available and sold in the cosmetics and medical markets for over 30 years. This device is mainly used for *in vivo* measurements. Many authors have used it to prove the effectiveness of surgical treatments [Stroumza *et al.*, 2015].

The Cutometer measures the deformation of an area of skin subjected to mechanical suction and its ability to recover. The measuring principle of the device is based on the application of a negative pressure within a suction chamber placed on the surface of the skin. A negative pressure is produced with a pump in the device and pulls the skin into the opening of the measuring probe. The area of skin to be measured is aspirated into the 2mm diameter opening of the probe (Figure A.12.b). The depth of skin penetration within the probe opening is determined in a non-contact manner using an optical method. Depending on the depth of skin penetration into the probe, the incoming light intensity is different.

The mechanical test therefore consists of measuring the deformation of the skin inside the chamber as a function of time and the negative pressure applied. The test begins with a quasi-instantaneous application of a constant vacuum and maintains this vacuum for a set period of time (similar to a creep test for polymers). The pressure then stops and the skin returns to its initial state.

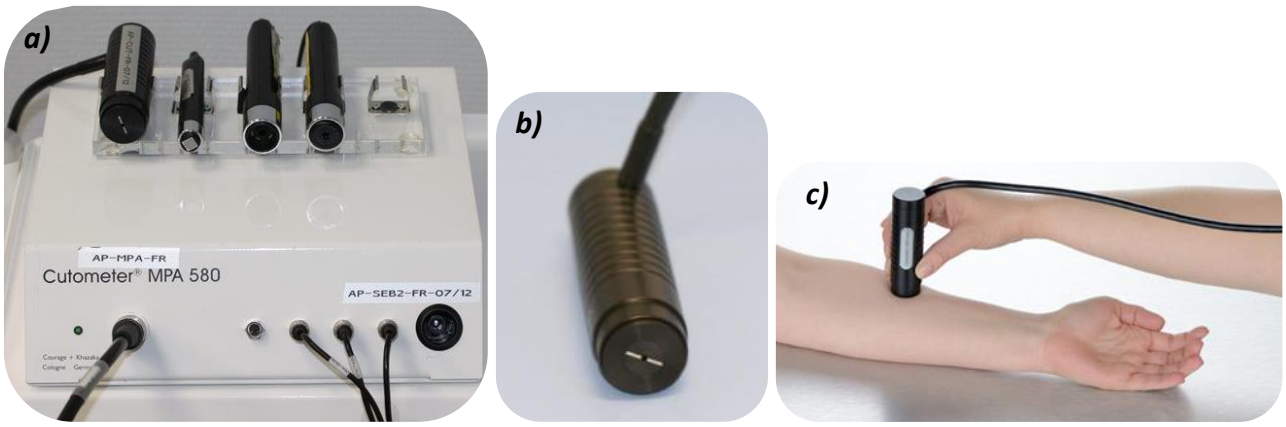

Figure A.12: Cutometer®. a) Photo of equipment. b) Photo of probe with suction chamber. c) Photo of Cutometer test.

The pressure exerted by the operator on the probe is the main measurement bias (Figure A312.c). The Cutometer user guide itself recommends that only one experimenter be assigned to the measurements.

The skin's ability to resist suction and its ability to return to its original state after the vacuum is removed are determined. Skin penetration depth (mm) is plotted against time (s). A theoretical curve for a Cutometer test, taken from the device's user guide, is shown in Figure A.13. The curve displayed is made up of two phases: the aspiration phase and the relaxation phase. The following data can be obtained from this curve, providing information on the elasticity and viscosity of the skin:

- Ue: immediate elongation (purely elastic component)
- Uv: delayed elongation (viscoelastic component)
- Ur: immediate retraction (elastic return)
- Ua: elongation recovered at the end of the stress cycle
- Uf: final elongation (total deformation: elastic + viscoelastic)

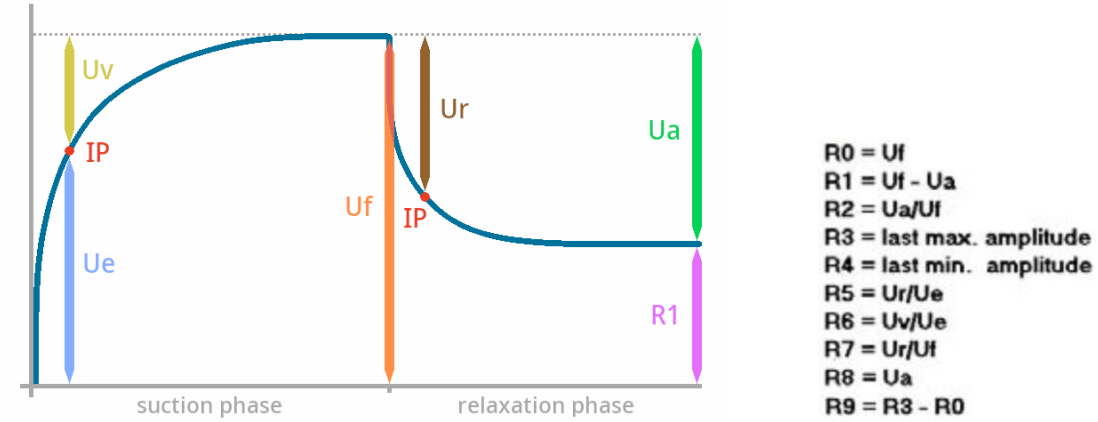

Figure A13: Theoretical curve for a Cutometer test, with all the measurable parameters.

These data enable to calculate biomechanical parameters, also presented in Figure A.13, such as:

- $R_0 = U_f$: maximum amplitude. This parameter reflects the penetration depth in mm after the suction phase. It therefore represents the firmness of the skin (strength to resist suction). The more U_f decreases, the firmer the skin.
- $R_2 = U_a/U_f$: gross elasticity. Portion between the maximum amplitude and the deformation capacity of the skin. The more the value tends towards 1, the more elastic the skin is.
- $R_5 = U_r/U_e$: net elasticity. Elastic portion between the suction region and the relaxation region. The more R5 tends towards 1, the more elastic the skin.
- $R_6 = U_v/U_e$: viscoelastic portion of the curve. The lower the value, the greater the elasticity.
- $R_7 = U_r/U_f$: portion of the immediate elastic recovery in proportion to the total amplitude. The more R7 tends towards 1, the more elastic the skin.

As in traction, this typical shape of the curve on human skin is due to the networks of elastin and collagen fibres present in the skin. The first very straight rise in the curve can be linked mainly to the movements of elastin, which is easy to pull and very flexible. The second part of the rise is mainly

due to collagen taking over. Collagen fibres are more resistant to suction and less flexible than elastin fibres. Immediately after the depression is eliminated, in the second part of the curve, collagen ensures the rapid return of the skin and elastin takes over, returning the skin to its original state.

B) Comparison of the Cutometer® with our Mécapeau instrumentation

The Cutometer and Mécapeau are two devices used to assess the viscoelastic properties of human skin. The first is a commercial device that is widely used for scientific studies in cosmetics and medicine, while the second is a specific device developed to offer different mechanical measurements and provide additional information for these fields of application.

Compared with the Cutometer, whose principle is based on mechanical suction tests, the Mécapeau device is based on mechanical extension tests, where a stretch is applied parallel to the skin surface. The advantage of our device is that it allows directional mechanical tests to be carried out, enabling skin anisotropy to be measured by performing tests in different directions on the skin. Another advantage is that our mechanical tests are carried out in the plane of the skin, unlike tests with the Cutometer, which means that the underlying structures of the skin tissue are not stressed.

The results obtained using the Cutometer are adimensional biomechanical parameters (the R parameters) that enable the viscoelastic properties of the skin to be measured. These parameters are specific to the Cutometer device. The Mécapeau instrumentation, on the other hand, provides a range of biomechanical parameters that are commonly used to analyse the mechanical behaviour of any type of material. The results obtained are therefore usable and comparable for internal studies, but can also be compared with other studies in the scientific literature. Tensile tests and dynamic mechanical analysis are universal and can be used to obtain mechanical parameters such as the material's modulus of elasticity and viscoelastic moduli, for example.

Despite this, the Cutometer is considered to be a standard method for determining skin elasticity, supported by numerous scientific studies. The aim of the research work carried out in this thesis is to develop and propose an innovative equipment that is complementary to the Cutometer for measuring the viscoelastic properties of the skin. This device has been developed for *ex vivo* measurements, but it can also be used for *in vivo* measurements, which provides additional and complementary data to the tests carried out with a Cutometer.

Appendix 5: Injuries and wound healing

The skin is characterised by a high capacity for regeneration and healing. Even small wounds, such as small cuts, are an attack on the skin. When a wound occurs, the body naturally initiates a natural biological phenomenon: healing. This is a complex repair process during which the body must stop the bleeding, protect, clean, and close the wound. The damaged tissue must be reconstituted as close as possible to the original tissue. Depending on the depth of the wound, two healing processes can then take place:

- Healing of superficial lesions (epidermal damage)
- Healing of deep lesions (damage to the dermis or even the hypodermis)

A) Healing of superficial lesions

Superficial lesions may be abrasions (scraping of a part of the skin) or minor burns, for example. The basal cells of the epidermis surrounding the wound detach from the basement membrane, enlarge and migrate towards the centre of the lesion to fill the space (*Figure A14*). When cells from opposite edges of the wound meet, a cellular response, contact inhibition, stops their progression. Migration ceases completely when all sides of each cell come into contact with other epidermal cells.
As the basal cells of the epidermis migrate, a hormone called epidermal growth factor (EGF) stimulates the division of basal stem cells to replace those that have migrated into the wound. The displaced basal epidermal cells divide to produce new layers and thus thicken the regenerated epidermis. Regeneration results in permanent repair of the epidermis.

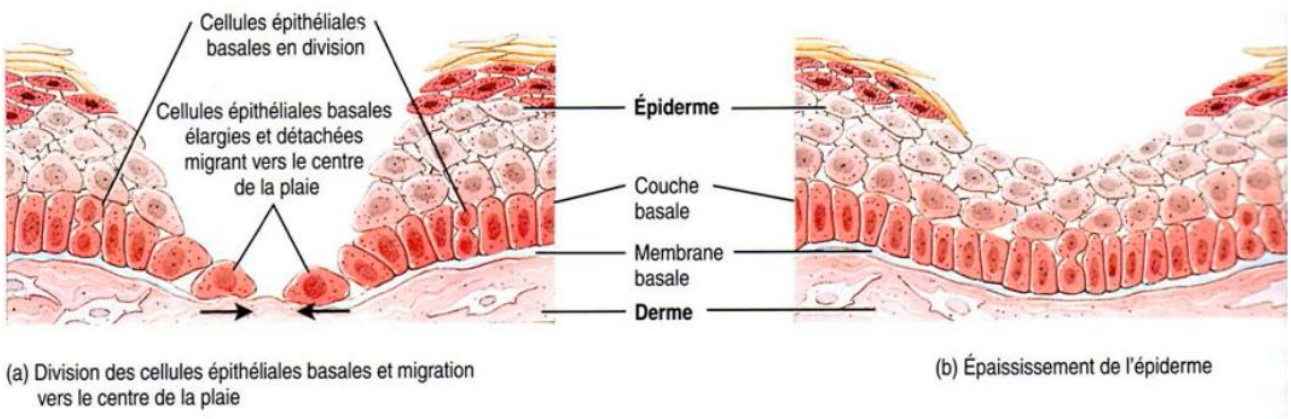

Figure A14: Healing of superficial lesions – Image from BNM Santé-Cicatrisation

B) Healing of deep lesions

It is triggered when an injury reaches the dermis or the hypodermis. The repair process is more complex because several layers of tissue are damaged. It leads to the formation of scar tissues which do not allow the skin to fully recover its previous functions. Healing takes place in four phases.

- The inflammatory phase (*Figure A15.a*)

This phase allows for the elimination of the aggressor agent and cellular debris as well as the repair of the damaged tissue. Whatever the type of wound, healing always begins with the appearance of inflammatory phenomena: vasodilatation (linked to redness and heat) and increased vascular permeability (linked to oedema and heat).

Immediately after the trauma, there is tissue oedema. Coagulation is induced by activation of thrombokinase which is released. This results in the formation of fibrin in the form of a clot. This prevents too much blood loss. A few minutes later, exudation begins, which will ensure the defence against infection and the detersion of the wound. The platelets enclosed in the clot release growth factors at the wound site and attract inflammatory cells. Then, it is the turn of monocytes, macrophages, and phagocytes to intervene. They orchestrate the stages of tissue repair by phagocytosing necrotic tissue, foreign bodies, and bacteria and by stimulating the growth of new blood vessels (angiogenesis), the growth of fibroblasts and the proliferation of keratinocytes. Thus, by phagocytosis and proteolysis, necrotic tissue and other tissue debris, germs and toxins are removed.

- The migration phase

The blood clot turns into a scab due to the proliferation of fibrin filaments, which is the beginning of the development of the scar. The epithelial cells mass under this clot to close the wound. Fibroblasts from the connective tissue migrate to the centre of the lesion and begin to synthesise scar tissue (composed of collagen fibres and glycoproteins) while damaged blood vessels regenerate. The fibroblasts in the dermis are particularly active during the healing process. The tissue that fills the wound during this phase is called granulation tissue.

- The proliferation (or budding) phase

This is the massive proliferation of cells, blood vessels and fibres. It is characterised by extensive growth of epithelial cells beneath the scab, the disordered deposition of collagen fibres by fibroblasts and the continued regeneration of blood vessels.

- The maturation phase (*Figure A15.b*)

This is the phase of scar remodelling. Maturation is also the longest phase; it continues for more than a year. Initially, the wound retracts under the influence of myofibroblasts. Then, as the granulation tissue becomes progressively depleted of water and contains fewer and fewer vessels, it becomes firmer. Collagen production decreases and the randomly placed collagen fibres become organised. The number of fibroblasts decreases and the blood vessels return to normal. The skin will remain more or less white because the melanocyte count will be replenished later. The crust falls off as soon as the epidermis has regained its normal thickness.

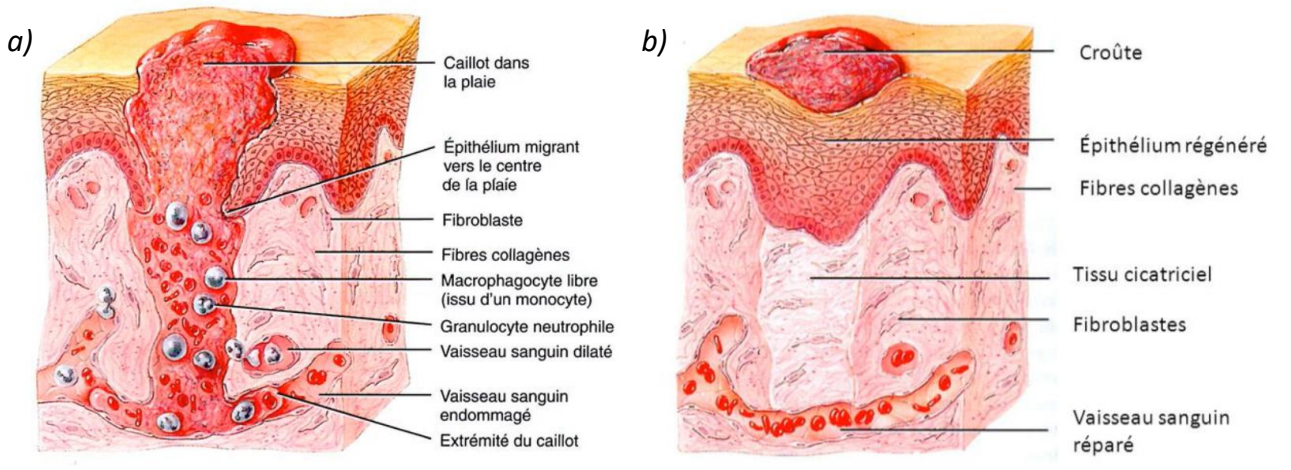

Figure A15: Healing of deep lesions. a) Inflammatory phase. b) Maturation phase – Image from BNM Santé-Cicatrisation

Normally, after 6 months, a scar should be soft and painless. However, scarring disorders can lead to disharmonious scars: keloid scars, hypertrophic scars, etc.

Résumé de la thèse

La peau est l'enveloppe du corps humain assurant le rôle de première barrière protectrice de notre organisme. Les propriétés mécaniques de la peau humaine jouent un rôle clé dans son intégrité car elles confèrent au tissu cutané sa capacité à rester intact. La mesure des propriétés mécaniques de la peau présente ainsi de nombreux intérêts comme celui de disposer d'une méthode d'évaluation objective des effets de produits médicaux ou cosmétiques, ainsi que celui de quantifier les pathologies cutanées qui pourraient les affecter.

Dans ce contexte, un instrument spécifique pour évaluer les propriétés mécaniques de la peau humaine *ex vivo* a été développé. L'objectif de cet appareillage est de caractériser à la fois les propriétés mécaniques conventionnelles tirées d'un essai de traction à vitesse d'étirement constante, et les deux composantes mécaniques, élasticité et dissipation, issues d'un essai de spectrométrie mécanique afin d'éventuellement discriminer chaque phénomène. L'approche proposée est d'établir un lien phénoménologique entre viscoélasticité et structure de la peau.

La première partie de cette thèse a été consacrée à un travail instrumental afin que l'appareillage mesure de façon précise et fiable les propriétés mécaniques de tissus déformables. Son développement et son amélioration continue ont finalement permis de caractériser ces propriétés sur des explants de peau humaine *ex vivo.*

Les premiers tests sur les explants de peau humaine *ex vivo* ont permis de confronter et d'adapter l'instrumentation à l'étude d'échantillons biologiques. Tout d'abord, des études préliminaires portant, entre autres, sur le pré-conditionnement, l'état de pré-tension et l'anisotropie mécanique, ont été réalisées afin de valider la fiabilité de l'instrumentation et des méthodes développées. Une fois l'ensemble de ces notions étudiées, une caractérisation complète des propriétés viscoélastiques des explants a pu être réalisée. Cette caractérisation a également permis d'étudier leur viabilité dans le temps et la notion de vieillissement cutané.

Cette instrumentation brevetée, associée à l'utilisation d'explants de peau *ex vivo* dans des conditions physiologiques pendant plusieurs jours, a finalement permis d'évaluer l'effet de différentes contraintes sur les propriétés mécaniques de la peau. Une étude portant sur les vergetures a révélé que ces zones cutanées endommagées étaient caractérisées par une forte anisotropie mécanique et présentaient des propriétés viscoélastiques dégradées. Par ailleurs, une étude portant sur la congélation des explants, processus utilisé pour conserver les tissus dans le temps, a montré que le fait de congeler la peau semble avoir un léger effet de rigidification sur ses propriétés mécaniques. Enfin, l'effet d'un *stress* enzymatique sur la peau, imitant un processus naturel de vieillissement accéléré du tissu, a été examiné. Cette dernière étude a démontré la dégradation significative des propriétés mécaniques des explants exposés à des enzymes protéolytiques : collagénase et élastase. Un lien avec des analyses histologiques est proposé.

Ces différentes études menées lors de ce travail de thèse ont permis de montrer que cette instrumentation peut contribuer à répondre à des questions scientifiques et techniques et peut aider au développement de produits destinés aux traitements. En effet, elle pourrait permettre d'analyser et d'évaluer de manière objective les effets de différentes agressions extérieures (exposition aux rayons UV, pollution par un produit chimique ou par atmosphère, incision, etc.) et les effets de produits médicaux ou dermo-cosmétiques (crèmes hydratantes, crèmes anti-vergetures, pansements cicatrisants, etc.) sur les propriétés viscoélastiques de la peau humaine.

Abstract

Skin is the envelope of the human body, acting as our body's first protective barrier. The mechanical properties of human skin play a key role in skin integrity, as they confer its ability to remain intact to the cutaneous tissue. Measuring the mechanical properties of the skin therefore has many benefits, such as providing a method for objectively assessing the effects of medical or cosmetic products, and for quantifying skin pathologies that could affect them.

In this context, a specific instrument for assessing the mechanical properties of human skin *ex vivo* has been developed. The aim of this equipment is to characterise both the conventional mechanical properties obtained from a tensile test at a constant stretching rate, and the two mechanical components, elasticity and dissipation, obtained from a mechanical spectrometry test, in order to discriminate each phenomenon. The proposed approach is to establish a phenomenological link between viscoelasticity and skin structure.

The first part of the thesis was devoted to instrumental work to ensure that the equipment accurately and reliably measures the mechanical properties of deformable tissues. Its development and continuous improvement finally enabled these properties to be characterised on *ex vivo* human skin explants.

Initial tests on *ex vivo* human skin explants enabled to confront and adapt the instrumentation with the study of biological samples. Firstly, preliminary studies were carried out on pre-conditioning, pre-tension state and mechanical anisotropy, to validate the reliability of the instrumentation and the methods developed. Once all these concepts had been studied, the viscoelastic properties of the explants were fully characterised. This characterisation also enabled to study their viability over time and the notion of skin ageing.

This patented device, combined with the use of *ex vivo* skin explants under physiological conditions for several days, has finally allowed to assess the effect of different stresses on the mechanical properties of the skin. A study of stretch marks revealed that these damaged areas of skin were characterised by high mechanical anisotropy and had degraded viscoelastic properties. In addition, a study of explant freezing, a process used to preserve tissue over time, showed that freezing the skin appears to have a slight stiffening effect on its mechanical properties. Finally, the effect of enzymatic stress on the skin, mimicking a natural process of accelerated tissue ageing, was studied. This last study demonstrated a significant deterioration in the mechanical properties of explants exposed to proteolytic enzymes: collagenase and elastase. A link with histological analyses is proposed.

The various studies carried out during this thesis have shown that this instrumentation can contribute to answering scientific and technical questions and could help in the development of products intended for treatments. Indeed, it could be used to objectively analyse and assess the effects of various external stresses (exposure to UV rays, chemical or atmospheric pollution, incisions, etc.) and the effects of medical or dermo-cosmetic products (moisturising creams, stretch mark creams, healing dressings, etc.) on the viscoelastic properties of human skin.

Résumé de thèse vulgarisé

La peau est l'enveloppe du corps humain assurant le rôle de première barrière protectrice de notre organisme. Les propriétés mécaniques de celle-ci jouent un rôle clé dans son intégrité en lui conférant sa capacité à rester intact. Un instrument spécifique permettant d'évaluer les propriétés mécaniques de la peau humaine est proposé afin de mieux comprendre leurs liens avec la structure du tissu et leurs évolutions sous des contraintes extérieures. En caractérisant avec cet appareil des échantillons de peau *ex vivo* dans des conditions physiologiques pendant plusieurs jours, nous proposons de mieux appréhender ce tissu et d'aider au développement de produits destinés aux traitements. En effet, l'instrument permet de caractériser de façon précise les effets de différents *stress* sur les propriétés d'élasticité et de déformabilité de la peau. Il est ainsi possible d'évaluer de façon objective certains phénomènes cutanés (vergetures) ou l'effet de produits médicaux ou cosmétiques.

Popularised abstract

Skin is the envelope of the human body, acting as our body's first protective barrier. The mechanical properties of the skin play a key role in its integrity, as they confer to the cutaneous tissue its ability to remain intact. A specific instrument for assessing the mechanical properties of human skin is proposed, with the aim of gaining a better understanding of their links with tissue structure and how they change under external stress. By characterising *ex vivo* skin samples under physiological conditions for several days, we propose to gain a better understanding of this tissue and help to develop products for cure. The instrument enables to precisely characterise the effects of various stresses on the elasticity and deformability properties of the skin. This enables to objectively assess certain skin phenomena (stretch marks) or the effect of medical or cosmetic products.

ECOLE DOCTORALE :
Sciences Exactes et leurs Applications (ED 211)

LABORATOIRE :
Institut des Sciences Analytiques et de Physico-Chimie pour l'Environnement et les Matériaux (IPREM)

CONTACT

Bastien BLANCHARD
bastienblanchard64@gmail.com

UNIVERSITÉ DE PAU ET DES PAYS DE L'ADOUR